MOLECULAR IMMUNE RESPONSES OF LUMPFISH (*CYCLOPTERUS LUMPUS*) TO *AEROMONAS SALMONICIDA*

By

Setu Chakraborty, B.Sc. (Hons.), M.Sc.

A Thesis Submitted to the School of Graduate Studies

in Partial Fulfilment of the

Requirements for the Degree of

Doctor of Philosophy

Department of Ocean Sciences

Memorial University of Newfoundland

Spring 2023

St. John's, Newfoundland, and Labrador

Abstract

Lumpfish (*Cyclopterus lumpus*) have been utilized to biocontrol sea-lice (e.g., *Lepeophtheirus salmonis*) infestations in Atlantic salmon (*Salmo salar*) farms in the North Atlantic region. *Aeromonas salmonicida* subsp. *salmonicida* is a Gram-negative facultative intracellular pathogen infecting several fish species, including lumpfish. Here, I established an *A. salmonicida* systemic infection model in lumpfish. Juvenile lumpfish were intraperitoneally (ip) injected with different doses of *A. salmonicida* strain J223. *A. salmonicida* median lethal dose (LD_{50}) was calculated at 10^2 colony-forming units (CFU)/dose. Samples from blood, head kidney, spleen, and liver were collected at different time points to determine the infection kinetics. Triplicated RNA samples from the head kidney, spleen, and liver of non-infected and infected (10^4 CFU/dose) lumpfish at 3 and 10 days post-infection (dpi) were utilized for RNA sequencing (RNA-Seq). Analysis of RNA-Seq data suggested that *A. salmonicida* could induce lethal infection in lumpfish by septic-like shock, suppression of the adaptive immune system, impairment of the DNA repair system, and disruption of cytoskeleton structure. Thus, an effective vaccine for lumpfish against *A. salmonicida* is highly needed. Here, I evaluated the immune protective effect of *A. salmonicida* bacterins and outer membrane proteins (OMPs) expressing iron-regulated outer membrane proteins (IROMPs) in lumpfish. However, my results demonstrate that vaccines do not confer protection to lumpfish against *A. salmonicida* J223. Additionally, I observed that formalin-killed *A. salmonicida* J223 bacterins do not increase IgM titers in lumpfish serum. Instead, the bacterins downregulate genes encoding IgM, MHC-II, and CD4, which indicates immune suppression and vaccine's inability to trigger humoral and cell-mediated immune responses. Furthermore, different post-transcriptional factors (e.g., microRNAs (miRNAs)) that significantly determine an organism's disease state are not explored yet in lumpfish. Therefore, I characterized miRNA

encoding genes in lumpfish from three developmental stages (adult, embryos, and larvae) in this study, providing the reference miRNAome for future functional studies. Altogether, 443 unique mature miRNAs were identified in lumpfish. Transcriptomics analysis suggested organ-specific and age-specific expression of miRNAs. This thesis contributes significantly to understanding lumpfish- *A. salmonicida* interactions and provides guidelines for future host-pathogen interaction and vaccine studies.

General summary

Lumpfish is a cleaner fish that biocontrols sea-lice infestations in Atlantic salmon. *Aeromonas salmonicida* subsp. *salmonicida* is a bacterial pathogen infecting several fish species, including lumpfish. Here, I proposed an *A. salmonicida* infection model in lumpfish. Juvenile lumpfish were infected with different doses of *A. salmonicida* strain J223. I determined that ~10^2 J223 cells can kill 50% of the lumpfish population. Samples from blood, head kidney, spleen, and liver were collected at different time points. Triplicated RNA samples from the head kidney, spleen, and liver of non-infected and infected lumpfish at 3 and 10 days post-infection (dpi) were used for RNA sequencing (RNA-Seq). Analysis of RNA-Seq data suggested that *A. salmonicida* could induce a lethal condition in lumpfish, suppress its immune system, impair the DNA repair system, and disrupt cytoskeleton structure. Thus, an effective vaccine for lumpfish against *A. salmonicida* is needed. Here, I evaluated the immune protective effect of formalin-inactivated *A. salmonicida* and its outer membrane proteins (OMPs) in lumpfish. However, my results demonstrate that vaccines do not protect lumpfish against *A. salmonicida* J223. Additionally, I observed that formalin-killed *A. salmonicida* J223 bacterins suppressed the immune responses of lumpfish. Furthermore, different post-transcriptional factors (e.g., microRNAs (miRNAs)) that significantly determine an organism's disease state are not explored yet in lumpfish. Therefore, I characterized miRNA encoding genes in lumpfish from three developmental stages (adult, embryos, and larvae) in this study, providing the reference miRNAome for future functional studies. Altogether, 443 unique mature miRNAs were identified in lumpfish. Transcriptomics analysis suggested organ-specific and age-specific expression of miRNAs. This thesis contributes significantly to understanding lumpfish- *A. salmonicida* interactions and provides guidelines for future host-pathogen interaction and vaccine studies.

Acknowledgments

Throughout my Ph.D. research, I have received excellent guidance and support. I would like to first and foremost want to acknowledge and thank my parents for their endless love and support. They may not have understood everything I was doing, but they were always there for me. I must acknowledge my husband and son, who supported me throughout this entire process to make me successful. I am sincerely grateful to my supervisor, Dr. Javier Santander, for your guidance, knowledge, and leadership. Juggling a Ph.D. while working was challenging, but you were always there to provide encouragement and direction. To Dr. Rune Andreassen and his lab for providing me with enormous support in completing one thesis chapter at the Oslo Metropolitan University. I also thank my Ph.D. committee, Dr. Matthew Rise, and Dr. Mani Larijani. In that sense, I would also like to thank my collaborators Danny Boyce, manager of the Dr. Joe Brown Aquatic Research Building (JBARB), JBARB staff, and Steve Hill and Gord Nash at the Cold-Ocean Deep-Sea Research Facility (CDRF). I am also grateful for all colleagues I have met along the way. To those in the Santander lab, I have learned so much from many of you and I would not have made it this far without your help. It was a privilege to work alongside you. I would like to acknowledge Canada First - Ocean Frontier Institute (sub-module J3), NSERC-Discovery grant (RGPIN-2018-05942), and Atlantic Fisheries Fund, Canada, for funding my research.

Co-authorship statement

All primary intellectual and practical contributions reported in this thesis were completed by Setu Chakraborty and Javier Santander. Chapters 2, 3, and 4 identified co-authors for their significant contributions (Section 1.11):

Chapter 2: Setu Chakraborty, Ahmed Hossain, Trung Cao, Hajarooba Gnanagobal, Cristopher Segovia, Stephen Hill, Jenifer Monk, Jillian Porter, Danny Boyce, Jennifer R. Hall, Gabriela Bindea, Surendra Kumar, Javier Santander.

Chapter 3: Setu Chakraborty, Hajarooba Gnanagobal, Ahmed Hossain, Trung Cao, Ignacio Vasquez, Danny Boyce, Javier Santander.

Chapter 4: Setu Chakraborty, Nardos T. Woldemariam, Tina Visnovska, Matthew L. Rise, Danny Boyce, Javier Santander, Rune Andreassen.

Table of contents Page no.

1. Chapter one: Introduction ……1

1.1. Global expansion of the aquaculture industry and food security ……..…….....1

1.2. Aquaculture in Canada ……..……..……...2

1.3. Sea-lice: one of the most significant challenges in salmon aquaculture ..…….3

1.4. Sea-lice control in salmon aquaculture …….....6

1.4.1. Physical methods ……..…….....6

1.4.2. Chemical treatments ……...……7

1.4.3. Biological methods ……...……..8

1.5. Lumpfish ……9

1.5.1. Taxonomy and Distribution …….……...9

1.5.2. Physical and genetic characteristics …….……...11

1.5.3. Feeding and Reproduction ……..…….…….....13

1.5.4. Production ……..…..……13

1.5.5. Research on lumpfish diseases, immunity against infections, and vaccinology ……...14

1.6. *Aeromonas salmonicida* ……...16

1.7. Host-pathogen interactions ……..18

1.8. Vaccinology ……..…19

1.9. Major gaps in knowledge …….……..……..….24

1.10. Main objectives and thesis structure …….……....24

1.11. Publications arising from this thesis …….....26

1.12. References ……28

2. Chapter two: Multi-organ transcriptome response of lumpfish (*Cyclopterus lumpus*) to *Aeromonas salmonicida* subsp. *salmonicida* systemic infection ……52

2.1. Abstract ……52

2.2. Introduction …….....53

2.3. Materials and methods …….……55

2.3.1. Bacterial strain, culture media, and reagents ……..55

2.3.2. Bacteria inoculum preparation ……56

2.3.3. Ethics statement ……...….56

2.3.4. Fish holding ……...……...56

2.3.5. Lumpfish infection and lethal dose 50 (LD_{50}) determination ….....57

2.3.6. A. salmonicida tissue colonization ……...57

2.3.7. Histopathology …….……58

2.3.8. RNA purification ……..……58

2.3.9. Library preparation and RNA-Seq ……...62

2.3.10. Reference transcriptome assembly and downstream analysis ……64

2.3.11. de novo transcriptome assembly, contig abundance, and functional annotation ……...65

2.3.12. Gene filtration and GO enrichment analysis ….……...……66

2.3.13. RT-qPCR analyses ……67

2.4. Results ……..69

2.4.1. LD_{50} determination and A. salmonicida infection kinetics in lumpfish ……...……69

2.4.2. Quality statistics ……72

2.4.3. Global profile of differentially expressed genes and transcripts identified using reference genome-guided transcriptome assembly ……..…73

2.4.4. Global profile of differentially expressed transcripts identified by de novo transcriptome assembly analysis …….80

2.4.5. GO enrichment analysis ……..…..92

2.4.6. Analysis of the most significant differentially expressed genes ……...99

2.4.7. RT-qPCR verification analysis ……..…..……109

2.5. Discussion ……..…….114

2.6. Conclusions ……..……..125

2.7. References ……..……130

3. Chapter three: Inactivated *Aeromonas salmonicida* suppresses the humoral and cell-mediated immunity of lumpfish (*Cyclopterus lumpus*) ……..….148

3.1. Abstract ……..…148

3.2. Introduction ……..….149

3.3. Materials and Methods ……..……153

3.3.1. Bacterial strains, media, and reagents ……..…..153

3.3.2. Bacterin preparation ……..153

3.3.3. Bacterial outer membrane proteins preparations ……..……155

3.3.4. Vaccine pre-evaluation ……..…..……156

3.3.5. Bacteria inoculum preparation ……..…..157

3.3.6. Ethics statement ……..…….157

3.3.7. Fish holding ……..……157

3.3.8. Lumpfish immunization using a common garden experiment ……..…….158

3.3.9. Challenge of immunized lumpfish ……...160

3.3.10. Direct enzyme-linked immunosorbent assay (dELISA) ……160

3.3.11. RNA Preparation ……....162

3.3.12. cDNA synthesis and RT-qPCR ……164

3.4. Results ……166

3.4.1. A. salmonicida bacterin integrity and presence of VapA determination ……166

3.4.2. Survival of vaccinated lumpfish after challenge with A. salmonicida ……..169

3.4.3. IgM titers in immunized lumpfish determined by ELISA ……172

3.4.4. Gene expression analyses reveal the suppression of humoral and cell-mediated immunity of lumpfish ……...……174

3.5. Discussion ……..177

3.6. Conclusions ……..…..181

3.7. References ……..…183

4. Chapter four. Characterization of miRNAs in Embryonic, Larval, and Adult Lumpfish Provides a Reference miRNAome for *Cyclopterus lumpus* …….……...…..199

4.1. Abstract ……..….....199

4.2. Introduction ……200

4.3. Materials and Methods …….....202

4.3.1. Fish holding …….....202

4.3.2. Ethics statement ……..203

4.3.3. Sample collection ……203

4.3.4. RNA extraction ……203

4.3.5. High-throughput sequencing (HTS) …… 205

4.3.6. Analysis of sequencing data ……205

4.3.7. Disclosing putative differentially expressed and/or organ and developmental stage enriched miRNAs ……209

4.3.8. RT-qPCR ……210

4.4. Results ……212

4.4.1. Total RNA extraction, library preparation, and small RNA sequencing ……212

4.4.2. Characterization of lumpfish miRNA ……212

4.4.3. Abundance of miRNAs within organs and developmental stages ……213

4.4.4. Comparison of mature miRNA expression between organs and early developmental stages ……221

4.5. Discussion ……228

4.6. Conclusions ……233

4.7. References ……234

5. Chapter five: Conclusions and prospects ……247

5.1 Findings and future directions ……247

5.2 Conclusions ……256

5.3 References ……258

List of figures

Figure 1.1. Different life stages of *L. salmonis*. ……...……5

Figure 1.2. Lumpfish distribution …….10

Figure 1.3. Lumpfish (*Cyclopterus lumpus*) physical appearance……..……..12

Figure 1.4. *Aeromonas salmonicida* subsp. *salmonicida* infection. …….....……17

Figure 1.5. The immune response following immunization with an antigen. ….……..……21

Figure 2.1. RNA-Seq sample collection and data analysis workflow ……..……60

Figure 2.2. Quality of the RNA samples and sequenced reads. ……...….63

Figure 2.3. *Aeromonas salmonicida* infection kinetics in lumpfish. …….……70

Figure 2.4. Global gene expression profile of different lumpfish organs infected with *A. salmonicida*. ……..74

Figure 2.5. Clusterization of gene expression profile in different lumpfish organs infected *A. salmonicida*. ……..75

Figure 2.6. Clusterization of gene expression profile in different lumpfish organs infected *A. salmonicida*. ……..……...…….76

Figure 2.7. Gene expression profile comparison. …….79

Figure 2.8. Quality of transcriptome assembly. ……...…….84

Figure 2.9. Transcripts expression profile comparison. ……..….87

Figure 2.10. Principal component analysis, correlation analysis, and hierarchical clustering. ……89

Figure 2.11. Comparison of DEGs and DETs identified by reference genome-guided and *de novo* transcriptome assembly. ……..……..….91

Figure 2.12. ClueGO-based enriched gene ontology (GO) terms in lumpfish lymphoid organs at 3 dpi with *A. salmonicida*. ……..…….……93

Figure 2.13. ClueGO-based enriched gene ontology (GO) terms in lumpfish lymphoid organs at 10 dpi with *A. salmonicida*. ……..……..94

Figure 2.14. ClueGO-based enriched gene ontology (GO) terms in lumpfish lymphoid organs. ……96

Figure 2.15. Most significant DEGs (lowest FDR adjusted *p*-value) in all organs studied after *A. salmonicida* infection in lumpfish. …….…….100

Figure 2.16. Most significant DEGs (lowest FDR adjusted *p*-value) in the head kidney after *A. salmonicida* infection in lumpfish. ……..…….102

Figure 2.17. Most significant DEGs (lowest FDR adjusted *p*-value) in the spleen after *A. salmonicida* infection in lumpfish. …….…….103

Figure 2.18. Most significant DEGs (lowest FDR adjusted *p*-value) in the liver after *A. salmonicida* infection in lumpfish. ……..……105

Figure 2.19. Gene expression correlation between RT-qPCR and RNA-Seq data of 14 selected DEGs. ……..……..…..110

Figure 2.20. Gene expression correlation between RT-qPCR and RNA-Seq data of 14 gene expressions. ……..……112

Figure 2.21. *Aeromonas salmonicida* J223 infected lumpfish. ……..…….121

Figure 2.22. *Aeromonas salmonicida* infection model in lumpfish lymphoid organs. ……..……..…..127

Figure 3.1. Experimental workflow. ……...…159

Figure 3.2. One percent agarose gel electrophoresis of RNA samples of control fish (n=3) and A^+W/A^-W bacterin injected fish (n=3). ……...……163

Figure 3.3. *A. salmonicida* bacterin integrity and presence of VapA determination. ……..……..……..168

Figure 3.4. The cumulative survival rate of intraperitoneally (ip) immunized lumpfish after ip challenge with *A. salmonicida* (10^4 CFU/dose). ……..……170

Figure 3.5. Quantification of post-challenge IgM levels is lumpfish by dELISA. ……..……173

Figure 3.6. Expression of transcripts related to cytokines (*il1b, il8a, il8b, il10,*), immunoglobulin (*igm-h1, igm-h2*, and *igm-mu-1*), adaptive immunity markers *mhc-ii*, *cd4*, and *cd8* in lumpfish spleen in response to *A. salmonicida* (A-layer +/-) bacterins at 6 wpi. ……..……175

Figure 4.1. Experimental workflow used for characterization of lumpfish miRNAome…..…..207

Figure 4.2. miRNA diversity in lumpfish tissue/organs, and early developmental stages…….215

Figure 4.3. Twenty most abundant miRNAs in lumpfish brain, muscle, gill, liver, spleen, and head kidney…….……..217

Figure 4.4. Twenty most abundant miRNAs in lumpfish embryos and larvae……...220

Figure 4.5. Verification of tissue-specific expression of conserved miRNAs. ……..226

List of tables

Table 2.1. Quality of the RNA……...61

Table 2.2. Primers used in this study……..…67

Table 2.3. Trimming and mapping statistics…….....72

Table 2.4. Differentially expressed genes (DEGs) identified by reference transcriptome assembly…….78

Table 2.5. Differentially expressed transcripts (DETs) identified by reference transcriptome assembly…….80

Table 2.6. Trinity statistics……..…81

Table 2.7. Alignment statistics……..……82

Table 2.8. Differentially expressed transcripts (DETs) identified by *de novo* transcriptome assembly……...…..85

Table 2.9. Significant differential regulation of adaptive immune marker ($log_2FC \leq -1.0$ or ≥ 1.0, FDR ≤ 0.05) identified from RNA-Seq analysis…….……...…106

Table 3.1. RNA quality……...…162

Table 3.2. Primers used in this study……..164

Table 4.1. Concentration and quality of RNA samples……..204

Table 4.2. Primers used in RT-qPCR analysis of mature miRNAs……211

Table 4.3. Mature miRNAs suggested as highly expressed in one organ compared to others……....221

Table 4.4. Mature miRNAs suggested as highly expressed in embryos or larvae……..223

Abbreviation

ADORA3: Adenosine receptor A3

AEN: Apoptosis-enhancing nuclease

ANOVA: Analysis of variance

APC: Antigen-presenting cells

APR: Acute phase response

BCL-3: B-cell lymphoma 3

BLAST: Basic local alignment search tool

BP: Biological process

BPIFCL: Bactericidal permeability-increasing protein

BUSCO: Benchmarking universal single-copy orthologs

C: Complement component

CC: Cellular component (CC)

CCL19: C-C motif chemokine-like 19

CCL20: C-C motif chemokine-like 20

CD209: Cluster of differentiation 209

CD4: Cluster of differentiation 4

CD74: Cluster of differentiation 74

CD79: Cluster of differentiation 79

CD8: Cluster of differentiation 8

CDRF: Cold-Ocean Deep-Sea Research Facility

CEACAM1: Carcinoembryonic antigen-related cell adhesion molecule 1

CFB: Complement factor B

CFU: Colony-forming units

CLCGWB: CLC Genomics Workbench v20.0

CLRs: C-type lectin receptors

Ct: Fluorescence threshold cycle

CXCR3: Chemokine receptor type 3

DAPI: 4′,6-diamidino-2-phenylindole

DDIT4: DNA damage-inducible transcript 4 protein

DDR: DNA damage response

DEGs: Differentially expressed genes

DETs: Differentially expressed transcripts

DFO: Fisheries and Oceans Canada

DIC: Disseminated intravascular coagulation

DOS: Department of Ocean Sciences

DPI: Days post-infection

DSBs: DNA double-strand breaks

DTAF: 5-([4,6-dichlorotriazinyl] amino) fluorescein hydrochloride)

ECPs: Extracellular products

EF1: Elongation factor 1-alpha

ELISA: Enzyme-linked immune sorbent assay

ERCC-1: DNA excision repair protein

ETF3D: Eukaryotic translation initiation factor 3 subunit D

F3: Coagulation factor IIIa

FAO: Food and Agriculture Organization

FBB: fibrinogen beta chain

FBG: fibrinogen gamma chain

FC: Fold-change

FDR: False discovery rate

GO: Gene ontology

HAMP: Hepcidin antimicrobial peptide

HP: Haptoglobin

HTS: High-throughput sequencing

IgM: Immunoglobulin M

IGP2: ATP-dependent RNA helicase lgp2

IL: Interleukin

IL1R2: Interleukin 1 receptor 2

IROMPs: Iron-regulated outer membrane proteins

IS: Insertion sequences

JBARB: Dr Joe Brown aquatic research building

LD50: Median lethal dose

LFC: Log_2 fold-change

Ln: Logarithm

LPS: Lipopolysaccharide

MF: Molecular function

MHC: Major histocompatibility complex

miRNA: MicroRNA

MUN: Memorial University of Newfoundland

NCBI: National Center for Biotechnology Information

NFIL3: Nuclear factor interleukin-3-regulated protein

NFκB: Nuclear factor kappa-light-chain-enhancer of activated B cells

NK: Natural killer cells

NLRs: NOD-like receptors

NOD1: Nucleotide binding oligomerization domain containing 1

NTS: Non-typhoidal Salmonella

NW: Non-washed

OMPs: Outer membrane proteins

OSC: Ocean Sciences Centre

PABPC1: Polyadenylate-binding protein 1

PAMPs: Pathogen-associated molecular patterns

PARP1: Poly (ADP-ribose) polymerase 1

PBS: phosphate-buffered saline

PCA: Principal component analysis

PIT: Passive integrated transporter

PRR: Pattern recognition receptor

PS: Extracellular polysaccharide

R&D: Research and development

RIN: RNA integrity number

RISC: RNA-induced silencing complex

RNA-Seq: RNA-sequencing

RPL32: Ribosomal protein L32

RPS: Relative percentage survival

RQ: Relative quantity

RSEM: RNA-Seq by expectation maximization

RT-qPCR: Real-time quantitative polymerase chain reaction

SAA5: Serum amyloid A 5

SAPs: Serum amyloid proteins

SD: Standard deviation

SDS-PAGE: Sodium dodecyl-sulfate polyacrylamide gel electrophoresis

SOCS3: Suppressor of cytokine signaling 3

SRA: Sequence read archive

T3SS: Type three secretion system

TLRs: Toll-like receptors

TMM: Trimmed mean of M-values

TNFα: Tumor necrosis factor

TOI: Target of interest

TSA: Trypticase soy agar

TSB: Trypticase soy broth

TUBA1A: Tubulin alpha-1A chain

UV: Ultraviolet

UVC: Ultraviolet-C

WCV: Whole cell vaccine

WPI: Weeks post-immunization

List of Supplementary files

File S2.1. Differentially expressed genes (DEGs) identified by reference genome-guided transcriptome assembly ($log_2FC \geq 1$ or ≤ -1, FDR ≤ 0.05).

File S2.2. Differentially expressed transcripts (DETs) identified by reference genome-guided transcriptome assembly ($log_2FC \geq 1$ or ≤ -1, FDR ≤ 0.05).

File S2.3. Differentially expressed transcripts (DETs) identified by *de novo* transcriptome assembly analysis (log2FC ≥ 1 or ≤ -1, *p* value ≤ 0.05).

File S2.4. BLASTN analysis results.

File S2.5. List of all novel genes identified by *de novo* transcriptome analysis.

File S2.6. Global view of gene ontology enrichment.

File S2.7. Gene ontology enrichment.

File S2.8. Top most significant genes.

File S2.9. Genes associated with enriched pathways of interest.

Supplementary data 1. ClueGOSourceFiles_CyclopterusLumpus.

File S4.1. miRNAs analysed by RT-qPCR.

File S4.2. List id unique mature miRNA.

File S4.3. Mature miRNAs suggested as differentially expressed by DESeq2 analysis when comparing embryos against all others.

Table S4.1. Descriptive data from small RNA sequenced samples in Bioproject PRJNA679415.

Table S4.2. All evolutionarily conserved and novel lumpfish miRNA genes discovered in different organs and developmental stages.

Table S4.3. Normalized read counts of individual mature miRNAs from sequencing data in each sample sequenced.

Table S4.4. Relative distribution of miRNAs within organs and within developmental stages.

1. Chapter one: Introduction

1.1 Global expansion of the aquaculture industry and food security

The present global population is 8.01 billion, and it is increasing by 0.84% annually [1]. The Food and Agriculture Organization (FAO) evaluated that global agricultural production would need to be increased by at least 60% to feed the projected 9.7 billion growing population in 2050 [2]. The rising human population affects food security by overexploiting agricultural land [3]. In addition, overexploitation of ocean fisheries causes fish stocks to decline [4]. Global fish consumption has increased by 3% annually from 1961 to 2019, twice as high as the world population growth [5, 6]. FAO estimated that the proportion of fish stocks within biologically sustainable levels decreased from 90% in 1974 to 64.6% in 2019 [5, 6]. As capture fishery production has been declining since the late 1980s, aquaculture has been responsible for developing seafood supply for human consumption [5, 6]. For example, global fish production reached approximately 178 million tonnes in 2020, of which 87.5 million tonnes came from aquaculture production [6]. Aquaculture is likely the fastest-growing food-producing sector, valued at USD 281 billion in 2020 [4, 6, 7]. Aquaculture generated jobs for 20.5 million people in 2018 [4]. This sector has considerable potential to contribute to the global animal protein demand projected during the next 30 years [5, 6]. Given the worldwide aquaculture sector's contribution to food security and the global economy, the aquaculture sector's sustainable development is a requirement to meet future demand from the world population [8].

1.2 Aquaculture in Canada

Today aquaculture is an established practice in several parts of the world. In Canada, aquaculture was started 50 years ago to enhance natural stocks, and now it has become a large-scale commercial industry [9]. Atlantic Salmon (*Salmo salar*), Chinook salmon (*Oncorhynchus tshawytscha*), coho salmon (*Oncorhynchus kisutch*), Arctic char (*Salvelinus alpinus*), rainbow trout (*Oncorhynchus mykiss*), brown trout (*Salmo trutta*), lake trout (*Salvelinus namaycush*), brook trout (*Salvelinus fontinalis*), Eastern and Pacific oyster (*Crassostrea virginica* and *Crassostrea gigas*), Blue mussel (*Mytilus edulis, Mytilus trossulus)* and Mediterranean mussel (*Mytilus galloprovincialis*), and clam (e.g. *Venerupis philippinarum*) are well-established aquaculture industries in Canada that valued at ~$1.2 billion [10]. The farming of several other species, e.g., sablefish (*Anopoploma fimbria*), tilapia (*Oreochromis niloticus*), halibut (*Hippoglossus hippoglossus*), is at various stages of development, which generates 1.6% (~$22 million) of total Canadian aquaculture value [11, 12].

Today aquaculture in Canada generates $3.86 billion in economic activity and employs over 14,500 Canadians in every province and the Yukon [13]. Aquaculture constitutes about 20% of total seafood production and 33% of Canada's total fisheries value [11]. Over the last ten years, the aquaculture production value has increased by 63% [11]. In 2019 Canada's total aquaculture production was estimated at 187,026 tonnes, valued at 1.2 billion dollars. This production was essentially from offshore farming of Atlantic salmon, representing 118,632 tonnes of volume and 0.91 billion dollars of value [14, 15]. Canada is the fourth-largest farmed salmon producer in the world after Norway, the United Kingdom, and Chile [16]. According to a 2009 study, Canada's farmed salmon industry provides more than 10,000 jobs alone [11]. Atlantic Canadian production occurs mainly on the southern coasts of New Brunswick, Nova Scotia, and the island portion of

Newfoundland and Labrador. Sixty percent of Atlantic Canadian salmon production occurs in New Brunswick's Bay of Fundy region. However, Newfoundland and Labrador, and Nova Scotia are rapidly increasing salmon production. In fact, since 2006, salmonid production (Atlantic salmon and steelhead trout) in Newfoundland and Labrador has increased by 195% in volume (Statistics Canada, 2010) [17].

1.3 Sea-lice: one of the most significant challenges in salmon aquaculture

Diseases are a fundamental challenge in aquaculture. Globally industry-wide losses due to diseases exceed US$6 billion annually, while in Canada, annual losses due to infectious diseases caused by viruses, bacteria, and parasites in the salmon industry can be approximately $90 million [18, 19]. One of the most prominent disease challenges currently restraining the global Atlantic salmon aquaculture is infestation by caligid sea-lice, specifically *Lepeophtheirus salmonis* and *Caligus spp* [20-24]. Sea-lice are naturally abundant in the marine environment. They are reported in Canadian salmon farms during autumn while adult wild salmon return to their spawning grounds carrying high sea-lice numbers and infesting farmed salmon [25].

Sea-lice are a group of grossly visible host-dependent copepod ectoparasites with vast reproductive potential [20-24]. The *caligidae* family of copepod ectoparasites comprises 30 genera and 509 valid species [26]. Among them, *Lepeophtheirus* and *Caligus*, collectively known as sea-lice, are causing the most significant economic impact of any group of parasites in salmonid fish culture; in particular, the species *Lepeophtheirus salmonis* (Krøyer, 1837) is the most notorious one [27]. The salmon louse, *L. salmonis*, is a parasite of salmonids in the *Salmo*, *Oncorhynchus*, and *Salvelinus* genera with a circumpolar distribution in the Northern Hemisphere [27, 28].

Different life stages of *L. salmonis* are nauplii, copepodites, chalimi, pre-adults, and adults. Nauplii are non-infectious, free-swimming, and non-feeding planktonic larvae. The infectious

larval copepodite starts to search for hosts to attach to survive and remain embedded on the host skin. The immature chalimus feeding is restricted to the host skin around the attachment point until they turn into mobile pre-adults and adults that move freely over the host skin (Figure 1.1) [28]. The attached sea-lice feed on salmon mucus, blood, and skin, which leads to significant physical and biochemical damage, including skin lesions, loss of protective skin function, secondary infections due to immunosuppression, and osmoregulatory failure. Additionally, it causes chronic stress to the fish and reduces fish growth and appetite [20, 24, 28-30].

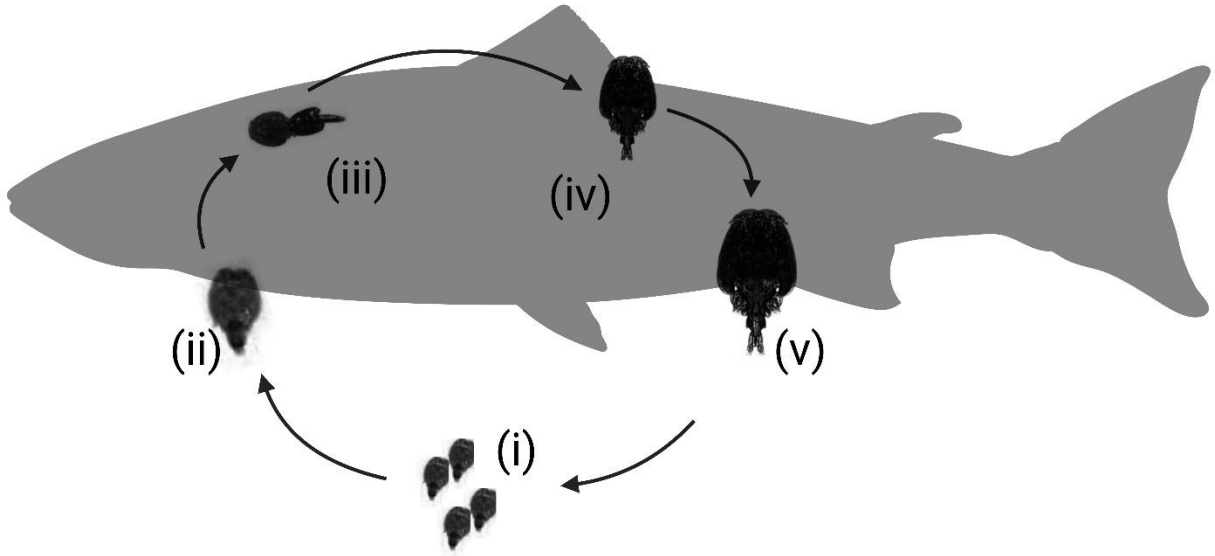

Figure 1.1. Different life stages of *L. salmonis*. (i) nauplii, (ii) copepodites, (iii) chalimi, (iv) pre-adults, and (v) adults on salmon skin. Figure 1.1 was created with BioRender.com.

Besides biochemical and physical damages, there are significant economic impacts due to production losses and treatment costs [20, 29]. The global economic impact of sea-lice was estimated at US$807 million in 2015, with costs likely to rise since then [20]. A survey in Norway shows that the percent of total biomass growth lost per production cycle due to average sea-lice infestations varies from 3.62 to 16.55%, despite control, and depends on farm location, which generates damages of US$0.46 per kg of harvested biomass, equivalent to 9% of farm revenues [31].

Fisheries and Oceans Canada (DFO) and coastal provincial governments take regulatory measures to control sea-lice levels on salmon farms. Typically, in Canada, sea-lice are controlled through early harvesting, in-feed medications, and topical pesticides. The development of alternate methods for managing sea-lice is also being encouraged through integrated pest-management strategies and investment in research [32].

1.4 Sea-lice control in salmon aquaculture

The salmon aquaculture industry has been dealing with sea-lice infestations since its origin [33]. Several preventative and control methods have been implemented to minimize sea-lice prevalence and reduce their impact on both farmed and wild fish. Such methods are categorized into physical, chemical, and biological methods [34].

1.4.1 Physical methods

Additions of filtration and sieving devices (e.g., plankton nets or tarpaulin skirts) around salmon cages can reduce sea-lice infestation [35]. Closed cages can reduce the abundance of sea-lice reproduction within the cages without adversely affecting fish survival or growth rates [36]. Another option is snorkel sea cages, which allow salmon to access the surface via an enclosed tube, impervious to sea-lice larvae. Snorkel sea cages can prevent an effective sea-lice infestation

on farmed salmon with little or no, adverse effects on fish growth [37, 38]. However, snorkel sea cages may affect salmon behavior, which must be considered in welfare assessments of their use. The placement of conducting cables around the cages can inactivate sea-lice and reduce infection rates by using electric pulses [34]**.**

Study shows that culturing Atlantic salmon under natural light and at 4 to 12 m deep in the water column, especially in areas where salinity is lower at the water surface, significantly reduces sea-lice infestation [39]. Also, irradiation by ultraviolet-C (UVC) light is found to be highly effective at suppressing lice reproduction; however, UVC exposure leads to cataract-like pathologies at an early age, skin damage, and behaviors indicating discomfort [40]. Furthermore, sea-lice removal technologies using brushes or water jets (e.g., hydrolicer), novel bath treatments using warm water (thermolicer) or freshwater, and air-desiccation can control sea-lice infestation [20, 29].

1.4.2 Chemical treatments

Traditionally, the salmon aquaculture industry has relied heavily upon parasiticides either as bath treatments (e.g., azamethiphos, cypermethrin, deltamethrin, hydrogen peroxide, organophosphates) or feed (e.g., emamectin benzoate, teflubenzuron) [41, 42]. Three commercial products are currently approved against sea-lice in Canada: (a). Slice® (Merck Animal Health), which contains emamectin benzoate and is used as an in-feed parasiticide, (b) Interox® Paramove® 50 (Solvay Interox Pty Ltd.), which contains hydrogen peroxide and is applied as a bath treatment, (c) Calicide® (Nutreco), which has tebflubenzuron and delivered in feed [34]. However, the continuous and frequent use of chemical parasiticides can lead to genetic mutation of sea-lice [43, 44] and resistance to chemotherapeutic [29, 42, 45, 46]. Sea-lice resistance to emamectin benzoate, hydrogen peroxide, azamethiphos, pyrethroids, deltamethrin, and

cypermethrin has been reported several times; however, the mechanism of resistance is not fully elucidated yet [41, 42, 47-63].

1.4.3 Biological methods

Biological methods include selective breeding [64], vaccination [65, 66], and the use of cleaner fish [20, 35, 67-69]. Selective breeding for disease resistance is a long-established practice; however, it is still in the exploration phase for sea-lice [70-73]. Identifying the lice-resistant individuals and the genes involved in the host response to infection can improve the control strategies. Developing a vaccine against sea-lice remains elusive [35, 74, 75]. Another biological pest control strategy is using cleaner fish [20]. The most used cleaner fish for controlling sea-lice in salmon farms in the northern hemisphere are European wrasse (*Labridae*), such as ballan (*Labrus bergylta* A.), corkwing (*Symphodus melops* L.), goldsinny (*Ctenolabrus rupestris* L.) wrasses and lumpfish (*Cyclopterus lumpus*). Ballan wrasse, widespread in Scotland and Norway, is not a native species in Canada. Instead, a different wild-caught wrasse, cunner (*Tautogolabrus adspersus*), has been used in Atlantic Canada. However, wrasse is an efficient cleaner fish but tends to become inactive in winter [69]. On the other hand, lumpfish continue to feed on sea-lice, both *L. salmonis* and *C. elongatus*, at low temperatures, indicating that lumpfish is a suitable cold-water option for the biological delousing of Atlantic salmon [35, 67, 68, 76, 77].

1.5 Lumpfish

1.5.1 Taxonomy and distribution

The lumpfish was first named and characterized by Linnaeus in 1758 [78]. It is a bony fish (class: Osteichthyes, infraclass: Teleostei) belonging to the Order Scorpaeniformes, family *Cyclopteridae*, and genus *Cyclopterus* [78].

Lumpfish occur naturally in the North Atlantic and southern parts of the Arctic Ocean (Figure 1.2), and it populates bays and channels and extends off the coasts of Iceland, Norway, Canada, Scotland, Ireland, and Portugal [79-89]. Adult lumpfish spend most of the year far from the shore, up to several hundred meters deep; however, adult fish and juvenile breeding occur in shallow coastal water [81].

Figure 1.2. Lumpfish distribution. Lumpfish can be found in the North Atlantic and southern parts of the Arctic Ocean, including, coasts of Iceland, Norway, Canada, Scotland, Ireland, and Portugal

1.5.2 Physical and genetic characteristics

A short, swollen, and tadpole-like body with a cartilaginous and gelatinous humpback characterizes lumpfish. The ventral fins unite into a sucking disk that is attached to floating objects (Figure 1.3). It cannot swim well and prefers to adhere to a flat and smooth substrate, like plastic, or stick with stone or floating seaweed [90]. The lumpfish has 25 diploid chromosomes (2n) [91, 92]. There are three genetically distinct populations of lumpfish in the North Atlantic, Maine–Canada–Greenland (Northwest), Iceland–Norway (Northeast), and the Baltic Sea [84].

Figure 1.3. **Lumpfish (*Cyclopterus lumpus*) physical appearance.** A short, swollen, and tadpole-like body with a cartilaginous and gelatinous humpback together with the ventral fins unite into a sucking disk.

1.5.3 Feeding and reproduction

Juvenile lumpfish are used to feed on a wide range of near-surface plankton. Adult lumpfish feed on euphausiids, pelagic amphipods, jellyfish, and small fish such as herring and sand lance [80, 81].

Lumpfish spawning occurs on the rocky sea substrate on both sides of the North Atlantic [82, 93-95]. Lumpfish exhibit a sexual dimorphism while breeding [81, 82]. They have an extended courtship involving nest cleaning, fin brushing, and quivering [81, 82]. Each female lumpfish produces an average of 1000,000 eggs per spawning season, depending on body size. Males fertilize pink eggs onto the nest's surface, mold the eggs into the nest, produce funnel-like depressions in the egg mass, remain there throughout the incubation period, and defend the egg mass against invertebrate predators [81, 82].

1.5.4 Production

The number of cleaner fish used by the salmon farming industry has increased exponentially since 2008 [69, 96]. Commercial production of lumpfish juveniles is ongoing in Norway, and it is an emergent species in the aquaculture industry in Atlantic Canada. Marbase Marystown Inc. is North America's first lumpfish hatchery in Newfoundland and Labrador, Canada. Together with that, the Ocean Sciences Centre (OSC) of the Memorial University of Newfoundland (MUN) is home to Canada's leading cleaner fish research and development (R&D) facility. Lumpfish production and genomic research are ongoing in these facilities [97]. Extensive commercial lumpfish aquaculture will help to alleviate economic, environmental, and ethical concerns [69, 98]. Primarily, commercial lumpfish production relies on the capture of wild broodstock, which is unsustainable, because, in recent decades, a significant decrease in lumpfish spawning stocks in the North Atlantic region suggests the overexploitation of natural stock [69,

84]. Therefore, lumpfish must be reared in captivity to supply the salmon farming industry with the number of lumpfish required for sea-lice control.

1.5.5 Research on lumpfish diseases, immunity against infections, and vaccinology

The cultivation of lumpfish is a relatively novel aquaculture. However, diseases caused by various pathogens preclude this industry's development. The knowledge of lumpfish diseases has increased in recent years, alongside research into its immune system that may foster vaccine development against different pathogens [99, 100].

Recent studies have revealed that lumpfish have a similar innate immune response to other teleosts; for instance, macrophages display phagocytosis and respiratory burst [101], and IgM^+ B-cells have phagocytic activity [102]. Antimicrobial peptides and proteins involved in complement activation, inflammation, and pathogen lysis have been identified by proteomic analysis of lumpfish skin mucus [103]. Lumpfish interleukin (IL) 1 (IL-1) signaling pathways, four ligands of the IL-1 family in lumpfish (i.e., IL-1β type I and type II, IL-18, and the novel IL-1 family members (nIL-1F)), tumor necrosis factor-alpha (TNF-α) and IL-6 were identified and characterized at mRNA and gene levels [104, 105]. Transcriptomics analysis of lumpfish primary macrophages infected with bacterial pathogen revealed the upregulation of genes encoding proteins involved in cell signaling, cytokines, pathogen recognition components, including 13 toll-like receptors (TLRs), nucleotide binding oligomerization domain containing 1 (NOD1), nucleotide binding oligomerization domain containing 2 (NOD2), IL-1β, IL-8, IL-6, TNFα, IL-17A/F3, IL-17C, and several components of the complement system [106]. *Renibacterium salmoninarum* infection in lumpfish showed upregulation of genes encoding cytokines (*interleukin 1 beta (il1β), interleukin 8a (il8a), interleukin 8b (il8b)*), pattern recognition receptor (*toll-like receptor 5* (*tlr5a*), interferon-induced effectors (*radical S-adenosyl methionine domain-containing*

protein 2/viperin (*rsad2)* and three gene isoforms of *interferon-induced GTP-binding protein* (*mxa, mxb, mxc*)), and acute phase reactants (*hepcidin antimicrobial peptide* (*hamp), serum amyloid A 5* (*saa5*)) at 28 days post-infection (dpi) [107]. In contrast, cell-mediated adaptive immunity-related genes (*T-cell surface glycoprotein CD4a* (*cd4a), T-cell surface glycoprotein CD4b* (*cd4b), lymphocyte antigen 6 complex locus protein G6f (ly6g6f), T-cell surface glycoprotein CD8 alpha chain (cd8α), HLA class II histocompatibility antigen gamma chain* (*cd74*)) were downregulated at 28 dpi, but *cd74* was significantly upregulated at 98 dpi [107]. Vaccination studies in lumpfish indicate the total levels of Immunoglobulin M (IgM) in sera are lower than in salmon, but lumpfish produce specific antibodies upon immunization and can mount protective adaptive immune response [108-110]. Real-time quantitative polymerase chain reaction (RT-qPCR) analyses showed that the oral immunization of lumpfish larvae resulted in a subtle stimulation of canonical immune transcripts such as *il8b, interleukin 10* (*il10), immunoglobulin heavy chain variable region a* (*igha), immunoglobulin mu heavy chain a (ighma), immunoglobulin mu heavy chain b (ighmb), C-C motif chemokine-like 19* (*ccl19), C-C motif chemokine-like 20* (*ccl20), cd8a, cd74,* and *ATP-dependent RNA helicase lgp2* (*lgp2)* [109].

On the other hand, there is growing interest in identifying major pathogens infecting lumpfish in Atlantic Canada [111]. Bacterial infections are among the significant factors contributing to reduced production and profits [112]. Several studies identify bacterial pathogens in lumpfish, including *Pseudomonas anguilliseptica*, *Vibrio anguillarum*, *Pasteurella sp.*, *Piscirickettsia salmonis*, and *Aeromonas salmonicida* [110, 113-116]. Typical and atypical *A. salmonicida* outbreaks in farmed salmon and lumpfish have been reported in the UK, Norway, and Canada [20, 69, 100, 113, 117-119]. Still, there is no successful vaccine against some *A.*

salmonicida strains in lumpfish. Antibacterial treatments against *A. salmonicida* are also unsuccessful in lumpfish [120].

1.6 Aeromonas salmonicida subsp. salmonicida

Isolates with different phenotypic characteristics have been classified into typical and atypical groups [121]. The typical strains correspond to *A. salmonicida* subsp. *salmonicida,* and the atypical correspond to *A. salmonicida* subsp. *achromogenes, masoucida, smithia,* and *pectinolytica* [121]. *A. salmonicida* subsp. *salmonicida* is one of the oldest known fish pathogens, endemic worldwide in both fresh and marine water in a broad host range [121-124]. This Gram-negative, non-motile, rod-shaped, facultative intracellular, and gamma proteobacterium is the etiologic agent of furunculosis (Figure 1.4A). Furunculosis is a systemic disease of salmonids characterized by high mortality and morbidity in the aquatic production system, which produces hemorrhagic and necrotic lesions in the skin and gut (Figure 1.4B-D) [124-129]. *A. salmonicida* is well equipped to resist the host defense ways. It can enter the fish through skin, gills, and gastrointestinal tract by removing mucus [121, 130]. Many virulence factors (e.g., structural components like flagella, fimbriae, lipopolysaccharide (LPS), and outer membrane proteins (OMPs)), affect the intestinal barrier function in fish and facilitate translocation by increasing receptor-mediated endocytosis and paracellular permeability [121, 130].

A. salmonicida Type I pilus system contributes to host tissue colonization [131]. Also, the VapA layer in the outer membrane of *A. Salmonicida,* along with LPS, assists in adhering and spreading throughout the host tissues (Figure 1.4E) [121, 128, 132]. Using the type three secretion system (T3SS), *A. salmonicida* secrete toxins and effector proteins (e.g. AexT, Ati2, AopH, AopO, AopN, AopP, and AopS) into the host cell cytoplasm, suppress host immunity mechanisms, and induces apoptosis (Figure 1.4E) [121, 128]. Additionally, extracellular products, such as haemolysins, lipases and proteases, iron acquisition systems and quorum sensing (QS) communication contribute to the host pathogenicity [121].

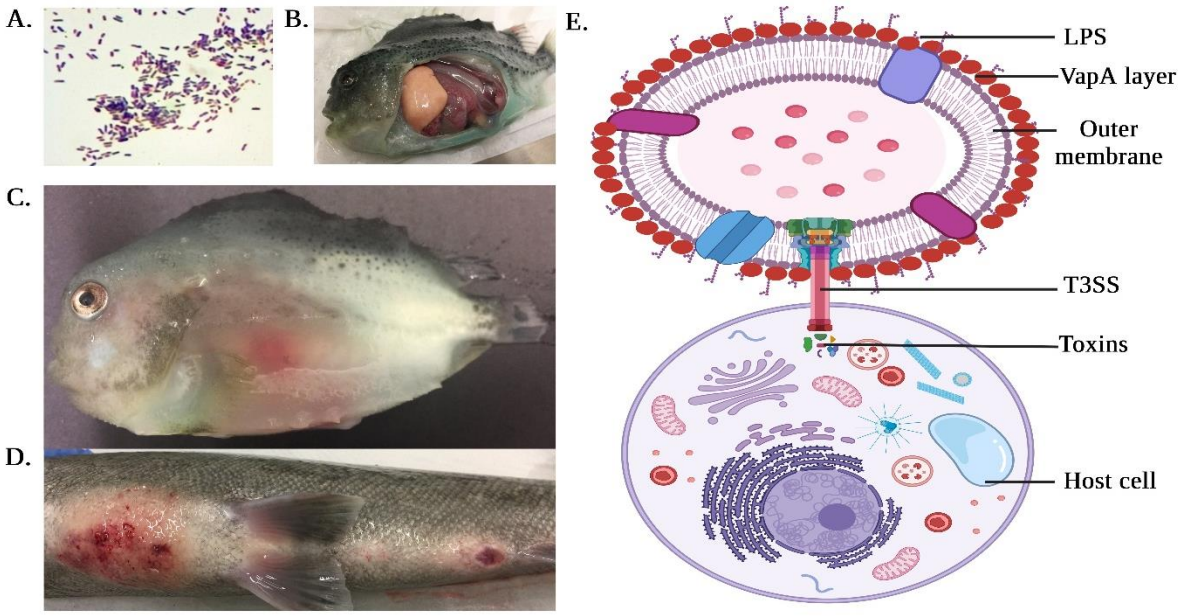

Figure 1.4. *Aeromonas salmonicida* subsp. *salmonicida* infection. A. Gram staining of *A. salmonicida* subspecies *salmonicida*; B-C. *A. salmonicida* subspecies *salmonicida* infection in lumpfish shows internal organ haemorrhage; D. *A. salmonicida* subspecies *salmonicida* infection in Atlantic salmon develops furuncles on skin; E. A model of *A. salmonicida* attachment to the host cell and secretion of toxins in the host cell cytoplasm. It shows that the VapA layer in the outer membrane of *A. salmonicida*, along with lipopolysaccharide (LPS), assists in adhering and spreading throughout the host tissues. Using the type three secretion system (T3SS), *A. salmonicida* secrete toxins into the host cell cytoplasm. Figure 1.4A-D are original pictures that were taken while conducting the experimental work for this thesis. Figure 1.4E was created with BioRender.com, while the concept was adopted from Origgi et al. 2016 [133].

1.7 Host-pathogen interactions

Properly understanding bacterial pathogens and the host's resulting disease state is key to developing effective vaccines for several terrestrial pathogens. Teleostei, the most diverse infraclass within the class Actinopterygii, comprises ~ 70 orders, ~ 500 families, and ~ 30,000 species (i.e., approximately half of all extant vertebrate species) [134]. The immune system's composition and response of teleosts toward a pathogen could be various. For example, most studied fish have genes for both major histocompatibility complex I (MHCI) and MHCII molecules, but the Atlantic cod (*Gadus morhua*) has lost the genes for MHCII and its accessory molecules [135]. Instead, cod has expanded the number of MHCI genes and a unique composition of its Toll-like receptor (TLR) families to compensate for adaptive and innate immunity without MHCII [135].

Similarly, bacterial pathogens are diverse and respond differently to different fish hosts. For example, the genome-based analysis revealed that *A. salmonicida* isolates from different geographical origins are diverse [136, 137]. A total of 109 genome sequences of *A. salmonicida* in the GenBank database revealed that the number and size of plasmids are very diverse among different isolates [137, 138]. Even if the plasmids are stable, the repertoire may change [137]. Furthermore, genome analysis showed that strains with high chromosome sequence similarity have substantial differences in structure [139]. Genetic diversity influences the outcome of host-pathogen interactions [140]. Host-pathogen interactions are essential to understand infectious diseases, as well as their prevention and treatment [141, 142]. Therefore, elucidating the interspecies differences and host-pathogen interactions will help increase the efficacy of future therapies and vaccine initiatives.

Transcriptomics analysis using different laboratory techniques (e.g., RNA-Sequencing) is one of the methods to examine host-pathogen interactions that simultaneously measure the expression of thousands of genes, demonstrating differences in the transcriptome in response to an infection [143]. On the other hand, different post-transcriptional factors, including small non-coding RNAs, play an important role in determining an organism's disease state by regulating gene expression related to many cellular functions. MicroRNAs (miRNAs) are a major class of small non-coding RNAs that function as guide molecules in RNA silencing by negatively regulating gene expression at the messenger RNA (mRNA) level or by promoting a large proportion of cellular mRNA degradation [144-152]. They are a large family of post-transcriptional regulators that are ~22 nucleotides long and found in animals, plants, and some viruses [150, 152]. Functional studies indicate that miRNAs have unique, diverse expression patterns and regulate almost every cellular process in animals, including developmental, physiological, and pathophysiological processes in living organisms [144-152]. Additionally, miRNAs are connected to many diseases, and miRNA-mediated clinical trials have shown promising results for treating such diseases, including viral and bacterial infections [145, 146, 152]. Researchers use state-of-the-art tools, such as high-throughput sequencing (HTS), to characterize the miRNAome repertoire, understand the host immune strategies activated against the pathogen, and how the pathogen overcomes host-mediated immune responses directed against it [153]. Such information could help to develop vaccine therapeutics against the pathogen [145, 146, 152].

1.8 Vaccinology

The concept of fish vaccination was first published in the period 1935–1938, when the immune mechanisms behind protective immunization were mostly unknown [154]. In 1938 Snieszko et al. showed that fish build up protective immunity after injecting with killed bacteria.

Subsequently, his group developed commercial fish vaccination methods, which were employed successfully in carp culture in central Europe [154]. Duff published the first oral immunization of fish in 1942, where chloroform-killed *Bacterium* (*Aeromonas*) *salmonicida* induced protection to cutthroat trout (*Oncorhynchus clarkii*) against furunculosis after an injection challenge [154, 155]. After then, there were not many reports about vaccination in aquaculture for several years because of the disinterest in immunoprophylaxis due to the availability of antimicrobial compounds [156]. The first vaccine for fish was licensed in the USA in 1976 for aquaculture [156]. Since then, the use of vaccines has expanded along with the growth of the aquaculture industry. For example, furunculosis has been controlled by the use of protective vaccines containing formalin-inactivated *A. salmonicida* bacterins in Atlantic salmon, rainbow trout, and Arctic char [157-164].

Vaccination is the most critical measure to prevent bacterial infection in aquaculture [165]. The vaccine contains a non-virulent, innocuous form of the given pathogen, which can initiate the innate immune response that shapes memory adaptive immune responses (Figure 1.5) [166]. The principle of vaccination is immune memory, where a subsequent exposure to a pathogen induces an enhanced immune response against the previously encountered pathogen [167].

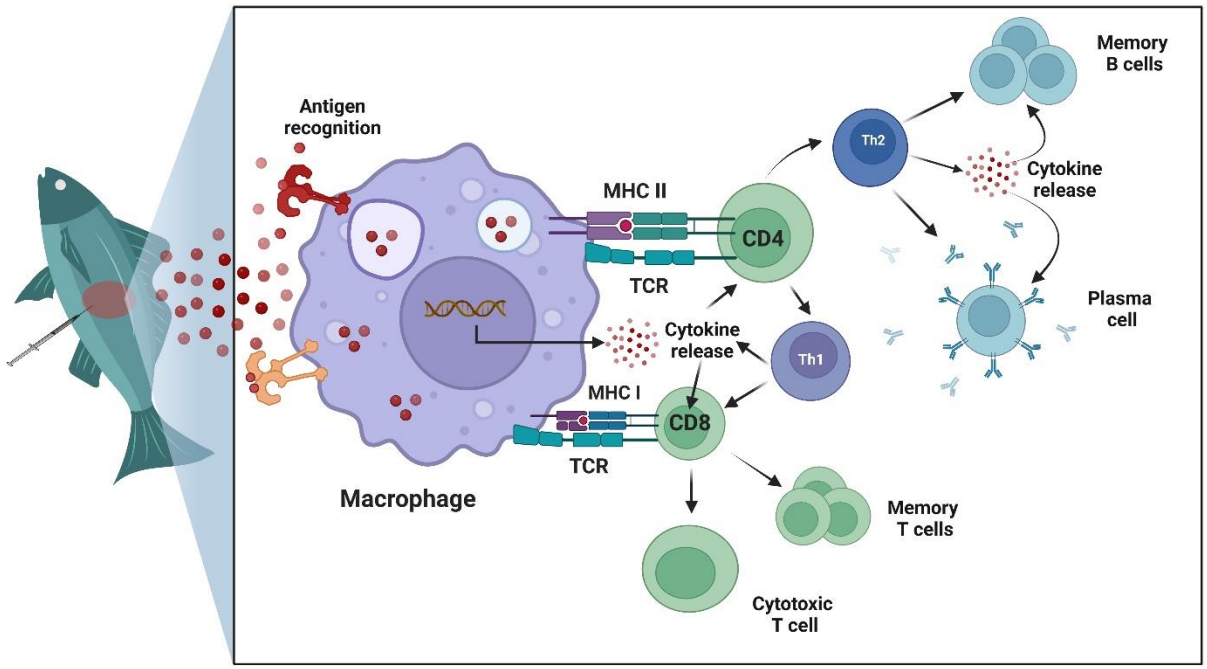

Figure 1.5. **The immune response following immunization with an antigen.** The vaccine is injected into fish and the antigen is taken up by antigen-presenting cells (APC, e.*g.*, macrophages). The presentation of the vaccine antigen by MHC molecules on the cell surface activates T cells through the T cell receptor (TCR). The T cells drive B cell activation, which results in the production of short-lived plasma cells that actively secrete antibodies specific for the vaccine antigen and long-lived memory B cells that mediate immune memory. Furthermore, activated T cells are $CD8^+$ (cluster of differentiation 8/ T cell transmembrane glycoprotein) memory T cells that can proliferate rapidly when they encounter a pathogen and $CD8^+$ cytotoxic T cells that can kill infected cells. The figure was created with BioRender.com. The concept was adopted from Bedekar 2022 [168].

There are numerous innate immune cells in fish. Among them, macrophages are considered as the principal phagocytic cells contributing to innate immune defenses [169]. Functionally, macrophages are equipped with many pattern recognition receptors (PRRs) (e.g., TLRs, C-type lectin receptors (CLRs), NOD-like receptors (NLRs)) that detect a multitude of pathogen-associated molecular patterns (PAMPs) and initiate phagocytosis of the foreign entity [170]. At least 20 different TLRs have been identified in fish species [171, 172]. However, TLRs that bind and recognize PAMPs derived from bacteria are TLR2 (peptidoglycan, lipoteichoic acid), TLR5 (flagellin), TLR9, and TLR21 (CpG DNA) [173-181]. Subsequent PRRs binding to PAMPs initiates a signaling cascade that stimulates transcription factors (such as nuclear factor kappa-light-chain-enhancer of activated B cells (NFκB)), leading to the inflammatory response by upregulating genes involved in cytokine synthesis [182]. Furthermore, macrophages present antigens by MHC molecules to circulating lymphocytes in the blood and spleen that initiates the adaptive immune system, capable of initiating protective memory immune responses against foreign particles [183]. T and B lymphocytes can detect those antigens with TCR or B cell receptor (BCR), respectively. A series of DNA recombination events in the gene segments encoding these receptors provides an immense phenotypic diversity to recognize a wide array of antigenic epitopes [184]. Activated $CD4^+$ (cluster of differentiation 4/ T cell surface glycoprotein) T cells and $CD8^+$ (cluster of differentiation 8/ T cell transmembrane glycoprotein) T cells can produce cytokines and cytotoxic proteins to direct immune responses [185]. On the other hand, activated B cells will transform into plasma cells to secrete antigen-specific antibodies [186]. Antibody development and production are critical when dealing with most bacterial pathogens because it prevents bacterial pathogen's growth and colonization by complement activation, neutralization, and/or opsonization to enhance phagocytosis [187]. Furthermore, the production of memory B cells and

$CD8^+$ memory T cells trigger more robust and efficient immune protection once they encounter a pathogen. The requirement to consistently stimulate immunological memory/protection is mandatory to design an effective vaccine for aquaculture production [188].

Vaccinated fish are less at risk of contracting infections than unvaccinated fish [167, 189, 190]. The choice of vaccine type and delivery method depends on several factors that include vaccine safety, production costs relative to what the farmer can justify compared with the value of the fish, efficacy, and type of immune response induced close to what is needed to obtain protection [167, 189, 190]. Vaccines for fish are usually inactivated whole-cell vaccines (WCV), subunit vaccines, and live attenuated vaccines [188]. However, the duration of immunity for inactivated vaccines is short unless formulated for antigen retention at the injection site, requiring adjuvants to form a depot at the injection site [167, 189, 190]. The addition of an adjuvant will result in the antigen's retention for a prolonged period and a slow antigen release [167, 189, 190]. Adjuvants are compounds used in vaccine preparation that increase vaccine efficacy by promoting APC maturation or retaining antigens within tissues without compromising the resulting immune response [167, 189, 190]. A vaccine containing purified antigens alone could produce a minor antibody response with little to no T cell activation [189, 190].

However, not all formulations confer immunological memory. Antigens prepared for vaccination or the pathogen could trigger adaptive immune suppression, hindering protective disease control measures [191-193]. For example, vaccination against *Salmonella* is challenging because non-typhoidal *Salmonella* (NTS) targets and suppresses B cell lymphopoiesis and activation and IgG-secreting plasma cells against NTS [191]. Intraperitoneal injection (ip) of inactivated phase I *Coxiella burnetii* WCV into mice resulted in marked and persistent suppression of the proliferative response of spleen cells [192]. A vaccine formulation based on bacterial surface

antigens was unsuccessful against ulcerative *A. salmonicida* in carp (*Cyprinus carpio*) because the pathogenesis was characterized by a state of immune suppression [193].

Disease control or elimination requires the induction of protective immunity in a sufficient proportion of the population [194]. This is best achieved by immunization programs capable of inducing long-term protection, a hallmark of adaptive immunity by maintaining antigen-specific immune effectors and/or by the induction of immune memory cells that may be sufficiently efficient and rapidly reactivated into immune effectors in case of pathogen exposure [195].

1.9 Major gaps in knowledge

Cleaner fish farming is still in its infancy. Still, many aspects of lumpfish biology and their immune functions remain unknown or poorly described. Health management is a critical priority as disease outbreaks throughout all life stages are responsible for significant losses in the aquaculture industry. Research is required to characterize immune function in these species, host-pathogen interaction, and develop vaccines against the most virulent bacteria (e.g., *A. salmonicida*). Furthermore, before the current research, there was no report regarding lumpfish small RNAs, e.g., miRNA repertoire. The characterization of lumpfish small RNA is essential for future functional studies.

1.10 Main objectives and thesis structure

Drawing from some of the main knowledge gaps, the present work explores: the pathogenicity of *A. salmonicida* in lumpfish; strategies to develop a vaccine for lumpfish with a comparison to current industrial methods; the reason for vaccine ineffectiveness; and provides a reference miRNAome for lumpfish by characterizing the miRNAs of embryonic, larval, and adult lumpfish for future functional studies.

To explore the pathogenicity of *A. salmonicida* in lumpfish, in chapter 2, I characterized the kinetics of *A. salmonicida* subsp. *salmonicida* J223 (lab collection) infection in juvenile lumpfish. Here, I profiled the transcriptome of the main lymphoid organs, including head kidney, spleen, and liver, at 3 and 10 days post-infection (dpi). The main objectives of this chapter were the determination of lethal dose 50 (LD_{50}) of *A. salmonicida* J223 in lumpfish and lumpfish transcriptome response to the *A. salmonicida* early and lethal infection. High-throughput RNA-Seq data of three lymphoid organs, head kidney, spleen, and liver, were assembled through the *de novo* transcriptome assembler and reference genome-guided transcriptome assembler to reveal organ-specific response to the infection.

In chapter 3, I primarily aimed to develop a vaccine for lumpfish against *A. salmonicida* subsp. *salmonicida*. For this purpose, I evaluated the immune protective effect of *A. salmonicida* outer membrane proteins (OMPs) and bacterins in lumpfish with and without the Vap A layer (A^+/A^-). The finding of the primary investigation leads to the hypothesis that the inactivated *A. salmonicida* J223 does not trigger memory immune responses and confer protection to lumpfish. To further investigate, I tested the biomarkers for adaptive immune responses by enzyme-linked immune sorbent assay (ELISA) and RT-qPCR analyses.

In chapter 4, I aimed to identify and characterize miRNA genes in lumpfish by HTS analysis, followed by the miRDeep analysis of different lumpfish sample types (i.e., adult lumpfish brain, muscle, gill, liver, spleen, and head kidney, as well as the early developmental stages of embryos and larvae). This chapter's main objectives were to provide the first reference miRNAome in lumpfish and identify the organ-specific expression of some miRNAs.

Finally, in Chapter 5, I summarized the research findings and highlighted the main conclusions, indicating how they may improve our understanding of *A. salmonicida* pathogenicity

and vaccine development in lumpfish with aquaculture applications. It also provides directions for future research in these areas.

1.11 Publications arising from this thesis

The results presented in this thesis have been published as follows:

a) Chakraborty S, Hossain A, Cao T, Gnanagobal H, Segovia C, Hill S, Monk J, Porter J, Boyce D, Hall JR, Bindea G, Kumar S, Santander J. Multi-organ transcriptome response of lumpfish (*Cyclopterus lumpus*) to *Aeromonas salmonicida* subspecies *salmonicida* systemic Infection. Microorganisms. 2022;10(11):2113.

   Author contributions: Conceptualization: Javier Santander (JS), Setu Chakraborty (SC); Methodology: JS, SC, Ahmed Hossain (AH), Trung Cao (TC), Hajarooba Gnanagobal (HG), Jennifer Hall (JH), Surendra Kumar (SK), Cristopher Segovia (CS), Dany Boyce (DB), Gabriel Bindea (GB); Investigation: SC, AH, TC, HG, JH, SK, CS, DB, JS; Writing original draft: SC, SK, JH, JS; Resources: JS, DB; Writing - Review & Editing: HG, TC, AH, MD, JH, SK, CS, DB, JS; Visualization: JS, SC, SK, CS, GB; Supervision: JS; Funding acquisition: JS, DB.

b) Chakraborty S, Gnanagobal H, Hossain A, Cao T, Vasquez I, Boyce D, Santander J. Inactivated *Aeromonas slmonicida* suppresses the humoral and cell-mediated immunity of lumpfish (*Cyclopterus lumpus*). Frontiers in Veterinary Science (submitted).

   Author contributions: Conceptualization: JS, SC; Methodology: JS, SC, HG, AH, TC, Ignacio Vasquez (IV), DB; Investigation: SC, HG, AH, TC, IV, DB, JS; Writing original-draft: SC; Resources: JS, DB; Writing - Review & Editing: HG, AH, TC, IV, DB, JS; Visualization: SC; Supervision: JS; Funding acquisition: JS, DB.

c) Chakraborty S, Woldemariam NT, Visnovska T, Rise ML, Boyce D, Santander J, Andreassen R. Characterization of miRNAs in embryonic, larval, and adult lumpfish provides a reference miRNAome for *Cyclopterus lumpus*. Biology (Basel). 2022;11(1):130.

Author contributions: Conceptualization: Rune Andreassen (RA), JS, Matthew L. Rise (MR), SC; Methodology: RA, JS, SC, Nardos Tesfaye Woldemariam (NW), Tina Visnovska (TV), DB; Investigation: RA, JS, SC, NW, TV; Writing original-draft: SC, RA; Resources: RA, JS, DB; Writing - Review & Editing: RA, JS, MR, SC, NW, TV; Visualization: SC; Supervision: RA, JS; Funding acquisition: RA, JS, DB.

1.12 References

1. Worldometer. https://www.worldometers.info/world-population/.
2. FAO. The future of food and agriculture: Trends and challenges. 2017. https://www.fao.org/3/i6583e/i6583e.pdf
3. Gupta GS. Land degradation and challenges of food security. Review of European Studies. 2019;11(1).
4. FAO. The State of World Fisheries and Aquaculture 2020. 2020. https://www.fao.org/3/ca9229en/ca9229en.pdf.
5. FAO. The State of World Fisheries and Aquaculture 2018. 2018. https://www.fao.org/3/i9540en/i9540en.pdf.
6. FAO. The State of World Fisheries and Aquaculture 2022. 2022. https://www.fao.org/publications/home/fao-flagship-publications/the-state-of-world-fisheries-and-aquaculture/en.
7. DFO. Aquaculture collaboration. 2019. https://www.dfompo.gc.ca/aquaculture/collaboration-eng.html.
8. Nadarajah S, Flaaten O. Global aquaculture growth and institutional quality. Marine Policy. 2017;84:142-51.
9. DFO. Aquaculture. 2021. https://www.dfo-mpo.gc.ca/stats/aquaculture-eng.htm.
10. DFO. Aquaculture: Farmed species profiles. 2021. https://www.dfompo.gc.ca/aquaculture/sector-secteur/species-especes/index-eng.htm.
11. DFO. Aquaculture statistics. 2013. https://www.dfo-mpo.gc.ca/aquaculture/sector-secteur/stats-eng.htm.
12. CAIA. Aquaculture species index. 2023.

https://www.aquaculture.ca/aquaculture-speciesindex.

13. CAIA. Canadian aquaculture. 2023. https://www.aquaculture.ca/benefits-to-canadians-index.

14. DFO. Aquaculture Production and Value. 2021. https://www.dfo-mpo.gc.ca/stats/aqua/aqua21-eng.htm

15. DFO. Aquaculture Value Added Account. 2021. https://www.dfo-mpo.gc.ca/stats/aqua/va21pub-eng.htm.

16. DFO. Farmed Salmon. 2017. https://www.dfo-mpo.gc.ca/aquaculture/sector-secteur/species-especes/salmon-saumon-eng.htm.

17. ACOA. Aquaculture in Atlantic Canada - Atlantic Salmon. https://www.canada.ca/en/atlantic-canada-opportunities/services/aquaculture-in-atlantic-canada.html

18. DFO. Evaluation of bacterial kidney disease (BKD) impacts on the Canadian salmon aquaculture industry. 2010. https://www.cahsbc.ca/wpcontent/uploads/2019/03/BKDWhitePaper_FinalApr2010_WithAppendices.pdf.

19. Akazawa N, Alvial A, Baloi AP, Blanc P, Brummett RE, Burgos JM, Chamberlain GC, Chamberlain GW, Forster J, Hao NV, Ibarra R, Kibenge F, Lightner DV, Loc TH, Nikuli HL, Omar I, Ralaimarindaza, Reantaso M, St-Hilaire S, Towner R, Tung H, Villarreal M, Wyk M Van. Reducing disease risk in aquaculture (English). Agriculture and environmental services discussion paper. World Bank Group. 2014.

20. Brooker AJ, Papadopoulou A, Gutierrez C, Rey S, Davie A, Migaud H. Sustainable production and use of cleaner fish for the biological control of sea-lice: recent advances and current challenges. Veterinary Record. 2018;183(12):383.

21. Lam CT, Rosanowski SM, Walker M, St-Hilaire S. Sea-lice exposure to non-lethal levels of emamectin benzoate after treatments: a potential risk factor for drug resistance. Scientific Reports. 2020;10(1):932.

22. Karbowski CM, Finstad B, Karbowski N, Hedger RD. Sea-lice in Iceland: assessing the status and current implications for aquaculture and wild salmonids. Aquaculture Environment Interactions. 2019;11:149-60.

23. Aaen SM, Helgesen KO, Bakke MJ, Kaur K, Horsberg TE. Drug resistance in sea-lice: a threat to salmonid aquaculture. Trends in Parasitology. 2015;31(2):72-81.

24. Abolofia J, Asche F, Wilen JE. The Cost of Lice: Quantifying the impacts of parasitic sea-lice on farmed salmon. Marine Resource Economics. 2017;32(3):329-49.

25. DFO. Average number of lice per fish on BC salmon farms. 2020. https://www.pac.dfo-mpo.gc.ca/aquaculture/reporting-rapports/lice-ab-pou/index-eng.html.

26. Walter, T.C.; Boxshall, G. (2023). World of Copepods Database. Accessed at https://www.marinespecies.org/copepoda on 2023-07-03. doi:10.14284/356.

27. Costello MJ. Ecology of sea-lice parasitic on farmed and wild fish. Trends in Parasitology. 2006;22(10):475-83.

28. Torrissen O, Jones S, Asche F, Guttormsen A, Skilbrei OT, Nilsen F, Horsberg TE, Jackson D. Salmon lice impact on wild salmonids and salmon aquaculture. Journal of Fish Diseases. 2013;36(3):171-94.

29. Overton K, Dempster T, Oppedal F, Kristiansen TS, Gismervik K, Stien LH. Salmon lice treatments and salmon mortality in Norwegian aquaculture: a review. Reviews in Aquaculture. 2018;11(4):1398-417.

30. Barker SE, Bricknell IR, Covello J, Purcell S, Fast MD, Wolters W, Bouchard DA. Sea-lice, *Lepeophtheirus salmonis* (Kroyer 1837), infected Atlantic salmon (*Salmo salar* L.) are more susceptible to infectious salmon anemia virus. PLoS One. 2019;14(1):e0209178.

31. Costello MJ. The global economic cost of sea-lice to the salmonid farming industry. Journal of Fish Diseases. 2009;32(1):115-8.

32. DFO. Managing disease and parasites. 2020.

33. Margolis L. The identity of the species of *lepeophtheirus* (copepoda) parasitic on Pacific salmon (genus *oncorhynchus*) and Atlantic salmon (*Salmo sala*r). Canadian Journal of Zoology. 1958;36(6):889-93.

34. Yossa R, Dumas A. Approaches for controlling sea-lice infestation in global salmon farming: What is applicable in Canadian aquaculture industry. Journal of Applied Aquaculture. 2016;28(4):314-29.

35. Hemmingsen W, MacKenzie K, Sagerup K, Remen M, Bloch-Hansen K, Dagbjartarson Imsland AK. *Caligus elongatus* and other sea-lice of the genus *Caligus* as parasites of farmed salmonids: A review. Aquaculture. 2020;522.

36. Nilsen A, Nielsen KV, Biering E, Bergheim A. Effective protection against sea-lice during the production of Atlantic salmon in floating enclosures. Aquaculture. 2017;466:41-50.

37. Stien LH, Dempster T, Bui S, Glaropoulos A, Fosseidengen JE, Wright DW, Oppedal F. 'Snorkel' sea-lice barrier technology reduces sea-lice loads on harvest-sized Atlantic salmon with minimal welfare impacts. Aquaculture. 2016;458:29-37.

38. Oppedal F, Samsing F, Dempster T, Wright DW, Bui S, Stien LH. Sea-lice infestation levels decrease with deeper 'snorkel' barriers in Atlantic salmon sea-cages. Pest Management Science. 2017;73(9):1935-43.

39. Hevrøy EM, Boxaspen K, Oppedal F, Taranger GL, Holm JC. The effect of artificial light treatment and depth on the infestation of the sea louse *Lepeophtheirus salmonis* on Atlantic salmon (*Salmo salar* L.) culture. Aquaculture. 2003;220(1-4):1-14.

40. Barrett LT, Bui S, Oppedal F, Bardal T, Olsen RE, Dempster T. Ultraviolet-C light suppresses reproduction of sea-lice but has adverse effects on host salmon. Aquaculture. 2020;520.

41. Denholm I, Devine GJ, Horsberg TE, Sevatdal S, Fallang A, Nolan DV, Powell R. Analysis and management of resistance to chemotherapeutants in salmon lice, *Lepeophtheirus salmonis* (*Copepoda: Caligidae*). Pest Management Science. 2002;58(6):528-36.

42. Igboeli OO, Fast MD, Heumann J, Burka JF. Role of P-glycoprotein in emamectin benzoate (SLICE®) resistance in sea-lice, *Lepeophtheirus salmonis*. Aquaculture. 2012;344-349:40-7.

43. Fjørtoft HB, Besnier F, Stene A, Nilsen F, Bjørn PA, Tveten AK, Finstad B, Aspehaug V, Glover KA. The Phe362Tyr mutation conveying resistance to organophosphates occurs in high frequencies in salmon lice collected from wild salmon and trout. Scientific Reports. 2017;7(1):14258.

44. Agusti-Ridaura C, Bakke MJ, Helgesen KO, Sundaram AY, Bakke SJ, Kaur K, Horsberg TE. Candidate genes for monitoring hydrogen peroxide resistance in the salmon louse, *Lepeophtheirus salmonis*. Parasites & Vectors. 2020;13:1-16.

45. Jones PG, Hammell KL, Gettinby G, Revie CW. Detection of emamectin benzoate tolerance emergence in different life stages of sea-lice, *Lepeophtheirus salmonis*, on farmed Atlantic salmon, *Salmo salar* L. Journal of Fish Diseases. 2013;36(3):209-20.

46. Fjørtoft HB, Nilsen F, Besnier F, Stene A, Tveten AK, Bjørn PA, Aspehaug VT, Glover KA. Losing the 'arms race': multiresistant salmon lice are dispersed throughout the North Atlantic Ocean. Royal Society Open Science. 2021;8(5):210265.

47. Sutherland BJ, Poley JD, Igboeli OO, Jantzen JR, Fast MD, Koop BF, Jones SR. Transcriptomic responses to emamectin benzoate in Pacific and Atlantic Canada salmon lice *Lepeophtheirus salmonis* with differing levels of drug resistance. Evolutionary Applications. 2015;8(2):133-48.

48. G Geary T, Moreno Y. Macrocyclic lactone anthelmintics: spectrum of activity and mechanism of action. Current Pharmaceutical Biotechnology. 2012;13(6):866-72.

49. He L, Gao X, Wang J, Zhao Z, Liu N. Genetic analysis of abamectin resistance in *Tetranychus cinnabarinus*. Pesticide Biochemistry and Physiology. 2009;95(3):147-51.

50. Ghosh R, Andersen EC, Shapiro JA, Gerke JP, Kruglyak L. Natural variation in a chloride channel subunit confers avermectin resistance in *C. elegans*. Science. 2012;335(6068):574-8.

51. J Wolstenholme A, M Kaplan R. Resistance to macrocyclic lactones. Current Pharmaceutical Biotechnology. 2012;13(6):873-87.

52. Carmichael SN, Bron JE, Taggart JB, Ireland JH, Bekaert M, Burgess ST, Skuce PJ, Nisbet AJ, Gharbi K, Sturm A. Salmon lice (*Lepeophtheirus salmonis*) showing varying emamectin benzoate susceptibilities differ in neuronal acetylcholine receptor and GABA-gated chloride channel mRNA expression. BMC Genomics. 2013;14(1):1-16.

53. Bruno D, Raynard R. Studies on the use of hydrogen peroxide as a method for the control of sea-lice on Atlantic salmon. Aquaculture International. 1994;2:10-8.

54. Thomassen J. A new method for control of salmon lice. Fish Farming Technology: CRC Press; 2020.

55. Fiander H, Schneider H. Dietary ortho phenols that induce glutathione S-transferase and increase the resistance of cells to hydrogen peroxide are potential cancer chemopreventives that act by two mechanisms: the alleviation of oxidative stress and the detoxification of mutagenic xenobiotics. Cancer Letters. 2000;156(2):117-24.

56. Spitz DR, Adams DT, Sherman CM, Roberts RJ. Mechanisms of cellular resistance to hydrogen peroxide, hyperoxia, and 4-hydroxy-2-nonenal toxicity: the significance of increased catalase activity in H_2O_2-resistant fibroblasts. Archives of Biochemistry and Biophysics. 1992;292(1):221-7.

57. Nakamura K, Kanno T, Mokudai T, Iwasawa A, Niwano Y, Kohno M. Microbial resistance in relation to catalase activity to oxidative stress induced by photolysis of hydrogen peroxide. Microbiology and Immunology. 2012;56(1):48-55.

58. Uhlich GA. KatP contributes to OxyR-regulated hydrogen peroxide resistance in Escherichia coli serotype O157: H7. Microbiology. 2009;155(11):3589-98.

59. Helgesen KO, Romstad H, Aaen SM, Horsberg TE. First report of reduced sensitivity towards hydrogen peroxide found in the salmon louse *Lepeophtheirus salmonis* in Norway. Aquaculture Reports. 2015;1:37-42.

60. Smissaert H. Cholinesterase inhibition in spider mites susceptible and resistant to organophosphate. Science. 1964;143(3602):129-31.

61. Kaur K, Helgesen KO, Bakke MJ, Horsberg TE. Mechanism behind resistance against the organophosphate azamethiphos in salmon lice (*Lepeophtheirus salmonis*). PloS one. 2015;10(4):e0124220.

62. Weston DP, Poynton HC, Wellborn GA, Lydy MJ, Blalock BJ, Sepulveda MS, Colbourne JK. Multiple origins of pyrethroid insecticide resistance across the species complex of a nontarget aquatic crustacean, *Hyalella azteca*. Proceedings of the National Academy of Sciences. 2013;110(41):16532-7.

63. Sevatdal S, Fallang A, Ingebrigtsen K, Horsberg TE. Monooxygenase mediated pyrethroid detoxification in sea-lice (*Lepeophtheirus salmonis*). Pest Management Science. 2005;61(8):772-8.

64. Robledo D, Gutierrez AP, Barria A, Lhorente JP, Houston RD, Yanez JM. Discovery and functional annotation of quantitative trait loci affecting resistance to sea-lice in Atlantic salmon. Frontiers in Genetics. 2019;10:56.

65. Carpio Y, Basabe L, Acosta J, Rodríguez A, Mendoza A, Lisperger A, Zamorano E, González M, Rivas M, Contreras S, Haussmann D. Novel gene isolated from *Caligus rogercresseyi*: a promising target for vaccine development against sea-lice. Vaccine. 2011;29(15):2810-20.

66. Casuso A, Valenzuela-Muñoz V, Benavente BP, Valenzuela-Miranda D, Gallardo-Escárate C. Exploring sea-lice vaccines against early stages of infestation in Atlantic Salmon (*Salmo salar*). Vaccines. 2022; 10(7).

67. Imsland AK, Reynolds P, Eliassen G, Hangstad TA, Nytrø AV, Foss A, Vikingstad E, Elvegård TA. Assessment of growth and sea-lice infection levels in Atlantic salmon stocked in small-scale cages with lumpfish. Aquaculture. 2014;433:137-42.

68. Imsland AKD, Hanssen A, Nytro AV, Reynolds P, Jonassen TM, Hangstad TA, Elvegard TA, Urskog TC, Mikalsen B. It works! Lumpfish can significantly lower sea-lice infestation in large-scale salmon farming. Biology Open. 2018;7(9).

69. Powell A, Treasurer JW, Pooley CL, Keay AJ, Lloyd R, Imsland AK, Garcia de Leaniz C. Use of lumpfish for sea-lice control in salmon farming: challenges and opportunities. Reviews in Aquaculture. 2018;10(3):683-702.

70. Jones CS, Lockyer AE, Verspoor E, Secombes CJ, Noble LR. Towards selective breeding of Atlantic salmon for sea louse resistance: approaches to identify trait markers. Pest Management Science. 2002;58(6):559-68.

71. Robinson NA, Robledo D, Sveen L, Daniels RR, Krasnov A, Coates A, Jin YH, Barrett LT, Lillehammer M, Kettunen AH, Phillips BL. Applying genetic technologies to combat infectious diseases in aquaculture. Reviews in Aquaculture. 2022.

72. Yáñez JM, Houston RD, Newman S. Genetics and genomics of disease resistance in salmonid species. Frontiers in Genetics. 2014;5.

73. Houston RD, Bean TP, Macqueen DJ, Gundappa MK, Jin YH, Jenkins TL, Selly SL, Martin SA, Stevens JR, Santos EM, Davie A. Harnessing genomics to fast-track genetic improvement in aquaculture. Nature Reviews Genetics. 2020;21(7):389-409.

74. Bui S, Oppedal F, Sievers M, Dempster T. Behaviour in the toolbox to outsmart parasites and improve fish welfare in aquaculture. Reviews in Aquaculture. 2019;11(1):168-86.

75. Raynard RS, Bricknell IR, Billingsley PF, Nisbet AJ, Vigneau A, Sommerville C. Development of vaccines against sea-lice. Pest Management Science. 2002;58(6):569-75.

76. Boissonnot L, Karlsen C, Reynolds P, Austad M, Stensby-Skjærvik S, Remen M, Imsland AK. Welfare and survival of lumpfish (*Cyclopterus lumpus*) in Norwegian commercial Atlantic salmon (*Salmo salar*) production. Aquaculture. 2023 Jul 15;572:739496.

77. Imsland A, Remen M, Sagerup K, Mathisen R, Myklebust EA, Reynolds P. Possible Use of Lumpfish to Control *Caligus elongatus* Infestation on Farmed Atlantic Salmon: A Mini Review. Journal of Ocean University of China. 2020;19(5):1133-9.

78. Integrated Taxonomic Information System – Report. https://www.itis.gov/servlet/SingleRpt/SingleRpt?search_topic=TSN&search_value=167612#null

79. Marcos-Lopez M, Donald K, Stagg H, McCarthy U. Clinical *Vibrio anguillarum* infection in lumpsucker *Cyclopterus lumpus* in Scotland. Veterinary Record. 2013;173(13):319.

80. Daborn GR, Gregor RS. Occurrence, distribution, and feeding habits of juvenile lumpfish, *Cyclopterus lumpus* L. in the Bay of Fundy. Canadian Journal of Zoology. 1983;61:797-801.

81. Goulet D, Green JM, Shears TH. Courtship, spawning, and parental care behavior of the lumpfish, *Cyclopterus lumpus* L., in Newfoundland. Canadian Journal of Zoology. 1986;64:1320-5.

82. Alberta OT, Torstensenb E, Bertelsenc B, Jonssond ST, Pettersene IH, Holstf JC. Age-reading of lumpsucker (*Cyclopterus lumpus*) otoliths: dissection, interpretation and comparison with length frequencies. Fisheries Research. 2002;55:239-52.

83. Norethberg G, Johannesen A, Arge R. Cryopreservation of lumpfish *Cyclopterus lumpus* (Linnaeus, 1758) milt. PeerJ. 2015;3:e1003.

84. Pampoulie C, Skirnisdottir S, Olafsdottir G, Helyar SJ, Thorsteinsson V, Jónsson SÞ, Fréchet A, Durif CM, Sherman S, Lampart-Kałużniacka M, Hedeholm R. Genetic structure of the

lumpfish *Cyclopterus lumpus* across the North Atlantic. ICES Journal of Marine Science. 2014;71(9):2390-7.

85. Bañón R, Garazo A, Fernández A. Note about the presence of the lumpsucker *Cyclopterus lumpus* (*Teleostei*, *Cyclopteridae*) in Galician waters (NW Spain). Journal of Applied Ichthyology. 2008;24(1):108-9.

86. Cox P, Anderson M. A study of the lumpfish (*Cyclopterus lumpus* L.). Contributions to Canadian Biology and Fisheries. 1922;1(1):1-20.

87. Kennedy J, Jónsson SÞ, Kasper JM, Ólafsson HG. Movements of female lumpfish (*Cyclopterus lumpus*) around Iceland. ICES Journal of Marine Science. 2015;72(3):880-9.

88. Kasper JM, Bertelsen B, Olafsson HG, Holst JC, Sturlaugsson J, Jonsson SP. Observations of growth and postspawning survival of lumpfish *Cyclopterus lumpus* from mark-recapture studies. Journal of Fish Biology. 2014;84(6):1958-63.

89. Vasconcelos P, Monteiro CC, Santos MN, Gaspar MB. First record of the lumpfish (*Cyclopterus lumpus* Linnaeus, 1758) off the Algarve coast (southern Portugal): southward extension of the species distributional range. Journal of Applied Ichthyology. 2004;20:159-60.

90. Davenport J. Synopsis of biological data on the lumpsucker, *Cyclopterus lumpus* (Linnaeus, 1758). FAO Fishery Synopsis. 1985;147:1-40.

91. Holborn MK, Einfeldt AL, Kess T, Duffy SJ, Messmer AM, Langille BL, Brachmann MK, Gauthier J, Bentzen P, Knutsen TM, Kent M. Reference genome of lumpfish *Cyclopterus lumpus* Linnaeus provides evidence of male heterogametic sex determination through the AMH pathway. Molecular Ecology Resources. 2022;22(4):1427-39.

92. Li MF, Clyburne S. New cell line from the marine lumpfish, *Cyclopterus lumpus*. Journal of the Fisheries Board of Canada. 1977;34(1):134-9.

93. Hedeholm R, Blicher ME, Grønkjær P. First estimates of age and production of lumpsucker (*Cyclopterus lumpus*) in Greenland. Fisheries Research. 2014;149:1-4.

94. Kyushin K. The embryonic and larval development, growth, survival and changes in body form, and the effect of temperature on these characteristics of the smooth lumpsucker, *Aptocyclub ventricobub (Pallas)*. Bulletin of the Faculty of Fisheries Hokkaido University. 1975;26(1):49-72.

95. Davenport J, Kjørsvik E. Buoyancy in the lumpsucker *Cyclopterus Lumpus*. Journal of the Marine Biological Association of the United Kingdom. 1886;66(1):159-74.

96. Barrett LT, Overton K, Stien LH, Oppedal F, Dempster T. Effect of cleaner fish on sea-lice in Norwegian salmon aquaculture: a national scale data analysis. International Journal of Parasitology. 2020. 1;50(10-11):787-96.

97. Cleaner fish R&D at Memorial University of Newfoundland helps spawn new industry [press release]. 2021. https://genomeatlantic.ca/cleaner-fish-rd-at-memorial-university-of-newfoundland-helps-spawn-new-industry/.

98. Overton K, Barrett LT, Oppedal F, Kristiansen TS, Dempster T. Sea-lice removal by cleaner fish in salmon aquaculture: a review of the evidence base. Aquaculture Environment Interactions. 2020;12:31-44.

99. Menanteau-Ledouble S, Kumar G, Saleh M, El-Matbouli M. *Aeromonas salmonicida*: updates on an old acquaintance. Diseases of Aquatic Organism. 2016;120(1):49-68.

100. Rønneseth A, Haugland GT, Brudal E, Wergeland HI. Bacterial diseases and vaccination of farmed lumpfish (*Cyclopterus lumpus L.*). 17th International Conference on Diseases of Fish And Shellfish. 2015.

101. Haugland GT, Jakobsen, R. A., Vestvik, N., Ulven, K., Stokka, L., Wergeland, H. I. Phagocytosis and respiratory burst activity in lumpsucker (*Cyclopterus lumpus* L.) leucocytes analysed by flow cytometry. PLoS One. 2012;7(10):e47909.

102. Ronneseth A, Ghebretnsae DB, Wergeland HI, Haugland GT. Functional characterization of IgM+ B cells and adaptive immunity in lumpfish (*Cyclopterus lumpus* L.). Development and Comparative Immunology. 2015;52(2):132-43.

103. Patel DM, Brinchmann, MF. Skin mucus proteins of lumpsucker (*Cyclopterus lumpus*). Biochemistry and Biophysics Reports. 2017;9:217-25.

104. Eggestøl H, Lunde HS, Knutsen TM, Haugland GT. Interleukin-1 ligands and receptors in lumpfish (*Cyclopterus lumpus* L.): molecular characterization, phylogeny, gene expression, and transcriptome analyses. Frontiers in Immunology. 2020;11:502.

105. Eggestøl H, Lunde HS, Haugland GT. The proinflammatory cytokines TNF-α and IL-6 in lumpfish (*Cyclopterus lumpus* L.) -identification, molecular characterization, phylogeny and gene expression analyses. Development and Comparative Immunology. 2020;105:103608.

106. Eggestøl HØ, Lunde HS, Rønneseth A, Fredman D, Petersen K, Mishra CK, Furmanek T, Colquhoun DJ, Wergeland HI, Haugland GT. Transcriptome-wide mapping of signaling pathways and early immune responses in lumpfish leukocytes upon in vitro bacterial exposure. Scientific Reports. 2018;8(1):5261.

107. Gnanagobal H, Cao T, Hossain A, Dang M, Hall JR, Kumar S, Van Cuong D, Boyce D, Santander J. Lumpfish (*Cyclopterus lumpus*) is susceptible to *Renibacterium salmoninarum* infection and induces cell-mediated immunity in the chronic stage. Frontiers in Immunology. 2021:4647.

108. Erkinharju T, Lundberg MR, Isdal E, Hordvik I, Dalmo RA, Seternes T. Seternes. Studies on the antibody response and side effects after intramuscular and intraperitoneal injection of Atlantic lumpfish (*Cyclopterus lumpus* L.) with different oil-based vaccines. Journal of Fish Diseases. 2017;40(12):1805-13.

109. Dang M, Cao T, Vasquez I, Hossain A, Gnanagobal H, Kumar S, Hall JR, Monk J, Boyce D, Westcott J, Santander J. Oral immunization of larvae and juvenile of lumpfish (*Cyclopterus lumpus*) against *Vibrio anguillarum* does not influence systemic immunity. Vaccines. 2021;9(8):819.

110. Rønneseth A, Haugland GT, Colquhoun DJ, Brudal E, Wergeland HI. Protection and antibody reactivity following vaccination of lumpfish (*Cyclopterus lumpus L*.) against atypical *Aeromonas salmonicida*. Fish and Shellfish Immunology. 2017;64:383-91.

111. Vasquez I, Cao T, Chakraborty S, Gnanagobal H, O'Brien N, Monk J, Boyce D, Westcott JD, Santander J. Comparative Genomics Analysis of *Vibrio anguillarum* Isolated from Lumpfish (*Cyclopterus lumpus*) in Newfoundland Reveal Novel Chromosomal Organizations. Microorganisms. 2020;8(11):1666.

112. Gudmundsdottir BK, Bjornsdottir B. Vaccination against atypical furunculosis and winter ulcer disease of fish. Vaccine. 2007;25(30):5512-23.

113. Rouleau FD, Vincent AT, Charette SJ. Genomic and phenotypic characterization of an atypical *Aeromonas salmonicida* strain isolated from a lumpfish and producing unusual granular structures. Journal of Fish Diseases. 2018;41(4):673-81.

114. Ellul RM, Walde C, Haugland GT, Wergeland H, Rønneseth A. Pathogenicity of *Pasteurella* sp. in lumpsuckers (*Cyclopterus lumpus* L.). Journal of fish diseases. 2019;42(1):35-46.

115. Mjølnerød EB, Nilsen HK, Gulla S, Riborg A, Bottolfsen KL, Wiklund T, Christiansen D, López Romalde JÁ, Scholz F, Colquhoun DJ. Multilocus sequence analysis reveals different lineages of *Pseudomonas anguilliseptica* associated with disease in farmed lumpfish (*Cyclopterus lumpus L.*). PLoS One. 2021;16(11):e0259725.

116. Marcos-López M, Ruane NM, Scholz F, Bolton-Warberg M, Mitchell SO, Murphy O'Sullivan S, Irwin Moore A, Rodger HD. *Piscirickettsia salmonis* infection in cultured lumpfish (*Cyclopterus lumpus* L.). Journal of Fish Diseases. 2017;40(11):1625-34.

117. Boily F, Malcolm G, Johnson SC. Characterization of *Aeromonas salmonicida* and furunculosis to inform pathogen transfer risk assessments in British Columbia. DFO Canadian Science Advisory Secretariat (CSAS). 2019;Res. Doc. 2019/016:39.

118. Gulla S, Duodu S, Nilsen A, Fossen I, Colquhoun DJ. *Aeromonas salmonicida* infection levels in pre- and post-stocked cleaner fish assessed by culture and an amended qPCR assay. Journal of Fish Diseases. 2016;39(7):867-77.

119. Gulla S, Krossøy B, Vågnes O, Colquhoun D. Specific subtypes of atypical *Aeromonas salmonicida* represent a significant risk to 'cleaner fish' used in norwegian salmon farming. 17th International Conference on Diseases of Fish And Shellfish. 2015.

120. Kverme KO, Kallekleiv M, Larsen K, Rønneseth A, Wergeland HI, Samuelsen OB, Haugland GT. Antibacterial treatment of lumpfish (*Cyclopterus lumpus*) experimentally challenged with *Vibrio anguillarum*, atypical *Aeromonas salmonicida* and *Pasteurella atlantica*. Journal of Fish Diseases. 2022;45(1):153-63.

121. R Beaz-Hidalgo MJF. *Aeromonas* spp. whole genomes and virulence factors implicated in fish disease. Journal of Fish Diseases. 2013;36(4):371-88.

122. Fish FF. Furunculosis in Wild Trout. Copeia. 1937;1937(1):37-40.

123. Duijn JCV. Taxonomy of the Fish Furunculosis Organism. Nature. 1962;4846:1127.

124. Janda JM, Abbott SL. The genus *Aeromonas*: taxonomy, pathogenicity, and infection. Clininal Microbiology Reviews. 2010;23(1):35-73.

125. Gaelle Porcheron CMD. Interplay between iron homeostasis and virulence: Fur and RyhB as major regulators of bacterial pathogenicity. Veterinary Microbiology. 2015;179(1-2):2-14.

126. Ebanks RO, Dacanay A, Goguen M, Pinto DM, Ross NW. Differential proteomic analysis of *Aeromonas salmonicida* outer membrane proteins in response to low iron and in vivo growth conditions. Proteomics. 2004;4(4):1074-85.

127. Takashi Aoki BIH. The outer membrane proteins of the fish pathogens *Aeromonas hydrophila*, *Aeromonas salmonicida* and *Edwardsiella tarda*. FEMS Microbiology Letters. 1985;27:299-305.

128. Dallaire-Dufresne S, Tanaka KH, Trudel MV, Lafaille A, Charette SJ. Virulence, genomic features, and plasticity of *Aeromonas salmonicida* subsp. *salmonicida*, the causative agent of fish furunculosis. Veterinary Microbiology. 2014;169(1-2):1-7.

129. Vanden Bergh P, Heller M, Braga-Lagache S, Frey J. The *Aeromonas salmonicida* subsp. *salmonicida* exoproteome: global analysis, moonlighting proteins and putative antigens for vaccination against furunculosis. Proteome Science. 2013;11(44):1-12.

130. Ringø E, Jutfelt F, Kanapathippillai P, Bakken Y, Sundell K, Glette J, Mayhew TM, Myklebust R, Olsen RE. Damaging effect of the fish pathogen *Aeromonas salmonicida* ssp. *salmonicida* on intestinal enterocytes of Atlantic salmon (*Salmo salar* L.). Cell Tissue Research. 2004;318(2):305-11.

131. Dacanay A, Boyd JM, Fast MD, Knickle LC, Reith ME. *Aeromonas salmonicida* Type I pilus system contributes to host colonization but not invasion. Diseases of Aquatic Organisms. 2010;88(3):199-206.

132. Ellis AE. Immunity to bacteria in fish. Fish & Shellfish Immunology. 1999;9:291-308.

133. Frey J, Origgi FC. Type III secretion system of *Aeromonas salmonicida* undermining the Host's immune response. Frontiers in Marine Science. 2016;3:130.

134. Ravi V, Venkatesh B. The divergent genomes of teleosts. Annual Review of Animal Biosciences. 2018;6(402):47-68.

135. Star B, Nederbragt AJ, Jentoft S, Grimholt U, Malmstrøm M, Gregers TF, Rounge TB, Paulsen J, Solbakken MH, Sharma A, Wetten OF. The genome sequence of Atlantic cod reveals a unique immune system. Nature. 2011;477(7363):207-10.

136. Vincent AT, Trudel MV, Freschi L, Nagar V, Gagné-Thivierge C, Levesque RC, Charette SJ. Increasing genomic diversity and evidence of constrained lifestyle evolution due to insertion sequences in *Aeromonas salmonicida*. BMC Genomics. 2016;17:44.

137. Vincent AT, Hosseini N, Charette SJ. The *Aeromonas salmonicida* plasmidome: a model of modular evolution and genetic diversity. Annals of the New York Academy of Sciences. 2021;1488(1):16-32.

138. NCBI. Genome: *Aeromonas salmonicida*. .

139. Vasquez I, Hossain A, Gnanagobal H, Valderrama K, Campbell B, Ness M, Charette SJ, Gamperl AK, Cipriano R, Segovia C, Santander J. Comparative Genomics of Typical and Atypical *Aeromonas salmonicida* Complete Genomes Revealed New Insights into Pathogenesis Evolution. Microorganisms. 2022;10(1).

140. Sironi M, Cagliani R, Forni D, Clerici M. Evolutionary insights into host–pathogen interactions from mammalian sequence data. Nature Reviews Genetics. 2015;16(4):224-36.

141. Abreu R, Giri P, Quinn F. Host-pathogen interaction as a novel target for host-directed therapies in tuberculosis. Frontiers in Immunology. 2020;11.

142. Jo EK. Interplay between host and pathogen: immune defense and beyond. Experimental & Molecular Medicine. 2019;51(12):1-3.

143. Byron SA, Van Keuren-Jensen KR, Engelthaler DM, Carpten JD, Craig DW. Translating RNA sequencing into clinical diagnostics: opportunities and challenges. Nature Reviews Genetics. 2016 May;17(5):257-71.

144. Michlewski G, Caceres JF. Post-transcriptional control of miRNA biogenesis. Cold Spring Harbor Laboratory Press for the RNA Society. 2019;25:1-16.

145. Bhaskaran M, Mohan M. MicroRNAs: history, biogenesis, and their evolving role in animal development and disease. Veterinary Pathology. 2014;51(4):759-74.

146. Bronevetsky Y, Ansel KM. Regulation of miRNA biogenesis and turnover in the immune system. Immunological Reviews. 2013;253(1):304-16.

147. Correia de Sousa M, Gjorgjieva M, Dolicka D, Sobolewski C, Foti M. Deciphering miRNAs' Action through miRNA Editing. International Journal of Molecular Sciences - MDPI. 2019;20(24).

148. Ha M, Kim VN. Regulation of microRNA biogenesis. Nature Reviews Molecular Cell Biology. 2014;15(8):509-24.

149. Hammond SM. An overview of microRNAs. Advanced Drug Delivery Reviews. 2015;87:3-14.

150. Krol J, Loedige I, Filipowicz W. The widespread regulation of microRNA biogenesis, function and decay. Nature Reviews Genetics. 2010;11(9):597-610.

151. Matsuyama H, Suzuki HI. Systems and synthetic microRNA biology: from biogenesis to disease pathogenesis. International Journal of Molecular Sciences. 2019;21(1).

152. Saliminejad K, Khorram Khorshid HR, Soleymani Fard S, Ghaffari SH. An overview of microRNAs: Biology, functions, therapeutics, and analysis methods. Journal of Cellular Physiology. 2019;234(5):5451-65.

153. Sudhagar A, Kumar G, El-Matbouli M. Transcriptome analysis based on RNA-Seq in understanding pathogenic mechanisms of diseases and the immune system of fish: a comprehensive review. International Journal of Molecular Sciences. 2018;19(1).

154. Van Muiswinkel WB. A history of fish immunology and vaccination I. The early days. Fish & Shellfish Immunology. 2008;25(4):397-408.

155. Duff DC. The oral immunization of trout against *Bacterium salmonicida*. The Journal of Immunology. 1942 May;44(1):87-94.

156. Gudding R, Van Muiswinkel WB. A history of fish vaccination: science-based disease prevention in aquaculture. Fish & shellfish immunology. 2013;35(6):1683-8.

157. Bergh PV, Burr SE, Benedicenti O, von Siebenthal B, Frey J, Wahli T. Antigens of the type-three secretion system of *Aeromonas salmonicida* subsp. *salmonicida* prevent protective immunity in rainbow trout. Vaccine. 2013;31(45):5256-61.

158. Villumsen KR, Raida MK. Long-lasting protection induced by bath vaccination against *Aeromonas salmonicida* subsp. *salmonicida* in rainbow trout. Fish & Shellfish Immunology. 2013;35(5):1649-53.

159. Lim J, Hong S. Characterization of *Aeromonas salmonicida* and *A. sobria* isolated from cultured salmonid fish in Korea and development of a vaccine against furunculosis. Journal of Fish Diseases. 2020;43(5):609-20.

160. Marana MH, Skov J, Chettri JK, Krossøy B, Dalsgaard I, Kania PW, Buchmann K. Positive correlation between *Aeromonas salmonicida* vaccine antigen concentration and protection in vaccinated rainbow trout *Oncorhynchus mykiss* evaluated by a tail fin infection model. Journal of Fish Diseases. 2017;40(4):507-16.

161. Rømer Villumsen K, Dalsgaard I, Holten-Andersen L, Raida MK. Potential role of specific antibodies as important vaccine induced protective mechanism against *Aeromonas salmonicida* in rainbow trout. PLoS One. 2012;7(10):e46733.

162. Romstad AB, Reitan LJ, Midtlyng P, Gravningen K, Emilsen V, Evensen Ø. Comparision of a serological potency assay for furunculosis vaccines (*Aeromonas salmonicida* subsp. *salmonicida*) to intraperitoneal challenge in Atlantic salmon (*Salmo salar* L.). Biologicals. 2014;42(2):86-90.

163. Rømer Villumsen K, Koppang EO, Raida MK. Adverse and long-term protective effects following oil-adjuvanted vaccination against *Aeromonas salmonicida* in rainbow trout. Fish & Shellfish Immunology. 2015;42(1):193-203.

164. Braden LM, Whyte SK, Brown AB, Iderstine CV, Letendre C, Groman D, Lewis J, Purcell SL, Hori T, Fast MD. Vaccine-induced protection against furunculosis involves pre-emptive priming of humoral immunity in Arctic charr. Frontiers in Immunology. 2019;4;10:120.

165. Assefa A, Abunna F. Maintenance of fish health in aquaculture: review of epidemiological approaches for prevention and control of infectious disease of fish. Veterinary Medicine International. 2018.

166. Evensen Ø. Immunology and vaccinology of farmed aquatic animals. Aquaculture Health Management. 2020.

167. Moser M, Leo O. Key concepts in immunology. Vaccine. 2010;28.

168. Bedekar MK, Kole S. Fundamentals of fish vaccination. Vaccine Design: Springer; 2022.

169. Soza-Ried C, Hess I, Netuschil N, Schorpp M, Boehm T. Essential role of c-myb in definitive hematopoiesis is evolutionarily conserved. Proceedings of the National Academy of Sciences of the United States of America. 2010;107(40):17304-8.

170. Mogensen TH. Pathogen recognition and inflammatory signaling in innate immune defenses. Clinical Microbiology Reviews. 2009;22(2):240-73.

171. Zhang J, Kong X, Zhou C, Li L, Nie G, Li X. Toll-like receptor recognition of bacteria in fish: ligand specificity and signal pathways. Fish & Shellfish Immunology. 2014;41(2):380-8.

172. Nie L, Cai SY, Shao JZ, Chen J. Toll-like receptors, associated biological roles, and signaling networks in non-mammals. Frontiers in Immunology. 2018;9:1523.

173. Ribeiro CM, Hermsen T, Taverne-Thiele AJ, Savelkoul HF, Wiegertjes GF. Evolution of recognition of ligands from Gram-positive bacteria: similarities and differences in the TLR2-mediated response between mammalian vertebrates and teleost fish. Journal of Immunology. 2010;184(5):2355-68.

174. Basu M, Swain B, Sahoo BR, Maiti NK, Samanta M. Induction of toll-like receptor (TLR) 2, and MyD88-dependent TLR- signaling in response to ligand stimulation and bacterial infections in the Indian major carp, mrigal (*Cirrhinus mrigala*). Molecular Biology Reports. 2012;39(5):6015-28.

175. Samanta M, Swain B, Basu M, Panda P, Mohapatra GB, Sahoo BR, Maiti NK. Molecular characterization of toll-like receptor 2 (TLR2), analysis of its inductive expression and associated

down-stream signaling molecules following ligands exposure and bacterial infection in the Indian major carp, rohu (*Labeo rohita*). Fish & Shellfish Immunology. 2012;32(3):411-25.

176. Hwang SD, Asahi T, Kondo H, Hirono I, Aoki T. Molecular cloning and expression study on Toll-like receptor 5 paralogs in Japanese flounder, *Paralichthys olivaceus*. Fish & Shellfish Immunology. 2010;29(4):630-8.

177. Wang W, Shen Y, Pandit NP, Li J. Molecular cloning, characterization and immunological response analysis of Toll-like receptor 21 (TLR21) gene in grass carp, *Ctenopharyngodon idella*. Development and Comparative Immunology. 2013;40(3-4):227-31.

178. Gao H, Wu L, Sun JS, Geng XY, Pan BP. Molecular characterization and expression analysis of Toll-like receptor 21 cDNA from *Paralichthys olivaceus*. Fish & Shellfish Immunology. 2013;35(4):1138-45.

179. Franch R, Cardazzo B, Antonello J, Castagnaro M, Patarnello T, Bargelloni L. Full-length sequence and expression analysis of Toll-like receptor 9 in the gilthead seabream (*Sparus aurata* L.). Gene. 2006;378:42-51.

180. Munoz I, Sepulcre MP, Meseguer J, Mulero V. Molecular cloning, phylogenetic analysis and functional characterization of soluble Toll-like receptor 5 in gilthead seabream, *Sparus aurata*. Fish & Shellfish Immunology. 2013;35(1):36-45.

181. Iliev DB, Skjæveland I, Jørgensen JB. CpG oligonucleotides bind TLR9 and RRM-Containing proteins in Atlantic Salmon (*Salmo salar*). BMC Immunology. 2013;12(12):1-12.

182. Takeuchi O, Akira S. Pattern recognition receptors and inflammation. Cell. 2010;140(6):805-20.

183. Flajnik MF, Kasahara M. Origin and evolution of the adaptive immune system: genetic events and selective pressures. Nature Reviews Genetics. 2010;11(1):47-59.

184. Nemazee D. Role of B cell antigen receptor in regulation of V(D)J recombination and cell survival. Immunologic Research. 2000;21(2-3):259–63.

185. Abbas AK, Murphy KM, Sher A. Functional diversity of helper T lymphocytes. Nature. 1996;383:787-93.

186. LeBien TW, Tedder TF. B lymphocytes: how they develop and function. Blood. 2008;112(5):1570-80.

187. Forthal DN. Functions of Antibodies. Microbiology Spectrum. 2014;2(4):1-17.

188. Ma J, Bruce TJ, Jones EM, Cain KD. A review of fish vaccine development strategies: conventional methods and modern biotechnological approaches. Microorganisms. 2019;7(11).

189. Semple SL, Dixon B. Salmonid antibacterial immunity: an aquaculture perspective. Biology (Basel). 2020;9(10).

190. Tafalla C, Bogwald J, Dalmo RA. Adjuvants and immunostimulants in fish vaccines: current knowledge and future perspectives. Fish & Shellfish Immunology. 2013;35(6):1740-50.

191. Takaya A, Yamamoto T, Tokoyoda K. Humoral Immunity vs. *Salmonella*. Frontiers in Immunology. 2020;10:3155.

192. Damrow TA, Williams JC, Waag DM. Suppression of in vitro lymphocyte proliferation in C57BL/10 ScN mice vaccinated with phase I *Coxiella burnetii*. Infection and Immunity. 1985;47(1):149-56.

193. Evenberg D, de Graaff P, Fleuren W, van Muiswinkel WB. Blood changes in carp (*Cyprinus carpio*) induced by ulcerative *Aeromonas salmonicida* infections. Veterinary Immunology and Immunopathology. 1986;12(1):321-30.

194. Pollard AJ, Bijker EM. A guide to vaccinology: from basic principles to new developments. Nature Reviews Immunology. 2021;21(2):83-100.

195. Clem AS. Fundamentals of vaccine immunology. Journal of Global Infectious Diseases. 2011;3(1):73.

2. Chapter two: Multi-Organ transcriptome response of lumpfish (*Cyclopterus lumpus*) to *Aeromonas salmonicida* subsp. *salmonicida* systemic infection.

2.1 Abstract

Lumpfish (*Cyclopterus lumpus*) are utilized as cleaner fish to biocontrol sea-lice (*Lepeophtheirus salmonis*) infestations in Atlantic salmon (*Salmo salar*) farms in the North Atlantic region. *Aeromonas salmonicida*, a Gram-negative facultative intracellular pathogen, is the causative agent of furunculosis in several fish species, including lumpfish. The molecular immune response of lumpfish to *A. salmonicida* infection was unknown. In this study, I established an *A. salmonicida* systemic infection model in lumpfish and examined the transcriptome profile of central and peripherical lymphoid tissues. Lumpfish (55.9 ± 6.4 g (mean ± SD)) were intraperitoneally (ip) injected with different doses of *A. salmonicida* to calculate the median lethal dose (LD_{50}). Samples of blood, head kidney, spleen, and liver were collected at different time points to determine the infection kinetics. I determined that *A. salmonicida* LD_{50} is 10^2 colony-forming units (CFU) per dose. I found that the lumpfish head kidney is the primary target organ of *A. salmonicida*. Triplicated biological samples were collected from head kidney, spleen, and liver from non-infection and infected lumpfish at 3 and 10 dpi for RNA-sequencing (RNA-Seq). RNA-Seq generated 79,705,149 ± 7,628,565 (mean ± SD) paired-end reads. The reads were *de novo* and reference genome-guided assembled. The reference genome-guided transcriptome assembly resulted in 6,246 differentially expressed genes (DEGs) ($\log_2FC \leq -1.0$ or ≥ 1.0, FDR $\leq$ 0.05). The *de novo* assembly resulted in 403,204 transcripts, which added 1307 novel genes not identified by the reference genome-guided transcriptome assembly. Differential gene expression and gene ontology (GO) enrichment analyses suggested that *A. salmonicida* could induce lethal infection in lumpfish by uncontrolled and detrimental blood coagulation, complement activation,

inflammation, DNA damage, suppression of the adaptive immune system, and prevention of cytoskeleton formation, which results in death. *A. salmonicida* might inhibit the NF-κB signaling pathway and positively regulate the apoptotic process in lumpfish. These results agree with the fish's lethargy before the onset of the disease and mortality and coincided with the effect of *A. salmonicida* virulence factors. This study provided insight into the interactions between a marine teleost and *A. salmonicida*.

2.2 Introduction

Lumpfish (*Cyclopterus lumpus*) has been utilized as a cleaner fish species to biocontrol sea-lice (e.g., *Lepeophtheirus salmonis*) infestations in Atlantic salmon (*Salmo salar*) farms in Atlantic Canada, Iceland, the US, the UK, and Norway [1–4]. Lumpfish cultivation is becoming an emergent aquaculture industry in the North Atlantic region since its utilization significantly reduces or eliminates the application of toxic chemotherapeutics [2-6].

Bacterial diseases are a health concern for lumpfish delousing performance and survival rates in sea-cages [3,4]. *Aeromonas salmonicida,* a facultative intracellular pathogen, endemic worldwide in fresh and marine water and the etiologic agent of furunculosis [7–10], is one of the most frequent pathogens of lumpfish [3,4,11,12]. *A. salmonicida* infection causes a cascade of events that usually result in fish death [13–15].

Recent studies have revealed that lumpfish have a similar innate immune system to other teleosts; for instance, macrophages display phagocytosis and respiratory burst [16], and IgM^+ B-cells have phagocytic activity [17]. Proteomic analysis of lumpfish skin mucus has identified antimicrobial peptides and proteins involved in complement activation, inflammation, and pathogen lysis [18]. Transcriptomics analysis of primary macrophages infected with *Vibrio anguillarum* revealed the upregulation of genes encoding proteins involved in cell signaling,

cytokines, and pathogen recognition components, e.g., toll-like receptors (TLRs), NOD-like receptors (NLRs), interleukins (ILs), and several components of the complement system [19]. *Renibacterium salmoninarum* infection in lumpfish showed the upregulation of cytokines, pattern recognition receptors (PRR), iron regulation, and acute phase reactant-related genes. In contrast, cell-mediated adaptive immunity-related genes were downregulated [20]. Vaccination studies in lumpfish indicate that the total levels of immunoglobulin (IgM) in sera are lower than in salmon; lumpfish produce specific antibodies upon immunization and can mount an effective adaptive immune response [21–23]. Real-time quantitative polymerase chain reaction (RT-qPCR) analyses showed that the oral immunization of lumpfish larvae induced canonical cytokines and chemokines-related genes [23]. However, *A. salmonicida* infection kinetics in lumpfish and lumpfish transcriptomic response to *A. salmonicida* infection had not been explored before this study. Therefore, in this study, I characterized the kinetics of *A. salmonicida* infection in lumpfish and profiled the transcriptome response of head kidney, spleen, and liver at 3 and 10 days post-infection (dpi). The head kidney and the spleen are the central lymphoid organs in teleost fishes [24], and the liver is involved in critical biochemical processes in fish (e.g., metabolism) [25]. Besides, the liver is also considered as a lymphoid organ because non-parenchymal cells of the liver take part in antigen presentation and immunomodulatory functions [26-28], and these immune defense mechanisms of the liver are present in teleost fish [29].

I determined that *A. salmonicida* kills lumpfish in a dose-dependent manner, and the lethal dose 50 (LD_{50}) was determined as 10^2 colony-forming units (CFU) per dose. I found that the lumpfish head kidney is the primary target organ of *A. salmonicida*. Using reference genome-guided and *de novo* transcriptome assembly analysis, I identified tissue-specific gene expression profiles in the head kidney, spleen, and liver. This study suggests uncontrolled and detrimental

blood coagulation, complement activation, and inflammation could cause a septic-like shock, which leads to hypoxia, internal organ hemorrhages, and suppression of the adaptive immune system. The analysis also suggests an impairment of the DNA repair system, which results in cell cycle arrest and death. These findings relate to the effects of the type three secretion system (T3SS) effectors described in *A. salmonicida* (e.g., destabilize cytoskeleton structure by depolymerizing microfilament and microtubules, induce apoptosis [30]. Similarly, the gene ontology (GO) enrichment analysis indicates that downregulated genes in the spleen are associated with cytoskeleton structure formation. Upregulated genes are associated with the positive regulation of the apoptotic process. Overall, this study provides fundamental knowledge to understand the *A. salmonicida* infection model in a marine environment and provides valuable guidance for future pathogenicity studies.

2.3 Materials and Methods

2.3.1 Bacterial strain, culture media, and reagents

Virulent *A. salmonicida* J223 (CP048223) [31–33] isolated from Atlantic salmon in 1999 was used in this study. A single colony of *A. salmonicida* J223 [34] was grown routinely in a 16 mm diameter glass tube containing 3 mL of Trypticase Soy Broth (TSB, Difco, Franklin Lakes, New Jersey, USA) at 15 °C with aeration (180 rpm) for 48 h. TSB was supplemented with bacto agar (1.5%; Difco) and Congo-red (0.01%; Sigma-Aldrich, St. Louis, Missouri, USA) when required. Bacterial growth was monitored by spectrophotometry using a Genesys 10 UV spectrophotometer (Thermo Scientific, Madison, Wisconsin, USA) and by plating to count CFU/mL [35].

2.3.2 Bacteria inoculum preparation

A. salmonicida J223 was initially grown in 3 mL of TSB media for 48 h. Subsequently, 300 µL of fresh culture was added to a 250 mL flask containing 30 mL of TSB media and incubated for 18 h at 15 °C with aeration (180 rpm) in an orbital shaker up to an optical density (OD_{600}) of 0.7 (~1 x 10^8 CFU/mL) according to the previous description [31]. The bacterial cells were harvested by centrifugation (4200 × *g* for 10 min at 4 °C), washed three times with phosphate-buffered saline (PBS; 136 mM NaCl, 2.7 mM KCl, 10.1 mM Na_2HPO_4, 1.5 mM KH_2PO_4 (pH 7.2)) [36], and finally resuspended in 300 µL of PBS. The concentrated bacterial inoculum was serially diluted in PBS (1:10) and quantified by plating it onto Trypticase Soy Agar (TSA) to determine CFU/mL.

2.3.3 Ethics statement

The experiments were performed according to the Canadian Council on Animal Care guidelines and accepted by Memorial University of Newfoundland's Institutional Animal Care Committee (protocols #18-01-JS; #18-02-JS) [37].

2.3.4 Fish holding

Juvenile specific-pathogen-free lumpfish 55.9 ± 6.4 g (mean ± SD) were obtained from the Dr. Joe Brown Aquatic Research Building (JBARB) at the Department of Ocean Sciences (DOS), Memorial University of Newfoundland (MUN), Canada [37]. All the infection assays were conducted at the nationally certified marine AQ3 biocontainment unit at the Cold-Ocean Deep-Sea Research Facility (CDRF), DOS, MUN. Lumpfish were kept in 500 L tanks, with flow-through (7.5 L min^{-1}) of filtered and UV treated seawater (8–10 °C), ambient photoperiod (winter-spring), and 95–110% air saturation. The fish were fed daily using a commercial diet (Skretting – Europa 15; crude protein (55%), crude fat (15%), crude fiber (1.5%), calcium (3%), phosphorus

(2%), sodium (1%), vitamin A (5000 IU/Kg), vitamin D (3000 IU/Kg) and vitamin E (200 IU/Kg)) with a ration of 0.5% of their body weight per day.

2.3.5 Lumpfish infection and lethal dose 50 (LD_{50}) determination

Lumpfish were transferred from JBARB to the AQ3 biocontainment facility in 500 L tanks containing 60 fish each and acclimated for 2 weeks under optimal conditions (described above). LD_{50} of *A. salmonicida* J223 was evaluated in naïve lumpfish according to established protocols in the relevant literature [38]. Briefly, the fish were anesthetized with 40 mg of MS222 (Syndel Laboratories, Vancouver, British Colombia, Canada) per liter of seawater and intraperitoneally (ip) injected with 100 µL of 10^1, 10^2, 10^3, 10^4, and 10^5 CFU of *A. salmonicida* J223 per dose. Five independent tanks were utilized for monitoring the mortality, and five other separate tanks were used for sampling. An additional non-infected group served as a control. Fish were visually inspected for any signs of the disease. The LD_{50} dose was determined for *A. salmonicida* in lumpfish according to the Reed and Muench method [39] and the Karber method [40]. Kaplan-Meier estimator and Log-rank tests were used to obtain survival fractions after the challenges and determine the differences between treatments. A one-way ANOVA was followed by Tukey's multiple comparisons test ($p \leq 0.05$ was considered as significant). Statistical analyses and data visualization were performed using GraphPad Prism 7.0 (La Jolla, San Diego, California, USA).

2.3.6 A. salmonicida tissue colonization

Five fish were netted at each of 0, 3, 7, 10, 14, 21, and 33 dpi and immediately euthanized with an overdose of MS222 (400 mg/L). The head kidney, spleen, and liver were aseptically removed, placed in the sterile homogenizer bags (Nasco whirl-pak®, Thermo Fisher Scientific, Waltham, Massachusetts, USA), weighed, and suspended in PBS to a final volume of 1 mL (weight: volume). Afterward, the tissues were homogenized, the suspensions were serially diluted

(1:10), and the suspensions were spread onto the TSA plate. Similarly, 1 mL of blood was collected, serially diluted, and spread onto the TSA plate. The plates were incubated at 15 °C for 4 days to determine the number of *A. salmonicida* CFU per gram of tissue or 1 mL of blood, respectively. The Tukey's multiple comparisons test followed one-way ANOVA ($p \leq 0.05$ was considered significant). Statistical analyses and data visualization were performed using GraphPad Prism 7.0.

2.3.7 Histopathology

Sections of lumpfish head kidney, spleen, and liver were collected from the non-infected control and infected fish at 3 and 10 dpi. Tissues were submerged in 10% formalin for three days at room temperature. The fixed tissues were removed from formalin and stored in PBS at 4 °C until further processing for paraffin-embedded tissue block according to established procedures [41]. Tissues were sectioned, and 5 µm sections were stained with hematoxylin and eosin (Leica Biosystems, Concord, Ontario, Canada) and visualized under a light microscope (Olympus CX21, New York, USA).

2.3.8 RNA purification

The tissue (~100 mg) of head kidney, spleen, and liver were sampled from 3 non-infected lumpfish and 3 infected lumpfish (10^4 CFU/dose) at 3 and 10 dpi (Figure 2.1) for RNA-Seq and RT-qPCR analyses, similar to other studies [42–47]. Lumpfish tissues (n = 27) were preserved in 500 µL of RNAlater (Invitrogen™, ThermoFisher, Waltham, Massachusetts, USA) according to the manufacturer's instructions until further processing. RNA was extracted from fish tissues using the mirVana RNA isolation kit (Invitrogen™, ThermoFisher, Waltham, Massachusetts, USA) following the manufacturer's instructions. RNA samples were treated with TURBO DNase (TURBO DNA-free™ Kit, Invitrogen™, ThermoFisher, Waltham, Massachusetts, USA)

following the manufacturer's instructions for the complete digestion of DNA and removal of remaining DNase and divalent cations, such as magnesium and calcium. Purified RNA samples were quantified for concentration and evaluated for purity using a spectrophotometer (Genova-nano, Jenway, Stone, Staffordshire, England), and evaluated for integrity using 1% agarose gel electrophoresis (Table 2.1).

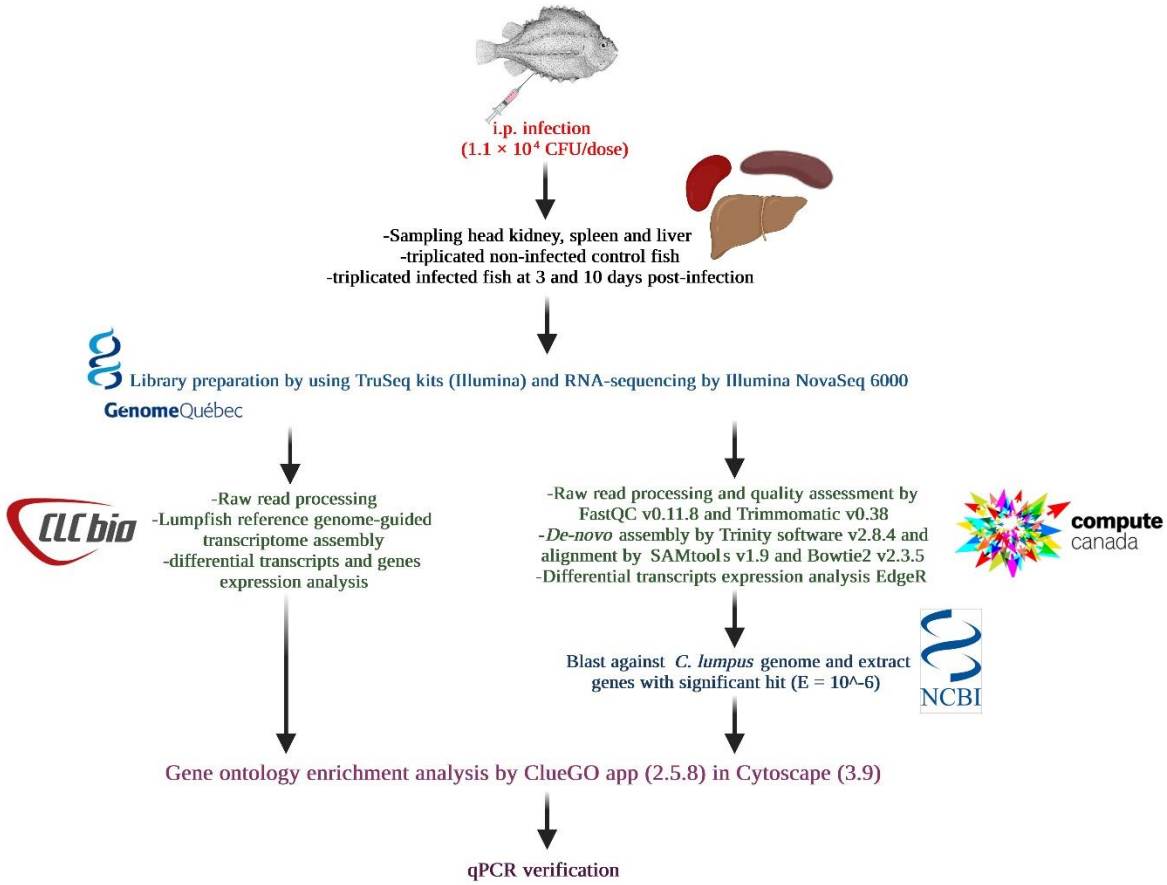

Figure 2.1. RNA-Seq sample collection and data analysis workflow.

Table 2.1. Quality of the RNA.

Sample name[a]	28S/18S[b]	RIN[c]	Concentration (ng/µl)	260/280[d]	260/230[e]
Control Head kidney1	1.53	9.2	852.84	2.07	2.31
Control Head kidney 2	0.90	7.8	955.81	2.06	2.19
Control Head kidney 3	1.48	9.3	299.90	2.05	2.24
3 dpi Head kidney 1	1.12	8.7	280.09	2.07	1.29
3 dpi Head kidney 2	0.65	6.8	847.86	2.09	2.10
3 dpi Head kidney 3	0.91	8.2	227.22	2.08	1.67
10 dpi Head kidney 1	1.11	8.7	229.25	2.02	1.79
10 dpi Head kidney 2	1.36	9.0	225.24	2.06	1.51
10 dpi Head kidney 3	0.50	5.4	1083.98	2.00	2.33
Control Spleen1	0.94	7.6	356.49	2.03	1.52
Control Spleen 2	1.66	8.6	366.55	2.05	2.16
Control Spleen 3	1.08	8.7	286.33	2.05	2.05
3 dpi Spleen 1	1.42	9.2	521.28	2.08	1.98
3 dpi Spleen 2	1.67	9.5	339.04	2.04	1.56
3 dpi Spleen 3	1.62	9.0	470.40	1.95	2.33
10 dpi Spleen 1	1.01	6.8	875.61	2.05	2.31
10 dpi Spleen 2	0.81	6.7	687.89	2.05	2.27
10 dpi Spleen 3	1.30	8.7	639.58	2.06	1.91
Control Liver1	1.18	8.6	346.84	2.03	1.52
Control Liver 2	1.7	7.6	356.49	2.05	2.16
Control Liver 3	1.32	10.0	912.41	2.05	2.05
3 dpi Liver 1	0.56	7.3	927.85	2.08	1.46
3 dpi Liver 2	1.62	9.6	586.10	2.09	1.85
3 dpi Liver 3	1.65	9.5	466.16	1.99	2.09
10 dpi Liver 1	1.13	8.7	780.28	2.06	2.23
10 dpi Liver 2	1.04	7.4	1351.75	2.05	2.33
10 dpi Liver 3	1.81	9.8	522.96	2.08	1.96

[a] dpi: days post-infection.

[b] 28S: structural ribosomal RNA (rRNA) for the large subunit (LSU) of eukaryotic cytoplasmic ribosomes. 18S: rRNA, a part of the ribosomal RNA. The S represents Svedberg units.

[c] RIN: The RNA integrity number is a tool to estimate the integrity of total RNA samples. The RIN extension automatically assigns an integrity number to a eukaryote total RNA sample analyzed on the Agilent 2100 Bioanalyzer.

[d] 260/280 Ratio: 260 nm and 280 nm are the absorbance wavelengths used to assess the purity of DNA and RNA. A ratio of ~2.0 is considered pure for RNA. A lower absorbance ratio may indicate the presence of protein, phenol, or other contaminants that have an absorbance close to 280 nm. Subtraction of non-nucleic acid absorbance at 320 nm, is also needed to calculate this ratio. Formula:

DNA Purity (A_{260}/A_{280}) = (A_{260} reading – A_{320} reading) ÷ (A_{280} reading – A_{320} reading).

[e] 260/230 Ratio: The ratio of absorbance at 260 and 230 nm can be used as a secondary measure of DNA or RNA purity. In this case, a ratio between 2.0 - 2.2 is considered pure. If the ratio is lower than this expected range, it may indicate contaminants in the sample that absorb at 230nm.

2.3.9 Library preparation and RNA-Seq

Library construction and sequencing services were performed at Genome Quebec, Quebec, Canada. Briefly, the quality of RNA was evaluated using a Bioanalyzer 2100 (Agilent, Santa Clara, California, USA) (Figure 2.2, Table 2.1). Libraries were generated from 250 ng of total RNA using the NEBNext® Multiplex Oligos for Illumina® (Dual Index Primers Set 1; Adapter 1: 3´-AGATCGGAAGAGCACACGTCTGAACTCCAGTCAC-5´; Adapter 2: 3´-AGATCGGAAGAGCGTCGTGTAGGGAAAGAGTGT-5´) and sequenced in a NovaSeq 6000 Sequencer (Illumina) using a NovaSeq 6000 S4 100 bp PE flow cell. The raw data were deposited in the NCBI Sequence Read Archive (SRA) (Accession number PRJNA596743).

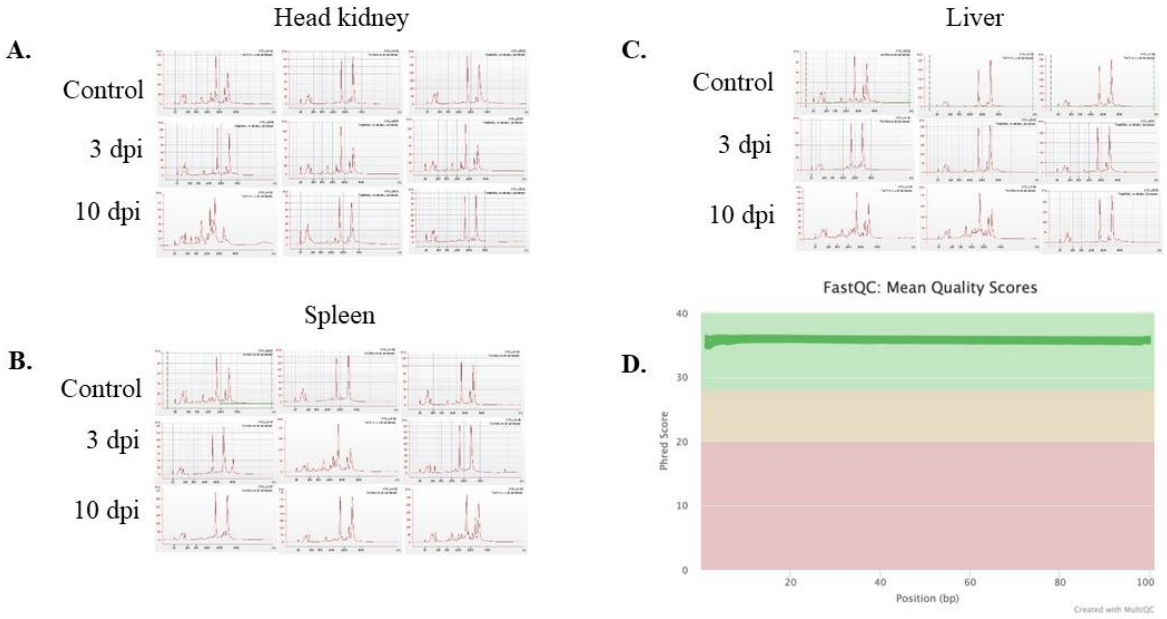

Figure 2.2. Quality of the RNA samples and sequenced reads. A. Quality of RNA samples collected from head kidney of non-infected control and 3 and 10 days post-infected lumpfish analyzed in Bioanalyzer 2100; B. Quality of RNA samples collected from spleen of non-infected control and 3 and 10 days post-infected lumpfish analyzed in Bioanalyzer 2100; C. Quality of RNA samples collected from liver of non-infected control and 3 and 10 days post-infected lumpfish analyzed in Bioanalyzer 2100; D. Sequence quality histograms: the mean quality value across each base position in the read after trimming adapter sequence and low quality reads.

2.3.10 Reference transcriptome assembly and downstream analysis

After RNA sequencing, paired-end raw reads were mate-paired and filtered to remove low-quality reads using the CLC Genomics Workbench v20.0 (CLCGWB; Qiagen, Hilden, Germany) with default parameters (mate-paired read information, minimum distance = 1; maximum distance = 1000). Adapter trimming was done by the CLCGWB using the trim reads tool with default parameters (quality trimming, trim using quality scores, limit: 0.05, and trim ambiguous nucleotides, the maximum number of ambiguities = 2). The quality of the reads was checked using the FastQC [48], and a MultiQC [49] report was generated before and after trimming. CLCGWB then mapped trimmed reads against the lumpfish genome (NCBI accession number PRJNA625538) using the RNA-Seq analysis tool. Reads mapping and transcript counts were conducted using the following settings: mismatch cost = 2, insertion and deletion costs = 3, minimum length fraction and minimum similarity fraction = 0.8, the maximum number of hits for a read = 10, and strand-specific = both. Gene expression quantification and normalization of the mapped reads were performed by an alignment-dependent expectation-maximization (EM) algorithm [50] based on the RSEM and eXpress methods [51]. The TPM values were then computed from the counts assigned to each transcript after normalization by the trimmed mean of M-values (TMM) [52]. A global correlation analysis was performed using $\log_2$-transformed TPM values (x + 1) of each gene, and transcripts and correlations were estimated by the Pearson method. Abundance data were subsequently subjected to differential expression analyses using the CLCGWB and the differential expression tool based on a negative binomial general linear model (GLM) [53]. A standard selection of biologically significant differentially expressed genes (DEGs) and differentially expressed transcripts (DETs) were performed with cut-off values of $\log_2$ fold-change (FC) ≤ -1.0 or ≥ 1.0 and a false discovery rate (FDR) $p \leq 0.05$.

2.3.11 de novo transcriptome assembly, contig abundance, and functional annotation

Adaptor sequences and reads ≤ 50 base pairs (bp) were trimmed using the Trimmomatic v0.38 [54]. Reads were assembled into a *de novo* transcriptome using the Trinity software (v2.8.4) with default parameters [55]. Assembled contigs shorter than 200 bp were excluded from the analysis. I examined the read representation of the assembly by aligning the processed reads on *de novo* assembled transcriptome using the SAMtools v1.9 [56] and Bowtie2 v2.3.5 [57]. I also examined how successfully assembled protein-coding transcripts were reconstructed to full or near full-length using the BLAST$^+$ [58] and Swissprot/TrEMBL. The *de novo* transcriptome assembly quality and completeness were evaluated using BUSCO version 3 [59] against a predefined set of 4584 Actinopterygian single copy orthologs from the orthoDB v9 database.

RSEM (v1.3.1) [60] was used to quantify TPMs in the Trinity package. Trinotate v3.1.1, a functional annotation pipeline, was used to generate an annotation report for the potential biological function of the assembled contigs [61]. Trinotate uses the TransDecoder v5.5 [55] to identify protein-coding regions in each assembled transcript. BLAST$^+$ variants (blastn, blastx, and blastp) against sequence databases downloaded locally (last accessed, January 2021), including RefSeq-rna, RefSeq-protein, nt, nr, and SwissProt, were used to annotate the *de novo* assembled transcriptome. The transcriptomes were further annotated for remote homologs and protein domains using HMMER v3.2.1 and Pfam v3.2.1 [62,63]. The SignalP v5.0 [64] and tmhmm v2.0c [65] software tools were used to predict signal peptides and transmembrane domains, respectively.

A differential expression analysis was performed using DESeq2 [66] and edgeR [53]. Within each pairwise comparison, only transcripts with an FDR adjusted *p*-value ≤ 0.05 were considered significantly differentially expressed. The differential expression analysis was conducted at the isoform level to identify the DETs in each organ at different timepoint.

2.3.12 Gene filtration and GO enrichment analysis

DEGs identified by reference transcriptomic assembly analysis were filtered ($log_2FC \leq -1.0$ or ≥ 1.0, p-value ≤ 0.05) for the GO enrichment analysis. On the other hand, DETs identified by *de novo* reference assembly analysis and edgeR analysis were utilized for the nucleotide blast against the lumpfish genome in NCBI to extract the corresponding gene symbols. Those genes were added to the GO term enrichment analyses. To obtain an overall view, GO enrichment analysis of all DEGs of head kidney, spleen, and liver at 3 dpi and 10 dpi were conducted by the ClueGO App (2.5.8) [67] in Cytoscape 3.9 [68] using ClueGO source files for lumpfish (Supplementary data 1). ClueGO source files were created using a GO OBO file downloaded on 24 March 2022. Fisher's exact test was conducted to study the enrichment of GO terms with a *p*-value cut-off ≤ 0.05 for 3 dpi and a *p*-value cut-off ≤ 0.00001 for 10 dpi. A differential *p*-value cut-off and the GO term fusion strategy were employed to reduce the redundancy of the GO terms and simplify the network. To obtain a global view, GO enrichment analysis of DEGs ($n = 600$ for 10 dpi; 300 most significant DEGs (lowest FDR adjusted *p*-value) from each assembly analysis of head kidney, spleen, and liver at 3 dpi and 10 dpi were conducted by ClueGO. Fisher's exact test was conducted to study the enrichment of GO terms with a *p*-value cut-off ≤ 0.05. The GO term fusion strategy was employed. However, to explore the *A. salmonicida* pathogenecity, GO enrichment analysis associated with biological processes of upregulated and downregulated DEGs in the head kidney 3 dpi and 10 dpi, spleen 3 dpi and 10 dpi, and liver 3 dpi and 10 dpi was conducted by setting the network specificity at medium in the ClueGO. Fisher's exact test was conducted to study the enrichment of GO terms with a *p*-value cut-off ≤ 0.05 (3 dpi) and ≤ 0.001 (10 dpi). The GO term fusion strategy was applied.

2.3.13 RT-qPCR analyses

To verify the RNA-Seq analyses, expression levels of 14 genes were measured in the same 27 RNA samples that were subjected to RNA-Seq analyses. These genes were selected based on their TPM values as they were expressed in individual samples from at least one group (i.e., control, 3 dpi or 10 dpi) in all three tissues (i.e., head kidney, liver, and spleen). In all cases, first-strand cDNA templates were synthesized, and RT-qPCR amplifications were performed as described previously [20,23]. The sequences, efficiencies, and amplicon sizes, and for all primer pairs used in the RT-qPCR analyses are presented in Table 2.2.

Table 2.2. Primers used in this study.

Gene name (*Gene symbol*) Trinity ID	Nucleotide sequence (5'-3')	Efficiency[a] (%)	Amplicon size (bp)
complement component 6 (*c6*) (DN137_c0_g1_i25)	F: CTGTCACCCCTCCACAGAGT R: GTTGCATGTCAGCGTTGAGT	98.8	100
C-X-C motif chemokine receptor 3 (LOC117745182 */cxcr3*) (DN2498_c0_g1_i8)	F: AGAGTTCACTGTGGGGGTTG R: GACTGCACCTGGTGACCTTT	93.9	106
galectin-3-binding protein (LOC117735282*/ igals3bp*) (DN1760_c1_g1_i3)	F: GTGCCTCAGAACGGTCTCTC R: GGCCATGTTGTCCTTGAAGT	96	114
glutathione S-transferase alpha 4 (*gsta4.1*) (DN1192_c0_g1_i2)	F: CCTATGGTGGAAATGGATGG R: CATGACCCGGTCTTTGAGAT	92.9	108
hepcidin anti-microbial peptide b (LOC117728128 / *hampb*) (DN2492_c0_g1_i7)	F: CGTCGTGCTCACCTTCATTT R: CTGGGTTGTCAACGCTCAT	91.9	95
interleukin 1 receptor type 2 (LOC117750249*/ il1r2*) (DN49226_c0_g1_i2)	F: CTCATTGATGAGCGGCAGTA R: GGGGTCAGAGGTCACAGAGA	92.5	111
interleukin 8b (il8b) alias *C-X-C motif chemokine ligand 8b* (*cxcl8b*) (DN2906_c0_g1_i1)	F: GTCTGAGAAGCCTGGGAGTG R: TCAGAGTGGCAATGATCTCG	87.4	138
BPI fold-containing family C- like (*bpifcl*) (DN1675_c0_g2_i3)	F: GTTTCCCGGACTTCTGATGA R: GGTACCATTTGGTTGGATGG	95.7	130

Gene name (*Gene symbol*) Trinity ID	Nucleotide sequence (5'-3')	Efficiency[a] (%)	Amplicon size (bp)
pentraxin 3 (*ptx3a*) (DN6917_c2_g1_i1)	F: GCCTCAAACCCAGAGATCAG R: GTCGGGAAGTTTGCATTTGT	90	105
ras-related protein ORAB-1 (LOC117743939/ *orab1*) (DN1973_c0_g3_i2)	F: ACAGGAGATCGACCGCTATG R: GAGTCTGCGAACTCCTTTGC	92.4	117
amyloid protein a (LOC117728776) (DN17527_c0_g1_i1)	F: AGAGTGGGTGCAGGAAAGAA R: GAAGTCCTGGTGGCCTGTAA	92.1	116
suppressor of cytokine signaling 3 (*socs3a*) (DN488_c0_g1_i2)	F: CATGCCTCAGAGCAAAGTGA R: AGCTGCAGGAGAGAGGTCTG	93.7	104
TNF receptor superfamily member 9 (LOC117733297/ *tnfrsf9*) (DN2095_c0_g3_i4)	F: AGGAGAAGAAAAGCCGATCC R: CTCGTGGAAACTGCACTCAA	94.4	115
toll-like receptor 5a (LOC117727165/ *tlr5a*) (DN8688_c0_g1_i1)	F: CCATCATGCACTTTGTACGG R: TGGACGAGTTTCAGCAGTTG	92.9	129

[a] efficiency with which primers bind to the target

In the experimental qPCR analyses, expression levels of the genes were normalized to expression levels of two endogenous control transcripts. The fluorescence threshold cycle (Ct) values of all 27 samples in the study were measured (in triplicate) for each of these transcripts using cDNA of 4 ng of input total RNA, and then analyzed using geNorm [69]. Based on this analysis, *eukaryotic translation initiation factor 3 subunit D* (*etf3d*) (geNorm M = 0.31) and *elongation factor 1-alpha* (*ef1a*) (geNorm M = 0.34) were selected as the two endogenous controls.

Endogenous control selection was followed by the experimental RT-qPCR analyses. cDNA representing 4 ng of input RNA was used as a template in the PCR reactions. On each plate, for every sample, the selected genes and endogenous controls were tested in triplicate, and a non-template control was included. The relative quantity (RQ) of each transcript was determined using the QuantStudio Real-Time PCR Software (version 1.3) (Applied Biosystems), where Ct values

were normalized with both *etf3d* and *ef1a* with amplification efficiencies incorporation. For each target of interest (TOI), the sample with the lowest normalized expression (mRNA) level was set as the calibrator sample (i.e., assigned an RQ value = 1.0).

To compare the TPM to the RQ values, the $\log_2$ normalized values were utilized. Statistical regression analyses and data visualization were performed using GraphPad Prism 7.0.

2.4 Results

2.4.1 LD_{50} determination and A. salmonicida infection kinetics in lumpfish

Five groups of 60 fish (duplicated tanks, total n = 600) were injected with five different doses of *A. salmonicida* J223 (10^1, 10^2, 10^3, 10^4, and 10^5 CFU/dose) to determine the LD_{50} and infection kinetics (Figure 2.3A). After 3 dpi, lack of appetite, erratic swimming, and internal hemorrhagic septicemia were observed. Fish started to die at 7–10 dpi, and there was no survival in the fish infected with the 10^3, 10^4, and 10^5 CFU/dose. Thirty-two percent of lumpfish survived after the infection with 10^2 CFU/dose (Figure 2.3A). In contrast, 93% of fish survived after the infection with the lowest dose tested (10^1 CFU/dose) (Figure 2.3A). The survivors and the non-infected control fish showed no symptoms of disease or mortality. The LD_{50} for *A. salmonicida* J223 in lumpfish was 187 CFU/dose according to the Reed and Muench method [39] and 273 CFU/dose according to the Karber method [40]. According to the log-rank (Mantel-Cox) test and log-rank test for trend, the survival curves and the trend were significantly different ($p < 0.0001$).

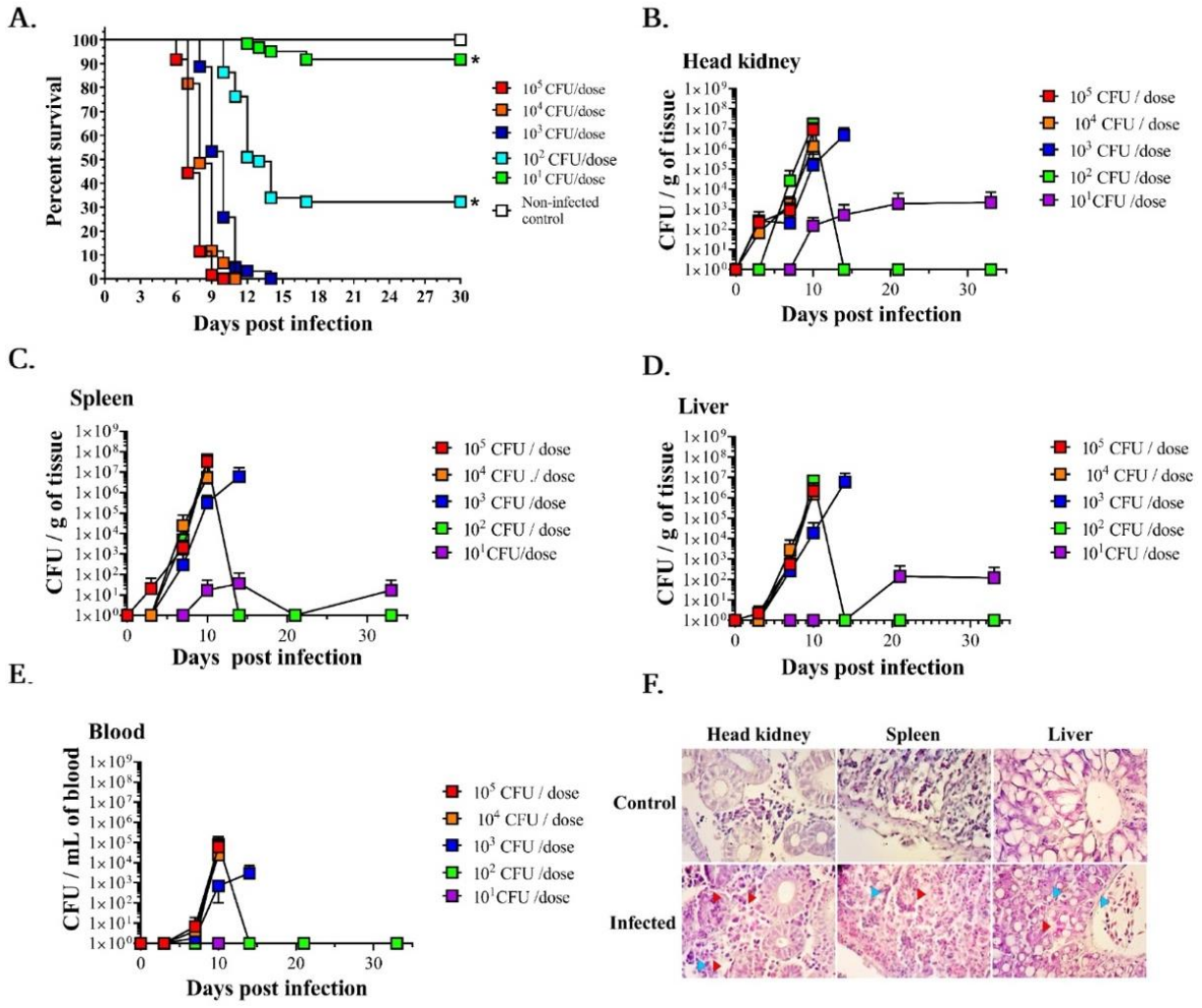

Figure 2.3. ***Aeromonas salmonicida*** **infection kinetics in lumpfish**. A. Survival of lumpfish to *A. salmonicida* infection. Lumpfish were ip injected with 5 different doses of *A. salmonicida* ranging from 1.1×10^1 to 1.1×10^5 CFU/dose. The survival percentage of lumpfish infected with these different doses were 93%, 32%, 0%, 0%, and 0% at 30 dpi, respectively; B-E. *A. salmonicida* colonization in the lumpfish lymphoid organs (head kidney, spleen, and liver) and blood at 3, 7, 10, 21, 33 dpi; B. *A. salmonicida* colonization in head kidney; C. *A. salmonicida* colonization in spleen; D. *A. salmonicida* colonization in liver; E. *A. salmonicida* colonization in blood. *:

indicates a significant statistical difference ($p < 0.05$); F. Histopathology of lumpfish tissues stained with hematoxylin and eosin. Lumpfish tissues were collected from control fish and infected fish (1.1×10^4 CFU/dose) and imaged from the stained slides under the light microscope (x 400). Blue and red arrows indicate inflammatory cells and necrosis, respectively.

A. salmonicida colonization was determined at 0, 3, 7, 10, 14, 21, and 33 dpi in different tissues (Figure 2.3B-2.3E). *A. salmonicida* was detected in the head kidney at 3 dpi in fish infected with 10^3–10^5 CFU/dose, but not when infected with 10^1–10^2 CFU/dose. I did not observe bacterial colonization in the liver, spleen, and blood at 3 dpi in lumpfish injected with the lowest doses (10^1–10^4 CFU/dose) (Figure 2.3C-2.3E). In contrast, a few fish infected with the 10^5 CFU/dose showed bacterial colonization in the spleen and liver at 3 dpi (Figure 2.3C-2.3D). *A. salmonicida* was first detected in blood at 7 dpi (Figure 2.3E). At 7 dpi, head kidney, spleen, and liver showed bacterial colonization in all doses tested except in the lowest doses evaluated (10^1 and 10^2 CFU/dose) (Figure 2.3B-D). At 10 dpi, bacterial colonization was detected in all the tissues except for the fish infected with 10^1 CFU/dose (Figure 2.3B-1E). Significant differences between bacterial loads were observed only in the spleen samples of the fish infected with 10^5 CFU/dose compared to the other groups ($p < 0.003$). At 14 dpi, 3 fish infected with the 10^3 CFU/dose showed bacterial colonization in all tissues sampled (Figure 2.3B-2.3E). After 15 dpi, no bacteria were detected in the remaining survivors in the 10^2 CFU/dose infected group. However, *A. salmonicida* was detected in the head kidney, spleen, and liver until 33 dpi in fish infected with 10^1 CFU/dose. These results suggest that *A. salmonicida* targets the head kidney and disseminates to other organs, causing a systemic infection.

Histopathological analysis indicated that *A. salmonicida* caused inflammation and tissue necrosis in head kidney, spleen, and liver (Figure 2.3F). Previously, intracellular *A. salmonicida*

was observed in lumpfish tissues at 3 and 10 dpi [70], and similar observations were determined in the current study.

2.4.2 Quality statistics

RNA samples were collected from the head kidney, spleen, and liver of triplicated non-infected control lumpfish and infected lumpfish (10^4 CFU/dose) at 3 and 10 dpi (Figure 2.1). RNA qualities are presented in table 2.1 and figure 2.2A-C. RNA sequencing generated 1.08 billion Illumina NovaSeq reads ranging from 66-95 million raw reads per sample, with an average length of 101 bp (Table 2.3). Transcriptome sequencing generated an average of 79,705,149 ± 7,628,565 paired-end reads. After trimming, reads were applied to reference genome-guided transcriptome assembly and *de novo* transcriptome assembly analysis (Figure 2.1). Qualities of the trimmed reads are presented in figure 2.2D.

Table 2.3. Trimming and mapping statistics.

Experimental conditions	Number of reads before trim	Number of reads after trim	Percentage trimmed (%)	Number of mapped reads	% of mapped reads
Control Head kidney1	90,833,894	89,460,642	98.49	88,772,934	99.23
Control Head kidney 2	82,357,896	81,214,335	98.61	80,651,238	99.30
Control Head kidney 3	95,840,032	94,471,719	98.57	93,794,340	99.28
3 dpi Head kidney 1	85,364,678	84,249,691	98.69	83,689,892	99.33
3 dpi Head kidney 2	69,166,462	68,321,181	98.78	67,915,962	99.40
3 dpi Head kidney 3	83,210,266	82,006,542	98.55	81,417,744	99.28
10 dpi Head kidney 1	74,687,068	73,641,866	98.60	80,640,940	109.5
10 dpi Head kidney 2	75,696,762	74,572,712	98.52	73,123,686	98.05
10 dpi Head kidney 3	83,134,430	81,500,846	98.04	74,020,234	90.82
Control Liver1	75,238,962	74,186,108	98.60	73,667,016	99.30
Control Liver 2	82,613,962	81,592,390	98.76	81,097,032	99.39
Control Liver 3	89,149,382	87,873,344	98.57	87,249,434	99.28
3 dpi Liver 1	73,482,382	72,624,442	98.83	72,205,844	99.42
3 dpi Liver 2	76,781,706	75,902,586	98.86	75,475,798	99.43
3 dpi Liver 3	78,365,294	77,336,892	98.69	76,810,090	99.31
10 dpi Liver 1	66,590,420	65,684,895	98.64	73,681,162	112.17
10 dpi Liver 2	84,053,066	82,945,239	98.68	72,873,446	87.85
10 dpi Liver 3	72,837,270	71,790,152	98.56	69,948,408	97.43

Experimental conditions	Number of reads before trim	Number of reads after trim	Percentage trimmed (%)	Number of mapped reads	% of mapped reads
Control Spleen1	82,894,516	81,638,490	98.48	81,023,884	99.24
Control Spleen 2	85,830,500	84,711,276	98.70	84,168,702	99.35
Control Spleen 3	80,510,892	79,352,845	98.56	78,781,698	99.28
3 dpi Spleen 1	67,505,126	66,241,078	98.13	65,565,504	98.98
3 dpi Spleen 2	95,481,322	94,028,713	98.48	93,300,368	99.22
3 dpi Spleen 3	79,665,640	78,523,117	98.57	77,967,908	99.29
10 dpi Spleen 1	75,150,950	74,159,068	98.68	65,230,402	87.96
10 dpi Spleen 2	74,330,220	73,364,626	98.70	82,383,274	112.29
10 dpi Spleen 3	71,265,916	70,388,130	98.77	71,286,900	101.27

2.4.3 Global profile of differentially expressed genes and transcripts identified using reference genome-guided transcriptome assembly

To study the lumpfish response to *A. salmonicida* infection, I profiled the global gene expression of the head kidney, spleen, and liver at 3 and 10 dpi, compared to non-infected fish using RNA-Seq. A global gene expression correlation analysis showed a high degree of correlation (R^2 = 0.89 to 0.98; $p < 0.0001$) between different experimental conditions (Figure 2.4). Principal component analysis (PCA) and heatmap results reveal a clear tissue and time point clusterization (Figures 2.5 and 2.6). Among all the organs studied, the spleen has the clearest clusterization (Figure 2.6).

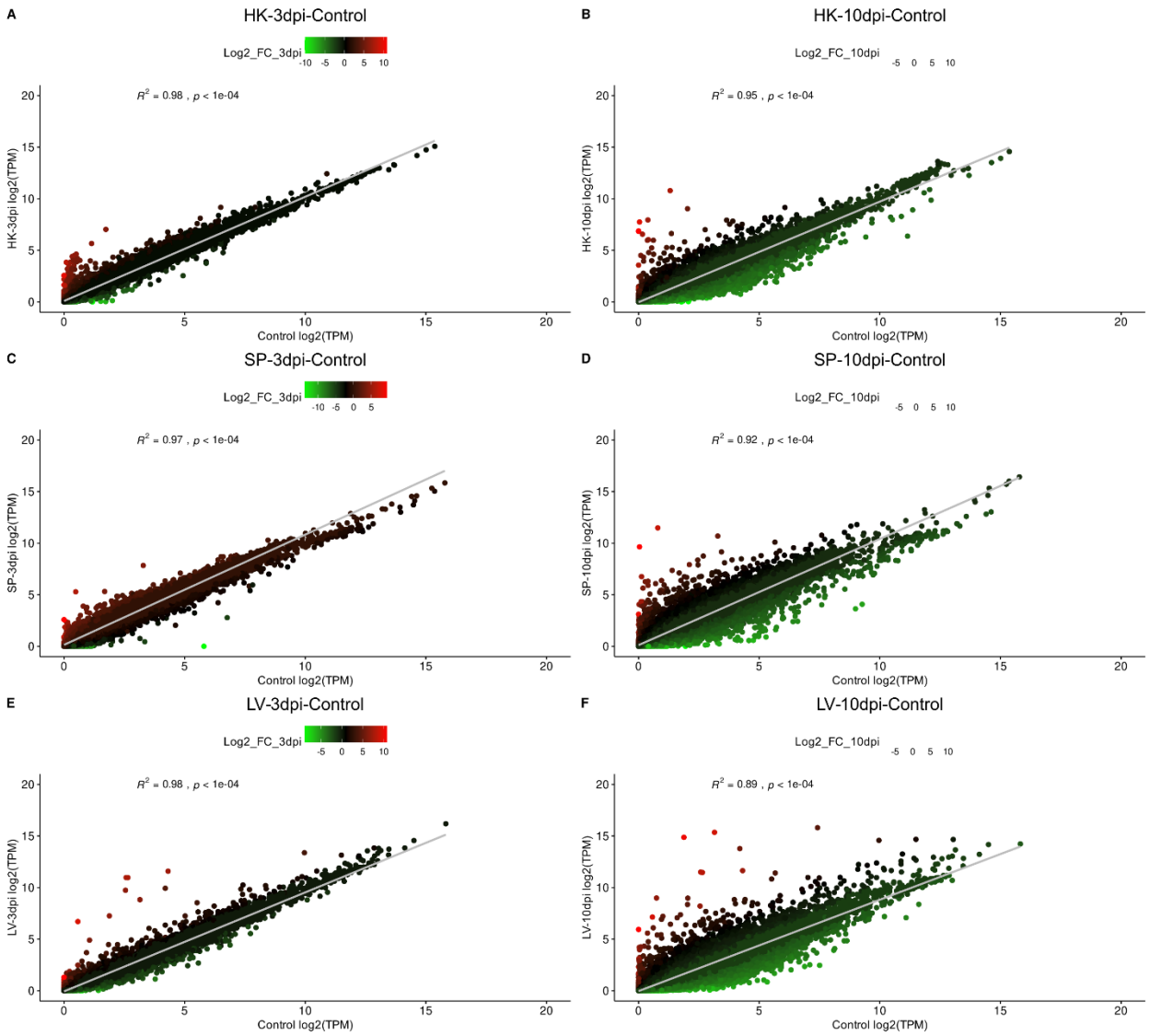

Figure 2.4. Global gene expression profile of different lumpfish organs infected with *A. salmonicida*. A. Scatter plot of RNA-Seq expression in head kidney 3 dpi; B. Scatter plot of RNA-Seq expression in head kidney 10 dpi; C. Scatter plot of RNA-Seq expression in spleen 3 dpi; D. Scatter plot of RNA-Seq expression in spleen 10 dpi; E. Scatter plot of RNA-Seq expression in liver 3 dpi; F. Scatter plot of RNA-Seq expression in liver 10 dpi. Each dot represents a gene, where red, green, and black represent upregulated, downregulated, and non-differentially expressed genes. HK: head kidney, SL: spleen, LV: liver.

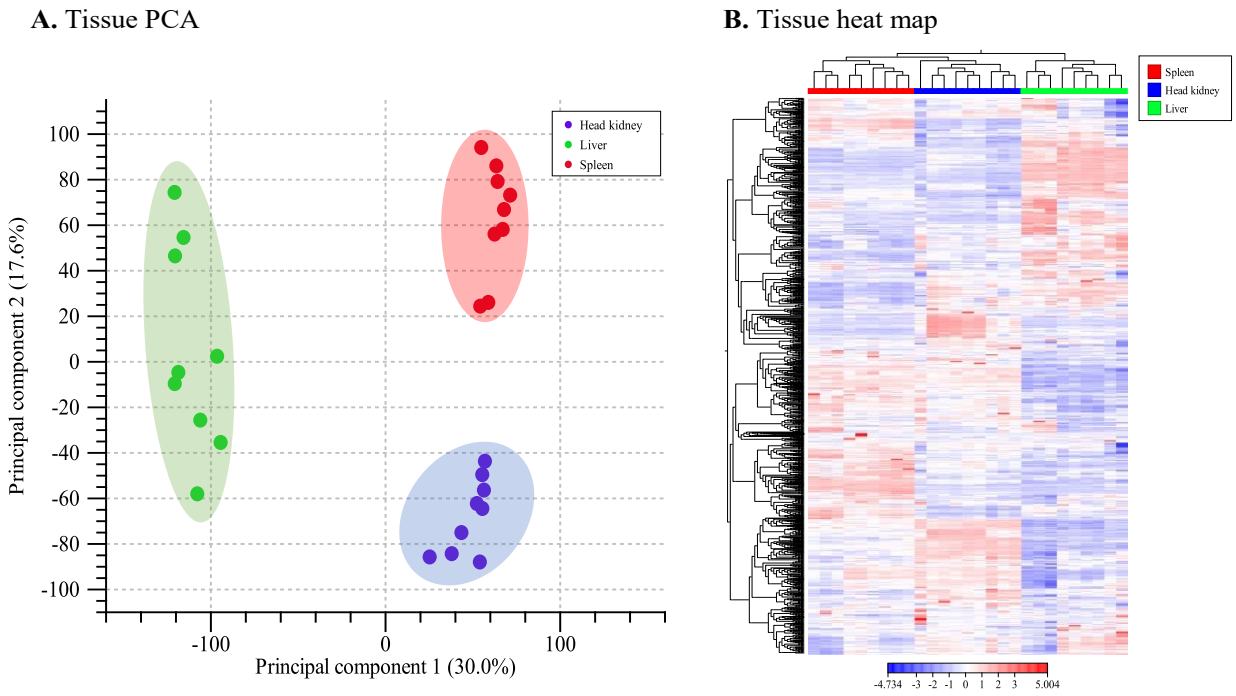

Figure 2.5. Clusterization of gene expression profile in different lumpfish organs infected *A. salmonicida*. A. Principal component analysis (PCA) of lumpfish head kidney, spleen, and liver; blue dot represents nine head kidney tissue samples, red dot represents nine spleen tissue samples, green dot represents nine liver tissue samples; B. Heatmap of differentially expressed genes in head kidney (blue), spleen (red), and liver (green) of lumpfish infected with *A. salmonicida* compared with non-infected control.

.

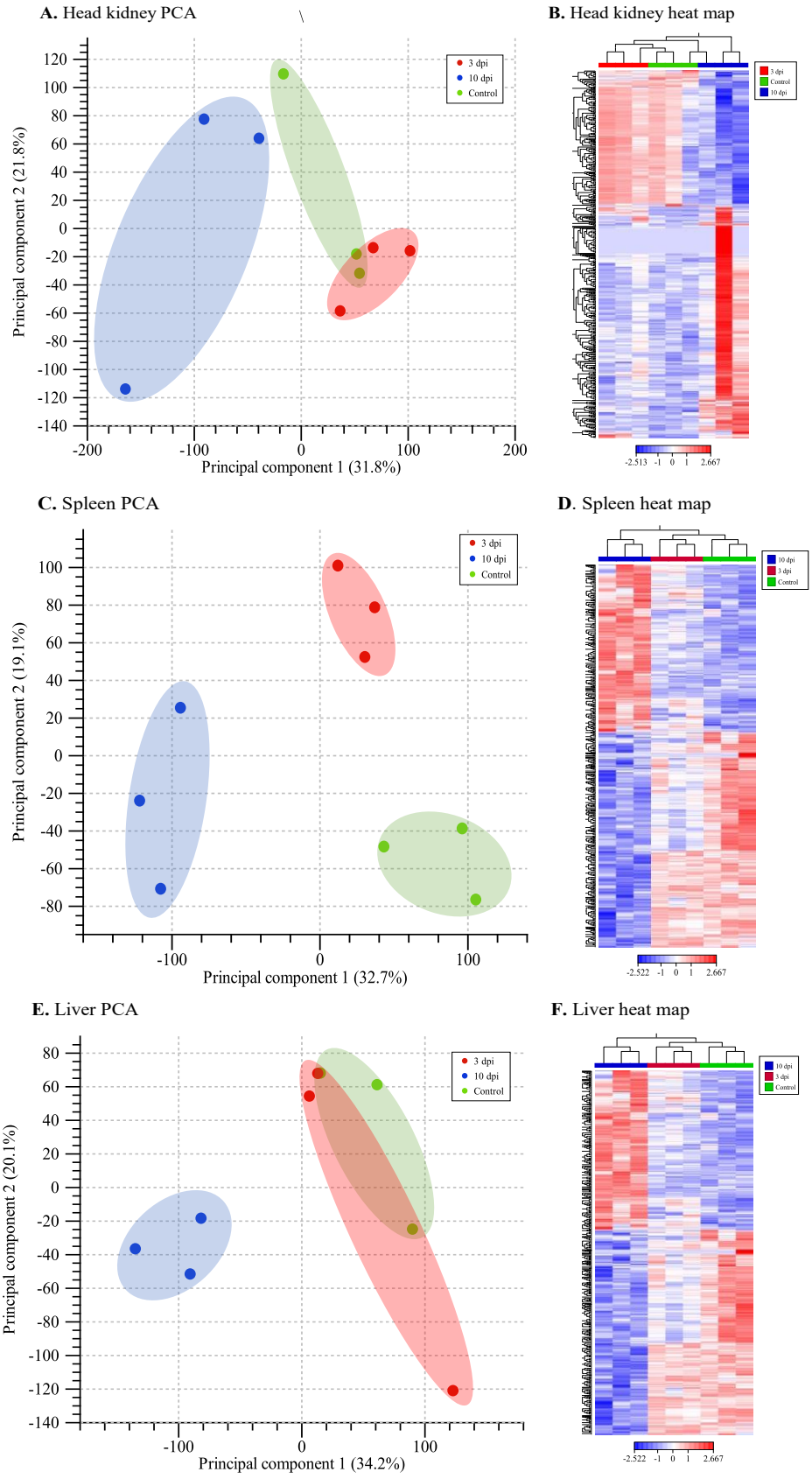
A. Head kidney PCA
B. Head kidney heat map
3 dpi
10 dpi
Control
Principal component 2 (21.8%)
Principal component 1 (31.8%)
C. Spleen PCA
D. Spleen heat map
Principal component 2 (19.1%)
Principal component 1 (32.7%)
E. Liver PCA
F. Liver heat map
Principal component 2 (20.1%)
Principal component 1 (34.2%)

Figure 2.6. Clusterization of gene expression profile in different lumpfish organs infected *A. salmonicida*. A. Principal component analysis (PCA) of lumpfish head kidney samples, green dot represents three control samples, red dot represents three 3 dpi samples, blue dot represents three 10 dpi samples; B. Heatmap of lumpfish head kidney infected with *A. salmonicida* compared with non-infected control; C. PCA of lumpfish spleen samples, green dot represents three control samples, red dot represents three 3 dpi samples, blue dot represents three 10 dpi samples; D. Heatmap of lumpfish spleen infected with *A. salmonicida* compared with non-infected control; E. PCA of lumpfish liver samples, green dot represents three control samples, red dot represents three 3 dpi samples, blue dot represents three 10 dpi samples; F. Heatmap of lumpfish liver infected with *A. salmonicida*.

The $\log_2$ fold-change (FC) ≤ -1.0 or ≥ 1.0 and FDR adjusted *p*-value of ≤ 0.05 were set as the cut-off criteria for sorting out significant differentially expressed genes. I found 102 DEGs in the head kidney at 3 dpi. These DEGs included 94 upregulated and 8 downregulated genes (Table 2.4, Figure 2.7A). Also, 1922 DEGs were identified in the head kidney at 10 dpi. These DEGs included 530 upregulated and 1392 downregulated genes (Table 2.4, Figure 2.7A). In the spleen, 637 DEGs were identified at 3 dpi, including 253 upregulated and 384 downregulated genes (Table 2.4, Figure 2.7B). In the spleen, 3133 DEGs were identified at 10 dpi, including 1368 upregulated and 1765 downregulated genes (Table 2.4, Figure. 2.7B). In the liver, 58 DEGs were identified at 3 dpi. These DEGs included 44 upregulated and 14 downregulated genes (Table 2.4, Figure 2.7C). Also, 2766 DEGs were identified in the liver at 10 dpi, including 1360 upregulated and 1406 downregulated genes (Table 2.4, Figure 2.7C). Gene identifier, description/annotation, fold-change, and FDR adjusted *p*-value are listed in File S2.1. A comparison between the head kidney, spleen, and liver 3 and 10 dpi showed that 309 DEGs were common to all organs, while the head kidney and the spleen shared 373 DEGs, the head kidney and the liver shared 196 DEGs, and the spleen and the liver shared 738 DEGs (Figure 2.7D).

Table 2.4. Differentially expressed genes (DEGs) identified by reference transcriptome assembly.

Tissues	Days post-infection (dpi)	Upregulated genes	Downregulated genes	Total DEGs
Head kidney	3	94	8	102
Head kidney	10	530	1392	1922
Spleen	3	253	384	637
Spleen	10	1368	1765	3133
Liver	3	44	14	58
Liver	10	1360	1406	2766

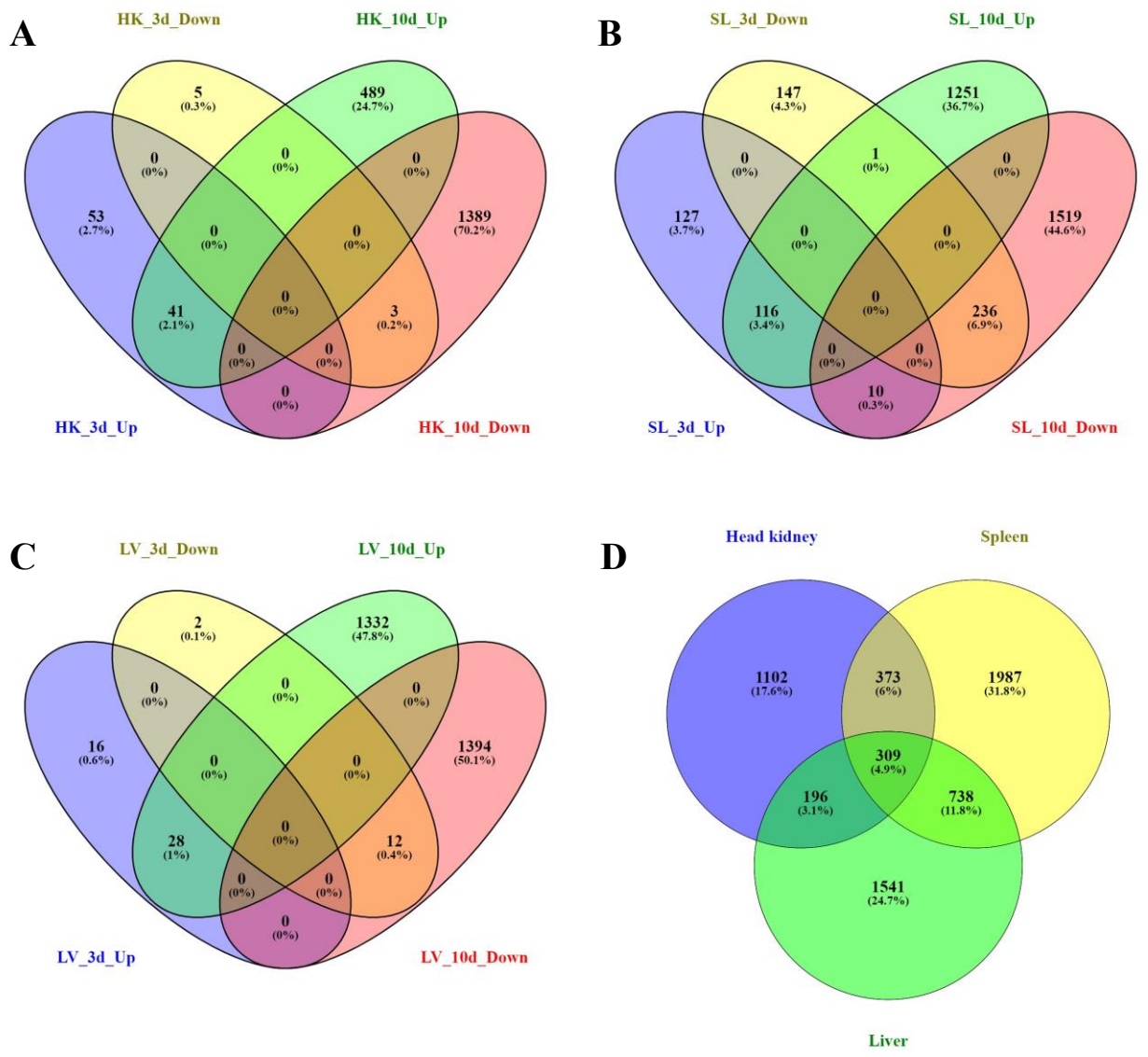

Figure 2.7. Gene expression profile comparison. A. Venn diagram of upregulated (Up) and downregulated (Down) DEGs ($log_2FC \leq -1.0$ or ≥ 1.0, FDR ≤ 0.05) in head kidney (HK) at 3 and 10 dpi; B. Venn diagram of upregulated (Up) and downregulated (Down) DEGs ($log_2FC \leq -1.0$ or ≥ 1.0, FDR ≤ 0.05) in spleen (SL) at 3 and 10 dpi; C. Venn diagram of upregulated (Up) and downregulated (Down) DEGs ($log_2FC \leq -1.0$ or ≥ 1.0, FDR ≤ 0.05) in the liver (LV) at 3 and 10 dpi; D. Venn diagram of all DEGs ($log_2FC \leq -1.0$ or ≥ 1.0, FDR ≤ 0.05) in head kidney, spleen, and liver.

Similarly, the $\log_2$FC ≤ -1.0 or ≥ 1.0 and FDR adjusted *p*-value of ≤ 0.05 were set as the cut-off criteria for sorting out significant DETs. I identified 133 DETs in the head kidney at 3 dpi, including 89 upregulated and 44 downregulated transcripts (Table 2.5). Also, 699 DETs were identified in the head kidney at 10 dpi, including 451 upregulated and 248 downregulated transcripts (Table 2.5). In the spleen, 614 DETs were identified at 3 dpi, including 237 upregulated and 377 downregulated transcripts (Table 2.5). In the head kidney, 2152 DETs were identified at 10 dpi, including 1173 upregulated and 979 downregulated transcripts (Table 2.5). In the liver, 33 DETs were identified at 3 dpi, including 27 upregulated and six downregulated genes (Table 2.5). Also, 1697 DETs were identified in the liver at 10 dpi, including 887 upregulated and 810 downregulated transcripts (Table 2.5). Gene identifier, fold-change, and FDR adjusted *p*-value are listed in File S2.2.

Table 2.5. Differentially expressed transcripts (DETs) identified by reference transcriptome assembly.

Tissues	Days post-infection (dpi)	Upregulated transcripts	Downregulated transcripts	Total DETs
Head kidney	3	89	44	133
Head kidney	10	451	248	699
Spleen	3	237	377	614
Spleen	10	1173	979	2152
Liver	3	27	6	33
Liver	10	887	810	1697

2.4.4 Global profile of differentially expressed transcripts identified by de novo transcriptome assembly analysis

To identify potential novel genes and transcripts, a *de novo* transcriptome analysis was conducted. Quality filtering and trimming were performed by Trimmomatic, and approximately

4.28% of the raw reads were removed (Table 2.6). The remaining high-quality reads (originating from the three different lymphoid tissues) were used to build a *de novo* transcriptome assembly using Trinity v2.8.4 assembler.

Table 2.6. Trinity statistics.

Total trinity transcripts	403,204
Total trinity genes	270,150
Percent GC	45.99
Contig N10	9165
Contig N20	6690
Contig N30	5231
Contig N40	4164
Contig N50	3235
Median contig length	497
Average contig	1296.15
Total assembled bases	522,614,427

The *de novo* assembly resulted in 403,204 transcripts with an average read length of 497 bp, representing 270,150 genes identified by Trinity (Table 2.6). The total length of all assembled transcripts is 522,614,427 bp with an N50 length of 3235 bp and GC content of 46%. I found that more than 98% of the reads were successfully aligned consistently for each sample (Table 2.7). Coding transcripts assessment was performed using the blastx search program in the database NCBI, RefSeq RNA, and SwissProt [71, 72].

Table 2.7. Alignment statistics.

Sample name	Aligned concordantly exactly 1 time	Aligned concordantly >1 times	Overall alignment rate (%)
Control Head kidney1	6056815 (14%)	33309331 (76.98%)	97.92
Control Head kidney 2	5561239 (14.17%)	30303899 (77.21%)	97.99
Control Head kidney 3	5823611 (12.66%)	36266811 (78.81%)	98.2
3 dpi Head kidney 1	5995555 (14.67%)	31412470 (76.87%)	97.79
3 dpi Head kidney 2	4668466 (14.02%)	26009476 (78.11%)	98.16
3 dpi Head kidney 3	5534685 (13.99%)	30610945 (77.4%)	97.93
10 dpi Head kidney 1	6204518 (15.73%)	28809529 (73.06%)	96.6
10 dpi Head kidney 2	4851800 (13.56%)	27816099 (77.73%)	97.66
10 dpi Head kidney 3	4818814 (13.3%)	28270093 (78.02%)	98.01
Control Spleen1	4935796 (13.74%)	27895313 (77.64%)	97.95
Control Spleen 2	4769616 (11.99%)	31464709 (79.13%)	98.33
Control Spleen 3	5384352 (12.62%)	33497395 (78.51%)	98.1
3 dpi Spleen 1	5420901 (15.39%)	26700202 (75.8%)	97.82
3 dpi Spleen 2	5093933 (13.8%)	28863984 (78.17%)	98.12
3 dpi Spleen 3	5421149 (14.45%)	28750313 (76.62%)	97.88
10 dpi Spleen 1	5355795 (14.93%)	27159109 (75.71%)	97.73
10 dpi Spleen 2	5198840 (14.71%)	26876759 (76.07%)	97.81
10 dpi Spleen 3	5145686 (15.11%)	25916830 (76.1%)	97.83
Control Liver1	4775243 (12.14%)	31337959 (79.64%)	98.18
Control Liver 2	5060475 (12.24%)	33095542 (80.03%)	98.29
Control Liver 3	3988922 (10.35%)	31537686 (81.8%)	98.49
3 dpi Liver 1	3499716 (10.92%)	25588309 (79.87%)	97.92
3 dpi Liver 2	4756240 (10.41%)	37275425 (81.56%)	98.44
3 dpi Liver 3	5063196 (10.72%)	38469695 (81.42%)	98.67
10 dpi Liver 1	3473492 (10.91%)	25995568 (81.64%)	98.55
10 dpi Liver 2	4197048 (10.44%)	33072408 (82.25%)	98.52
10 dpi Liver 3	3454200 (9.93%)	28709153 (82.54%)	98.5

I further evaluated the completeness of the transcriptome assembly using BUSCO. BUSCO pipeline for gene set completeness was assessed for eukaryotes (n = 303), vertebrates (n = 2586), and actinopterygian (n = 4584). The analysis reported that the majority of the actinopterygian core genes had been successfully recovered from the lumpfish *de novo* assembly. Specifically, of the 4584 single-copy orthologs searched, ~88% were completely recovered, and ~4% were partially recovered. Only ~8% of single-copy orthologs were classified as missing in the assembly. This data indicates a complete, consistent, high-quality lumpfish transcriptome assembly (Figure 2.8).

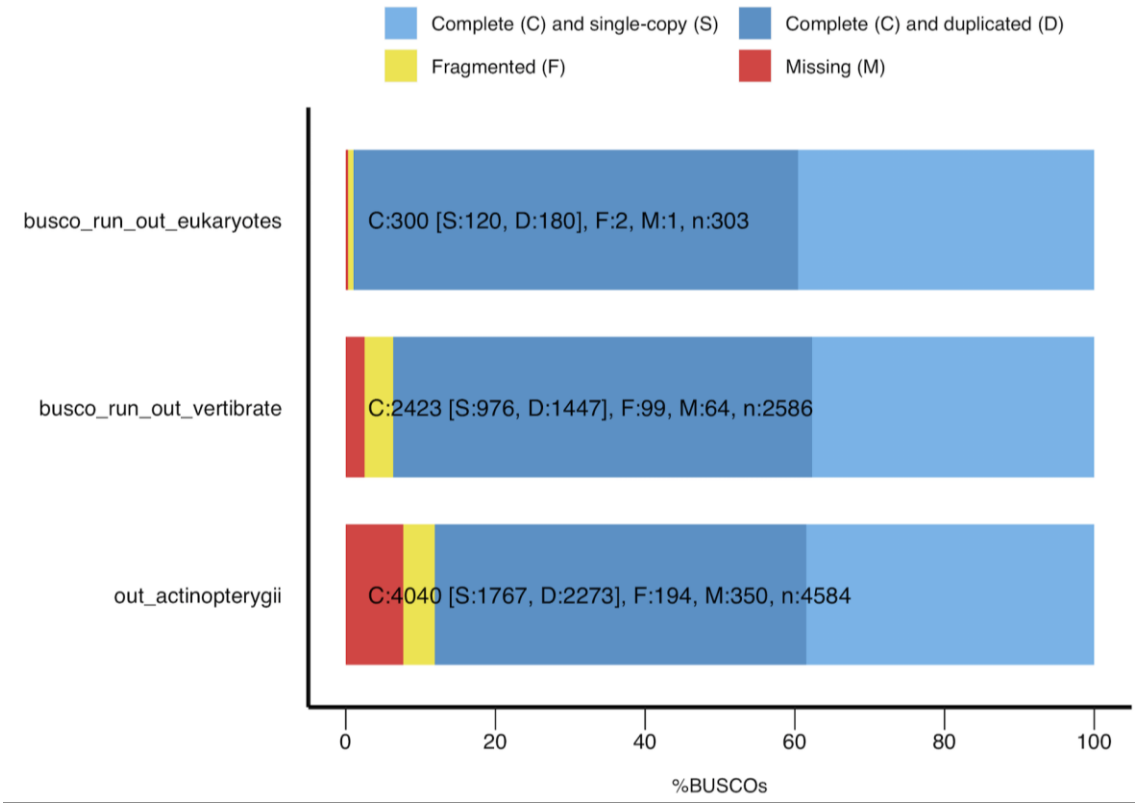

Figure 2.8. Quality of transcriptome assembly. BUSCO pipeline for gene set completeness was assessed for eukaryotes (n = 303), vertebrates (n = 2586), and actinopterygian (n = 4584). Here, ~88% actinopterygian core genes were completely recovered, while only ~8% of single-copy orthologs were classified as missing from the assembly. This data indicates a reasonably complete, consistent, and high-quality lumpfish transcriptome assembly.

DETs identified from the three lymphoid tissues at different time points are summarized in File S2.3. The lists of DETs identified by DESeq2 were generally higher and were almost accommodated within the edgeR DETs lists. I used the more conservative edgeR-generated DETs for further analysis (Table 2.8). The $\log_2$ fold-change (FC) ≤ -1.0 or ≥ 1.0 and FDR adjusted *p*-value of ≤ 0.05 were set as the cut-off criteria for sorting out significant DETs.

Table 2.8. Differentially expressed transcripts (DETs) identified by *de novo* transcriptome assembly.

Tissues	Days post-infection (dpi)	edgeR upregulated transcripts	edgeR downregulated transcripts	Total DETs
Head kidney	3	138	148	286
Head kidney	10	204	273	477
Spleen	3	214	287	501
Spleen	10	1005	1410	2415
Liver	3	56	77	133
Liver	10	1053	1040	2093

My analysis found 286 DETs in the head kidney 3 dpi. These DETs included 138 upregulated and 148 downregulated transcripts (Table 2.8, Figure 2.9A). 477 DETs were identified at 10 dpi, including 204 upregulated and 273 downregulated transcripts (Table 2.8, Figure 2.9A). 501 DETs were identified in spleen 3 dpi, including 214 upregulated and 287 downregulated transcripts (Table 2.8, Figure 2.9B). In the spleen, 2415 DETs were identified at 10 dpi. These DETs included 1005 upregulated and 1410 downregulated transcripts (Table 2.8, Figure 2.9B.). 133 DETs were identified in liver 3 dpi. These DETs included 56 upregulated and 77 downregulated transcripts (Table 2.8, Figure 2.9C). In liver, 2093 DETs were identified at 10 dpi. These DETs included 1053 upregulated and 1040 downregulated transcripts (Table 2.8, Figure 2.9C). A comparison between the head kidney, spleen, and liver showed that 56 DETs are common in all organs, while the head kidney and spleen share 53 DETs, the head kidney, and liver share 26 DETs, spleen and liver share 274 DETs (Figure 2.9D).

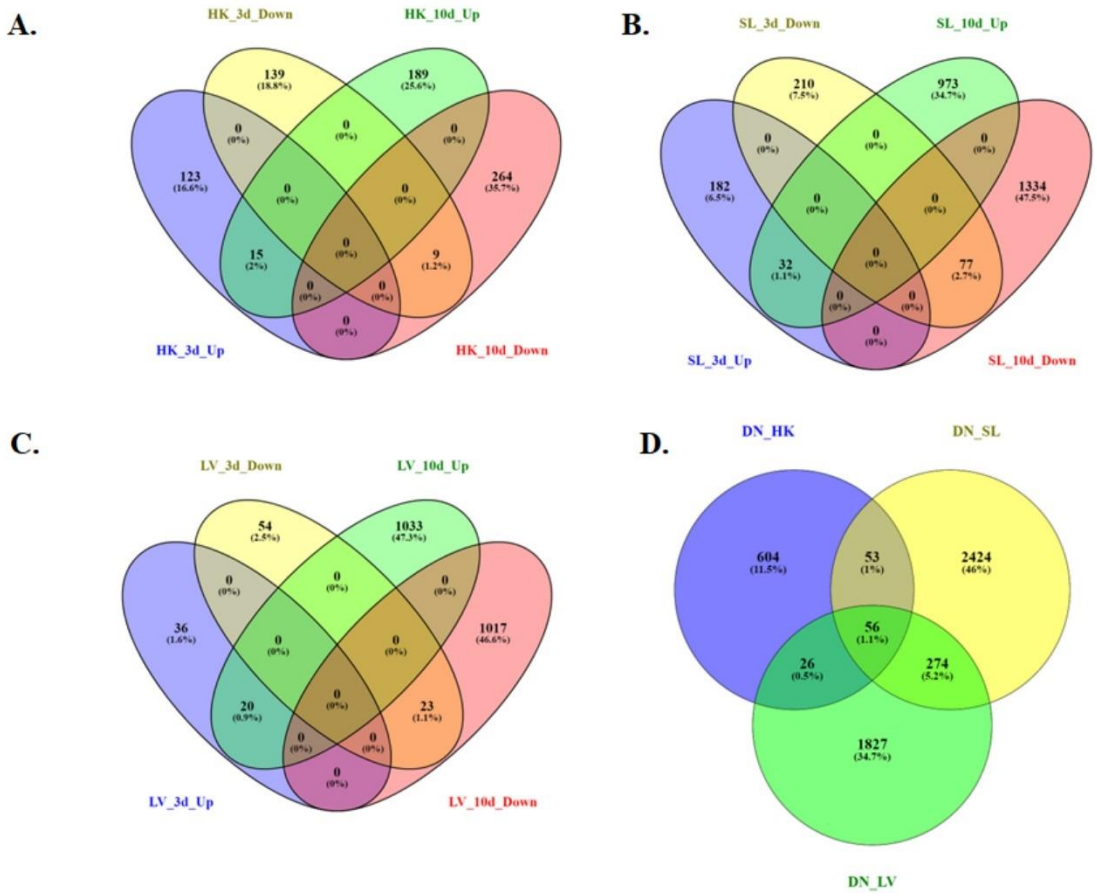

Figure 2.9. Transcripts expression profile comparison. A. Venn diagram of upregulated and downregulated DETs identified by *de novo* transcriptome assembly in head kidney at 3 and 10 dpi; B. Venn diagram of upregulated and downregulated DETs identified by *de novo* transcriptome assembly in spleen at 3 and 10 dpi; C. Venn diagram of upregulated and downregulated DETs identified by *de novo* transcriptome assembly in liver at 3 and 10 dpi; D. Venn diagram of all DETs in head kidney, spleen, and liver identified by *de novo* transcriptome assembly. DN- *de novo* transcriptome assembly. HK: Head kidney. SL: Spleen. LV: Liver. DETs: differentially expressed transcripts. Dpi: days post-infection. Filtration of DETs and DEGs are $\log_2 FC \leq -1.0$ or ≥ 1.0, FDR ≤ 0.05.

The hierarchical clustering of DETs expressed in abundance ($log_2FC \leq -5.0$ or ≥ 5.0 and FDR ≤ 0.05) visualized as in the heatmap supports the tissue and time point-specific clustering (Figure 2.10A). The heatmap also reveals that samples from uninfected lumpfish and infected animals clustered mostly within each tissue sub-cluster (Figure 2.10A). Also, I observed that the transcriptomic response was clearly separated based on infection time points in the spleen (Figure 2.10A). On the other hand, transcript responses in head kidney and liver samples from the pre-infected fish and infected fish at 3 dpi were not highly differentiated, indicating an early process of infection in these tissues (Figure 2.10A). I also assessed and visualized inter and intragroup variability using Pearson's correlation plots of correlation values between samples that agree with the hierarchical clustering analysis (Figure 2.10B).

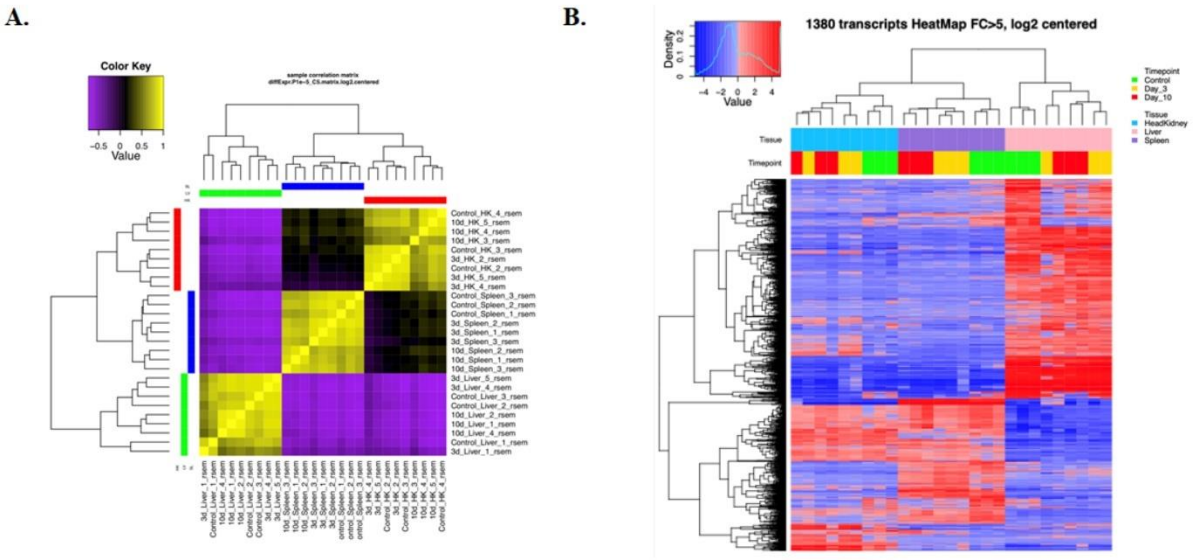

Figure 2.10. Principal component analysis, correlation analysis, and hierarchical clustering. A. Pearson's correlation plot visualizing the correlation values between samples; B. Hierarchical clustering of differentially expressed transcripts identified ($\log_2$FC ≤ -1.0 or ≥ 1.0, FDR ≤ 0.05) for each organ (head kidney, spleen, and liver) at 3 dpi and 10 dpi compared to non-infected control.

Furthermore, a blastn analysis of all DETs identified by *de novo* assembly was conducted against the lumpfish genome using Blast^{+} 2.12.0 to retrieve lumpfish gene symbols corresponding to those transcripts (File S2.4). The analysis identified 1954 genes that were common to the DEGs identified by the reference genome-guided transcriptome analysis. In total, 1307 unique genes were identified, which included 477 genes in the head kidney, 825 genes in the spleen, and 679 genes in the liver (Figure 2.11 and File S2.5). These unique genes were added to the DEGs list generated by the reference genome-guided transcriptome for GO enrichment analysis.

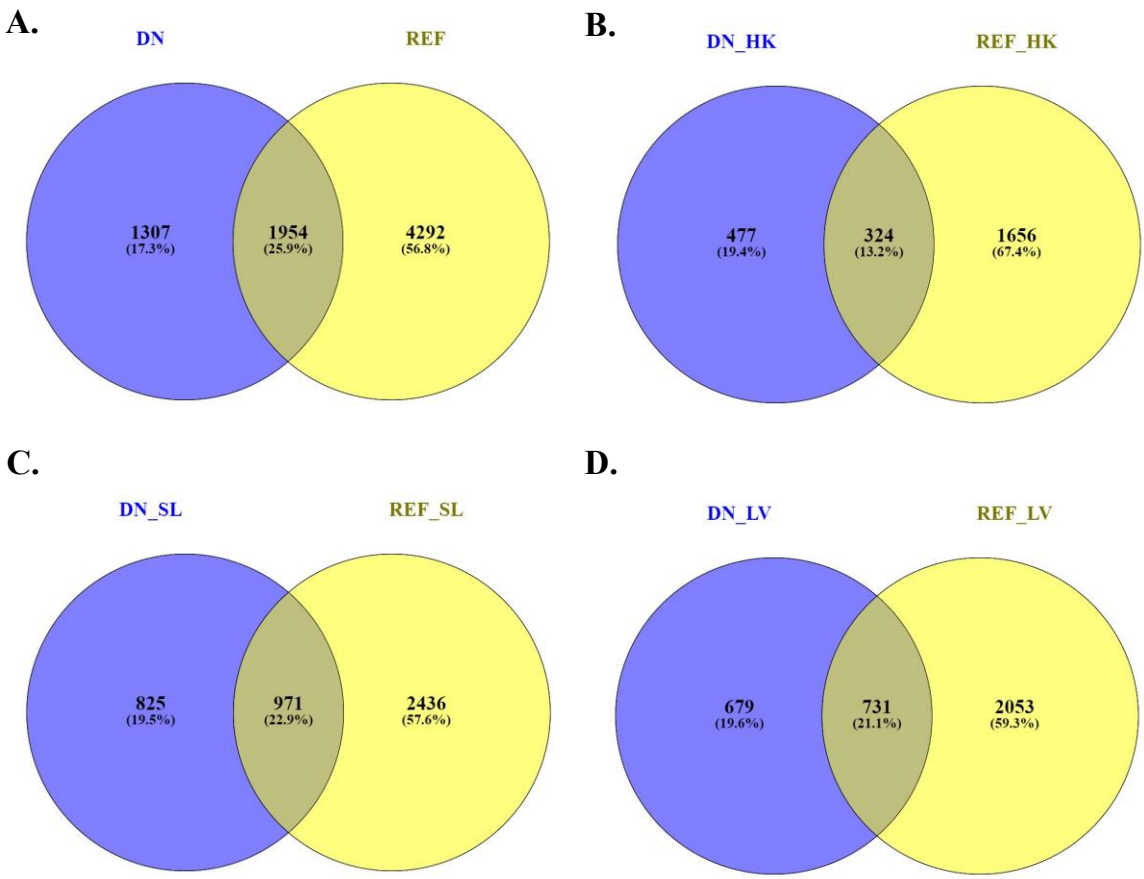

Figure 2.11. Comparison of DEGs and DETs identified by reference genome-guided and *de novo* transcriptome assembly. A. Comparison of DEGs identified by reference genome-guided and *de novo* transcriptome assembly; B. Comparison of DEGs identified by reference genome-guided and *de novo* transcriptome assembly in the head kidney; C. Comparison of DEGs identified by reference genome-guided and *de novo* transcriptome assembly in the spleen; D. Comparison of DEGs identified by reference genome-guided and *de novo* transcriptome assembly in the liver; REF: reference genome-guided transcriptome assembly. DN: *de novo* transcriptome assembly. HK: Head kidney. SL: Spleen. LV: Liver. DETs: differentially expressed transcripts. DEGs: differentially expressed genes. Filtration of DETs and DEGs are $\log_2 FC \leq -1.0$ or ≥ 1.0, FDR ≤ 0.05.

2.4.5 GO enrichment analysis

Overall, the GO enrichment analysis using a combination of all DEGs at 3 dpi and 10 dpi identified multiple enriched GO terms related to biological process (BP), molecular function (MF), and cellular component (CC) (Figure 2.12, 2.13, and File S2.6). This result suggests that nucleic acid metabolism and immune responses are mostly affected at the early point of infection. On the other hand, a lethal *A. salmonicida* infection could modulate lumpfish adaptive immune responses and metabolic processes.

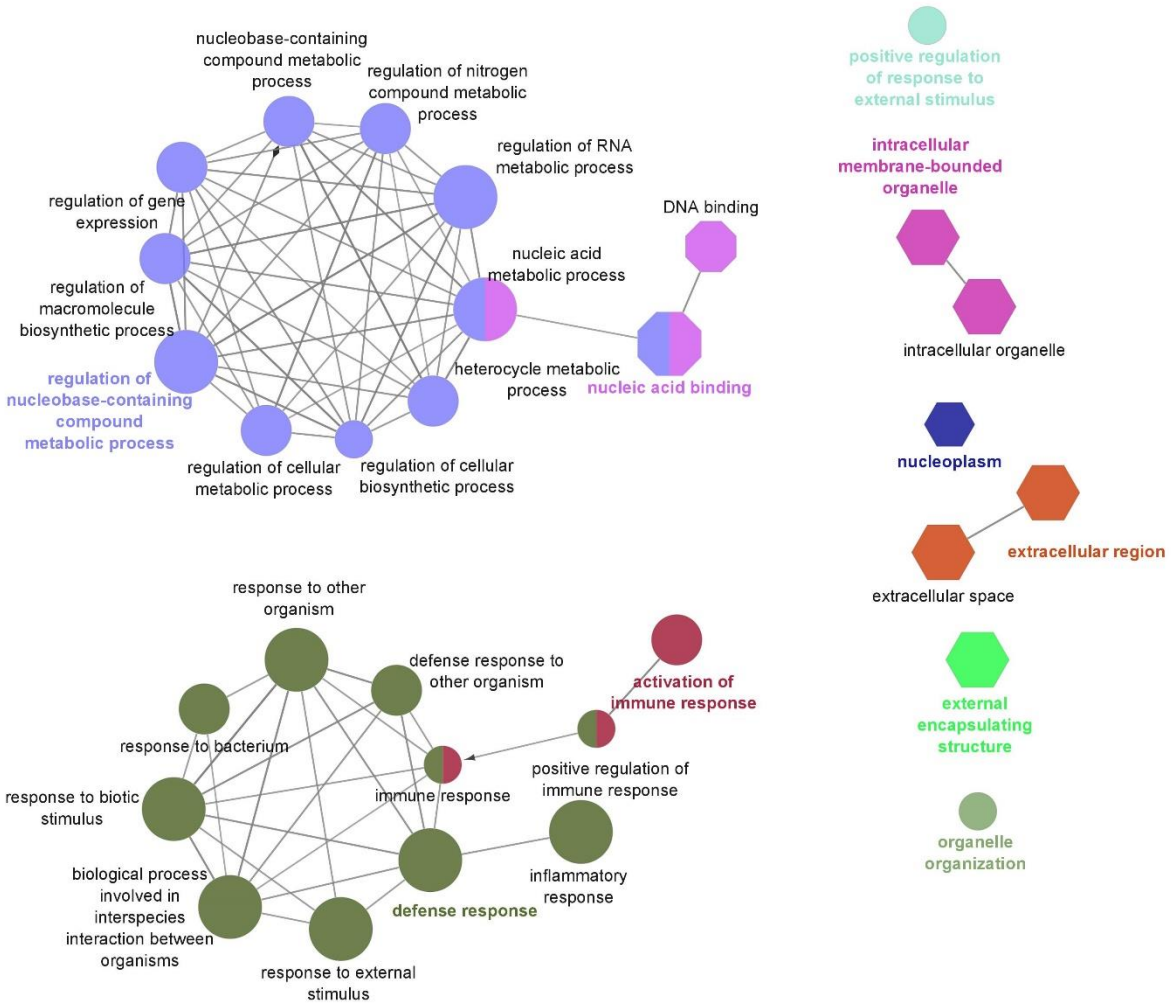

Figure 2.12. ClueGO-based enriched gene ontology (GO) terms in lumpfish lymphoid organs at 3 dpi with *A. salmonicida*. GO terms identified from DEGs in head kidney, spleen, and liver at 3 dpi. The shapes depict the database source i.e., GO biological process (ellipse), GO cellular component (hexagonal), GO molecular function (octagonal). The statistics of representative GO terms or pathways are tabulated in File S2.6.

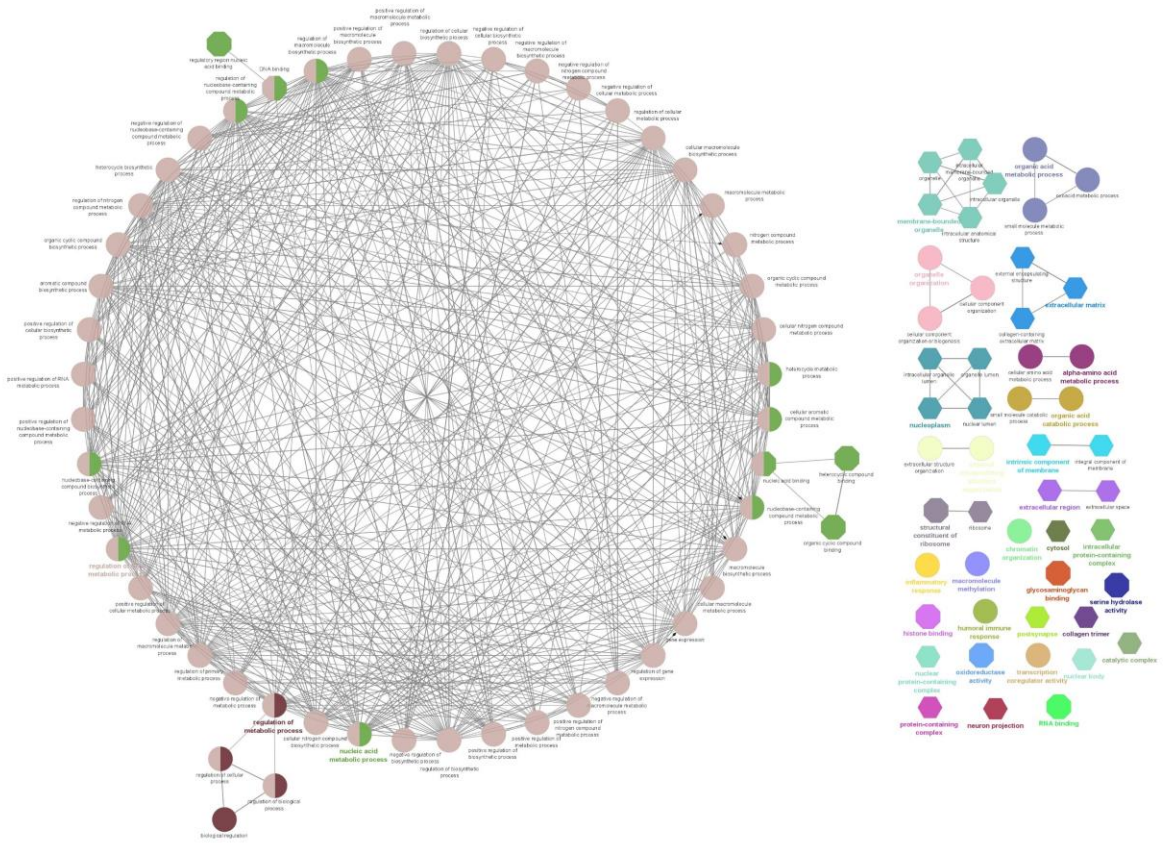

Figure 2.13. ClueGO-based enriched gene ontology (GO) terms in lumpfish lymphoid organs at 10 dpi with *A. salmonicida*. GO terms identified from DEGs in head kidney, spleen, and liver at 10 dpi. The shapes depict database source i.e., GO biological process (ellipse), GO cellular component (hexagonal), GO molecular function (octagonal). The statistics of representative GO terms or pathways are tabulated in File S2.6. High quality figure is provided in supplementary figure S2.1

The GO enrichment analysis using all DEGs in the head kidney at 3 dpi identified GO terms associated with BP (e.g., response to stimulus), MF (e.g., hydrolase activity), and CC (e.g., intracellular anatomical structure) (Figure 2.14A, File S2.6). The upregulated DEGs in the head kidney at 3 dpi were associated with acute phase response (APR), inflammatory response, complement activation, negative regulation of immune effector process, fibrin clot formation, and others (File S2.7). However, no GO terms were enriched by the downregulated DEGs of the head kidney at 3 dpi. All the DEGs of the spleen at 3 dpi showed their association with several enriched GO terms related to BP (e.g., cell adhesion, defense response, nucleic acid metabolic process), MF (DNA binding), and CC (e.g., extracellular region, external encapsulating structure) (Figure 2.14C, File S2.6). Upregulated DEGs were mostly associated with APR, complement component activation, humoral immune response, inflammatory responses, and many others (File S2.7). Downregulated DEGs of the spleen at 3 dpi were associated with ribosome assembly, cytoplasmic translation, and oxygen carrier (File S2.7). Furthermore, the DEGs of the liver at 3 dpi were only associated with response to stress (Figure 2.14E and File S2.6). Upregulated DEGs showed three enriched GO terms, such as APR, chemoattractant activity, and cellular response to interleukin-1 (File S2.7), and downregulated DEGs of the liver at 3 dpi were not associated with any GO terms.

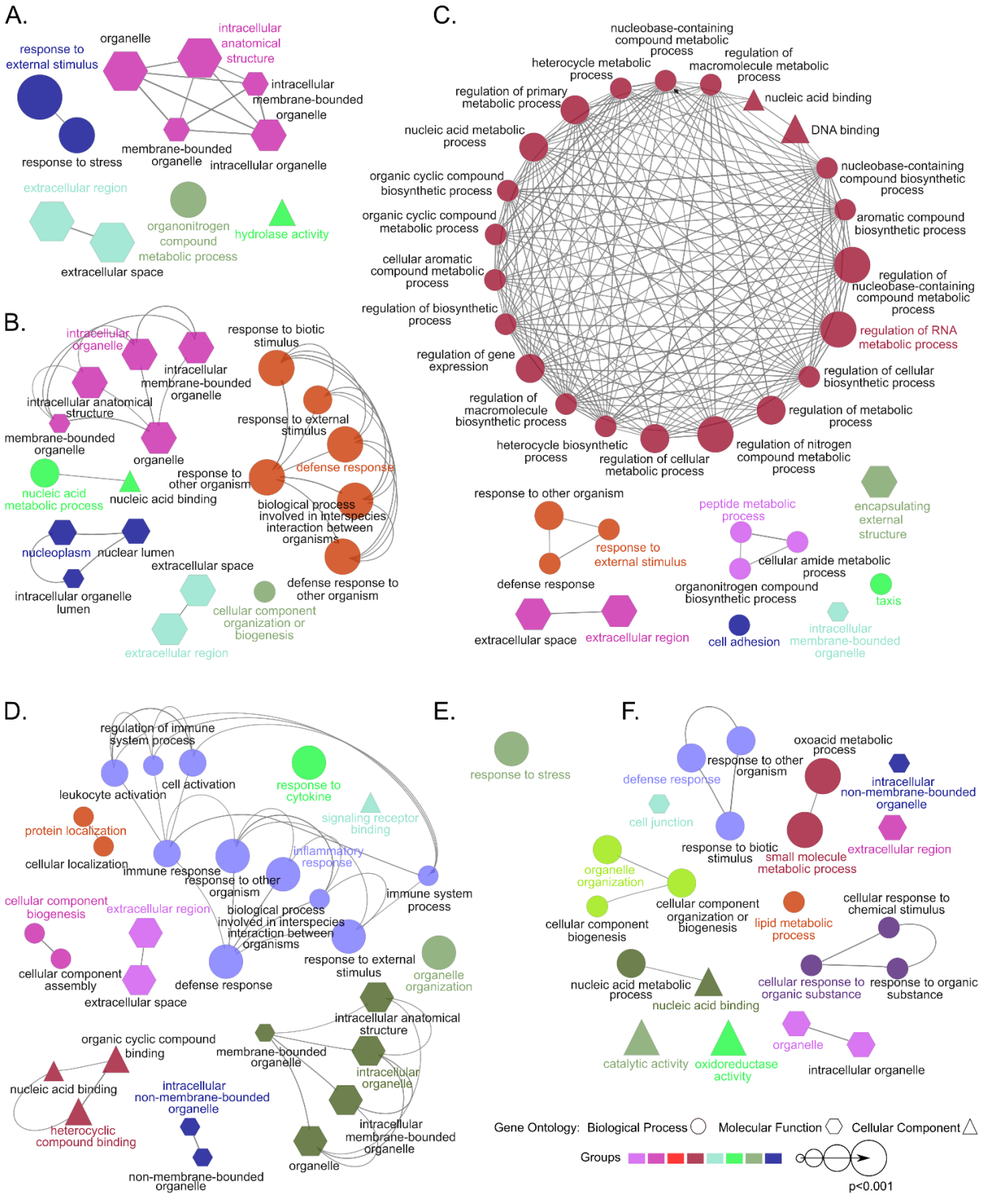
A.
organelle
intracellular anatomical structure
response to external stimulus
intracellular membrane-bounded organelle
response to stress
membrane-bounded organelle
intracellular organelle
extracellular region
organonitrogen compound metabolic process
hydrolase activity
extracellular space
B.
intracellular organelle
response to biotic stimulus
intracellular membrane-bounded organelle
intracellular anatomical structure
response to external stimulus
membrane-bounded organelle
organelle
response to other organism
defense response
nucleic acid metabolic process
nucleic acid binding
biological process involved in interspecies interaction between organisms
nucleoplasm
nuclear lumen
extracellular space
defense response to other organism
intracellular organelle lumen
cellular component organization or biogenesis
extracellular region
C.
nucleobase-containing compound metabolic process
heterocycle metabolic process
regulation of macromolecule metabolic process
regulation of primary metabolic process
nucleic acid binding
DNA binding
nucleic acid metabolic process
nucleobase-containing compound biosynthetic process
organic cyclic compound biosynthetic process
aromatic compound biosynthetic process
organic cyclic compound metabolic process
regulation of nucleobase-containing compound metabolic process
cellular aromatic compound metabolic process
regulation of RNA metabolic process
regulation of biosynthetic process
regulation of cellular biosynthetic process
regulation of gene expression
regulation of metabolic process
regulation of macromolecule biosynthetic process
heterocycle biosynthetic process
regulation of cellular metabolic process
regulation of nitrogen compound metabolic process
response to other organism
response to external stimulus
defense response
extracellular space
extracellular region
peptide metabolic process
encapsulating external structure
cellular amide metabolic process
organonitrogen compound biosynthetic process
taxis
cell adhesion
intracellular membrane-bounded organelle
D.
regulation of immune system process
cell activation
leukocyte activation
response to cytokine
signaling receptor binding
protein localization
cellular localization
immune response
inflammatory response
response to other organism
immune system process
cellular component biogenesis
extracellular region
biological process involved in interspecies interaction between organisms
response to external stimulus
organelle organization
cellular component assembly
defense response
extracellular space
intracellular anatomical structure
organic cyclic compound binding
membrane-bounded organelle
intracellular organelle
nucleic acid binding
intracellular non-membrane-bounded organelle
intracellular membrane-bounded organelle
heterocyclic compound binding
organelle
non-membrane-bounded organelle
E.
response to stress
F.
oxoacid metabolic process
response to other organism
defense response
intracellular non-membrane-bounded organelle
cell junction
response to biotic stimulus
small molecule metabolic process
extracellular region
organelle organization
cellular component organization or biogenesis
cellular response to chemical stimulus
cellular component biogenesis
lipid metabolic process
nucleic acid metabolic process
cellular response to organic substance
response to organic substance
nucleic acid binding
catalytic activity
oxidoreductase activity
organelle
intracellular organelle
Gene Ontology: Biological Process
Molecular Function
Cellular Component
Groups
p<0.001

Figure 2.14. ClueGO-based enriched gene ontology (GO) terms in lumpfish lymphoid organs. A. GO terms identified from DEGs in the head kidney at 3 dpi; B. GO terms identified from top 600 DEGs in the head kidney at 10 dpi; C. GO terms identified from DEGs in the spleen at 3 dpi; D. GO terms identified from top 600 DEGs in spleen at 10 dpi; E. GO terms identified from DEGs in liver at 3 dpi; F. GO terms identified from top 600 DEGs in liver at 10 dpi. Larger size denotes higher GO term significance. The shapes depict the database source i.e., GO biological process (ellipse), GO cellular component (hexagonal), GO molecular function (triangles). The statistics of representative GO terms or pathways are tabulated in File S2.6.

Furthermore, the 600 most significant DEGs (lowest FDR adjusted *p*-value) in the head kidney at 10 dpi were associated with eight enriched GO terms related to BP (e.g., defense response, nucleic acid metabolic process), 1 GO term related to MF (nucleic acid binding), and 10 GO terms related to CC (e.g., organelle, nucleoplasm, extracellular region) (Figure 2.14B and File S2.6). The 600 most significant DEGs (lowest FDR adjusted *p*-value) of the spleen at 10 dpi were associated with 16 enriched GO terms related to BP (e.g., immune response, inflammatory response, defense response), four GO terms associated with MF (signaling receptor binding, organic cyclic compound binding, heterocyclic compound binding, and nucleic acid binding), and nine GO terms associated with CC (e.g., organelle, extracellular region) (Figure 2.14D, File S2.6). The 600 most significant DEGs of the liver at 10 dpi were associated with 13 enriched GO terms related to BP (e.g., defense response, small molecule metabolic process, lipid metabolic process, and nucleic acid metabolic process), three GO terms related to MF (catalytic activity, nucleic acid binding, and oxidoreductase activity), and five GO terms related to CC (e.g., organelle, cell junction, extracellular region) (Figure 2.14F and File S2.6).

Furthermore, the GO enrichment analysis indicates that upregulated DEGs of the head kidney at 10 dpi were associated with APR, complement activation, inflammation, regulation of the apoptosis process, and negative regulation of the immune effector process (File S2.7). Upregulated DEGs in the spleen at 10 dpi were associated with complement activation, regulation of the apoptotic process, APR, blood coagulation, and inflammatory response (File S2.7). Upregulated DEGs of the liver at 10 dpi were associated with APR and inflammatory response (File S2.7).

Downregulated DEGs of the head kidney at 10 dpi were associated with metabolic processes, ion transport, and microtubule bundle formation (File S2.7). Downregulated DEGs in

the spleen at 10 dpi were associated with cytoskeleton organization, nucleic acid metabolic process, ribosome biosynthesis, and translation (File S2.7). Downregulated DEGs of the liver at 10 dpi were associated with metabolic processes, such as lipid, organic acid, amino acid, DNA, and RNA metabolic process, ion transport, DNA repair, double-strand break repair, and cell cycle (File S2.7).

2.4.6 Analysis of the most significant differentially expressed genes

I analyzed the 300 most significant DEGs based on the lowest FDR adjusted *p*-value in lumpfish head kidney, spleen, and liver (File S2.8). The results indicate that the most significantly overexpressed genes in the head kidney, spleen, and liver were *il1b*, *il8*, *il10*, *il6*, *hamp*, *haptoglobin* (*hp*), *ptx3*, *collagenase* (*mmp13b*), *c7b*, and *amyloid protein a* (Figure 2.15). In addition to this, the top significant upregulated genes in the head kidney at 3 dpi were *fibrinogen beta* and *gamma chain* (*fbb* and *fbg*) and *complement factor B* (*cfb*) (Figure 2.16). The top significant upregulated gene in the spleen at 3 dpi was *tubulin alpha-1A chain (tuba1a)*, and at 10 dpi were *tlr5*, *coagulation factor IIIa* (*f3*), and *socs3a* (Figure 2.17). The top significant upregulated genes in the liver at 10 dpi were *adenosine receptor A3* (*adora3*) and *carcinoembryonic antigen-related cell adhesion molecule 1* (*ceacam1*) (Figure 18). Most of these genes are involved with inflammation, complement activation, blood coagulation, and APR.

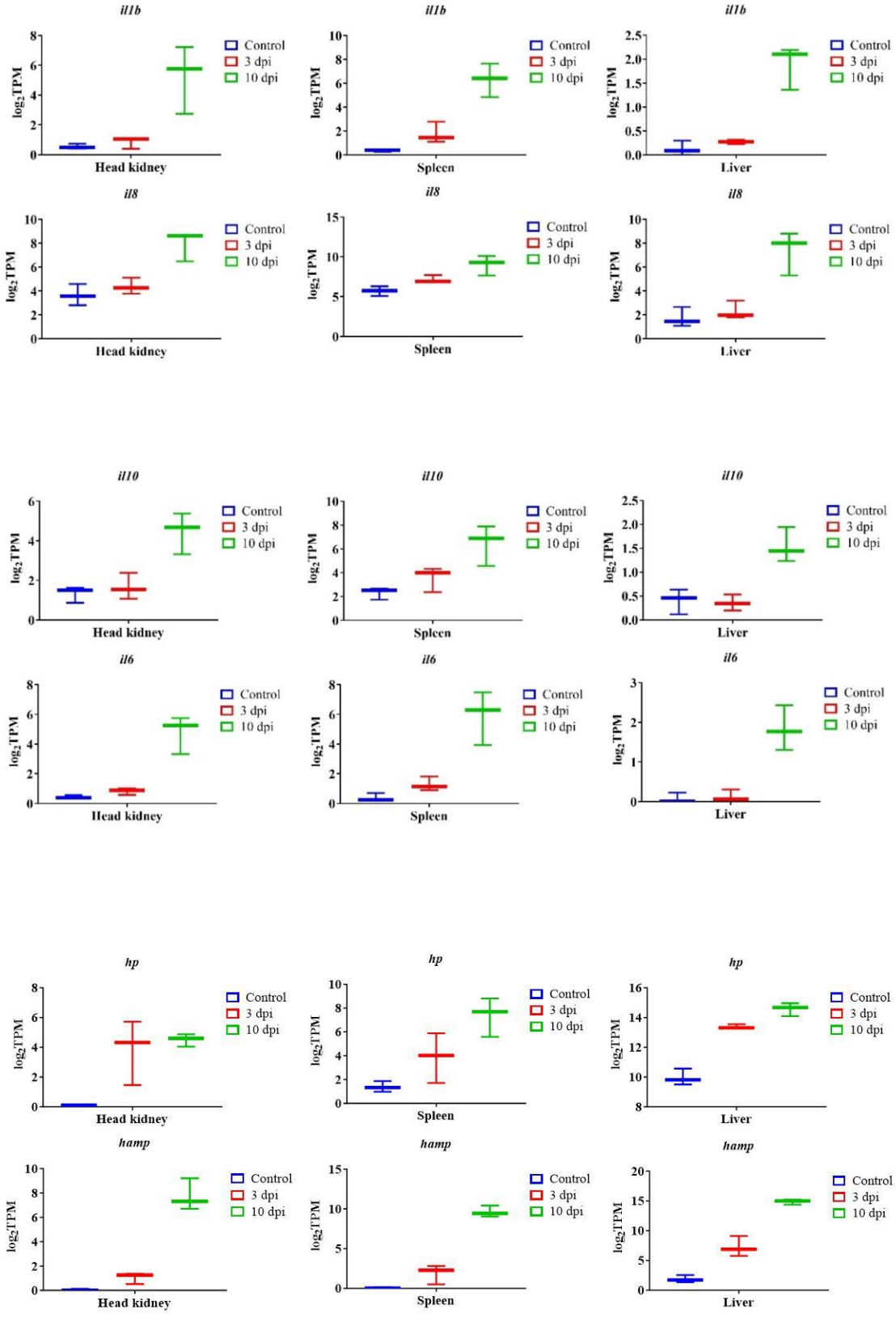
il1b
Head kidney
Spleen
Liver
il8
Head kidney
Spleen
Liver
il10
Head kidney
Spleen
Liver
il6
Head kidney
Spleen
Liver
hp
Head kidney
Spleen
Liver
hamp
Head kidney
Spleen
Liver
log2TPM
Control
3 dpi
10 dpi

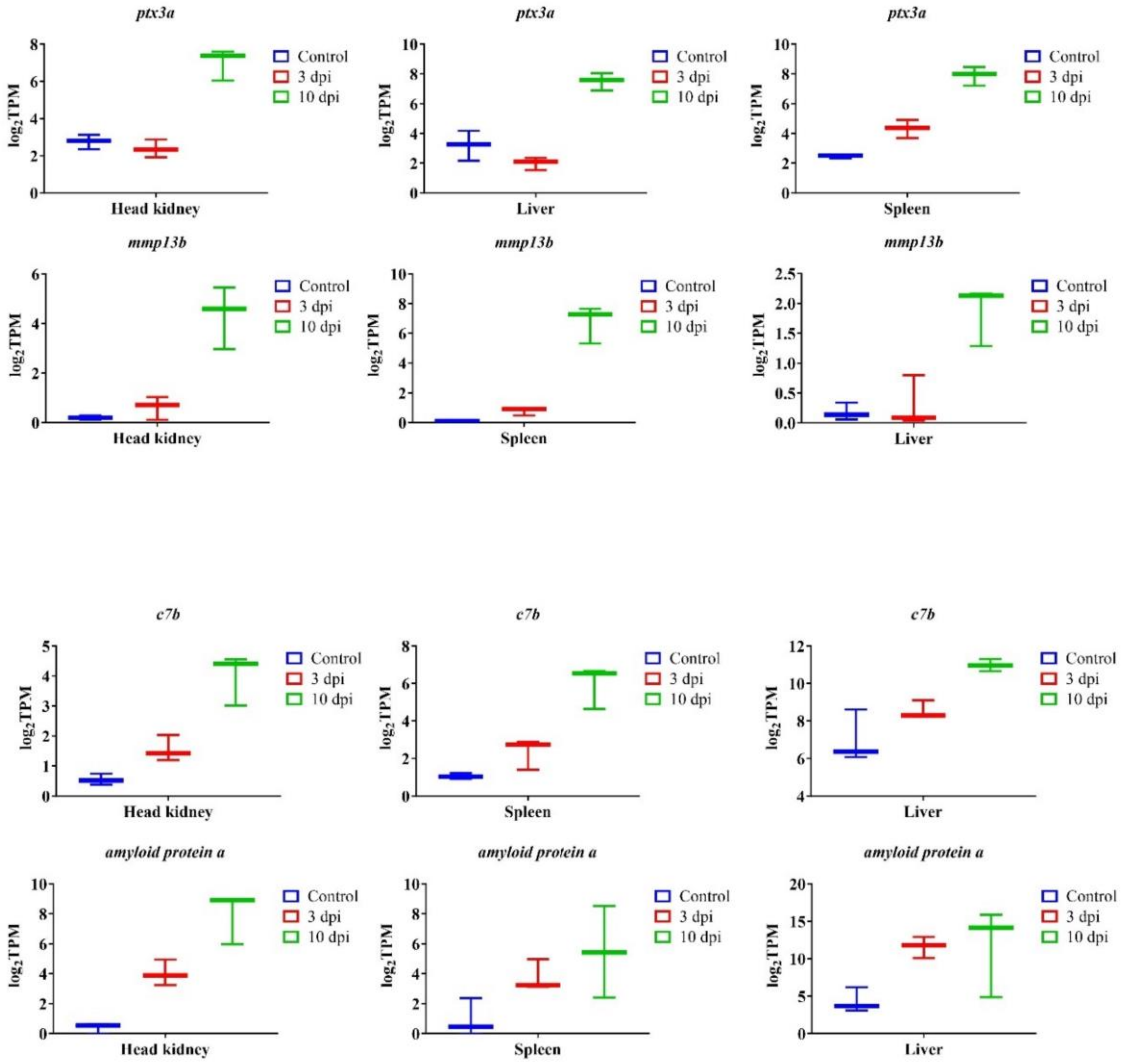

Figure 2.15. Most significant DEGs (lowest FDR adjusted *p*-value) in all organs studied after *A. salmonicida* infection in lumpfish. Bar plots represent the expression pattern (log_2TPM) of *interleukin-1 beta* (*il1b*), *interleukin-8* (*il8*), *interleukin-10* (*il10*), *interleukin-6* (*il6*), *haptoglobin (hp), hepcidin (hamp), pentraxin-related protein PTX3* (*ptx3*), *collagenase* (*mmp13b*), *complement component C7* (*c7*), and *amyloid protein a.*

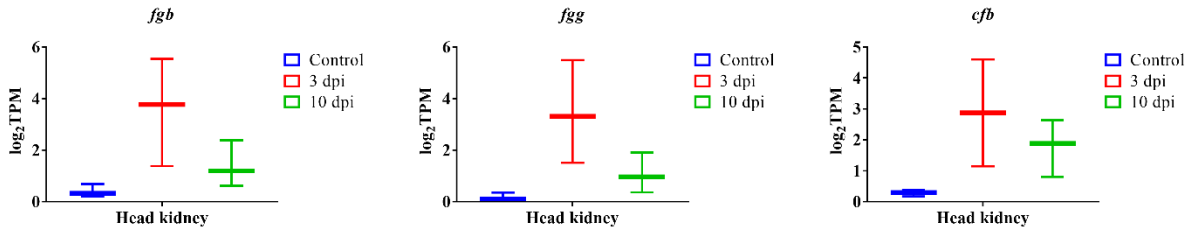

Figure 2.16. Most significant DEGs (lowest FDR adjusted *p*-value) in the head kidney after *A. salmonicida* infection in lumpfish. Bar plots represent the expression pattern (log_2TPM) of *fibrinogen beta* and *gamma chain* (*fgb* and *fgg*), *complement factor B* (*cfb*).

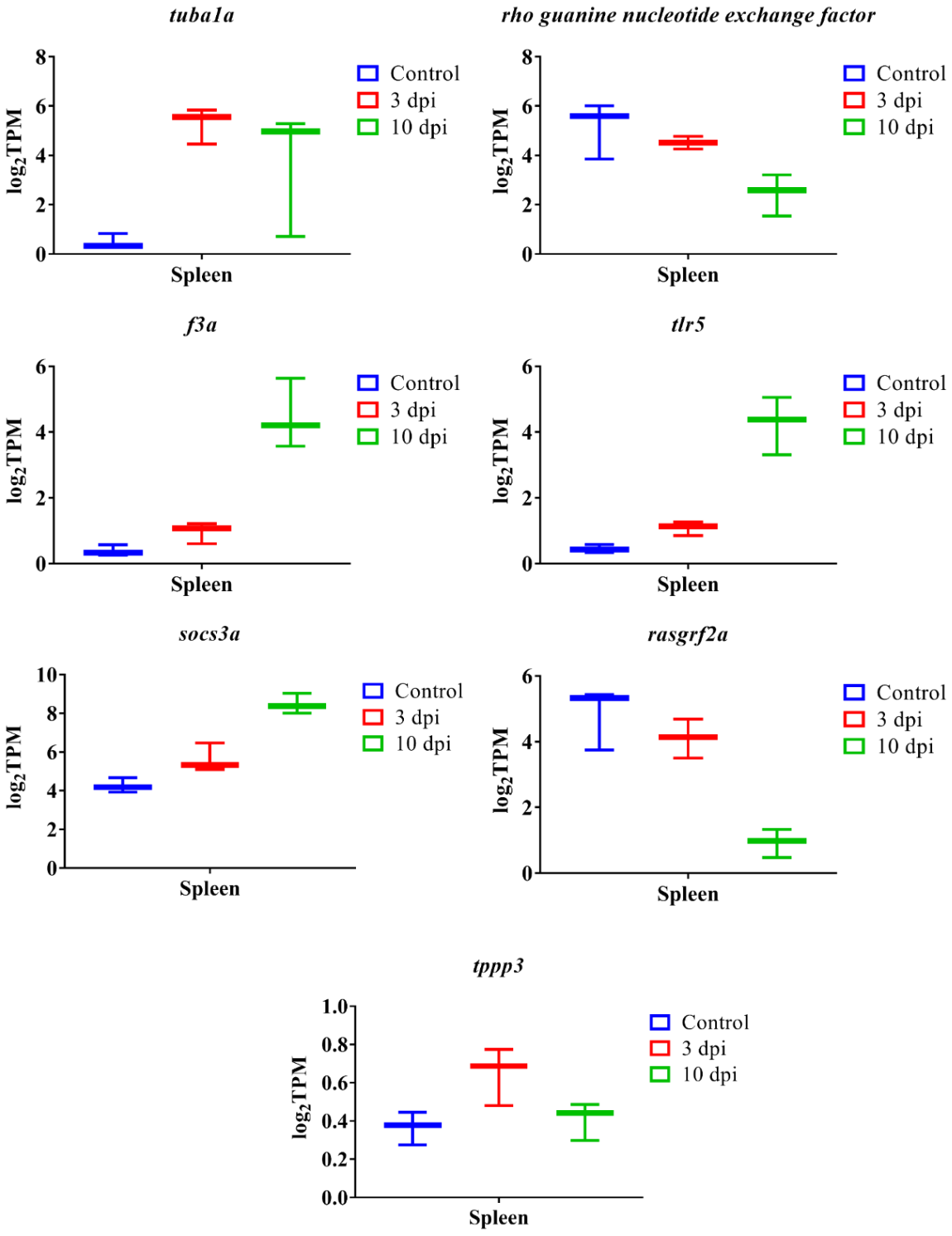
tuba1a
rho guanine nucleotide exchange factor
f3a
tlr5
socs3a
rasgrf2a
tppp3
log2TPM
Spleen
Control
3 dpi
10 dpi

Figure 2.17. Most significant DEGs (lowest FDR adjusted *p*-value) in the spleen after *A. salmonicida* infection in lumpfish. Bar plots represent the expression pattern (log_2TPM) of *tubulin alpha-1A chain (tuba1a), rho guanine nucleotide exchange factor*, *coagulation factor IIIa* (*f3a*), *toll-like receptor 5* (*tlr5*), *suppressor of cytokine signaling 3a* (*socs3a*), *ras-specific guanine nucleotide-releasing factor 2a* (*rasgrf2a*), *protein family member 3* (*tppp3*).

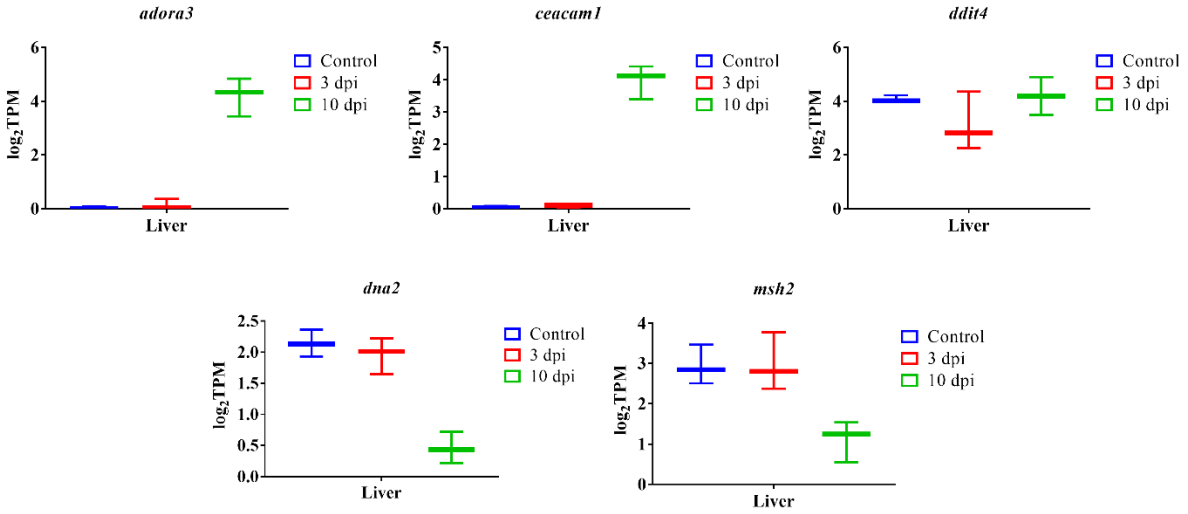

Figure 2.18. Most significant DEGs (lowest FDR adjusted *p*-value) in the liver after *A. salmonicida* infection in lumpfish. Bar plots represent the expression pattern (log_2TPM) of *adenosine receptor A3* (*adora3*), *carcinoembryonic antigen-related cell adhesion molecule 1* (*ceacam1*), *DNA damage-inducible transcript 4 protein (ddit4), DNA replication ATP-dependent helicase/nuclease DNA2* (*dna2*), and *DNA mismatch repair protein Msh2* (*msh2*).

Furthermore, I observed significant downregulation of genes encoding MHCII and IgM in all analyzed organs (Table 2.9). In addition, *cd79a*, *cd79b*, and *cd209* were downregulated in the head kidney, spleen, and liver (Table 2.9).

Table 2.9. Significant differential regulation of adaptive immune marker ($log_2FC \leq -1.0$ or ≥ 1.0, FDR ≤ 0.05) identified from RNA-Seq analysis.

Gene symbol	Description	Log_2 Fold Change					
		Head kidney		Spleen		Liver	
		3 dpi	10 dpi	3 dpi	10 dpi	3 dpi	10 dpi
LOC117737678	H-2 class II histocompatibility antigen gamma chain	-	-	-	-1.91	-1.37	-1.68
LOC117747618	H-2 class II histocompatibility antigen, E-S beta chain	-	-	-1.12	-2.35	-1.58	-1.76
LOC117731450	H-2 class II histocompatibility antigen, A-U alpha chain	-	-	-1.03	-2.75	-1.16	-2.12
LOC117747619	H-2 class II histocompatibility antigen, A-U alpha chain	-	-	-	-2.79	-1.76	-1.65
LOC117745568	H-2 class II histocompatibility antigen, A-U alpha chain	-	1.23	-	-	-	-3.18
LOC117742904	V-set and immunoglobulin domain-containing protein 1	-	-	-2.20	-5.07	-1.92	-3.44
si:ch211-139g16.8	Immunoglobulin superfamily member 6	-	-	-	-1.33	-1.04	-1.58
Sema3fa	Immunoglobulin (Ig) domain	-	-1.13	-	-1.81	-	-2.23

Gene symbol	Description	Log2 Fold Change					
		Head kidney		Spleen		Liver	
		3 dpi	10 dpi	3 dpi	10 dpi	3 dpi	10 dpi
vsig10	V-set and immunoglobulin domain-containing protein 10	-	-	-	-1.85	-	-1.18
LOC117747962	Immunoglobulin kappa light chain	-	-	-	-1.94	-	-1.34
LOC117737972	Polymeric immunoglobulin receptor	-	-	-	-1.97	-	-1.68
igsf8	Immunoglobulin superfamily member 8	-	-	-	-2.04	-	-
igsf5b	Immunoglobulin superfamily member 5	-	-2.05	-1.64	-2.24	-	-
tmigd1	Transmembrane and immunoglobulin domain containing 1	1.07	-4.07	-1.28	-2.56	-	-
LOC117750007	Immunoglobulin-like domain-containing receptor 1	-	-2.14	-1.42	-	-	-
vsig8b	V-set and immunoglobulin domain containing 8b	-	-2.61	-1.94	-	-	-
cd79a	B-cell receptor complex-associated protein alpha	-	-	-2.27	-5.76	-1.33	-2.49
cd79b	B-cell receptor complex-associated protein beta	-	-	-1.21	-4.75	-1.87	-5.44
LOC117735721	CD209	-1.08	-1.69	-	-1.96	-	-2.53
LOC117750415	CD209	-	-	-	-2.17	-1.31	-3.50
LOC117750406	CD209	-	-	-	-2.90	-	-3.59

Additionally, host genes are associated with cytoskeleton organization (e.g. *actin-binding LIM protein 1-like, cdc42 effector protein 1b, rho GTPase-activating protein 4-like, rho guanine nucleotide exchange factor 10-like protein, rho guanine nucleotide exchange factor 18, rho-related GTP-binding protein RhoH, tubulin beta chain, tubulin monoglycylase TTLL3-like, tubulin polyglutamylase TTLL7, ras-specific guanine nucleotide-releasing factor 2a* (*rasgrf2a*), *protein family member 3* (*tppp3*)) were downregulated in the spleen at 10 dpi (Figure 2.17, Files S2.1, S2.7, and S2.9).

A. salmonicida infection upregulated several regulators of NFκB activity, including *nuclear factor of kappa light polypeptide gene enhancer in B-cells inhibitor alpha* (*IκBα*), *B-cell lymphoma 3* (*bcl-3*), *tumor necrosis factor receptor superfamily member 11B* (*tnfrsf11b*), *apoptosis-enhancing nuclease* (*aen*), *DNA damage-inducible transcript 4 protein* (*ddit4*), *nfκb inhibitor* α (*nfkbi*α), and *nuclear factor interleukin-3-regulated protein* (*nfil3*) in lumpfish head kidney and spleen (Files S2.1 and S2.9).

A. salmonicida infection downregulated several genes (e.g. *BRCA1-associated RING domain protein 1* (*bard1*), *DNA replication ATP-dependent helicase/nuclease DNA2* (*dna2*), *DNA excision repair protein ERCC-1* (*ercc1*), *DNA repair endonuclease XPF* (*ercc4*), *E3 ubiquitin-protein ligase HERC2 isoform X1* (*herc2*), *DNA mismatch repair protein Msh2 (msh2), Poly(ADP-ribose) polymerase 1* (*parp1*), *DNA repair protein RAD52 homolog isoform X1* (*rad52*), *DNA repair and recombination protein RAD54-like* (*rad54l*)) involved in DNA damage repair in liver 10 dpi (Figure 2.18, Files S2.1, S2.7, and S2.9).

2.4.7 RT-qPCR verification analysis

The gene expression relationship between the $\log_2$ of the RQ values from the RT-qPCR and the $\log_2$ of the transcript per million reads (TPM) values from the RNA-Seq was determined for 14 selected genes, *complement component c6* (*c6*), *cxc chemokine receptor type 3* (*cxcr3*), *galectin-3-binding protein a* (*igals3bp*), *glutathione s-transferase alpha tandem duplicate 1* (*gsta4.1*), *hepcidin* (*hamp*), *interleukin 1 receptor 2* (*il1r2*), *interleukin 8* (*cxcl8b/il8*), *bactericidal permeability-increasing protein* (*bpifcl*), *pentraxin-related protein ptx3* (*ptx3a*), *ras-related protein orab-1* (*orab1*), *amyloid protein a, suppressor of cytokine signaling 3a* (*socs3a*), *tumor necrosis factor receptor superfamily member 9* (*tnfrsf9*), *toll-like receptor 5* (*tlr5a*). As shown in figure 2.19, there was a significant positive correlation between the RNA-Seq and RT-qPCR data. Correlation r^2 values ranged from 0.6 to 0.93 for all 14 genes. These results indicated that all examined DEGs were in agreement with the reference genome-guided RNA-Seq analysis. On the other hand, the RT-qPCR results for *c6, bpifcl, igals3bp, orab1* were not in good agreement with the *de novo* RNA-Seq analysis (Figure 2.20). However, the qRT-PCR results of all other DEGs evaluated agreed with the *de novo* RNA-Seq analysis, with correlation R^2 values ranging from 0.6 to 0.95 (Figure 2.20).

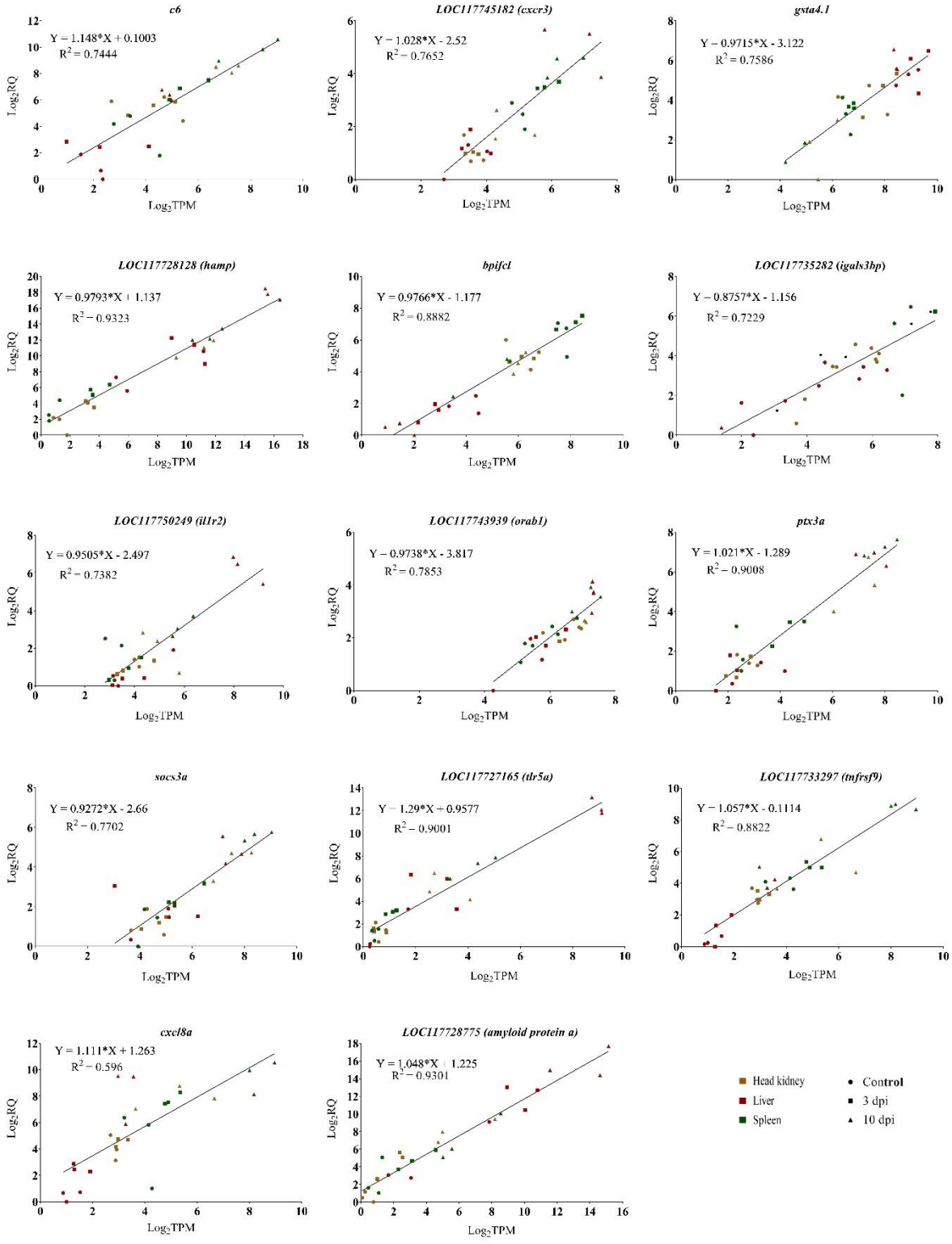
c6
Y = 1.148*X + 0.1003
R2 = 0.7444
LOC117745182 (cxcr3)
Y = 1.028*X - 2.52
R2 = 0.7652
gsta4.1
Y = 0.9715*X - 3.122
R2 = 0.7586
LOC117728128 (hamp)
Y = 0.9793*X + 1.137
R2 = 0.9323
bpifc1
Y = 0.9766*X - 1.177
R2 = 0.8882
LOC117735282 (igals3bp)
Y = 0.8757*X - 1.156
R2 = 0.7229
LOC117750249 (il1r2)
Y = 0.9505*X - 2.497
R2 = 0.7382
LOC117743939 (orab1)
Y = 0.9738*X - 3.817
R2 = 0.7853
ptx3a
Y = 1.021*X - 1.289
R2 = 0.9008
socs3a
Y = 0.9272*X - 2.66
R2 = 0.7702
LOC117727165 (tlr5a)
Y = 1.29*X + 0.9577
R2 = 0.9001
LOC117733297 (tnfrsf9)
Y = 1.057*X - 0.1114
R2 = 0.8822
cxcl8a
Y = 1.111*X + 1.263
R2 = 0.596
LOC117728775 (amyloid protein a)
Y = 1.048*X + 1.225
R2 = 0.9301
Log2RQ
Log2TPM
Head kidney
Liver
Spleen
Control
3 dpi
10 dpi

Figure 2.19. Gene expression correlation between RT-qPCR and RNA-Seq data of 14 selected DEGs. RNA-Seq data are presented as log_2TPM (X-axis), and RT-qPCR data are represented as log_2RQ (Y-axis). Three different colors represent gene expression in the head kidney (brown), spleen (red), and liver (green). The circle represents control samples, square represents 3 dpi, and triangle represents 10 dpi. Each symbol is an average of three fish at a particular time point in that tissue.

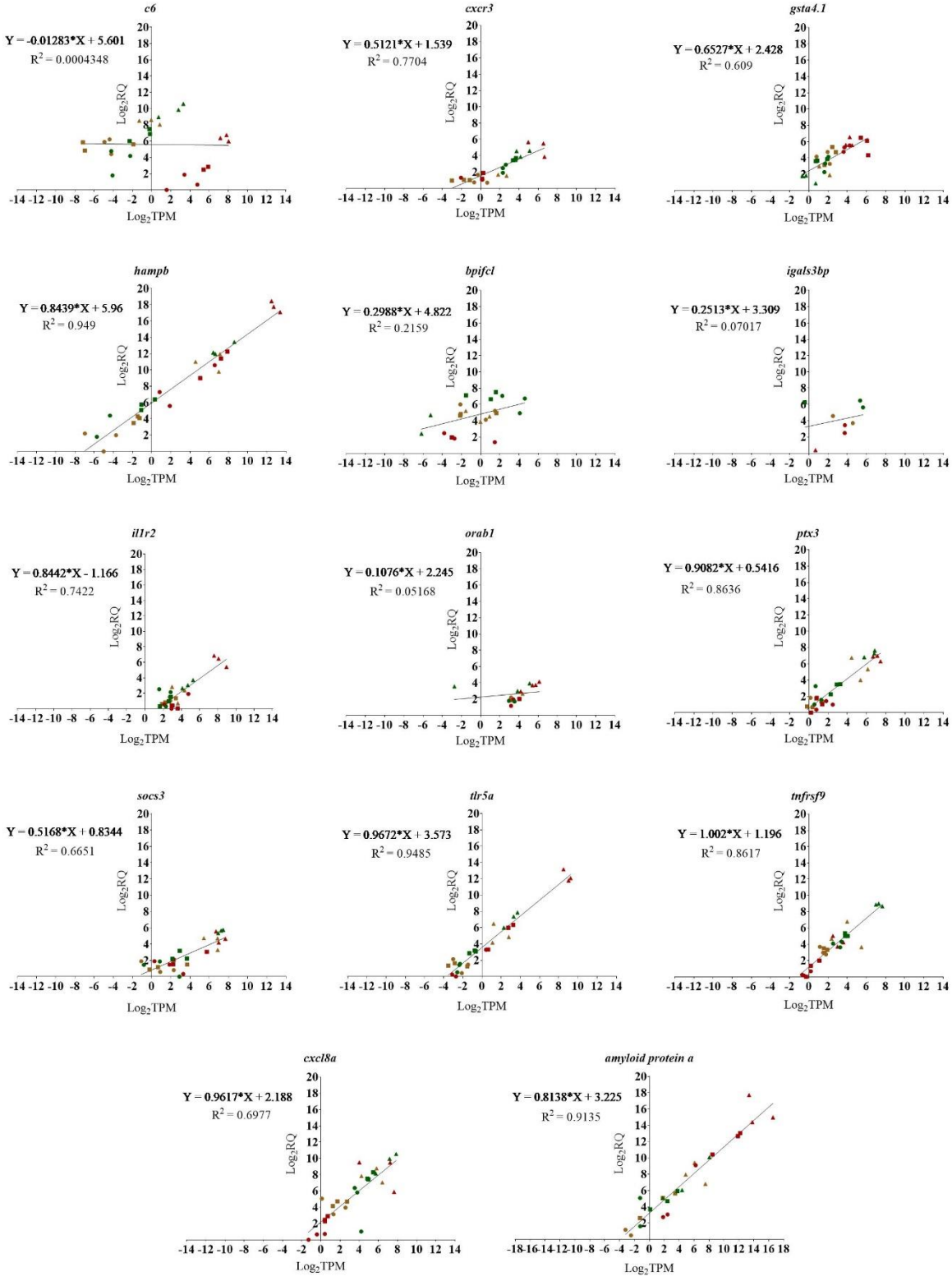
c6
Y = -0.01283*X + 5.601
R2 = 0.0004348
cxcr3
Y = 0.5121*X + 1.539
R2 = 0.7704
gsta4.1
Y = 0.6527*X + 2.428
R2 = 0.609
hampb
Y = 0.8439*X + 5.96
R2 = 0.949
bpifcl
Y = 0.2988*X + 4.822
R2 = 0.2159
igals3bp
Y = 0.2513*X + 3.309
R2 = 0.07017
il1r2
Y = 0.8442*X - 1.166
R2 = 0.7422
orab1
Y = 0.1076*X + 2.245
R2 = 0.05168
ptx3
Y = 0.9082*X + 0.5416
R2 = 0.8636
socs3
Y = 0.5168*X + 0.8344
R2 = 0.6651
tlr5a
Y = 0.9672*X + 3.573
R2 = 0.9485
tnfrsf9
Y = 1.002*X + 1.196
R2 = 0.8617
cxcl8a
Y = 0.9617*X + 2.188
R2 = 0.6977
amyloid protein a
Y = 0.8138*X + 3.225
R2 = 0.9135
Log2RQ
Log2TPM

Figure 2.20. Gene expression correlation between RT-qPCR and RNA-Seq data of 14 gene expressions. *de novo* RNA-Seq data are presented as log_2TPM (X axis). RT-qPCR data are represented as log_2RQ (Y- axis). Three different colors represent gene expression in head kidney (brown), spleen (red), and liver (green). The circle represents control samples, the square represents 3 dpi, and the triangle represents 10 dpi. Each symbol is an average of three fish in a particular time point in that tissue.

2.5 Discussion

Lumpfish are the emergent cleaner fish species in the North Atlantic region [1-6]. However, diseases, including bacterial infections, are affecting the performance of lumpfish and its extended utilization [3]. *A. salmonicida* is a globally distributed pathogen that infects and kills lumpfish [3]. The infection kinetics of *A. salmonicida* in lumpfish and its response to early and lethal infection had not been described before this study. In this study, I established a reproducible *A. salmonicida* systemic infection model in lumpfish. Additionally, I examined the transcriptome profile of internal organs, including the head kidney, spleen, and liver of lumpfish injected with a lethal dose (10^4 CFU) of *A. salmonicida*, during early (3 dpi) and late infection stages (10 dpi). Head kidney is known as a primary lymphoid organ as it is a hematopoietic tissue in the teleost, similar to the bone marrow of higher vertebrates [73]. B cell development, antigen sampling, and antigen retention have been described in teleosts head kidney [24,73,74]. The spleen is the primordial secondary lymphoid organ that contains macrophages, MHC class II+ cells, and T cells [24,73,75,76]. The liver is also a vital organ that takes part in metabolism and defense, and it is also considered as a lymphoid organ, as non-parenchymal cells of the liver take part in antigen presentation and immunomodulatory functions [25,26,28,29]. In addition, the liver encompasses large populations of natural killer (NK) cells and T cells [26,28]. This study analyzed the transcriptome response of the head kidney, spleen, and liver of lumpfish during a lethal *A. salmonicida* infection.

The virulence of different *A. salmonicida* isolates vary in different fish hosts. For instance, *A. salmonicida* DH170821-10 showed relatively lower pathogenicity with an LD_{50} of 6.4×10^3 CFU/dose in rainbow trout (*Oncorhynchus mykiss*) and coho salmon (*Oncorhynchus kisutch*) [77]. Another study described two highly pathogenic strains of *A. salmonicida*, MT1057, and MT423,

with an LD_{50} of 10^2 CFU/dose in Atlantic salmon but a lower virulence in halibut (*Hippoglossus hippoglossus)*, with an LD_{50} of 10^6 CFU/dose [78]. This study showed that *A. salmonicida* J223 (Santander lab collection) is highly virulent for Newfoundland lumpfish. I determined that an ip infection of 10^2 bacterial cells per dose can kill 50 percent of the infected lumpfish population, which is similar to rainbow trout, Chinese perch (*Siniperca chuatsi*), and Atlantic salmon [78,79]. The hyper-virulence of *A. salmonicida* J223 strain in lumpfish was further verified by another study conducted by Santander lab, where a bath infection of lumpfish with 10^6 CFU/mL of *A. salmonicida* J223 caused 100% lethality within 14 dpi (unpublished data).

Subsequently, *A. salmonicida* infection kinetics in different organs was determined for different doses used to infect lumpfish. All lethal doses (10^3–10^5 CFU/dose) showed the presence of *A. salmonicida* in the head kidney at 3 dpi, suggesting that this organ is the primary *A. salmonicida* target, and from there, it spreads to the spleen and liver, and finally, after 7 dpi, *A. salmonicida* infection in lumpfish becomes systemic (Figure 2.3). Similar to my findings, previous studies indicated that 3 to 4 days is a typical incubation period for *A. salmonicida*, where the bacterium rapidly disperses in head kidneys, followed by spleen and liver [80,81]. Lumpfish infected with a low dose of *A. salmonicida* (10^1 CFU/dose) established a persistent infection, as bacterial colonies were still detected after 30 dpi without causing mortalities. While *A. salmonicida* J223 strain lethal doses cause acute infections, in low doses it might cause chronic infections.

Similarly, *Pseudomonas aeruginosa* can cause both symptomatic acute and chronic infections. While acute infections often spread rapidly and can damage tissues as well as contribute to high mortality by sepsis, chronic infections can be carried on for years [82]. I did not explore the further mechanism of *A. salmonicida* mediated chronic infection here. Future studies to

consider how *A. salmonicida* can utilize strategies to evade immune clearance to cause chronic infections would be helpful to explore the pathogenesis in marine teleosts.

To understand the transcriptome dynamics and the impact of *A. salmonicida* on gene expression levels, high-throughput RNA-Seq technology was used. RNA-Seq can effectively analyze transcript sequences and estimate gene expression levels that can be applied to the identification of DETs or DEGs between different experimental conditions [83,84]. Illumina-based RNA-Seq results in millions of short reads which need to be assembled into transcript sequences [85]. An RNA-Seq analysis allows for the distinguishing between individual transcripts (isoform) of a gene [85]. Analysis of DETs is essential in identifying differences between tissues [84]. However, the alignment of RNA-Seq reads to a certain gene allows researchers to study gene expression [86,87]. Gene expression estimation from the expression levels of transcripts provides more robust results [88]. Gene expression estimation allows researchers to determine DEGs under different conditions. Analyzing DEGs is more applicable for biological analysis, e.g., GO enrichment analysis [89]. This study utilized two different approaches: *de novo* and reference-based, to assemble the transcriptome. With the availability of the reference genome, a reference-based assembly is more effective than a *de novo* assembly [90]; however, studies showed that the *de novo* assemblies were able to identify a complete gene content [55,60,91-95]. I applied the *de novo* assembly approach at the isoform level, which allowed me to determine DETs in 3 and 10 dpi of the head kidney, spleen, and liver. However, the reference-based assembly approach allowed me to generate both DEGs and DETs using CLCGWB. My results demonstrate that the total number of DETs identified by the *de novo* transcriptome assembly analysis was higher than the total number of DETs identified by the reference genome-guided transcriptome assembly analysis (5265 vs 4261, $\log_2 FC \leq -1.0$ or ≥ 1.0, FDR ≤ 0.05), which is similar to Kovi et al. [91] (Files

S2.3 and S2.2). Intrinsic methodological issues of *de novo* analysis could generate misassembled transcripts [96]. The Trinity *de novo* assembler might yield more transcripts because of lacking strand-specific information [97]. Subsequently, a BLAST search of all *de novo* DETs against the lumpfish genome identified that only 4839 (91.9%) *de novo* DETs are protein-coding transcripts. Hereafter, the corresponding genes of these *de novo* DETs were compared with the reference-based DEGs. I observed that only 25.9% of the genes were shared between the *de novo* and reference-based analysis, 17.3% were unique in *de novo* analysis, and 56.8% were unique in the reference-based analysis (Figure 2.11).

In addition to this, the RT-qPCR verification analysis demonstrates that the overall gene expression levels were underestimated by *de novo* analysis (Figure 2.19 and 2.20). Previous studies have found that the reference-based method surpasses the *de novo* method for characterizing transcriptome and gene expression [96,98,99]. Still, this study suggested that each method captured unique transcripts. Therefore, I adopted an integrative approach for GO enrichment analysis to bring more benefits for the better exploration of *A. salmonicida* pathogenicity.

The number of DEGs and DETs was highest in the spleen, followed by the head kidney and liver at 3 dpi. Similarly, the number of DEGs and DETs was highest in the spleen, followed by liver and head kidney at 10 dpi. However, in most cases, the number of DETs was lower than that of DEGs. This is because the gene-level expression is global. One gene can have several transcripts as a result of alternative splicing in eukaryotes and not all the DETs were significant ($\log_2FC \leq -1.0$ or ≥ 1.0, $FDR \leq 0.05$). Therefore, I cannot compare between the gene and transcript expression. Thus, moving forward, I used the gene-level analysis.

The head kidney plays a key role in initiating the immune response in fish [73,100]. I observed that the initial inflammatory response was triggered in the head kidney at 3 dpi (File

S2.9). Histopathological analysis also observed the inflammation in the head kidney (Figure 2.3F). Such responses correlate with the infection kinetics of *A. salmonicida* (Figure 2.3B-2.3E). Nevertheless, the spleen also was infected very fast and showed large numbers of DEGs and enriched GO terms (Figures 2.3C, 2.14C, and Table 2.4). The spleen promotes humoral immunity [101,102] and identifies cell damage [103]. This could be a reason for having the highest spleen response during *A. salmonicida* infection. The liver controls biochemical processes, including metabolism [104]. Large numbers of metabolism-related genes were downregulated at 10 dpi in the liver (Files S2.6, S2.7, and S2.9). Interestingly, I observed fish lethargy (e.g., lack of appetite and swimming) starting at 7 dpi and continuing until death, which might relate to a metabolic arrest at the deadly point of the infection.

RNA-Seq analysis suggests that the most significantly upregulated genes are associated with inflammation, complement activation, blood coagulation, and APR (Figures 2.15-2.18). Furthermore, GO enrichment analysis indicates that inflammation and APR were enriched pathways in all three organs (Files S2.7 and S2.9). In addition, blood coagulation and complement activation were enriched in the head kidney and spleen (File S2.7). Inflammation is an immune defense mechanism in response to bacterial infection where leukocytes (neutrophils and monocytes/macrophages) secrete cytokines into the bloodstream. Cytokines, such as IL1 and IL6, stimulate hepatocytes to produce and secrete acute phase proteins (e.g., serum amyloid proteins (SAPs), haptoglobin (HP)) [105-107]. RNA-Seq results demonstrate the upregulation of genes related to inflammation and APR in lumpfish head kidney (e.g., *il1b, il6, il10, cxcl8a*, *serum amyloid A-3, hp, cxcr3, hamp, ptx3a, tlr5a*), spleen (e.g., *amyloid protein a, C-C motif chemokine 19 (ccl19), il1b, il6, cxcl3, cxcl8a, hp, cxcr3, hamp, ptx3a, tlr5a*), and liver (e.g., *amyloid protein a, saa3, ccl19, il1b, il6, cxcl8a, hp, cxcr3, hamp, ptx3a, tlr5a*) (Files S2.7 and S2.9). The

upregulation of several of these genes (*cxcr3*, *hamp*, *il1r2*, *cxcl8b/il8*, *ptx3a*, *amyloid protein a*, *tlr5a*) was further verified by the RT-qPCR experiment (Figure 2.19). Like lumpfish, *A. salmonicida* infection also induces inflammation and APR in Atlantic salmon, cod, rainbow trout, Arctic char, and zebrafish [13,15,32,81,108,109]. The blood coagulation system and complement cascade are closely linked to the inflammatory response and APR [110–112]. Upregulation of genes related to blood coagulation was observed in lumpfish head kidney at 3 dpi (e.g., *fibrinogen*, *prothrombin*, *plasminogen*, *antithrombin-III*) and spleen at 10 dpi (e.g., *thrombomodulin*, *platelet glycoprotein 4*, *coagulation factor XIII*, *coagulation factor IIIa*, and *coagulation factor VIII*, *von Willebrand factor*) (Files S2.1, S2.7, and S2.9). Furthermore, after RNA-Seq data analysis, the upregulation of genes *complement factor H*, *complement factor B*, *c3-like complement component* (*c3*), *c7*, *c8 alpha chain complement component* (*c8*), *c1r-A subcomponent-like complement component*, and *c6* were observed in the head kidney and spleen (Files S2.1 and S2.9). The RT-qPCR analysis confirmed the upregulation of *c6* in all three tissues. These results indicate that *A. salmonicida* infection may induce blood coagulation and complement activation in lumpfish, similar to observations made in zebrafish, Atlantic salmon, and Arctic char infections with *A. salmonicida* [13,15,81].

However, under some circumstances, these innate immune responses cause tissue damage and organ failure, eventually leading to death, a hallmark of sepsis [113]. During sepsis, the association of pattern recognition molecules with the pro-inflammatory mediators and activation of the NF-κB signaling cascade could cause the increased expression of proinflammatory cytokines [111]. Pro-inflammatory cytokines and complement components activate the coagulation cascade [114]. The coagulation system acts as a general host defense system to restrict the dissemination of pathogens by recruiting leukocytes, while fibrin promotes the adherence and

migration of cells [115]. However, overactivation of the coagulation system during acute bacteremia causes disseminated intravascular coagulation (DIC), microvascular thrombosis–induced hypoxia, and prolonged suppression of fibrinolysis, which contributes to multiorgan failure, abnormalities in host metabolism, immune suppression, septic-like shock, and death [111,115-118]. Interestingly, the downregulation of genes encoding hemoglobin subunits alpha and beta was identified in the spleen at 3 dpi, and the moribund lumpfish was visually noticed with signs of hypoxia (Files S2.1, S2.7, and S2.9).

The unrestricted activation of inflammation, blood coagulation, and complement systems break the blood/tissue barrier and damage the host tissue and organs [119]. Interestingly, excessive hemorrhages in the lumpfish body, eyes, gills, or at the base of the fins, muscles, and organ tissues and ascites were visually observed in moribund fish (Figure 2.21). These observations suggest that detrimental and uncontrolled inflammation, overactivation of blood coagulation, and complement components might lead to a septic-like shock, which plays a significant role in the *A. salmonicida*-mediated lethal infection of lumpfish. However, the septic response is an extremely complex reaction of inflammatory, anti-inflammatory, humoral and cellular processes, and circulatory abnormalities, which are highly variable with the non-specific nature of the signs [120]. Therefore, further investigation is required to confirm sepsis in lumpfish.

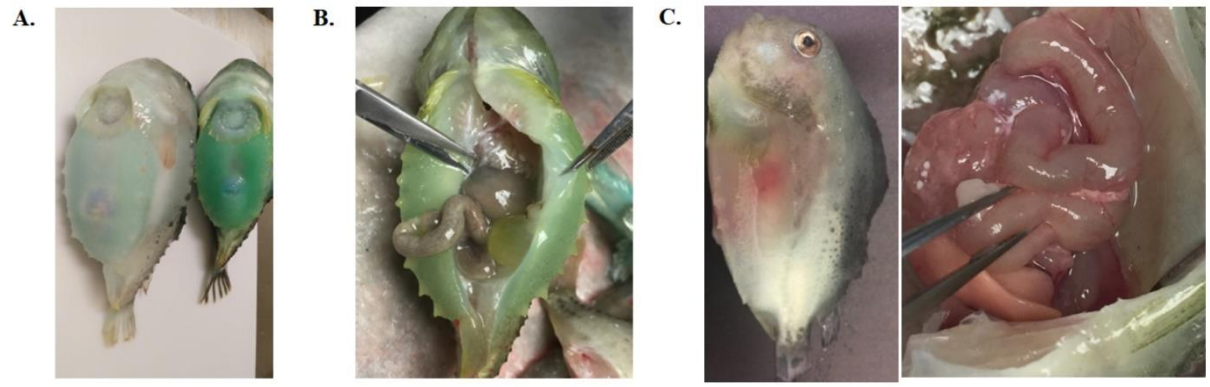

Figure 2.21. *Aeromonas salmonicida* J223 infected lumpfish. *A. salmonicida* infection causes: A. swelling; B. ascites; C. excessive hemorrhages in the lumpfish body and organ tissues of moribund fish.

Furthermore, *il10* was upregulated in all three lumpfish organs at 10 dpi (Figure 2.15). Previously, it was described that *A. salmonicida* elicits a significant increase in *il10* expression in head kidney leucocytes [121]. A similar effect was also described in Arctic char [81]. IL-10 can contribute to immune suppression by inducing a Treg-mediated response. Deleting the type three secretion system (T3SS) genes of *A. salmonicida* decreases the host cytokine expression significantly [121]. A fully virulent *A. salmonicida* downregulated specific innate and adaptive immune gene expression and reduced the survival of the infected rainbow trout [122-124]. Consequently, I observed the downregulation of genes encoding MHCII and IgM in all analyzed organs (Table 2.9). Previous research on *A. salmonicida* infection in trout showed the downregulation of immunoglobulin light chains, constant and variable domains [108,109]. In addition, *cd79a*, *cd79b*, and *cd209* were downregulated in the head kidney, spleen, and liver (Table 2.9). CD79a and CD79b are B-cell antigen receptor complex-associated proteins α and β chains that play a crucial role in B cells activation and antibody production [125]. CD209 is a C-type lectin, an essential PRR that participates in immune defense and microbial pathogenesis in mammals, and it is present on the surface of macrophages [126]. Previous studies on *A. salmonicida* infection in rainbow trout showed that *cd209* was downregulated [108,109]. All of these observations suggest *A. salmonicida*-mediated immune suppression in lumpfish.

A. salmonicida virulence factor AopO is an ortholog of the *Yersinia* YopO/YpkA serine/theonine kinase. This serine/threonine kinase inhibits phagocytosis by blocking the Rac-dependent Fcγ receptor internalization pathway [122]. I observed the downregulation of the low-affinity immunoglobulin gamma Fc region receptor II-b-like (*LOC117747925*) in the spleen at 3 dpi (File S2.1), suggesting that *A. salmonicida* J223 might cause an antiphagocytic effect in

lumpfish. However, this could result from the impact of an undetermined signaling cascade, which needs further verification.

At least six *A. salmonicida* T3SS-related virulence factors, AexT, Ati2, AopH, AopO, AopN, and AopS could be responsible for disrupting the host cytoskeleton structure, which allows this pathogen to colonize and survive inside the host [30,122]. The GTPase activating domain and the ADP-ribosylating domain of AexT act on small monomeric GTPases of the Rho family (Rho, Rac, and Cdc42) and actin, respectively, and causes actin depolymerization and cell rounding [30,122]. Ati2 of *Vibrio parahaemolyticus* is responsible for the local detachment of the actin-binding proteins from the plasma membrane and induces membrane blebbing and cytolysis by hydrolyzing the host phosphatidylinositol 4,5-bisphosphate [30,122]. AopH, an ortholog of *Yersinia* YopH, is responsible for altering the actin cytoskeleton by dephosphorylating the tyrosine residue [30,122]. AopO, an ortholog of *Yersinia* YopO, prevents the actin distribution in the host cell [30,122]. AopN, an *A. salmonicida* effector, binds and sequesters αβ-tubulin and inhibits microtubule polymerization that induces mitotic arrest [30,122]. AopS, an ortholog of *V. parahaemolyticus* VopS, could inhibit the actin assembly by preventing the interaction of Rho GTPases with its downstream effectors [30,122]. In this study, DEGs associated with cytoskeleton organization (e.g. *actin-binding LIM protein 1-like, cdc42 effector protein 1b, rho GTPase-activating protein 4-like, rho guanine nucleotide exchange factor 10-like protein, rho guanine nucleotide exchange factor 18, rho-related GTP-binding protein RhoH, tubulin beta chain, tubulin monoglycylase TTLL3-like, tubulin polyglutamylase TTLL7*, *rasgrf2a*, *tppp3*) were downregulated in the spleen at 10 dpi (Figure 9 and Files S1, S7, and S9). In addition, downregulation of genes related to microtubule bundle formation was observed in the head kidney at 10 dpi (e.g., genes encoding dynein assembly factors, dynein heavy chains, *tppp3*) (Figure 2.17 and Files S2.1, S2.7,

and S2.9). These findings indicate that the disruption of the lumpfish cytoskeleton might be possible by microfilament and microtubule depolymerization and mitotic arrest during *A. salmonicida* infection.

The *A. salmonicida* T3SS effector AopP induces apoptosis in affected cells by interfering with critical signal transduction pathways (i.e., NFκB signaling) that activate caspase 3 [30,122]. AopP hinders the NF-*κ*B signaling pathway by restraining the transportation of the p50/p65 protein complex (NFKB1/RelA) into the target cell's nucleus [30,122], resulting in the septicemia and furuncles formation (subcutaneous wounds) in host tissue [127]. I observed the upregulation of several genes that positively regulate the apoptosis process in the head kidney and spleen at 10 dpi (Files S2.1, S2.7, and S2.9). However, no caspases were differentially expressed in this study. I detected the upregulation of several regulators of the NFκB pathway, including IκBα inhibitor, *bcl-3*, *tnfrsf11b*, *aen*, *ddit4*, *nfkbia*, and *nuclear factor interleukin-3-regulated protein* (*nfil3*) (File S2.1 and S2.9). I did not observe the formation of furuncles in lumpfish skin that might be concurrent with no expression of caspases involved in apoptosis. A dual transcriptomic study and *in vitro* experiments to identify the dysregulation of *aopP* of *A. salmonicida* in lumpfish lymphoid organs could be valuable for future research.

Certain bacterial pathogens could cause chronic inflammation and/or produce genotoxins that can damage proteins, lipids, metabolites, DNA, and RNA. For example, *Helicobacter pylori* infection downregulates DNA mismatch repair and base excision repair mechanisms [128]. The bacterial toxin can be a source of DNA double-strand breaks (DSBs), causing cell death [129]. DSBs induce DNA damage response (DDR), resulting in cell cycle arrest [130]. My results indicate that *A. salmonicida* infection downregulates several genes involved in DNA damage/repair in the liver at 10 dpi (e.g., *bard1*, *dna2*, *ercc1*, *ercc4*, *herc2*, *msh2*, *parp1*, *rad52*,

rad54l) (Figure 2.18 and Files S2.1, S2.7, and S2.9). Therefore, several biological processes such as DNA replication, DNA and RNA metabolic processes, DSB repair, DNA repair, RNA metabolic process, gene expression, and cell cycle processes were enriched by the downregulated genes in liver 10 dpi (File S2.7). These findings suggest that *A. salmonicida* infection might provoke lumpfish DNA damage and cause cell cycle arrest in lumpfish liver.

Suitable biomarkers of sepsis and infection are necessary for monitoring fish disease conditions [131]. *hamp*, *hp*, *amyloid protein a*, *ptx3*, *mmp13b*, *il1b*, *il8*, *il10*, and *il6* were significantly upregulated in the head kidney, spleen, and liver of infected lumpfish, suggesting they could be used as biomarkers for the molecular diagnosis of *A. salmonicida* infection (Figure 2.15). Actually, most of these genes were suggested as biomarkers of sepsis in humans [132,133], suggesting a conserved response to septic shock in vertebrates. Genes encoding ras-related GTPase 1Ab, rho GTPase-related proteins, and microtubule-associated proteins might be proposed as biomarkers to identify *A. salmonicida*-specific infection (Figure 2.17 and File S2.8). In addition, *tlr5*, *c6*, *c7*, *fgb*, *fgg*, *f3a*, *socs3a*, *adora3*, *ceacam1*, *tppp3*, *tuba1a*, *ddit4*, *dna2*, and *msh2* can also potentially be proposed as biomarkers to detect *A. salmonicida* lethal infection in lumpfish. Multiplex RT-qPCR assays for these genes could then be developed to detect early *A. salmonicida* infection in lumpfish. These technologies could accelerate the identification of potential biomarkers for various diagnostic and therapeutic developments in the future lumpfish aquaculture industry and explore the response to septic shock in marine teleost.

2.6 Conclusions

A. salmonicida has evolved many mechanisms to counteract and modulate the host responses. Only 10^2 cells of *A. salmonicida* can kill 50% of the lumpfish population. Overall, this study characterizes *A. salmonicida* infection kinetics in lumpfish head kidney, spleen, and liver

(Figure 2.3) and proposes an infection model for lumpfish molecular responses at the early and lethal point of infection (Figure 2.22). The model suggests that *A. salmonicida* might induce lethal infection in lumpfish by uncontrolled and detrimental blood coagulation, complement activation, and inflammation. Such responses could lead to hypoxia, internal organ hemorrhages, suppression of the adaptive immune system, and impairment of the DNA repair system, which result in cell cycle arrest and, ultimately, death (Figure 2.22). Also, *A. salmonicida* might destabilize the cytoskeleton structure by depolymerizing microfilaments and microtubules to colonize and survive inside the lumpfish (Figure 2.22). In addition, *A. salmonicida* may be capable of inhibiting the NF-κB signaling pathway and the induction of the apoptotic process (Figure 2.22). These findings could help a global understanding of the molecular network of *A. salmonicida*-lumpfish host interactions, which is essential for developing effective treatments. Furthermore, this analysis provides a guideline for future experimental designs to study *A. salmonicida* pathogenesis in lumpfish.

3 days post-infection with *A. salmonicida*

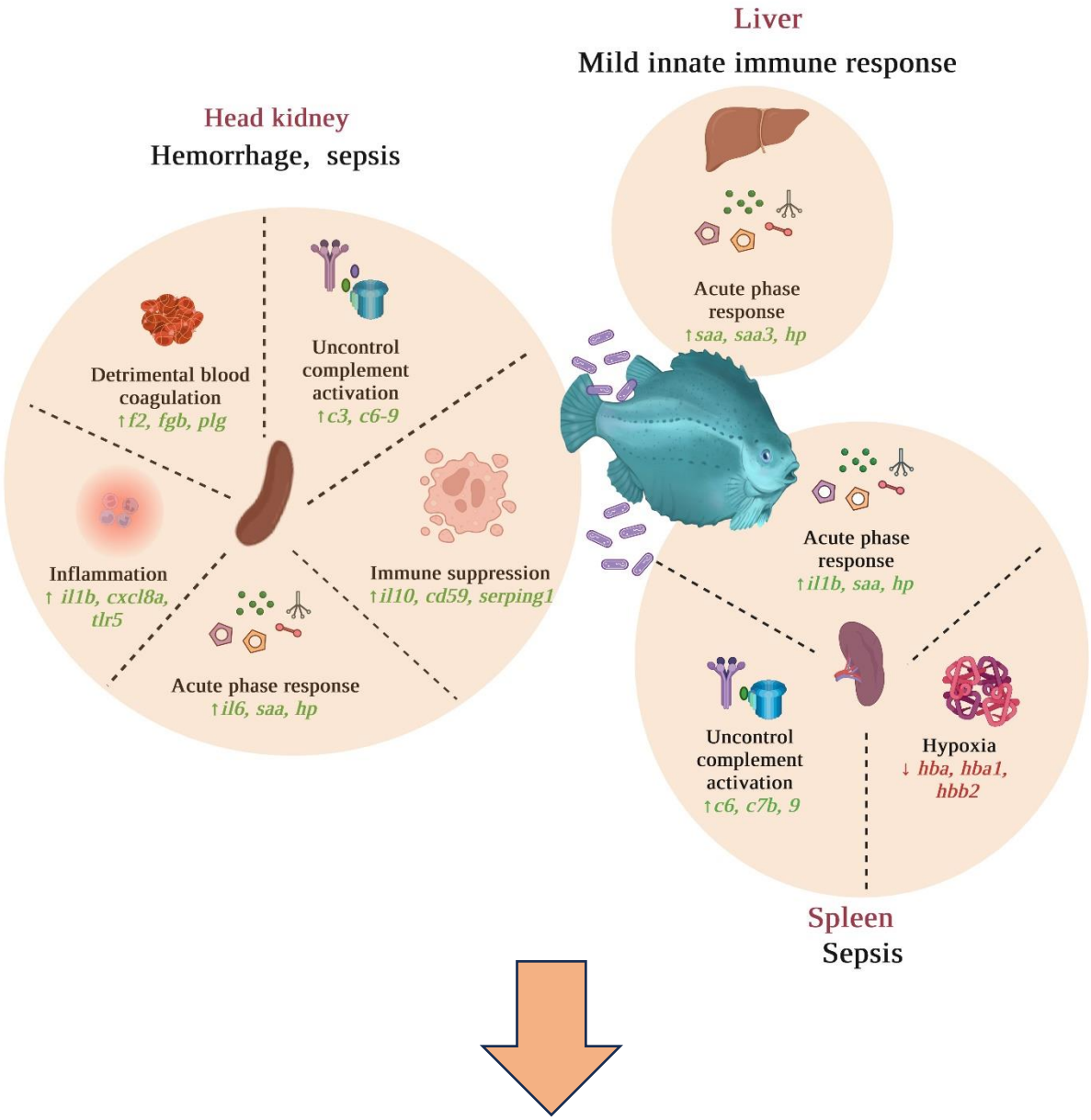

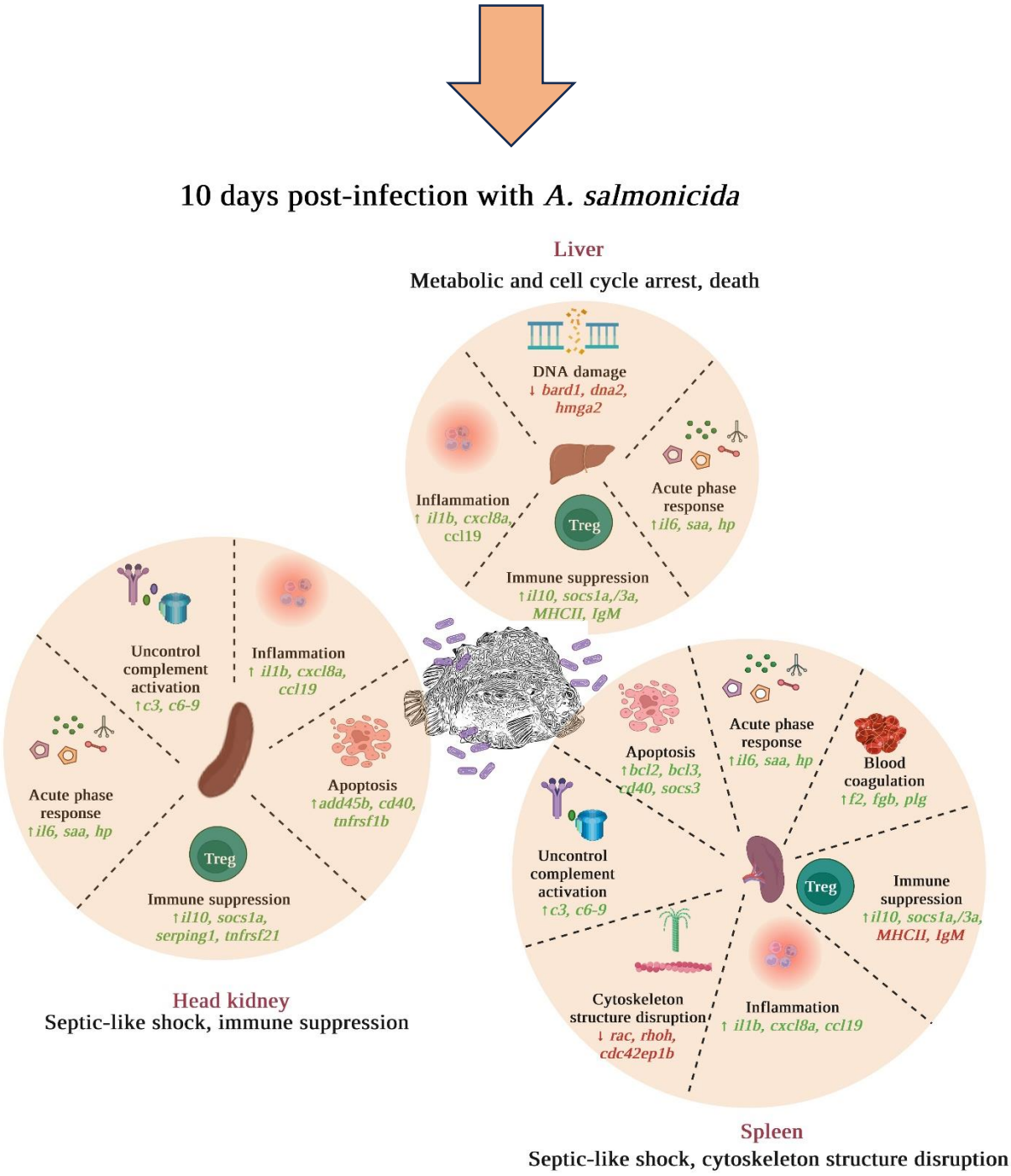
10 days post-infection with A. salmonicida
Liver
Metabolic and cell cycle arrest, death
DNA damage
↓ bard1, dna2, hmga2
Inflammation
↑ il1b, cxcl8a, ccl19
Acute phase response
↑il6, saa, hp
Treg
Immune suppression
↑il10, socs1a,/3a, MHCII, IgM
Uncontrol complement activation
↑c3, c6-9
Inflammation
↑ il1b, cxcl8a, ccl19
Acute phase response
↑il6, saa, hp
Apoptosis
↑add45b, cd40, tnfrsf1b
Treg
Immune suppression
↑il10, socs1a, serping1, tnfrsf21
Head kidney
Septic-like shock, immune suppression
Apoptosis
↑bcl2, bcl3, cd40, socs3
Acute phase response
↑il6, saa, hp
Blood coagulation
↑f2, fgb, plg
Uncontrol complement activation
↑c3, c6-9
Treg
Immune suppression
↑il10, socs1a,/3a, MHCII, IgM
Cytoskeleton structure disruption
↓ rac, rhoh, cdc42ep1b
Inflammation
↑ il1b, cxcl8a, ccl19
Spleen
Septic-like shock, cytoskeleton structure disruption

Figure 2.22. *Aeromonas salmonicida* infection model in lumpfish lymphoid organs. *A. salmonicida* early (3 dpi) and late (10 dpi) infection model shows that *A. salmonicida* could induce lethal infection in lumpfish by uncontrolled and detrimental blood coagulation, complement activation, and inflammation. Such responses might lead to hypoxia, internal organ hemorrhages, suppression of the adaptive immune system, and impairment of the DNA repair system, which results in cell cycle arrest and, ultimately, death. Also, *A. salmonicida* might destabilize the cytoskeleton structure by depolymerizing microfilaments and microtubules. Figure 2.22 was created with BioRender.com.

2.7 References

1. Eliasen K, Danielsen E, Johannesen Á, Joensen LL, Patursson EJ. The cleaning efficacy of lumpfish (*Cyclopterus lumpus L.*) in Faroese salmon (*Salmo salar* L.) farming pens in relation to lumpfish size and seasonality. Aquaculture. 2018;488:61-65.

2. Imsland AKD, Frogg N, Stefansson SO, Reynolds P. Improving sea-lice grazing of lumpfish (*Cyclopterus lumpus* L.) by feeding live feeds prior to transfer to Atlantic salmon (*Salmo salar* L.) net-pens. Aquaculture. 2019;511.

3. Powell A, Treasurer JW, Pooley CL, Keay AJ, Lloyd R, Imsland AK, Garcia de Leaniz C. Use of lumpfish for sea-lice control in salmon farming: challenges and opportunities. Reviews in Aquaculture. 2018;10(3): 683-702.

4. Brooker AJ, Papadopoulou A, Gutierrez C, Rey S, Davie A, Migaud H. Sustainable production and use of cleaner fish for the biological control of sea-lice: recent advances and current challenges. Veterinary Record. 2018;183(12):383.

5. Imsland AK, Reynolds P, Eliassen G, Hangstad, TA, Foss A, Vikingstad E, Elvegård TA. The use of lumpfish (*Cyclopterus lumpus* L.) to control sea-lice (*Lepeophtheirus salmonis* Krøyer) infestations in intensively farmed Atlantic salmon (*Salmo salar* L.). Aquaculture. 2014;424-425:18-23.

6. Imsland, A. K. D., Hanssen, A., Nytro, A. V., Reynolds, P., Jonassen, T. M., Hangstad, T. A., Elvegard, T. A., Urskog, T. C., Mikalsen, B. It works! Lumpfish can significantly lower sea-lice infestation in large-scale salmon farming. Biology Open. 2018;7 (9).

7. Fish FF. Furunculosis in Wild Trout. Copeia. 1937;1937(1):37-40.

8. Duijn JCV. Taxonomy of the Fish Furunculosis Organism. Nature. 1962;4846:1127.

9. Janda JM, Abbott SL. The genus *Aeromonas*: taxonomy, pathogenicity, and infection. Clinical Microbiology Reviews. 2010, 23 (1), 35-73.

10. Beaz-Hidalgo R, Figueras MJ. *Aeromonas* spp. whole genomes and virulence factors implicated in fish disease. Journal of Fish Diseases. 2013;36(4):371-388.

11. Gulla S, Duodu S, Nilsen, A, Fossen I, Colquhoun DJ. *Aeromonas salmonicida* infection levels in pre- and post-stocked cleaner fish assessed by culture and an amended RT-qPCR assay. Journal of Fish diseases. 2016;39(7):867-877.

12. Rouleau FD, Vincent AT, Charette S.J. Genomic and phenotypic characterization of an atypical *Aeromonas salmonicida* strain isolated from a lumpfish and producing unusual granular structures. Journal of Fish Diseases.2018;41(4):673-681.

13. Lin B, Chen S, Cao Z, Lin Y, Mo D, Zhang H, Gu J, Dong M, Liu Z, Xu A. Acute phase response in zebrafish upon *Aeromonas salmonicida* and *Staphylococcus aureus* infection: striking similarities and obvious differences with mammals. Molecular Immunology. 2007;44(4):295-301.

14. Long M, Nielsen TK, Leisner JJ, Hansen LH, Shen ZX, Zhang QQ, Li A. *Aeromonas salmonicida* subsp. *salmonicida* strains isolated from Chinese freshwater fish contain a novel genomic island and possible regional-specific mobile genetic elements profiles. FEMS Microbiology Letters. 2016;363(17).

15. Ewart KV, Belanger JC, Williams J, Karakach T, Penny S, Tsoi SC, Richards RC, Douglas SE. Identification of genes differentially expressed in Atlantic salmon (*Salmo salar*) in response

to infection by *Aeromonas salmonicida* using cDNA microarray technology. Development and Comparative Immunology. 2005;29(4):333-47.

16. Haugland GT, Jakobsen, RA, Vestvik N, Ulven K, Stokka L, Wergeland HI. Phagocytosis and respiratory burst activity in lumpsucker (*Cyclopterus lumpus* L.) leucocytes analysed by flow cytometry. PLoS One. 2012;7(10):e47909.

17. Ronneseth A, Ghebretnsae DB, Wergeland HI, Haugland GT. Functional characterization of IgM+ B cells and adaptive immunity in lumpfish (*Cyclopterus lumpus* L.). Development and Comparative Immunology. 2015;52(2):132-143.

18. Patel DM, Brinchmann MF. Skin mucus proteins of lumpsucker (*Cyclopterus lumpus*). Biochemistry and Biophysics Reports. 2017;9:217-225.

19. Eggestøl HØ, Lunde HS, Rønneseth A, Fredman D, Petersen K, Mishra CK, Furmanek T, Colquhoun DJ, Wergeland HI, Haugland GT. Transcriptome-wide mapping of signaling pathways and early immune responses in lumpfish leukocytes upon in vitro bacterial exposure. Scientific Reports. 2018;8(1):5261.

20. Gnanagobal H, Cao T, Hossain A, Dang M., Hall JR, Kumar S, Van Cuong D, Boyce D, Santander J. Lumpfish (*Cyclopterus lumpus*) is susceptible to *Renibacterium salmoninarum* infection and induces cell-mediated immunity in the chronic stage. Frontiers in Immunology. 2021; 12.

21. Ronneseth A, Haugland GT, Colquhoun DJ, Brudal E, Wergeland HI. Protection and antibody reactivity following vaccination of lumpfish (*Cyclopterus lumpus* L.) against atypical *Aeromonas salmonicida*. Fish & Shellfish Immunology. 2017;64:383-391.

22. Erkinharju T, Lundberg MR, Isdal E, Hordvik I, Dalmo RA, Seternes T. Studies on the antibody response and side effects after intramuscular and intraperitoneal injection of Atlantic lumpfish (*Cyclopterus lumpus* L.) with different oil-based vaccines. Journal of Fish Diseases. 2017;40(12):1805-1813.

23. Dang M, Cao T, Vasquez I, Hossain A, Gnanagobal H, Kumar S, Hall JR, Monk J, Boyce D, Westcott J, Santander J. Oral immunization of larvae and juvenile of lumpfish (*Cyclopterus lumpus*) against *Vibrio anguillarum* does not influence systemic immunity. Vaccines. 2021;9(8):819.

24. Zapata A, Diez B, Cejalvo T, Gutiérrez-de Frías C, Cortés A. Ontogeny of the immune system of fish. Fish & Shellfish Immunology. 2006;20(2):126-36.

25. Tocher DR. Metabolism and functions of lipids and fatty acids in teleost fish. Reviews in Fisheries Science. 2003;11(2):107-184.

26. Crispe IN. The liver as a lymphoid organ. Annual Review of Immunology. 2009;27:147-163.

27. Eckert C, Klein N, Kornek M, Lukacs-Kornek V. The complex myeloid network of the liver with diverse functional capacity at steady state and in inflammation. Frontiers in Immunology. 2015;6:179.

28. Thomson AW, Knolle PA. Antigen-presenting cell function in the tolerogenic liver environment. Nature Reviews Immunology. 2010;10(11):753-766.

29. González-Silvera D, Cuesta A, Esteban MÁ. Immune defence mechanisms presented in liver homogenates and bile of gilthead seabream (*Sparus aurata*). Journal of Fish Biology. 2021;99 (6):1958-1967.

30. Frey J, Origgi FC, Type III secretion system of *Aeromonas salmonicida* undermining the host's immune response. Frontiers in Marine Science. 2016;3(130).

31. Valderrama K, Saravia M, Santander J. Phenotype of *Aeromonas salmonicida* sp. *salmonicida* cyclic adenosine 3',5'-monophosphate receptor protein (Crp) mutants and its virulence in rainbow trout (*Oncorhynchus mykiss*). Journal of Fish Diseases. 2017;40(12):1849-1856.

32. Soto-Dávila M, Hossain A, Chakraborty S, Rise ML, Santander J. *Aeromonas salmonicida* subsp. *salmonicida* early infection and immune response of Atlantic cod (*Gadus morhua* L.) primary macrophages. Frontiers in Immunology. 2019;10(1237).

33. Soto-Dávila M, Valderrama K, Inkpen SM, Hall JR, Rise ML, Santander J. Effects of vitamin D2 (Ergocalciferol) and D3 (Cholecalciferol) on Atlantic salmon (*Salmo salar*) primary macrophage immune response to *Aeromonas salmonicida* subsp. *salmonicida* infection. Frontiers in Immunology. 2020;10.

34. Vasquez I, Hossain A, Gnanagobal H, Valderrama K, Campbell B, Ness M, Charette SJ, Gamperl AK, Cipriano R, Segovia C, Santander J. Comparative Genomics of Typical and Atypical *Aeromonas salmonicida* Complete Genomes Revealed New Insights into Pathogenesis Evolution. Microorganisms. 2022;10(1).

35. Leboffe MJ, Pierce BE. *Microbiology: laboratory theory & application*. Fourth edition. ed., Morton Publishing: Englewood, CO, 2015, p xvi, 896 pages.

36. Sambrook J, Russell W. *Molecular Cloning, A Laboratory Manual.* Cold Spring Harbor Press.: Long Island, NY, USA 2001.

37. Chakraborty S, Woldemariam NT, Visnovska T, Rise ML, Boyce D, Santander J, Andreassen R. Characterization of miRNAs in Embryonic, Larval, and Adult Lumpfish Provides a Reference miRNAome for *Cyclopterus lumpus*. Biology. 2022;11(1):130.

38. Vasquez I, Cao T, Hossain A, Valderrama K, Gnanagobal H, Dang M, Leeuwis RHJ, Ness M, Campbell B, Gendron R, Kao K, Westcott J, Gamperl AK, Santander J. *Aeromonas salmonicida* infection kinetics and protective immune response to vaccination in sablefish (*Anoplopoma fimbria*). Fish & Shellfish Immunology. 2020;104:557-566.

39. Reed LJ, Muench H. A simple method of estimating fifty percent endpoints. The American Journal of Hygiene. 1938:27(3):493-497.

40. Ahmed M. Acute Toxicity (Lethal Dose 50 Calculation) of Herbal Drug Somina in Rats and Mice. Pharmacology & Pharmacy. 2015;06(03):185-189.

41. Chandler D, Roberson RW. *Bioimaging: Current Concepts in Light and Electron Microscopy*. Jones and Bartlett Publishers, Sudbury, Massachusetts: 2009, p 440.

42. Bibert S, Guex N, Lourenco J, Brahier T, Papadimitriou-Olivgeris M, Damonti L, Manuel O, Liechti R, Götz L, Tschopp J, Quinodoz M. Transcriptomic signature differences between SARS-CoV-2 and Influenza Virus infected patients. Frontiers in Immunology. 2021;12.

43. Jia Z, Wu N, Jiang X, Li H, Sun J, Shi M, Li C, Ge Y, Hu X, Ye W, Tang Y, Shan J, Cheng Y, Xia XQ, Shi L. Integrative transcriptomic analysis reveals the immune mechanism for a CyHV-3-Resistant common carp strain. Frontiers in Immunology. 2021;12.

44. Prokop JW, Hartog NL, Chesla D, Faber W, Love CP, Karam R, Abualkheir N, Feldmann B, Teng L, McBride T. High-density blood transcriptomics reveals precision immune signatures of SARS-CoV-2 infection in hospitalized individuals. Frontiers in Immunology. 2021;12.

45. Roh H, Kim N, Lee Y, Park J, Kim BS, Lee MK, Park CI, Kim DH. Dual-organ transcriptomic analysis of rainbow trout infected with *Ichthyophthirius multifiliis* through co-expression and machine learning. Frontiers in Immunology. 2021;12.

46. Cai W, Kumar S, Navaneethaiyer U, Caballero-Solares A, Carvalho LA, Whyte SK, Purcell SL, Gagne N, Hori TS, Allen M. Transcriptome analysis of Atlantic salmon (*Salmo salar*) skin in response to sea-lice and infectious Salmon Anemia Virus co-infection under different experimental functional diets. Frontiers in Immunology. 2022;12.

47. Cohen-Gihon I, Israeli O, Tidhar A, Sapoznikov A, Evgy Y, Stein D, Aftalion M, Gur D, Orr I, Zvi A, Sabo T, Kronman C, Falach R. Transcriptome analysis of lungs in a mouse model of severe COVID-19. Frontiers in Virology. 2022;2.

48. Andrew S. FastQC: a quality control tool for high throughput sequence data. Babraham Bioinformatics, Babraham Institute, Cambridge, United Kingdom: 2010.

49. Ewels P, Magnusson M, Lundin S, Käller M. MultiQC: summarize analysis results for multiple tools and samples in a single report. Bioinformatics. 2016;32(19):3047-3048.

50. Li B, Ruotti V, Stewart RM, Thomson JA, Dewey CN. RNA-Seq gene expression estimation with read mapping uncertainty. Bioinformatics. 2009;26(4):493-500.

51. Teng M, Love MI, Davis CA, Djebali S, Dobin A, Graveley BR, Li S. Mason CE, Olson S, Pervouchine D, Sloan CA, Wei X, Zhan L, Irizarry RA, A benchmark for RNA-seq quantification pipelines. Genome Biology. 2016;17(1):74.

52. Pereira MB, Wallroth M, Jonsson V, Kristiansson E. Comparison of normalization methods for the analysis of metagenomic gene abundance data. BMC Genomics. 2018;19(1):274.

53. Robinson MD, McCarthy DJ, Smyth GK edgeR: a Bioconductor package for differential expression analysis of digital gene expression data. Bioinformatics. 2009;26(1):139-140.

54. Bolger AM, Lohse M, Usadel B. Trimmomatic: a flexible trimmer for Illumina sequence data. Bioinformatics. 2014;30(15):2114-20.

55. Haas BJ, Papanicolaou A, Yassour M, Grabherr M, Blood PD, Bowden J, Couger MB, Eccles D, Li B, Lieber M, MacManes MD. *De novo* transcript sequence reconstruction from RNA-seq using the Trinity platform for reference generation and analysis. Nature Protocols. 2013;8:1494.

56. Li H, Handsaker B, Wysoker A, Fennell T, Ruan J, Homer N, Marth G, Abecasis G, Durbin R. Genome Project Data Processing, S., The sequence alignment/map format and SAMtools. Bioinformatics. 2009;25(16):2078-9.

57. Langmead B, Salzberg SL. Fast gapped-read alignment with Bowtie 2. Nature Methods. 2012;9(4):357-9.

58. Camacho C, Coulouris G, Avagyan V, Ma N, Papadopoulos J, Bealer K, Madden TL. BLAST+: architecture and applications. BMC Bioinformatics. 2009 D;10:1-9.

59. Simao FA, Waterhouse RM, Ioannidis P, Kriventseva EV, Zdobnov EM. BUSCO: assessing genome assembly and annotation completeness with single-copy orthologs. Bioinformatics. 2015;31(19):3210-2.

60. Li B, Dewey CN. RSEM: accurate transcript quantification from RNA-Seq data with or without a reference genome. BMC Bioinformatics. 2011;12(1):323.

61. Bryant DM, Johnson K, DiTommaso T, Tickle T, Couger MB, Payzin-Dogru D Lee, TJ, Leigh ND, Kuo TH, Davis FG. A tissue-mapped axolotl de novo transcriptome enables identification of limb regeneration factors. Cell Reports. 2017;18(3):762-776.

62. Finn RD, Clements J, Eddy SR. HMMER web server: interactive sequence similarity searching. Nucleic Acids Research. 2011;39:W29-W37.

63. Mistry J, Chuguransky S, Williams L, Qureshi M, Salazar GA, Sonnhammer ELL, Tosatto SCE, Paladin L, Raj S, Richardson LJ, Finn RD, Bateman A. Pfam: The protein families database in 2021. Nucleic Acids Research. 2020;49(D1):D412-D419.

64. Almagro Armenteros JJ, Tsirigos KD, Sønderby CK, Petersen TN, Winther O, Brunak S, von Heijne G, Nielsen H. SignalP 5.0 improves signal peptide predictions using deep neural networks. Nature Biotechnology. 2019;37(4):420-423.

65. Sonnhammer EL, von Heijne G, Krogh A. A hidden Markov model for predicting transmembrane helices in protein sequences. Proceedings. International Conference on Intelligent Systems for Molecular Biology. 1998;6:175-82.

66. Love MI, Huber W, Anders S, Moderated estimation of fold change and dispersion for RNA-seq data with DESeq2. Genome Biology. 2014;15(12):550.

67. Bindea G, Mlecnik B, Hackl H, Charoentong P, Tosolini M, Kirilovsky A, Fridman WH, Pagès F, Trajanoski Z, Galon J. ClueGO: a Cytoscape plug-in to decipher functionally grouped gene ontology and pathway annotation networks. Bioinformatics. 2009;25(8):1091-3.

68. Shannon P, Markiel A, Ozier O, Baliga NS, Wang JT, Ramage D, Amin N, Schwikowski B, Ideker T. Cytoscape: a software environment for integrated models of biomolecular interaction networks. Genome Research. 2003;13(11):2498-504.

69. St-Pierre J, Grégoire JC, Vaillancourt C. A simple method to assess group difference in RT-qPCR reference gene selection using GeNorm: The case of the placental sex. Scientific Reports. 2017;7(1):16923.

70. Soto-Dávila, M, Chakraborty S, Santander J. Relative expression and validation of *Aeromonas salmonicida* subsp. *salmonicida* reference genes during ex vivo and in vivo fish infection. Infection, Genetics and Evolution. 2022;103:105320.

71. Roberts A, Schaeffer L, Pachter L. Updating RNA-Seq analyses after re-annotation. Bioinformatics. 2013;29(13):1631-1637.

72. Steijger T, Abril JF, Engström PG, Kokocinski F, Abril JF, Akerman M, Alioto T, Ambrosini G, Antonarakis SE, Behr J. Assessment of transcript reconstruction methods for RNA-seq. Nature Methods. 2013;10(12):1177-1184.

73. Bjørgen H, Koppang EO. Anatomy of teleost fish immune structures and organs. Immunogenetics. 2021;73(1),53-63.

74. Zwollo P, Cole S, Bromage E, Kaattari S. B cell heterogeneity in the teleost kidney: evidence for a maturation gradient from anterior to posterior kidney. The Journal of Immunology. 2005;174(11):6608-6616.

75. Flajnik MF. A cold-blooded view of adaptive immunity. Nature Reviews in Immunology. 2018;18(7):438-453.

76. Koppang EO, Fischer U, Moore L, Tranulis MA, Dijkstra JM, Köllner B, Aune L, Jirillo E, Hordvik I. Salmonid T cells assemble in the thymus, spleen and in novel interbranchial lymphoid tissue. Journal of Anatomy. 2010;217(6):728-739.

77. Lim J, Hong S, Characterization of *Aeromonas salmonicida* and *A. sobria* isolated from cultured salmonid fish in Korea and development of a vaccine against furunculosis. Journal of Fish Diseases. 2020;43(5):609-620.

78. Bricknell IR, Bowden TJ, Bruno DW, MacLachlan P, Johnstone R, Ellis AE. Susceptibility of Atlantic halibut, *Hippoglossus hippoglossus* (L.) to infection with typical and atypical *Aeromonas salmonicida*. Aquaculture. 1999;175(1):1-13.

79. Lin Q, Li J, Fu X, Liu L, Liang H, Niu Y, Huang C, Huang Z, Mo Z, Li N. Hemorrhagic gill disease of Chinese perch caused by *Aeromonas salmonicida* subsp. *salmonicida* in China. Aquaculture. 2020;519:734775.

80. Farto R, Milton DL, Bermudez MB, Nieto TP. Colonization of turbot tissues by virulent and avirulent *Aeromonas salmonicida* subsp. *salmonicida* strains during infection. Diseases of Aquatic Organisms. 2011;95(2):167-73.

81. Braden LM, Whyte SK, Brown ABJ, Iderstine CV, Letendre C, Groman D, Lewis J, Purcell SL, Hori T, Fast MD. Vaccine-induced protection against furunculosis involves pre-emptive priming of humoral immunity in Arctic Charr. Frontiers in Immunology. 2019;10(120).

82. Turner KH, Everett J, Trivedi U, Rumbaugh KP, Whiteley M. Requirements for *Pseudomonas aeruginosa* acute burn and chronic surgical wound infection. PLoS Genetics. 2014;10(7):e1004518-e1004518.

83. Wu Z, Wang X, Zhang X. Using non-uniform read distribution models to improve isoform expression inference in RNA-Seq. Bioinformatics. 2011;27(4):502-508.

84. Mortazavi A, Williams BA, McCue K, Schaeffer L, Wold B. Mapping and quantifying mammalian transcriptomes by RNA-Seq. Nature Methods. 2008;5(7):621-628.

85. Glaus P, Honkela A, Rattray M. Identifying differentially expressed transcripts from RNA-seq data with biological variation. Bioinformatics. 2012;28(13):1721-8.

86. Cloonan N, Forrest AR, Kolle G, Gardiner B, Faulkner GJ, Brown MK, Taylor DF, Steptoe AL, Wani S, Bethel G. Stem cell transcriptome profiling via massive-scale mRNA sequencing. Nature Methods. 2008;5(7):613-619.

87. Marioni JC, Mason CE, Mane SM, Stephens M, Gilad Y. RNA-seq: an assessment of technical reproducibility and comparison with gene expression arrays. Genome Research. 2008;18(9):1509-1517.

88. Wang X, Wu Z, Zhang X. Isoform abundance inference provides a more accurate estimation of gene expression levels in RNA-seq. Journal of Bioinformatics and Computational Biology. 2010;8(01):177-192.

89. Yi L, Pimentel H, Bray NL, Pachter L. Gene-level differential analysis at transcript-level resolution. Genome Biology. 2018;19(1): 53.

90. Martin JA, Wang Z. Next-generation transcriptome assembly. Nature Reviews Genetics. 2011;12(10):671-682.

91. Kovi MR, Abdelhalim M, Kunapareddy A, Ergon Å, Tronsmo AM, Brurberg MB, Hofgaard IS, Asp T, Rognli OA. Global transcriptome changes in perennial ryegrass during early infection by pink snow mould. Scientific Reports. 2016;6(1):1-15.

92. Grabherr MG, Haas BJ, Yassour M, Levin JZ, Thompson DA, Amit I, Adiconis X, Fan L, Raychowdhury R, Zeng Q. Full-length transcriptome assembly from RNA-Seq data without a reference genome. Nature Biotechnology. 2011:29(7):644-652.

93. Langmead B, Trapnell C, Pop M, Salzberg SL. Ultrafast and memory-efficient alignment of short DNA sequences to the human genome. Genome Biology. 2009;10(3):1-10.

94. Trapnell C, Williams BA, Pertea G, Mortazavi A, Kwan G, Van Baren MJ, Salzberg SL, Wold BJ, Pachter L. Transcript assembly and quantification by RNA-Seq reveals unannotated transcripts and isoform switching during cell differentiation. Nature Biotechnology. 2010;28(5):511-515.

95. Ward JA, Ponnala L, Weber CA. Strategies for transcriptome analysis in non-model plants. American Journal of Botany. 2012;99(2):267-276.

96. Lee SG, Na D, Park C, Comparability of reference-based and reference-free transcriptome analysis approaches at the gene expression level. BMC Bioinformatics. 2021;22(11):310.

97. Kovi MR, Amdahl H, Alsheikh M, Rognli OA. *De novo* and reference transcriptome assembly of transcripts expressed during flowering provide insight into seed setting in tetraploid red clover. Scientific Reports. 2017;7(1):44383.

98. Lu B, Zeng Z, Shi T. Comparative study of *de novo* assembly and genome-guided assembly strategies for transcriptome reconstruction based on RNA-Seq. Science China. Life Sciences. 2013;56(2):143-55.

99. Vijay N, Poelstra JW, Künstner A, Wolf JB. Challenges and strategies in transcriptome assembly and differential gene expression quantification. A comprehensive in silico assessment of RNA-seq experiments. Molecular Ecology. 2013;22(3):620-34.

100. Kumar R, Joy KP, Singh SM. Morpho-histology of head kidney of female catfish *Heteropneustes fossilis*: seasonal variations in melano-macrophage centers, melanin contents and effects of lipopolysaccharide and dexamethasone on melanins. Fish Physiology and Biochemistry. 2016;42(5):1287-1306.

101. Morales-Lange B, Agboola JO, Hansen JØ, Lagos L, Øyås O, Mercado L, Mydland LT, Øverland M. The spleen as a target to characterize immunomodulatory effects of down-stream processed *Cyberlindnera jadinii* yeasts in Atlantic salmon exposed to a dietary soybean meal challenge. Frontiers in Immunology. 2021;12.

102. Gong H, Wang Q, Lai Y, Zhao C, Sun C, Chen Z, Tao J, Huang Z. Study on immune response of organs of *Epinephelus coioides* and *Carassius auratus* after immersion vaccination with inactivated *Vibrio harveyi* vaccine. Frontiers in Immunology. 2021;11.

103. Bronte V, Pittet MJ. The spleen in local and systemic regulation of immunity. Immunity. 2013;39(5):806-818.

104. Rui L. Energy metabolism in the liver. Comparative Physiology. 2014;4 (1):177-197.

105. Charlie-Silva I, Klein A, Gomes JMM, Prado EJR, Moraes AC, Eto SF, Fernandes DC, Fagliari JJ, Junior JDC, Lima C. Acute-phase proteins during inflammatory reaction by bacterial infection: Fish-model. Scientific Reports. 2019;9 (1):4776.

106. Uhlar CM, Whitehead AS. Serum amyloid A, the major vertebrate acute-phase reactant. European Journal of Biochemistry. 1999;265(2):501-23.

107. Dinarello CA. Overview of the IL-1 family in innate inflammation and acquired immunity. Immunological Reviews. 2018;281(1):8-27.

108. Rebl A, Korytar T, Kobis JM, Verleih M, Krasnov A, Jaros J, Kuhn C, Kollner B, Goldammer T. Transcriptome profiling reveals insight into distinct immune responses to *Aeromonas salmonicida* in gill of two rainbow trout strains. Marine Biotechnology. 2014;16(3):333-48.

109. Long M, Zhao J, Li T, Tafalla C, Zhang Q, Wang X, Gong X, Shen Z, Li A. Transcriptomic and proteomic analyses of splenic immune mechanisms of rainbow trout (*Oncorhynchus mykiss*) infected by *Aeromonas salmonicida* subsp. *salmonicida*. Journal of Proteomics. 2015;122:41-54.

110. Stearns-Kurosawa DJ, Osuchowski MF, Valentine C, Kurosawa S, Remick DG. The pathogenesis of sepsis. Annual Review of Pathology. 2011;6:19-48.

111. O'Brien JM, Ali NA, Aberegg SK, Abraham E. Sepsis. The American Journal of Medicine. 2007;120(12):1012-1022.

112. Smith NC, Rise ML, Christian SL. A Comparison of the innate and adaptive immune systems in cartilaginous fish, ray-finned fish, and lobe-finned fish. Frontiers in Immunology. 2019;10:2292.

113. Cohen, J. The immunopathogenesis of sepsis. Nature. 2002;420(6917):885-891.

114. Amara U, Flierl MA, Rittirsch D, Klos A, Chen H, Acker B, Brückner UB, Nilsson B, Gebhard F, Lambris JD, Huber-Lang, M. Molecular intercommunication between the complement and coagulation systems. Journal of Immunology. 2010;185(9):5628-36.

115. Antoniak S. The coagulation system in host defense. Research and Practice in Thrombosis and Haemostasis. 2018;2(3):549-557.

116. Semeraro N, Ammollo CT, Semeraro F, Colucci M. Sepsis-associated disseminated intravascular coagulation and thromboembolic disease. Mediterranean Journal of Hematology and Infectious Diseases. 2010;2(3): e2010024-e2010024.

117. Levi M, van der Poll T. Coagulation and sepsis. Thrombosis Research. 2017;149:38-44.

118. Goeijenbier M, van Wissen M, van de Weg C, Jong E, Gerdes VEA, Meijers JCM, Brandjes DPM, van Gorp ECM. Review: Viral infections and mechanisms of thrombosis and bleeding. Journal of Medical Virology. 2012;84(10):1680-1696.

119. Lupu F, Keshari RS, Lambris JD, Mark Coggeshall K. Crosstalk between the coagulation and complement systems in sepsis. Thrombosis Research. 2014;133:S28-S31.

120. Pierrakos C, Vincent JL. Sepsis biomarkers: a review. Critical Care. 2010;14(1):R15.

121. Fast MD, Tse B, Boyd JM, Johnson SC. Mutations in the *Aeromonas salmonicida* subsp. *salmonicida* type III secretion system affect Atlantic salmon leucocyte activation and downstream immune responses. Fish and Shellfish Immunology. 2009;27(6):721-8.

122. Vanden Bergh P, Frey J. *Aeromonas salmonicida* subsp. *salmonicida* in the light of its type-three secretion system. Microbial Biotechnology. 2014;7(5):381-400.

123. Vanden Bergh P, Heller M, Braga-Lagache S, Frey J. The *Aeromonas salmonicida* subsp. *salmonicida* exoproteome: global analysis, moonlighting proteins and putative antigens for vaccination against furunculosis. Proteome Science. 2013;11(1):44-44.

124. Vanden Bergh P, Heller M, Braga-Lagache S, Frey J. The *Aeromonas salmonicida* subsp. *salmonicida* exoproteome: determination of the complete repertoire of Type-Three Secretion System effectors and identification of other virulence factors. Proteome Science. 2013;11(1):42.

125. Radaev S, Zou Z, Tolar P, Nguyen K, Nguyen A, Krueger PD, Stutzman N, Pierce S, Sun PD. Structural and functional studies of Ig alpha beta and its assembly with the B cell antigen receptor. Structure. 2010;18(8):934-943.

126. Jiang S, Sun L. Tongue Sole CD209: A Pattern-Recognition Receptor that Binds a Broad Range of Microbes and Promotes Phagocytosis. International Journal of Molecular Sciences. 2017;18(9).

127. Dallaire-Dufresne S, Tanaka KH, Trudel MV, Lafaille A, Charette SJ. Virulence, genomic features, and plasticity of *Aeromonas salmonicida* subsp. *salmonicida*, the causative agent of fish furunculosis. Veterinary Microbiology. 2014;169(1),1-7.

128. Machado AM, Figueiredo C, Seruca R, Rasmussen LJ. *Helicobacter pylori* infection generates genetic instability in gastric cells. Biochimica et Biophysica Acta. 2010;1806(1),58-65.

129. Rich T, Allen RL, Wyllie AH. Defying death after DNA damage. Nature. 2000;407(6805): 777-783.

130. Zgur-Bertok D. DNA damage repair and bacterial pathogens. PLoS Pathogens. 2013;9(11):e1003711.

131. Sun B, van Dissel D, Mo I, Boysen P, Haslene-Hox H, Lund H. Identification of novel biomarkers of inflammation in Atlantic salmon (*Salmo salar* L.) by a plasma proteomic approach. Developmental & Comparative Immunology. 2022;127:104268.

132. Barichello T, Generoso JS, Singer M, Dal-Pizzol F. Biomarkers for sepsis: more than just fever and leukocytosis—a narrative review. Critical Care. 2022;26(1);14.

133. Schrödl W, Büchler R, Wendler S, Reinhold P, Muckova P, Reindl J, Rhode H. Acute phase proteins as promising biomarkers: Perspectives and limitations for human and veterinary medicine. Proteomics. Clinical applications. 2016;10(11):1077-1092.

3. Chapter three: Inactivated *Aeromonas salmonicida* suppresses the humoral and cell-mediated immunity of lumpfish (*Cyclopterus lumpus*).

3.1. Abstract

Aeromonas salmonicida is a globally distributed aquatic pathogen that causes furunculosis in fish. The genome of this Gram-negative pathogen is very diverse, and several subspecies have been identified. Vaccine efficacy against *A. salmonicida* has been documented with successful reports in different fish species. Many *A. salmonicida* pathogenicity and vaccinology studies used different strains, which led to difficulties in reproducing results because of the genomic diversity of *A. salmonicida* strains. Recently, a hypervirulent strain of *A. salmonicida* was sequenced and characterized, which caused mass mortalities in Atlantic salmon, rainbow trout, and lumpfish. Using lumpfish as a model, I evaluated several antigen preparations against *A. salmonicida* J223. Here, I assessed the potential immune protective effect of *A. salmonicida* bacterins in the presence and absence of the virulence factors VapA layer and extracellular products secreted by *A. salmonicida*. Also, I evaluated the impact of outer membrane proteins (OMPs), including iron-regulated outer membrane proteins (IROMPs) of *A. salmonicida* in lumpfish. Triplicated groups of passive integrated transporter (PIT)-tagged lumpfish (10.3 ± 2.4 g (mean ± SD); n=48 per group) were intraperitoneally (ip) injected with the respective antigen formulation (*A. salmonicida* $VapA^+$ bacterin, $VapA^+$ bacterin with extracellular products, $VapA^-$ bacterin, $VapA^-$ bacterin with extracellular products, $VapA^+$ OMPs, $VapA^+$ IROMPs, $VapA^-$ OMPs, $VapA^-$ IROMPs) or control (TSB + adjuvant). Blood samples were collected every 2 weeks post-immunization (wpi) for IgM titers determination by enzyme-linked immune sorbent assay (ELISA), and spleen samples were collected at 6 wpi for gene expression evaluation by real-time quantitative polymerase chain reaction (RT-qPCR) assay. Immunized fish were ip challenged with 10^4 *A. salmonicida* cells/dose

at 8 wpi. Immunized and control fish died within 2 weeks post-challenge. ELISA analyses suggest that immunization with *A. salmonicida* J223 bacterins did not increase IgM titers. RT-qPCR results showed that genes having putative roles in adaptive immunity (e.g., *igm, mhc-ii,* and *cd4*) were downregulated. These results indicate that *A. salmonicida* J223 antigen preparations, including bacterin and OMPs, independent of VapA presence, suppress lumpfish immunity. Interestingly, a similar effect was observed in naïve lumpfish when infected with live *A. salmonicida* J223, suggesting the presence of virulence factors triggers immune suppression in lumpfish. My results will be valuable in developing an immune-protective vaccine against *A. salmonicida*.

3.2. Introduction

Aeromonas salmonicida was first identified in the 1890s during a disease outbreak at a Bavarian brown trout (*Salmo trutta*) hatchery [1]. Since then, *A. salmonicida* has been thoroughly studied and considered as an important fish pathogen due to its diverse host range, wide distribution, and significant economic impact on aquaculture, especially in salmonids [2].

Isolates with different phenotypic characteristics have been classified into typical and atypical groups [3]. The typical strains correspond to *A. salmonicida* subsp. *salmonicida,* and the atypical correspond to *A. salmonicida* subsp. *achromogenes, masoucida*, *smithia,* and *pectinolytica* [4-7]. Additionally, *A. salmonicida* can be divided into 14 subgroups based on variations in the gene that encodes for the A-layer protein (*vapA*) [8]. Moreover, the genome-based analyses revealed that *A. salmonicida* isolates from different geographical origins are much more diverse than previously thought [7, 9]. A total of 95 genome sequences of *A. salmonicida* (either completed or draft genomes) are available in the GenBank database (accessed in March 2023) (https://www.ncbi.nlm.nih.gov/genome/browse/#!/prokaryotes/540/).

The *A. salmonicida* genome is rich in mobile genetic elements, including plasmids, transposons, insertion sequences (ISs), and genomic islands [10]. Analysis of most of these genomes revealed that the number and size of plasmids vary among different isolates [9]. Plasmids can represent up to 40% of the genome [11], and plasmid repertoire is very diverse among *A. salmonicida* strains [9, 12]. Plasmids allow the bacterial genome to adapt rapidly by changing the gene repertoire [9, 11]. The type three secretion system (T3SS) of *A. salmonicida*, located in a large virulence plasmid, transfers several effector proteins and toxins into the host cell, suppressing the host immune response [13, 14]. Genomic variation within the virulence plasmid could affect T3SS functionality and virulence. For example, the typical strain J223 harbors a complete T3SS with additional copies of *aopN* and *acr2* virulence genes, correlating with the hypervirulence displayed by this strain [12, 15, 16].

A comparative genomic analysis of *A. salmonicida* strains showed that strains with high chromosome similarity have genomic structural differences. For example, typical *A. salmonicida* strain J223 has 99.21% and 99.17% of nucleotide identity with *A. salmonicida* strain O1-B526 and A449, respectively, but they display structural genomic differences (e.g., chromosomal inversion, insertions, and deletion) [12]. Genomic differences between *A. salmonicida* strains, host range, and environmental adaptation are related to ISs activity, which might result in the presence and absence of genes encoding for virulence factors, causing differences between strains that affect their phenotypes [7, 12, 17]. Typical strains harbor more active ISs than atypical strains, suggesting that atypical strains could have evolved from a recent endogenous mutagenesis event [12]. Such mutagenesis events indicate that there might be considerable flexibility in the capacity of the *A. salmonicida* genome to respond to diverse conditions.

Recent studies identified that the *A. salmonicida* species includes a myriad of strains with various ways of living and ecological niches [18]. The well-known strict psychrophiles have extensive host ranges in wild and farmed fish of all ages, and their infection occurs in freshwater, brackish, and marine environments [19-21]. Studies have been done to identify possible protective *A. salmonicida* antigens, e.g., the A-layer protein VapA, several outer membrane proteins (OMPs), including iron-regulated outer membrane proteins (IROMPs), extracellular products (ECPs) (e.g., protease, lipase, lipopolysaccharide (LPS)) and the T3SS consisting of effector and structural proteins [14, 22-35]. The potential of these virulence factors as vaccine candidates have been investigated in several fish species [24, 26, 36-44]. However, many of these vaccine studies used different strains of *A. salmonicida* and delivery routes for the infection challenges, which led to inconsistent results because of the genomic diversity within *A. salmonicida* [9, 12, 16, 44-48].

Lumpfish (*Cyclopterus lumpus* L.) farming has been increasing exponentially to reduce sea-lice (e.g., *Lepeophtheirus salmonis*, an ectoparasite) infestation from farmed Atlantic salmon in Europe and Canada [49-53]. Sea-lice impact the survival and welfare of salmon and cause substantial economic losses to the aquaculture industry [54, 55]. As anti-lice chemotherapeutic treatment results in parasite resistance, cleaner fish, like lumpfish, are successfully used to biocontrol sea-lice infestation in the North Atlantic region [56-58]. However, *A. salmonicida* infections are responsible for high mortality in lumpfish [16, 59]. Also, other farmed species, like sablefish (*Anoplopoma fimbria*), European perch (*Perca fluviatilis*), rainbow trout (*Oncorhynchus mykiss*), crucian carp (*Carassius auratus*), Atlantic halibut (*Hippoglossus hippoglossus*), and Arctic char (*Salvelinus alpinus*) are severely affected by *A. salmonicida* [60-64], suggesting that vaccines are lacking efficacy to control furunculosis outbreaks in species different than Atlantic

salmon. Efforts to develop vaccines against *A. salmonicida* in lumpfish are ongoing, but furunculosis remains recalcitrant [48, 52, 59, 65-70].

Inactivated whole *A. salmonicida* cell preparations do not confer immune protection in some fish species. For example, the A-layer protein was identified as highly immunogenic in fish when injected as whole *A. salmonicida* cell bacterin or purified preparations [38, 71, 72]. However, washed or unwashed formalin-killed virulent cells of *A. salmonicida* with or without the A-layer did not protect Brook trout (*Salvelinus fontinalis*) [39]. A potential reason for this could be the presence of virulence factors that cause immune suppression or the antigenic components of the vaccine could inhibit adaptive immune response. The antigenic component of an injected vaccine must be taken up by the antigen-presenting cells (APC) and presented by major histocompatibility complex (MHC) molecules that activate T cells. Activated T cells drive B cell activation and the production of memory B cells and $CD8^+$ memory T cells. $CD8^+$ memory T cells can proliferate rapidly once they encounter a pathogen and trigger immune protection [73].

In chapter 2, I identified that *A. salmonicida* subspecies *salmonicida* strain J223 causes an acute infection in lumpfish [16]. The lethal dose 50 (LD_{50}) was calculated as 10^2 CFU/dose, and 10^3 CFU/dose caused 100% mortality to lumpfish in 15 days. In addition, our group observed that mortality in lumpfish infected by a bath with *A. salmonicida* J223 (10^6 CFU/mL for 20 min) reached 100% in 14 days (unpublished data). *A. salmonicida* J223 infection also causes immune suppression by upregulating *il10* and downregulating immunoglobulins (*igm)* and *mhc-II* in lumpfish head kidney, spleen, and liver [16]. Therefore, I aimed to develop a vaccine for lumpfish against *A. salmonicida* J223. For this purpose, I evaluate the immune protective effect of *A. salmonicida* bacterins and OMPs/IROMPs with and without Vap A layer (A^+/A^-) in lumpfish. To further investigate the immune responses triggered by these antigen formulations in lumpfish, I

tested biomarkers for adaptive immune responses, including genes encoding MHC-II, $CD4^+$, $CD8^+$, and titers of IgM, by real-time quantitative polymerase chain reaction (RT-qPCR) and enzyme-linked immune sorbent assay (ELISA), respectively. My results indicate that the formalin-killed *A. salmonicida* bacterin and OMPs neither trigger memory immune responses nor confer protection to lumpfish. These results suggest that prevention of antigen presentation, B and T-cell activation could be a mechanism exerted by the virulence factors present in *A. salmonicida* J223.

3.3. Materials and Methods

3.3.1. Bacterial strains, media, and reagents

A. salmonicida strains J223 (A^+), J225, J227, and J228 (A^-; lab collection) were routinely grown from a single colony in a 16 mm diameter glass tube containing 3 mL of Trypticase Soy Broth (TSB, Difco, Franklin Lakes, New Jersey, USA) at 15 °C with aeration (180 rpm) for 48 h according to previous descriptions [15, 74-76]. Subsequently, 300 µL of fresh culture was added to a 250 mL Erlenmeyer flask containing 30 mL of TSB media and cultured at 15 °C with aeration (180 rpm) up to a desired optical density (OD_{600} nm). When required, TSB was supplemented with 1.5% bacto agar (Difco) and 0.01% Congo-red (TSA) (Sigma-Aldrich, St. Louis, Missouri, USA). Bacterial growth in TSB was monitored by the Genesys 10 UV spectrophotometer (Thermo Scientific, Madison, Wisconsin, USA) and by spreading of serially diluted growth medium on TSA plate to count colony forming units (CFU/mL). Bacterial cells were harvested by centrifugation (4,200 × *g* for 10 min at 4 °C).

3.3.2. Bacterin preparation

A. salmonicida strains were grown in 250 mL Erlenmeyer flasks containing 30 mL of TSB media supplemented with 2,2'-dipyridyl at 15 °C with aeration (180 rpm) up to OD_{600} 1.5 to induce

the expression of IROMPs [77]. The bacterial cells were harvested by centrifugation (4,200 × *g* for 10 min at 4 °C) and washed three times with phosphate-buffered saline (PBS; 136 mM NaCl, 2.7 mM KCl, 10.1 mM Na_2HPO_4, 1.5 mM KH_2PO_4 (pH 7.2)) [78] and then fixed with 50 mL of 6% formalin for 3 days at room temperature with gentle agitation. Formalin residues were removed by centrifugation at 4,200 × *g* for 10 min at 4 °C and washed 3 times with PBS. Inactivated cells were then resuspended in PBS and dialyzed (Molecular weight cut off 3.5 kDa; Spectra/Por, Cole Parmer, Laval, Quebec, Canada) at 4 °C with gentle stirring in 1 L of PBS for three consecutive days. Cell inactivation was confirmed by streaking the cells on the TSA plate. Then the inactivated strain J223, and a mix of J225, J227, and J228 strains were resuspended in 50 mL of PBS and stored at 4 °C until further utilization.

A second batch of bacterial strains was cultured under the previously described conditions and directly fixed with 0.2% formalin for 3 days at room temperature with gentle agitation. Cell inactivation was confirmed by streaking the culture on the TSA plate. The growth medium was saved because that contains ECPs secreted by the *A. salmonicida*. The inactivated cultures of J225, J227, and J228 strains were mixed in equal quantities (by volume). Both PBS-washed and unwashed preparation of J223 and mixed J225, J227, and J228 bacterins were quantified using flow cytometry and the Bacteria Counting Kit (Invitrogen™, ThermoFisher, Waltham, Massachusetts, USA) according to the manufacturer's instructions. A BD FACS Aria II flow cytometer (BD Biosciences, San Jose, California, USA) and BD FACS Diva v7.0 software were used for bacteria cell quantification. The number of bacterial cells/mL was calculated by dividing the number of signals in the bacterial frame by the number of signals in the microsphere frame, as described previously [79]. Washed and non-washed *A. salmonicida* J223 bacterin (hereafter referred to as A^+W and A^+NW, respectively) and the mix of *A. salmonicida* J225, J227, and J229

bacterin (hereafter referred to as A^-W and A^-NW, respectively) were mixed with CARBIGEN™, a terminally-sterilized, carbomer-based (Carbopol 934P) adjuvant to prepare the vaccine formulation according to manufacturer's instructions (MVP Adjuvants®, Phibro Animal Health Corporation, Teaneck, New Jersey, USA). Only TSB medium was mixed with the adjuvant to use as a control.

3.3.3. Bacterial outer membrane proteins preparations

A. salmonicida OMPs were prepared according to the established methods [80]. Briefly, *A. salmonicida* J223 and J227 were initially grown in 3 mL of TSB media from a single colony. Subsequently, 300 µL of fresh culture were added to 250 mL Erlenmeyer flasks containing 30 mL of TSB media supplemented with either 100 µM $FeCl_3$ or 2, 2'-dypyridyl, respectively at 15 °C with aeration (180 rpm) up to an optical density (OD_{600} nm) of 1.0. The cells were harvested by centrifugation at 10,000 g for 10 min at 4 °C and washed three times with PBS. *A. salmonicida* cells resuspended in Tris-OH/EDTA buffer pH 7.4 (20 mM Tris-OH; 1 mM EDTA; 1 mM PMSF) were lysed by passing the culture twice through a French press (Thermo Electron Corporation, Madison, Wisconsin, USA) at 10,000 psi (6.9 MPa; 40K cell). The lysed cell preparation was centrifuged at 7,000 g for 10 min at 4 °C to remove cell debris and unlysed cells. The supernatant was centrifuged at 16.000 g for 1 h at 4 °C, and the pellet was resuspended in 10 mL of 0.5% (w/v) Sarkosyl and incubated overnight on ice. The suspension was then centrifuged at 16,000 g for 1 h at 4 °C to obtain the OMPs. OMPs obtained from *A. salmonicida* J223 supplemented with $FeCl_3$ or 2, 2'-dipyridyl were denoted as A^+ OMPs or A^+ IROMPs, respectively. OMPs obtained from *A. salmonicida* J227 supplemented with FeCl3 or 2, 2'-dipyridyl were denoted as A^- OMPs or A^- IROMPs, respectively. The total OMPs were normalized to 5 µg/mL by using the

spectrophotometer (Genova-nano, Jenway, Stone, Staffordshire, England) and mixed with CARBIGEN™ to prepare the immunization dose.

3.3.4. Vaccine pre-evaluation

The presence and integrity of bacterins were assessed by staining with 5-([4,6-dichlorotriazinyl] amino) fluorescein hydrochloride (DTAF) solution (100 µg in dimethyl sulfoxide (DMSO); Sigma-Aldrich, St. Louis, Missouri, USA) according to established protocols [81] and 4′,6-diamidino-2-phenylindole (DAPI; Thermo Fisher Scientific, Waltham, Massachusetts, USA) according to the manufacturer's instructions. *A. salmonicida* strains labeled with DTAF and DAPI, were visualized with a Nikon AR1 laser scanning confocal microscope.

Furthermore, OMPs profiles were visualized by Sodium dodecyl-sulfate polyacrylamide gel electrophoresis (SDS-PAGE) electrophoresis. Proteins preparations were boiled for 10 min after resuspending in 100 µL of 2X SDS-buffer (glycerol 50%, 1M Tris-OH [pH 6.8], SDS 10%, bromophenol blue 0.5%, and β-mercaptoethanol 0.5%) [78]. Aliquots of 10 µL from each sample were separated in 10% SDS-PAGE at 120 V for 1.5 h using a Mini-PROTEAN®II Cell electrophoresis apparatus (Bio-Rad, Hercules, California, USA). The gel was stained for 30 min with a Coomassie blue solution (Coomassie blue 0.125% (*w*/*v*); methanol 50% (*v*/*v*); glacial acetic acid 10% (*v*/*v*); dH_2O up to 1 L) and destained with 30% methanol and 10% acetic acid solution until visualization.

A. salmonicida VapA was detected by Western blots. Briefly, SDS-PAGE gels and nitrocellulose membranes (0.2 µm, Bio-Rad, Hercules, California, USA) were submersed in transfer buffer (methanol 20% (*v*/*v*), 250 mM Tris-OH; 1.92 M glycine; dH_2O up to 1 L) for 5 min. OMPs were transferred by a semi-dry TRANS-BLOT®SD apparatus (Bio-Rad, Hercules, California, USA) at 20 V for 30 min. Membranes were incubated overnight in blocking buffer

(skim milk 0.5%; PBS-Tween 0.05% (PBS-T)) and washed three times with PBS-T for 5 min each. The membranes were incubated 1 h at room temperature with rabbit IgG anti-VapA (1:5000) [15], washed three times with PBS-T, and incubated 1 h with the goat anti-rabbit IgG alkaline-phosphate conjugate (1:5000) (Life Technologies, Thermo Fisher Scientific, Waltham, Massachusetts, USA). After washing three times, the protein was visualized by adding 1 mL of 5-bromo-4-chloro-3-indolyl phosphate (BCIP)-nitro blue tetrazolium (NBT) (Thermo Fisher Scientific, Waltham, Massachusetts, USA) to the membrane.

3.3.5. Bacteria inoculum preparation

A. salmonicida J223 was initially grown in 3 mL of TSB media. Subsequently, 300 µL of fresh culture were added to a 250 mL baffled Erlenmeyer flask containing 30 mL of TSB media and incubated at 15 °C with aeration (180 rpm) in an orbital shaker up to an optical density (OD_{600}) of 0.7 (~1 x 10^8 CFU/mL) according to previous descriptions [15]. The bacterial cells were harvested by centrifugation (4,200 × *g* for 10 min at 4 °C), washed three times with PBS, and finally resuspended in 300 µL of PBS. The concentrated bacterial inoculum was serially diluted in PBS (1:10) and quantified by plating it onto Trypticase Soy Agar (1.5%; TSA) to determine CFU/mL.

3.3.6. Ethics statement

The experiments were performed following the Canadian Council on Animal Care guidelines and approved by Memorial University of Newfoundland's Institutional Animal Care Committee (protocols #18-01-JS, #18-03-JS, and biohazard license L-01) [53].

3.3.7. Fish holding

Juvenile lumpfish (10.3 ± 2.4 g (mean ± SD)) were maintained at ~8–10 °C in 500 L tanks supplied with 95–110% air-saturated and U.V.-treated filtered flow-through seawater, and an

ambient photoperiod at the Dr. Joe Brown Aquatic Research Building (JBARB) at the Department of Ocean Sciences (DOS), Memorial University of Newfoundland (MUN), Canada for the immunization experiment [53]. Challenge assays were conducted at the AQ3 biocontainment Cold-Ocean Deep-Sea Research Facility (CDRF) at DOS, MUN. Lumpfish were kept in 500 L tanks, with flow-through (7.5 L/min) of UV-treated seawater (8-10 °C), ambient photoperiod (winter-spring), and 95-110% air saturation. Biomass density was maintained at 6.6 kg/m^3. The fish were fed daily using a commercial diet (Skretting – Europa 15; crude protein (55%), crude fat (15%), crude fiber (1.5%), calcium (3%), phosphorus (2%), sodium (1%), vitamin A (5000 IU/Kg), vitamin D (3000 IU/Kg) and vitamin E (200IU/Kg)) with a ration of 0.5% of their body weight per day.

3.3.8. Lumpfish immunization using a common garden experiment

Lumpfish were passive integrated transporter (PIT)-tagged and acclimated for 2 weeks at ~8–10 °C before immunization. After this period, independent groups of 48 fish were starved for 24 h, anesthetized with 40 mg of MS222 (Syndel Laboratories, Vancouver, BC, Canada) per liter of seawater. and intraperitoneally (ip) immunized with 100 μL of the A^+W (4.0×10^9 CFU/dose), A^+NW (5.8×10^7 CFU/dose), A^-W (5.1×10^8 CFU/dose), A^-NW (3.6×10^7 CFU/dose), A^+OMPs (500 ng/dose), $A^+IROMPs$ (500 ng/dose), A^-OMPs (500 ng/dose), and $A^-IROMPs$ (500 ng/dose). Control fish were injected with TSB and adjuvant (1:1). Fish were distributed randomly into three different tanks with an equal proportion of each group (Figure 3.1). Non-lethal blood samples (n=30; 6 fish each treatment) were taken from the caudal vein of anesthetized fish every 2 weeks post-immunization (wpi), and lethal spleen samples from euthanized fish (400 mg of MS222/ L of water) were taken at 6 wpi (n=30; 6 fish each treatment).

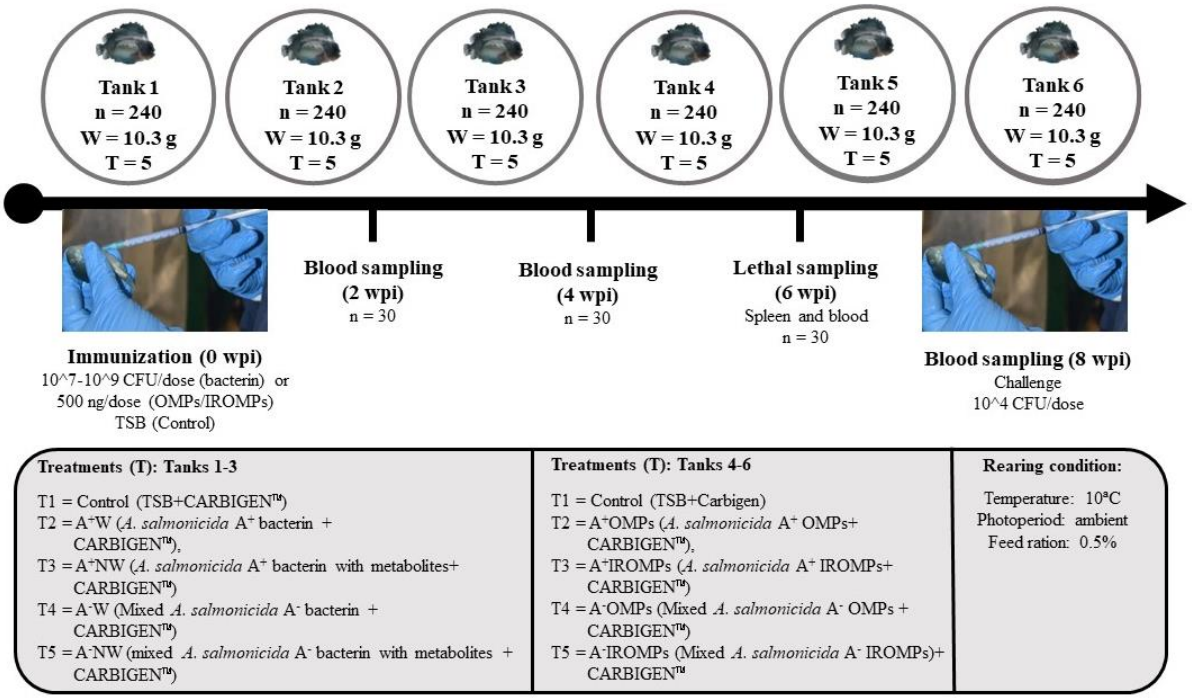

Figure 3.1. Experimental workflow. Four independent groups of 48 lumpfish were intraperitoneally (ip) immunized with *A. salmonicida* A^+/A^- and W/NW bacterin. Another four independent groups of 48 lumpfish were ip immunized with *A. salmonicida* A^+/A^- and OMPs/IROMPs. Control fish were injected with TSB and adjuvant CARBIGEN™ (1:1). Fish were distributed randomly into three different tanks with an equal proportion of each group. Non-lethal blood samples (n = 30; 6 fish each treatment) were taken every 2 wpi, and lethal spleen samples were taken at 6 wpi (n=30; 6 fish each treatment). n = number of fish, W = average weight of fish, T= number of treatments, wpi = weeks post-immunization.

3.3.9. Challenge of immunized lumpfish

Immunized lumpfish were transferred from JBARB to the AQ3 biocontainment facility and acclimated for 2 weeks under the previously described optimal conditions. The fish were anesthetized with 40 mg of MS222 per liter of seawater and ip injected with 100 μl of 10^4 CFU/dose of *A. salmonicida* at 8 wpi. Mortality was monitored daily, Kaplan-Meier estimator and Log-rank test were used to obtain survival fractions after the challenges and to determine the differences between treatments, respectively. One-way ANOVA was followed by Tukey's multiple comparisons test to obtain the *p*-value between groups ($p < 0.05$ was considered significant). Statistical analyses and data visualization were performed using GraphPad Prism 7.0 (La Jolla, San Diego, California, USA).

3.3.10. Direct enzyme-linked immunosorbent assay (dELISA)

Similar to the previous finding [60], I verified that high-affinity anti-lumpfish IgM chicken IgY binds strongly to the *A. salmonicida* J223 in a non-specific fashion that hindered us from conducting an indirect ELISA. Therefore, total lumpfish IgM titers were evaluated after immunization using dELISA.

The lumpfish serum samples were kept at 56 °C for 30 minutes to inactivate the complement and mixed with 100 μL of chloroform (Sigma-Aldrich, St. Louis, Missouri, USA) for 10 minutes at room temperature to remove fats. Serum samples were centrifuged at 4,000 g for 10 min at room temperature, and the supernatant was collected and stored at −80 °C until further utilization. Serum aliquots of 60 μL were serially diluted (1:2) in coating buffer (0.015 mM Na_2CO_3; 0.035 mM $NaHCO_3$; pH 9.8) in 96 well plates (Ultra-High Binding Polystyrene Microtiter, Thermo Fisher Scientific, Waltham, Massachusetts, USA). The plates were incubated

at 4 °C overnight, washed 3 times with PBS-Tween (PBS-T; 0.1%), and blocked with 150 µL of ChonBlock™ (Chondrex Inc., Woodinville, Washington States, USA) for 1 h at 37 °C. After this period, the plates were washed 3 times with PBS-T, inoculated with 100 µL of the secondary antibody (anti-lumpfish IgM chicken IgY (biotinylated); 1:10,000), and incubated at 37 °C for 1 h. Following incubation and washing, 100 µL of streptavidin-HRP (Southern Biotech, Southern Biotech, Birmingham, Alabama, USA; 1:10,000) was added, and the plates were incubated at 37 °C for 1 h. For visualization and color development, 50 µL of ultra-TMB (Invitrogen™, ThermoFisher, Waltham, Massachusetts, USA) were added, and the plates were incubated at room temperature (20-22 °C) for 15 min. Optical density was determined at 450 nm after adding 50 µL of stop solution (2 M H_2SO_4). IgM titers were evaluated in naïve animals (n = 6) at 2, 4, 6, and 8 wpi.

The standard curve was developed using established protocols [60]. Briefly, purified lumpfish IgM (lab collection, extracted from lumpfish serum) was serially diluted in coating buffer to 500, 250, 125, 62.5, 31.25, 15.63, 7.8, 3.9, 1.95, 0.98, 0.49, and 0.24 µg/ml and incubated overnight at 4 °C. Each concentration was evaluated in triplicate. After incubation and washing, 100 µL of IgY (1:10,000) were added and incubated at 37 °C for 1 h. Following incubation and washing, 100 µL of Streptavidin-HRP (1:10,000) were added and incubated at 37 °C for 1 h. For visualization and color development, 50 µL of ultra-TMB were added and incubated at room temperature (20-22 °C) for 15 min. Optical density was determined at 450 nm after adding 50 µL of stop solution (2 M H_2SO_4). The values were normalized using a natural logarithm standard curve of known concentrations. A one-way ANOVA multi-comparison analysis was performed to determine significant differences between treatments. Statistical analyses were performed using GraphPad Prism 7.0.

3.3.11. RNA Preparation

To study the lumpfish immune response to A^+ and A^- *A. salmonicida* bacterins, spleen samples (n = 3 per group) were extracted from control fish and fish immunized with A^+W and A^-W. Approximately 80-100 mg of tissue suspension in 500 µL of TRIzol reagent (Invitrogen™, ThermoFisher, Waltham, Massachusetts, USA) was homogenized using a motorized RNase-Free Pellet Pestle Grinder (Fisherbrand, Fisher Scientific, USA) and an additional 500 µL of TRIzol were added. RNA extractions were completed following the manufacturer's instructions. Extracted RNA samples were further purified using RNeasy MinElute Cleanup Kit (QIAGEN, Mississauga, Ontario, Canada) and TURBO DNA-free™ Kit (Invitrogen™, ThermoFisher, Massachusetts, USA). Purified RNA samples were quantified and evaluated for purity using a spectrophotometer at 260 nm wavelength (Genova-nano, Jenway, Stone, Staffordshire, England), and evaluated for integrity using 1% agarose gel electrophoresis [78] (Table 3.1 and Figure 3.2).

Table 3.1. RNA quality.

Sample Name	Concentration (µg/mL)	260/280[a]	260/230[b]
Control 1	535.32	2.07	1.30
Control 2	824.99	2.06	1.55
Control 3	905.18	2.05	1.70
A^+W 1	4940.7	2.09	2.09
A^+W 2	1360.60	2.07	1.86
A^+W 3	2957.90	2.08	2.06
A^-W 1	818.95	2.07	1.66
A^-W 2	909.79	2.07	1.70
A^-W 2	1368.80	2.09	1.76

[a] 260/280 Ratio: 260 nm and 280 nm are the absorbance wavelengths used to assess the purity of DNA and RNA. A ratio of ~2.0 is considered pure for RNA. A lower absorbance ratio may indicate the presence of protein, phenol, or other contaminants that have an absorbance close to 280 nm. Subtraction of non-nucleic acid absorbance at 320 nm, is also needed to calculate this ratio. Formula:

DNA Purity (A_{260}/A_{280}) = (A_{260} reading – A_{320} reading) ÷ (A_{280} reading – A_{320} reading)

[b] 260/230 Ratio: The ratio of absorbance at 260 and 230 nm can be used as a secondary measure of DNA or RNA purity. In this case, a ratio between 2.0 - 2.2 is considered pure. If the ratio is lower than this expected range, it may indicate contaminants in the sample that absorb at 230nm.

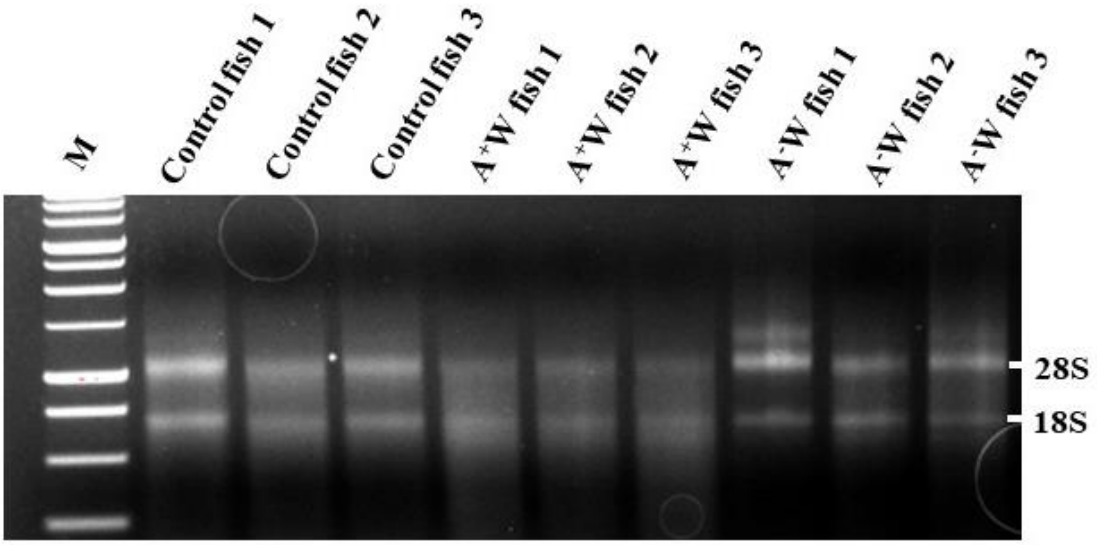

Figure 3.2. One percent agarose gel electrophoresis of RNA samples of control fish (n = 3) and A^+W/A^-W bacterin injected fish (n = 3). One microgram of RNA was run on a 1% agarose gel with ethidium bromide staining. Crisp 28S and 18S ribosomal RNA bands at ~2:1 ratio were indicative of acceptable RNA integrity. M = 1 kb molecular weight marker (Promega, Fisher Scientific, Ottawa, Ontario, Canada).

3.3.12. cDNA synthesis and RT-qPCR

First-strand cDNA templates for RT-qPCR were synthesized in 20 mL reactions from 1 mg purified RNA using SuperScript IV VILO Master Mix (Invitrogen™, ThermoFisher, Waltham, Massachusetts, USA) following the manufacturer's instructions. The sequences, amplicon sizes, and amplification efficiencies for all primer pairs used in the RT-qPCR analyses are presented in Table 3.2. Primer pairs for *interleukin 1b* (*i1b*), *interleukin 8a* (*il8a*), *interleukin 8b* (*il8b*), *interleukin 10* (*il10*), *immunoglobulin heavy chain 1* (*igm-h1*), *immunoglobulin heavy chain 2* (*igm-h2*), *immunoglobulin mu heavy chain 1* (*igm-mu-1*), *HLA class II histocompatibility antigen* (*mhc-II*), *cluster of differentiation 4* (*cd4-1* and *cd4-2*), and *cluster of differentiation 8* (*cd8*), and the endogenous control genes, 60S *ribosomal protein L32* (*rpl32*), *elongation factor 1-alpha* (*ef1a*), *eukaryotic translation initiation factor 3 subunit D* (*etf3d*), *polyadenylate-binding protein 1a* (pabpc1a) and *polyadenylate-binding protein 1b* (*pabpc1b*), were designed, and quality control (QC) was tested previously [82].

Table 3.2. Primers used in this study.

Gene Name	Symbol	Forward (F = 5'-3') Reverse (R = 5'-3')	Amplification Efficiency (%)	Amplicon Size (bp)
HLA class II histocompatibility	*mhc-II*	F: ACGCCAAGACACCTCTGACT R: GGAAGGTCTCGTTGAACTGC	89.8	108
immunoglobulin heavy chain 1	*igm-h1*	F: AGGACTGGAGTGGATTGGAA R: TGCATGGTCTGTCCGTTTAG	90.5	129
immunoglobulin heavy chain 2	*igm-h2*	F: GAATGGAACAAGGGGACAAA R: CGGTCGTTGAGTCTCTCCTC	89.6	108
immunoglobulin mu heavy chain 1	*igm-mu-1*	F: CAGCTTCTGGATTAGACTTTGA R: GATGTTGTTACTGTTGTGTTGG	90.2	107

Gene Name	Symbol	Forward (F = 5'-3') Reverse (R = 5'-3')	Amplification Efficiency (%)	Amplicon Size (bp)
interleukin 1 beta	*il1b*	F: ATTGTGTTCGAGCTCGGTTC R: CGAACTATGGTCCGCTTCTC	97.4	98
interleukin 8a	*il8a*	F: AAGTCATAGCCGGACTGTCG R: CCCTGCTGATGGAGTTGTCT	96.3	109
interleukin 8b	*il8b*	F: GTCTGAGAAGCCTGGGAGTG R: TCAGAGTGGCAATGATCTCG	87.3	138
interleukin 10	*il10*	F: AACCAGTGCTGTCGTTTCGT R: TGTCCAAGTCATCGTTTGCT	97.8	106
cluster of differentiation 4-1	*cd4-1*	F: CGTTAAGGTGCTGCAGATCA R: GCGGAAACCATTTCAGTTGT	84.9	122
cluster of differentiation 4-2	*cd4-2*	F: TGTGGGGTTAGCTCCTTCAC R: TGTTTGCGATCTCACCTTTG	94.2	138
cluster of differentiation 8	*cd8*	F: GCTTTGCTCTCTGGGCATAC R: TCCGGGTTCTTAAGTGGTTG	89.6	104
60S ribosomal protein L32	*rpl32*	F: GTAAGCCCAGGGGTATCGAC R: GGGCAGCATGTACTTGGTCT	92.9	107
elongation factor 1 alpha_a	*ef1a_a*	F: CAAGGGATGGAAGATTGAGC R: TGTTCCGATACCTCCGATTT	94.3	151
eukaryotic translation initiation factor 3 subunit D	*etif3d*	F: AGCCAGATCAACCTGAGCAT R: AGGCTGTACACCCGAATCAC	90.3	134
polyadenylate-binding protein 1_a	*pabpc1_a*	F: CAAGAACTTTGGGGAGGACA R: TGACAAAGCCAAATCCCTTC	86.39	125
polyadenylate-binding protein 1_b	*pabpc1_b*	F: GACTCAGGAGGCAGCTGAAC R: TCGCGCTCTTTACGAGATTT	91.99	102

In the experimental RT-qPCR analyses, the expression levels of the genes were normalized to the expression levels of two endogenous control genes. To select these endogenous controls, *rpl32*, *ef1a*, *etf3d*, *pabpc1a*, and *pabpc1b* were analyzed. The fluorescence threshold cycle (Ct) values of all 9 samples in the study were measured (in triplicate) for each of these transcripts using cDNA of 4 ng of input total RNA and then analyzed using geNorm [83]. *pabpc1b* and *rpl32* (geNorm M = 0.581) were selected as the two endogenous controls as they were the most stably expressed. RT-qPCR reactions were done in a final volume of 20 µL, containing 10 µL of 1 × PowerUp-SYBR Master Mix (Applied BioSystems, Foster City, California, USA), 1 µL (10 µM) of each primer, 6 µL of nuclease-free water (Ambion, Austin, Texas, USA), and 2 µL (4 ng) of cDNA. Samples were amplified and detected in a QuantStudio 3 (Applied BioSystems, ThermoFisher, Waltham, Massachusetts, USA). The reaction mixtures were incubated for 2 min at 95 °C, followed by 40 cycles of 1 s at 95 °C, 30 s at 60 °C, and finally 15 s at 95 °C, 1 min at 60 °C, and 15 s at 95 °C. On each plate, for every sample, the selected genes and endogenous controls were tested in triplicate, and a non-template control was included. Transcripts relative quantity (RQ) using the comparative $2^{-\Delta\Delta Ct}$ method [82].

3.4. Results

3.4.1. A. salmonicida bacterin integrity and presence of VapA determination

Bacterin integrity was checked in A^+W and A^-W. DAPI stains showed the presence of bacterial DNA. DTAF has an affinity toward carbohydrates, proteins, and polysaccharides components of the bacterial membranes [84, 85]. The staining results indicate the presence of an bacterial membrane around the bacterial genomic DNA (Figure 3.3A). Bacterial outer membrane proteins profile and VapA expression analyses were conducted by SDS-PAGE and Western blot. SDS-PAGE showed clear bands of IROMPs (~100-130 kDa) in A^+ IROMPs and A^- IROMPs

(3.3B). A clear band of VabA (~55-70 kDa) was also visualized in A^+ OMPs and A^+ IROMPs (3.3B). Additionally, the western blot of A^-OMPs, A^-IROMPs, A^+OMPs, and A^+IROMPs showed a clear band of VabA in A^+ OMPs and A^+ IROMPs (Figure 3.3C).

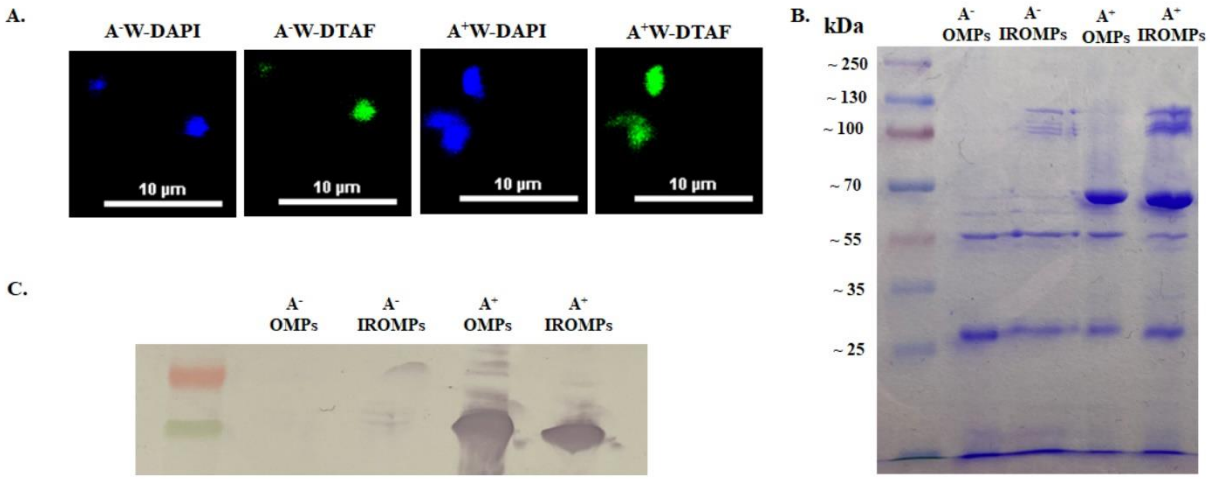

Figure 3.3. *A. salmonicida* bacterin integrity and presence of VapA determination. A. Confocal microscopy of *A. salmonicida* J223 VapA^{+} and *A. salmonicida* J225, J227, and J228 VapA^{-} strains labeled with 4,6-diamidino-2-phenylindole (DAPI), and 5-(4,6-dichlorotriazinyl) amino fluorescein (DTAF). Scale bars represent 10 µm of the area. DAPI stains showed the presence of bacterial DNA, and DTAF staining indicated the presence of bacterial membrane around the bacterial genomic DNA; B. SDS-PAGE represents the outer membrane proteins profile of A^{-}OMPs, A^{-}IROMPs, A^{+}OMPs, and A^{+}IROMPs stained with Coomassie Blue. Clear bands of IROMPs (~100-130 kDa) were visualized in A^{+} IROMPs and A^{-} IROMPs. Additionally, a clear band of VabA (~55-70 kDa) was visualized in A^{+} OMPs and A^{+} IROMPs; C. Western blot of A^{-} OMPs, A^{-}IROMPs, A^{+}OMPs, and A^{+}IROMPs. A clear band of VabA was visualized in A^{+} OMPs and A^{+} IROMPs.

3.4.2. Survival of vaccinated lumpfish after challenge with A. salmonicida

The challenge with *A. salmonicida* strain J223 resulted in > 90% and 100% mortality in lumpfish immunized with bacterin and OMPs, respectively, by 15 days post-infection (dpi). Mortality started at 8 dpi, and there was no significant difference in survival probability between the control and vaccinated groups (Figure 3.4). Morbid fish presented typical signs of acute infection, including apathetic behavior, external and internal hemorrhage, ascites accumulation in the peritoneal cavity, and swollen intestine. Relative Percentage Survival (RPS) was zero for each vaccine treatment at each time point. My results show that formalin-killed vaccines ($ECPs^{+/-}$), OMPs, and IROMPs from A^+ and A^- strains of *A. salmonicida* vaccine do not confer any protection to lumpfish against *A. salmonicida* J223.

A.

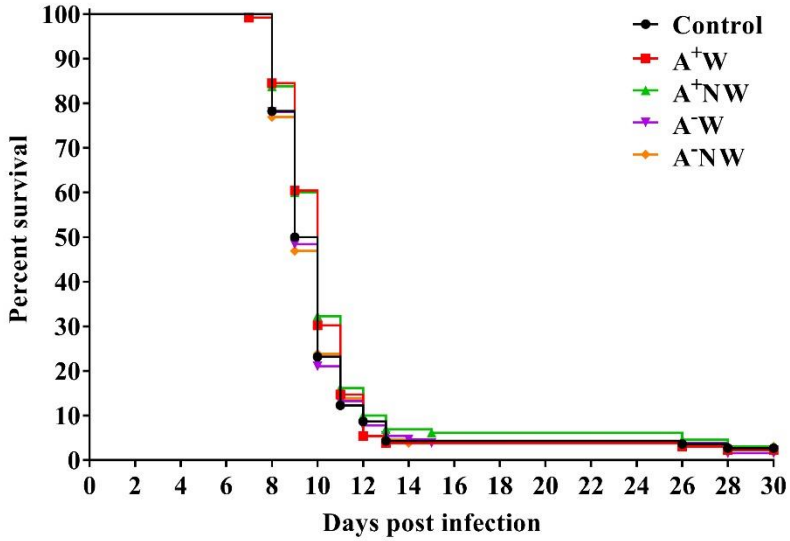
Percent survival
Days post infection
Control
A+W
A+NW
A-W
A-NW

B.

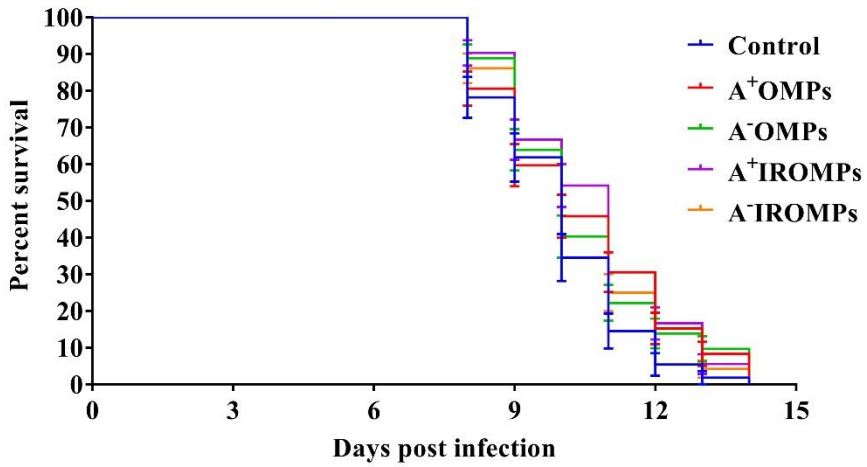
Percent survival
Days post infection
Control
A+OMPs
A-OMPs
A+IROMPs
A-IROMPs

Figure 3.4. The cumulative survival rate of intraperitoneally (ip) immunized lumpfish after ip challenge with *A. salmonicida* (10^4 CFU/dose). A. Survival rate of lumpfish injected with *A. salmonicida* (A^+/A^-; W/NW) bacterin. Less than 10% survived in control and vaccinated groups after 30 days post-challenge; B. Survival rate of lumpfish injected with *A. salmonicida* (A^+/A^-; OMPs/IROMPs) outer membrane proteins. No fish survived in both control or vaccinated groups. Control groups were mock vaccinated using the same inoculation route. Survival was assessed for 30 days. A^+: Vap A layer positive; A^-: Vap A layer negative; OMPs: Outer Membrane proteins; IROMPs: Iron Regulated Outer Membrane Proteins; W: PBS-washed cells; NW: Non-washed cells.

3.4.3. IgM titers in immunized lumpfish determined by ELISA

Previously it was determined that *A. salmonicida* J223 nonspecifically binds to the secondary IgY chicken antibody and goat IgG F(ab) [60]. Therefore, I determined the total plasma IgM titers using dELISA.

I developed a standard curve using different concentrations (500, 250, 125, 62.5, 31.25, 15.63, 7.8, 3.9, 1.95, 0.98, 0.49, and 0.24 µg/ml) of purified lumpfish IgM (Figure 3.5A). IgM concentrations were standardized using a natural logarithm (ln). The linear regression equation was determined to be $y = 0.0003001*X + 0.008771$ with $r^2 = 0.988$ ($p \leq 0.0001$) (Figure 3.5A). Total IgM was measured from non-lethal blood samples at 2, 4, 6, and 8 wpi, ranging from 5.5 to 6.1 µg/mL (Figure 3.5B). No significant differences in total IgM concentration were observed between the control and treatment groups. There was no increase in total antibody concentration over time in vaccinated fish. Instead, dELISA detects a decreasing tendency in antibody concentration in groups vaccinated with A^-W and A^-NW.

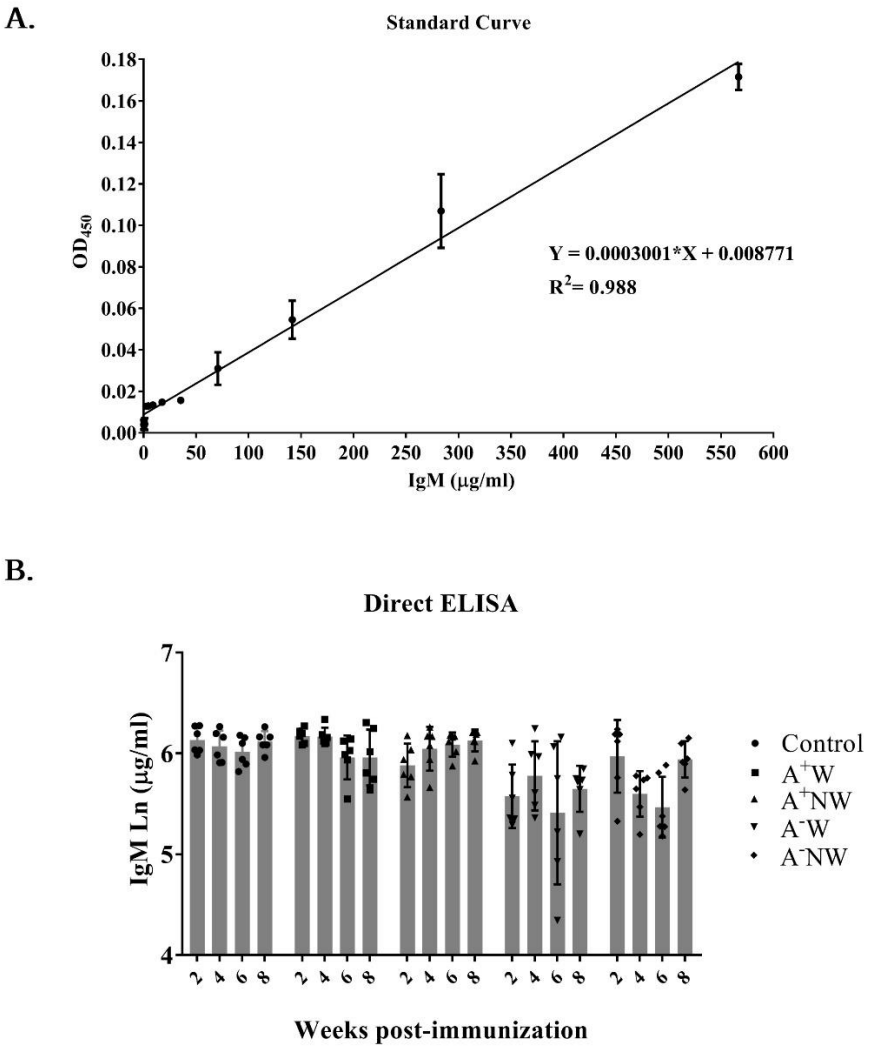

Figure 3.5. Quantification of post-challenge IgM levels is lumpfish by dELISA. A. Standard curve of purified IgM of known concentrations (500; 250, 125, 63.5, 31.8, 15.9, 7.9, 4, 2, 1 µg/mL); concentrations were standardized to the natural logarithm (ln); B. Total IgM quantification by dELISA in serum samples collected at 2, 4, 6, and 8 weeks post-immunization from the control and treatments (A^+W, A^+NW, A^-W, and A^-NW,) groups. There were no statistically significant differences detected.

3.4.4. Gene expression analyses reveal the suppression of humoral and cell-mediated immunity of lumpfish

The immune response of lumpfish to *A. salmonicida* vaccination was evaluated in the spleen at 6 wpi compared to control fish at the same time point. Expression levels of the 11 transcripts related to the innate and adaptive immune response were measured in control and A^+W or A^-W injected lumpfish. Transcript expression levels were compared between immunized fish and control fish (Figure 3.6). I observed that *i1b* was significantly upregulated in lumpfish immunized with A^-W ($p \leq 0.05$), but not in lumpfish immunized with A^+W bacterin. *il8a* was not dysregulated in A^+W and A^-W injected lumpfish. However, *il8b* was significantly downregulated by A^+W ($p \leq 0.05$) immunized fish. No significant differences in the expression of *il10* and *igm-h1* were observed in immunized fish compared to the control fish. *igm-h2* was downregulated by A^+W ($p \leq 0.05$) but not in A^-W treated fish. *igm-mu-1* was not dysregulated in both treatments. *mhc-II*, *cd4-1*, and *cd4-2* were significantly downregulated in A^+W ($p \leq 0.05$). Finally, I observed that *cd8* was upregulated by A^-W ($p \leq 0.05$) but not in A^+W immunized fish.

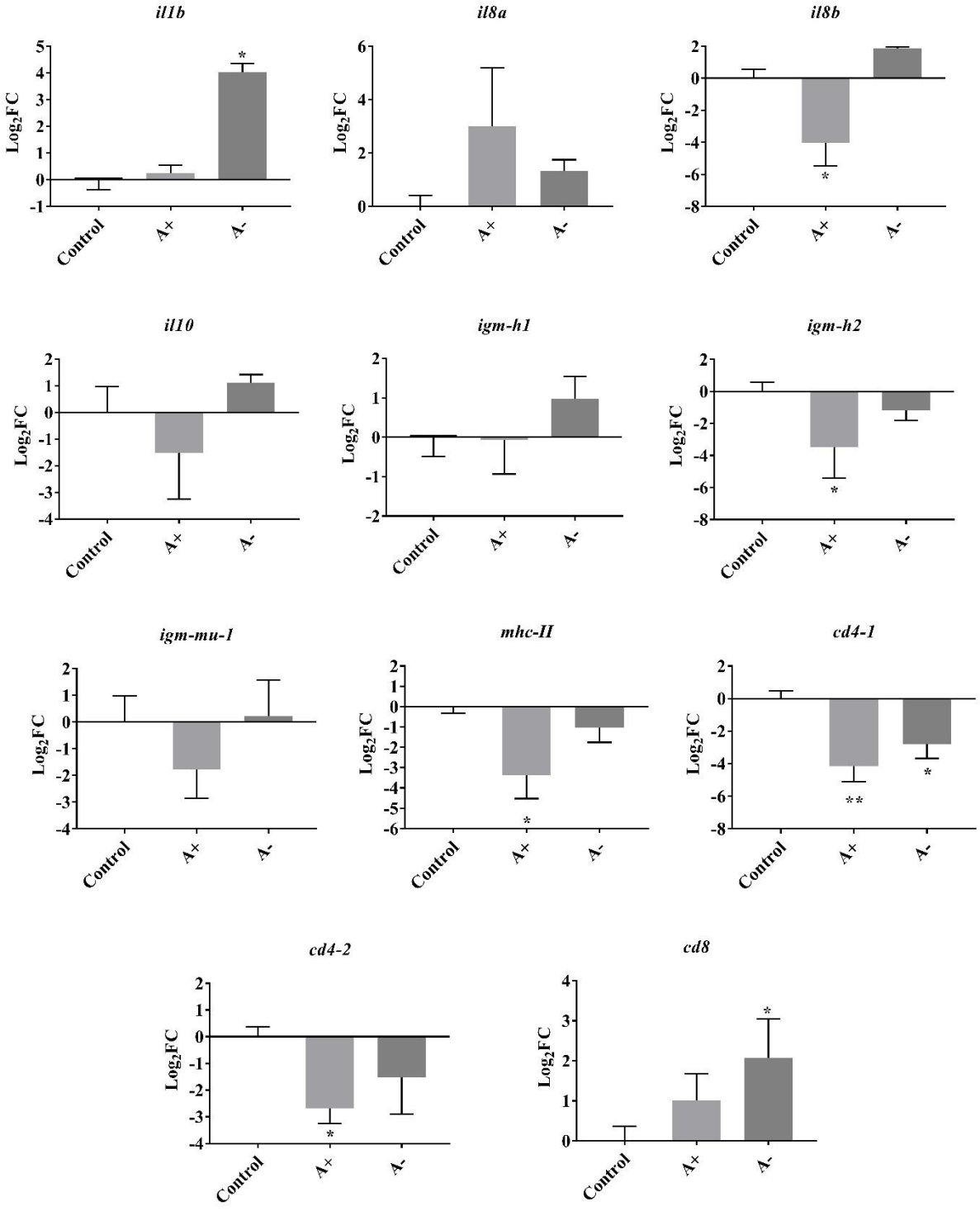
il1b
il8a
il8b
il10
igm-h1
igm-h2
igm-mu-1
mhc-II
cd4-1
cd4-2
cd8
Log2FC
Control
A+
A-

Figure 3.6. Expression of transcripts related to cytokines (*il1b, il8a, il8b, il10,*), immunoglobulin (*igm-h1, igm-h2,* and *igm-mu-1*), adaptive immunity markers *mhc-ii*, *cd4*, and *cd8* in lumpfish spleen in response to *A. salmonicida* (A-layer $^{+/-}$) bacterins at 6 wpi. Transcript expression levels in the spleen from the control (TSB-mock injected group) and immunized lumpfish at 6 wpi were analyzed using RT-qPCR. Relative expression was calculated using the $2^{-\Delta\Delta Ct}$ method and was $\log_2$ transformed; *rpl32* and *pabpc1b* were the endogenous control genes. A one-way ANOVA test, followed by the Sidak multiple comparisons *post hoc* test was used to identify significant differences between treatments (control and immunized groups) at a single time point. Asterisks (*) represent significant differences between treatments at each time point (*$p < 0.05$, **$p < 0.01$). Each value is mean ± SD (n = 3).

3.5. Discussion

A. salmonicida subsp. *salmonicida* is responsible for furunculosis in Atlantic salmon and many other fish species (e.g., lumpfish) [50]. *A. salmonicida* strain J223 was originally isolated from the Atlantic salmon in 1999 [15]. However, previously I observed that *A. salmonicida* J223 had counteracted and modulated the lumpfish responses and caused lethal infection [16]. Furthermore, no protective vaccine trial is described in lumpfish against *A. salmonicida* subsp. *salmonicida*. Therefore, I aimed to develop a vaccine for lumpfish against *A. salmonicida* J223.

For the past years, furunculosis has been partly controlled by the use of protective vaccines containing formalin-inactivated *A. salmonicida* bacterins in Atlantic salmon, rainbow trout, and Arctic char [37, 86-92]. Several studies explained virulence factors, including VapA layer, ECPs, OMPs (e.g., IROMPs) of *A. salmonicida* provided immune protection to these species [14, 22-44].

One of the essential virulence factors of *A. salmonicida* is its VapA-layer, encoded by the *vapA* gene, comprised of protein subunits tethered to the cell surface via LPS [22, 93-95]. The A-layer protects *A. salmonicida* against host cell complement and promotes bacterial autoagglutination, macrophage infiltration, and resistance [23, 94-96]. Specific mutants containing a disorganized A-layer are avirulent and provide significant protection to salmonids [95]. Thus, A-layers were considered as a necessary antigen for vaccines against furunculosis [24].

Furthermore, *A. salmonicida* produces many extracellular enzymes (e.g., lipases, proteases), which play a vital role in the proliferation of the bacterium and disease development [34, 94, 97]. Vaccines containing ECPs induce inflammatory reactions in Atlantic salmon [98]. *A. salmonicida* serine protease - beta-galactosidase hybrid protein conferred immune protection in Atlantic salmon against *A. salmonicida* [99]. Ellis et al. observed that rainbow trout immunized to extracellular antigens produce antibodies to ECP components (e.g., protease) [100].

Additionally, Gram-negative bacteria contain OMPs, which are essential for maintaining the selective permeability of the bacterial membrane and play an important role in ion uptake, iron acquisition, and resistance to antimicrobials, serum, and bile salts. Some of them have been recognized as potential vaccine candidates, and several studies have demonstrated their efficacy as vaccine candidates [48, 101-108]. Comparative reverse vaccinology of *A. salmonicida* suggested several OMPs (e.g., TonB-dependent siderophore receptor, the LPS assembly protein LptD, OMP assembly factor BamA, flagellar basal body rod protein FlgG, and secreted antigens flagellar hook assembly protein FlgD) as potential vaccine candidates for Atlantic salmon and lumpfish [48]. Additionally, the growth of *A. salmonicida* under iron-restricted conditions resulted in the expression of OMPs of 73, 76, and 85 kDa, which were not present when grown under in vitro iron-replete conditions [27]. Iron is a critical element of bacterial metabolism, and its availability contributes significantly to the pathogenic mechanism of most bacteria [109]. In order to cause a successful infection inside the host under iron-limited conditions, bacteria must acquire iron from the host using IROMPs (e.g., siderophores, transferrins, lactoferrins, ferritins, and hemoproteins) [110-112]. The IROMPs of *A. salmonicida* have been demonstrated to be protective antigens for fish [26, 113, 114].

Hereafter, I evaluated the immune protective effect of *A. salmonicida* formalin-killed bacterins ($A^{+/-}$; ECPs $^{+/-}$) and OMPs ($A^{+/-}$; IROMPs $^{+/-}$) in lumpfish. My results show that none of these vaccine formulations provide immune protection to lumpfish against *A. salmonicida* J223. The possible reasons for this could be the vaccine antigens mix does not trigger a long-lasting adaptive immune response or that the vaccine antigens suppress host immune responses.

An effective vaccine candidate usually contains an immunogenic antigen that can trigger innate defense mechanisms to generate robust and long-lasting adaptive memory immune

responses [115]. Antigen presentation by the MHC molecules allows antigen-specific B and T cell response and secretion of cytokines [115].

Several studies showed that antibody responses strongly correlate with protection against furunculosis. For example, ELISA confirmed that Atlantic salmon ip injected with A-layer negative *A. salmonicida* bacterin grown under iron-restricted conditions and supplemented with the extracellular polysaccharide (PS) antigen triggered anti-PS and anti-IROMPs antibody titers in fish serum and protect up to at least 9 months post-vaccination against a virulent *A. salmonicida* strain [113]. Other studies on Atlantic salmon also demonstrate antibody response and protection against virulent *A. salmonicida* strains [25, 90, 116].

Similarly, a significant correlation was found between the level of *A. salmonicida*-specific antibodies measured before the challenge and the endpoint survival of rainbow trout and Arctic char [89, 91, 92]. All these findings suggest that specific antibodies play an essential role in vaccine-mediated protection against *A. salmonicida*. Thus, I investigated the antibody response upon vaccination by ELISA at 2, 4, 6, and 8 wpi. Additionally, I checked the gene expression response level of *igm-h1*, *igm-h2*, and *igm-mu-1* to vaccination in lumpfish spleen at 6 wpi of three representing groups, control, A^+W, and A^-W. Interestingly, ELISA did not detect any increase in total antibody response in the vaccinated lumpfish serum compared to the control fish. Also, *igm-h2* was significantly downregulated by A^+ bacterin. Taken together, these results suggest that *A. salmonicida* J223, J225, J227, and J228 bacterins do not trigger humoral immune responses of lumpfish, and J223 bacterin suppresses the host's B cell response.

A. salmonicida is an intracellular pathogen that can reside within macrophages [46]. Cell-mediated immune responses are needed to eliminate intracellular microbial pathogens [117]. The activities of IL-1 and IL-8 form a direct bridge between innate and adaptive immunity [118]. The

immediate action of IL-1 on $CD4^+$ and $CD8^+$ T cells influences T cell differentiation [118, 119]. Wang et al. showed that co-vaccination of recombinant protein rENO with IL-8 enhanced humoral and cellular immunity (e.g., MHC-II, $CD4^+$, $CD8^+$) and increased survival against *Streptococcus iniae* infection in channel catfish [119]. A study observed that live *A. salmonicida* vaccines preferentially enhance T cell responsiveness and provide protection to rainbow trout [120]. However, my previous work also identified the upregulation of *il10* in lumpfish during *A. salmonicida* infection, which might be an indication of immune suppression. Therefore, I investigated the gene response of *i1b*, *il8a*, *il8b, il10, cd4-1*, *cd4-2*, and *cd8* towards vaccination in lumpfish spleen at 6 wpi of lumpfish immunized with *A. salmonicida*. I noticed that *A. salmonicida* A^+W and A^-W bacterins differentially immune modulate the lumpfish. For example, *il1b* was significantly upregulated in lumpfish immunized with A^- strains while no dysregulation was observed by A^+ bacterin. Furthermore, *il8b* was significantly downregulated in lumpfish immunized with A^+ strains, while no significant change was apparent in another group. However, *il8a* and *il10* were not significantly dysregulated by A^+ and A^- bacterin. Additionally, I observed the significant downregulation of *cd4-1, cd4-2,* and *mhc-II* by A^+ bacterin. However, *cd8* was not dysregulated by A^+ bacterin. These observations suggest that *A. salmonicida* J223 bacterin suppresses the innate immune response, antigen presentation, and T cell-mediated immune responses in lumpfish. Thus, it correlates with the no protection level conferred by *A. salmonicida* J223-based vaccine preparations.

However, significant upregulation of *il1b* and *cd8* by A^- *A. salmonicida* suggests the activation of cell-mediated immunity. Still, A^- bacterins did not trigger protective immunity to lumpfish against *A. salmonicida* J223. $A^{+/-}$ OMPs/IROMPs could also not confer protection to lumpfish. One possible reason for vaccine ineffectiveness could be the virulence factors of *A.*

salmonicida J223 strain. In chapter 2, I demonstrated that *A. salmonicida* J223 is a hypervirulent strain for lumpfish, and it could suppress the immune system of lumpfish and cause cell cycle arrest and sepsis-like clinical signs [12, 16]. Only 10^2 cells of *A. salmonicida* J223 can kill 50% of the lumpfish population. *A. salmonicida* J223 is equally virulent to Atlantic salmon (unpublished data) and rainbow trout [74]. Genome-wide analysis showed that J223 harbors additional copies of virulence factors *aopN* and *acr2* in the virulent pASal5 plasmid [12]. In addition to this, most of the genes encoding flagellar structural proteins and flagella-assembly-associated genes were identified in the J223 genome [12]. These findings suggest that additional virulence factors in *A. salmonicida* J223 strain make it hypervirulent and increase its ability to bypass vaccine-mediated response in the host.

3.6. Conclusions

I observed that all immunized fish had a similar pattern of mortality to the non-immunized control fish. Control and vaccinated fish died within two weeks post-challenge. Therefore, the results demonstrate that formalin-killed bacterial cells, OMPs, and IROMPs of A^+/A^- *A. salmonicida* derived from J223 do not confer immune protection to lumpfish against virulent *A. salmonicida*. ELISA results showed that formalin-killed *A. salmonicida* J223-derived bacterins, either in the presence or absence of VapA layer, do not increase IgM titers. Instead, it downregulates genes encoding IgM, MHC-II, and CD4, which indicates immune suppression. Although A^- *A. salmonicida* bacterin induced a cell-mediated immune response, still unable to protect lumpfish against *A. salmonicida* J223, which suggests that J223 has a strong immune evasion/suppression mechanism. Therefore, this study identified *A. salmonicida* subsp. *salmonicida* as a major lumpfish pathogen that can hijack fish defense mechanisms. However, the

tactics employed by the J223 strain to inactivate host defense are still a mystery, which needs to be revealed to develop a new immune protective vaccine.

3.7. References

1. Emmerich R. Über Eine Durch Bacterien Erzeugte Seuche Unter Den Forellen. 1894.

2. Austin B, Austin D. Diseases of farmed and wild fish. Aeromonadaceae representatives (*Aeromonas salmonicida*) in bacterial fish pathogens. 1993.

3. Smith IW. The classification of '*Bacterium salmonicida*'. Journal of General Microbiology. 1963;33:263-74.

4. Mc Carthy DH. The identification and significance of atypical strains of *Aeromonas salmonicida* [salmon and trout, carp, freshwater fish]. Bulletin de l'Office International des Epizooties (France). 1977;187:459-63.

5. Austin DA, McIntosh D, Austin B. Taxonomy of fish associated *Aeromonas* spp., with the description of *Aeromonas salmonicida* subsp. *smithia* subsp. *nov*. Systematic and applied Microbiology. 1989;11(3):277-90.

6. Pavan ME, Abbott SL, Zorzopulos J, Janda JM. *Aeromonas salmonicida* subsp. *pectinolytica* subsp. *nov*., a new pectinase-positive subspecies isolated from a heavily polluted river. International Journal of Systematic and Evolutionary Microbiology. 2000;50(3):1119-24.

7. Vincent AT, Trudel MV, Freschi L, Nagar V, Gagné-Thivierge C, Levesque RC, Charette SJ. Increasing genomic diversity and evidence of constrained lifestyle evolution due to insertion sequences in *Aeromonas salmonicida*. BMC Genomics. 2016;17(1):1-2.

8. Gulla S, Lund V, Kristoffersen AB, Sørum H, Colquhoun DJ. vapA (A-layer) typing differentiates *Aeromonas salmonicida* subspecies and identifies a number of previously undescribed subtypes. Journal of Fish Diseases. 2016;39(3):329-42.

9. Vincent AT, Hosseini N, Charette SJ. The *Aeromonas salmonicida* plasmidome: A model of modular evolution and genetic diversity. Annals of the New York Academy of Sciences. 2021;1488(1):16-32.

10. Charette SJ. Microbe profile: *Aeromonas salmonicida*: an opportunistic pathogen with multiple personalities. Microbiology. 2021;167(5):001052.

11. Casjens SR, Gilcrease EB, Vujadinovic M, Mongodin EF, Luft BJ, Schutzer SE, Fraser CM, Qiu WG. Plasmid diversity and phylogenetic consistency in the Lyme disease agent *Borrelia burgdorferi*. BMC Genomics. 2017;18(1):1-8.

12. Vasquez I, Hossain A, Gnanagobal H, Valderrama K, Campbell B, Ness M, Charette SJ, Gamperl AK, Cipriano R, Segovia C, Santander J. Comparative genomics of typical and atypical *Aeromonas salmonicida* complete genomes revealed new insights into pathogenesis evolution. Microorganisms. 2022;10(1):189.

13. Frey J, Origgi FC. Type III secretion system of *Aeromonas salmonicida* undermining the Host's immune response. Frontiers in Marine Science. 2016;3:130.

14. Burr SE, Stuber K, Wahli T, Frey J. Evidence for a type III secretion system in *Aeromonas salmonicida* subsp. *salmonicida*. Journal of Bacteriology. 2002;184(21):5966-70.

15. Valderrama K, Saravia M, Santander J. Phenotype of *Aeromonas salmonicida* sp. *salmonicida* cyclic adenosine 3′, 5′-monophosphate receptor protein (Crp) mutants and its virulence in rainbow trout (*Oncorhynchus mykiss*). Journal of Fish Diseases. 2017;40(12):1849-56.

16. Chakraborty S, Hossain A, Cao T, Gnanagobal H, Segovia C, Hill S, Monk J, Porter J, Boyce D, Hall JR, Bindea G. Multi-Organ transcriptome response of lumpfish (*Cyclopterus*

lumpus) to *Aeromonas salmonicida* subspecies salmonicida systemic infection. Microorganisms. 2022;10(11):2113.

17. Trudel MV, Tanaka KH, Filion G, Daher RK, Frenette M, Charette SJ. Insertion sequence AS5 (IS AS5) is involved in the genomic plasticity of *Aeromonas salmonicida*. Mobile Genetic Elements. 2013;3(3):e25640.

18. Vincent AT, Charette SJ. To be or not to be mesophilic, that is the question for *Aeromonas salmonicida*. Microorganisms. 2022;10(2):240.

19. Dacanay A, Knickle L, Solanky KS, Boyd JM, Walter JA, Brown LL, Johnson SC, Reith M. Contribution of the type III secretion system (TTSS) to virulence of *Aeromonas salmonicida* subsp. *salmonicida*. Microbiology. 2006;152(6):1847-56.

20. Wiklund T, Dalsgaard I. Occurrence and significance of atypical *Aeromonas salmonicida* in non-salmonid and salmonid fish species: a review. Diseases of Aquatic Organisms. 1998;32(1):49-69.

21. Menanteau-Ledouble S, Kumar G, Saleh M, El-Matbouli M. *Aeromonas salmonicida*: updates on an old acquaintance. Diseases of Aquatic Organisms. 2016;120(1):49-68.

22. Kay W, Buckley J, Ishiguro E, Phipps B, Monette J, Trust T. Purification and disposition of a surface protein associated with virulence of *Aeromonas salmonicida*. Journal of Bacteriology. 1981;147(3):1077-84.

23. Garduño RA, Moore AR, Olivier G, Lizama AL, Garduño E, Kay WW. Host cell invasion and intracellular residence by *Aeromonas salmonicida*: role of the S-layer. Canadian Journal of Microbiology. 2000;46(7):660-8.

24. Lund V, Arnesen A, Coucheron D, Modalsli K, Syvertsen C. The *Aeromonas salmonicida* A-layer protein is an important protective antigen in oil-adjuvanted vaccines. Fish & Shellfish Immunology. 2003;15(4):367-72.

25. Romstad AB, Reitan LJ, Midtlyng P, Gravningen K, Evensen Ø. Antibody responses correlate with antigen dose and in vivo protection for oil-adjuvanted, experimental furunculosis (*Aeromonas salmonicida* subsp. *salmonicida*) vaccines in Atlantic salmon (*Salmo salar* L.) and can be used for batch potency testing of vaccines. Vaccine. 2013;31(5):791-6.

26. Hirst I, Ellis AE. Iron-regulated outer membrane proteins of *Aeromonas salmonicida* are important protective antigens in Atlantic salmon against furunculosis. Fish & Shellfish Immunology. 1994;4(1):29-45.

27. Ebanks RO, Dacanay A, Goguen M, Pinto DM, Ross NW. Differential proteomic analysis of *Aeromonas salmonicida* outer membrane proteins in response to low iron and in vivo growth conditions. Proteomics. 2004;4(4):1074-85.

28. Menanteau-Ledouble S, Kattlun J, Nöbauer K, El-Matbouli M. Protein expression and transcription profiles of three strains of *Aeromonas salmonicida* ssp. *salmonicida* under normal and iron-limited culture conditions. Proteome Science. 2014;12(1):1-9.

29. Menanteau-Ledouble S, El-Matbouli M. Antigens of *Aeromonas salmonicida* subsp. *salmonicida* specifically induced in vivo in *Oncorhynchus mykiss*. Journal of Fish Diseases. 2016;39(8):1015.

30. Neelam B, Robinson RA, Price NC, Stevens L. The effect of iron limitation on the growth of *Aeromonas salmonicida*. Microbios. 1993;74(298):59-67.

31. Ellis A, Hastings T, Munro A. The role of *Aeromonas salmonicida* extracellular products in the pathology of furunculosis. Journal of Fish Diseases. 1981;4(1):41-51.

32. Ellis A. An appraisal of the extracellular toxins of *Aeromonas salmonicida* ssp. *salmonicida*. Journal of Fish Diseases. 1991;14(3):265-77.

33. Lee K, Ellis A. Glycerophospholipid: cholesterol acyltransferase complexed with lipopolysaccharide (LPS) is a major lethal exotoxin and cytolysin of *Aeromonas salmonicida*: LPS stabilizes and enhances toxicity of the enzyme. Journal of Bacteriology. 1990;172(9):5382-93.

34. Sakai D. Loss of virulence in a protease-deficient mutant of *Aeromonas salmonicida*. Infection and Immunity. 1985;48(1):146-52.

35. Burr SE, Pugovkin D, Wahli T, Segner H, Frey J. Attenuated virulence of an *Aeromonas salmonicida* subsp. *salmonicida* type III secretion mutant in a rainbow trout model. Microbiology. 2005;151(6):2111-8.

36. Bricknell I, Bowden T, Lomax J, Ellis A. Antibody response and protection of Atlantic salmon (*Salmo salar*) immunised with an extracellular polysaccharide of *Aeromonas salmonicida*. Fish & Shellfish Immunology. 1997;7(1):1-16.

37. Bergh PV, Burr SE, Benedicenti O, von Siebenthal B, Frey J, Wahli T. Antigens of the type-three secretion system of *Aeromonas salmonicida* subsp. *salmonicida* prevent protective immunity in rainbow trout. Vaccine. 2013;31(45):5256-61.

38. Bjørnsdottir R, Eggset G, Nilsen R, Jørgensen T. The A-layer protein of *Aeromonas salmonicida*: further characterization and a new isolation procedure. Journal of Fish Diseases. 1992;15(2):105-18.

39. Cipriano RC. Immunization of brook trout (*Salvelinus fontinalis*) against *Aeromonas salmonicida*: immunogenicity of virulent and avirulent isolates and protective ability of different antigens. Canadian Journal of Fisheries and Aquatic Sciences. 1982;39(1):218-21.

40. Cipriano RC. Immunogenic potential of growth products extracted from cultures of *Aeromonas salmonicida* for brook trout (*Salvelinus fontinalis*). Canadian Journal of Fisheries and Aquatic Sciences. 1982;39(11):1512-8.

41. Shieh H, MacLean J. Purification and properties of an extracellular protease of *Aeromonas salmonicida*, the causative agent of furunculosis. International Journal of Biochemistry. 1975;6(9):653-6.

42. Arnesen J, Bjørnsdottir R, Jørgensen T, Eggset G. Immunological responses in Atlantic salmon, *Salmo salar* L., against purified serine protease and haemolysins from *Aeromonas salmonicida*. Journal of Fish Diseases. 1993;16(5):409-23.

43. Tatner M. Modified extracellular product antigens of *Aeromonas salmonicida* as potential vaccines for the control of furunculosis in Atlantic salmon, *Salmo salar* L. Journal of Fish Diseases. 1991;14(3):395-400.

44. Marana MH, Jørgensen LV, Skov J, Chettri JK, Holm Mattsson A, Dalsgaard I. Subunit vaccine candidates against *Aeromonas salmonicida* in rainbow trout *Oncorhynchus mykiss*. PLoS One. 2017;12(2):e0171944.

45. Marquis H, Lallier R. Efficacy studies of passive immunization against *Aeromonas salmonicida* infection in brook trout, *Salvelinus fontinalis* (Mitchill). Journal of Fish Diseases. 1989;12(3):233-40.

46. Garduño RA, Thornton JC, Kay WW. Fate of the fish pathogen *Aeromonas salmonicida* in the peritoneal cavity of rainbow trout. Canadian Journal of Microbiology. 1993;39(11):1051-8.

47. Marsden M, Devoy A, Vaughan L, Foster T, Secombes C. Use of a genetically attenuated strain of *Aeromonas salmonicida* to vaccinate salmonid fish. Aquaculture International. 1996;4(1):55-66.

48. Chukwu-Osazuwa J, Cao T, Vasquez I, Gnanagobal H, Hossain A, Machimbirike VI, Santander J. Comparative reverse vaccinology of *Piscirickettsia salmonis*, *Aeromonas salmonicida*, *Yersinia ruckeri*, *Vibrio anguillarum* and *Moritella viscosa*, frequent pathogens of Atlantic salmon and lumpfish aquaculture. Vaccines. 2022;10(3):473.

49. Torrissen O, Jones S, Asche F, Guttormsen A, Skilbrei OT, Nilsen F. Salmon lice--impact on wild salmonids and salmon aquaculture. Journal of Fish Diseases. 2013;36(3):171-94.

50. Powell A, Treasurer, Jim W., Pooley, Craig L., Keay, Alex J., Lloyd, Richard, Imsland, Albert K., Garcia de Leaniz, Carlos. Use of lumpfish for sea-lice control in salmon farming: challenges and opportunities. Reviews in Aquaculture. 2018;10(3):683-702.

51. Brooker AJ, Papadopoulou A, Gutierrez C, Rey S, Davie A, Migaud H. Sustainable production and use of cleaner fish for the biological control of sea lice: recent advances and current challenges. Veterinary Record. 2018;183(12):383.

52. Chakraborty S, Cao T, Hossain A, Gnanagobal H, Vasquez I, Boyce D, Santander J. Vibrogen-2 vaccine trial in lumpfish (*Cyclopterus lumpus*) against *Vibrio anguillarum*. Journal of Fish Diseases. 2019;42(7):1057-64.

53. Chakraborty S, Woldemariam NT, Visnovska T, Rise ML, Boyce D, Santander J, Andreassen R. Characterization of miRNAs in embryonic, larval, and adult lumpfish provides a reference miRNAome for *Cyclopterus lumpus*. Biology. 2022;11(1):130.

54. Costello MJ. Ecology of sea lice parasitic on farmed and wild fish. Trends in Parasitology. 2006;22(10):475-83.

55. Costello MJ. The global economic cost of sea lice to the salmonid farming industry. Journal of Fish Diseases. 2009;32(1):115-8.

56. Aaen SM, Helgesen KO, Bakke MJ, Kaur K, Horsberg TE. Drug resistance in sea lice: a threat to salmonid aquaculture. Trends in Parasitology. 2015;31(2):72-81.

57. Imsland AKD, Hanssen, A., Nytro, A. V., Reynolds, P., Jonassen, T. M., Hangstad, T. A., Elvegard, T. A., Urskog, T. C., Mikalsen, B. It works! Lumpfish can significantly lower sea lice infestation in large-scale salmon farming. Biology Open. 2018;7(9).

58. North B. Cleaner Fish Biology and Aquaculture Applications Edited by J Treasurer. Published by 5M Publishing Ltd, Benchmark House, 8 Smithy Wood Drive, Sheffield S35 1QN, UK. 515 pages Hardback (ISBN 9781912158218). Animal Welfare. 2018;29(3):355-6

59. Erkinharju T, Dalmo RA, Hansen M, Seternes T. Cleaner fish in aquaculture: Review on diseases and vaccination. Reviews in Aquaculture. 2021;13(1):189-237.

60. Vasquez I, Cao T, Hossain A, Valderrama K, Gnanagobal H, Dang M, Santander S. *Aeromonas salmonicida* infection kinetics and protective immune response to vaccination in sablefish (*Anoplopoma fimbria*). Fish & Shellfish Immunology. 2020;104:557-66.

61. Lian Z, Bai J, Hu X, Lü A, Sun J, Guo Y. Detection and characterization of *Aeromonas salmonicida* subsp. *salmonicida* infection in crucian carp *Carassius auratus*. Veterinary Research Communications. 2020;44(2):61-72.

62. Bartkova S, Kokotovic B, Skall HF, Lorenzen N, Dalsgaard I. Detection and quantification of *Aeromonas salmonicida* in fish tissue by real-time PCR. Journal of Fish Diseases. 2017;40(2):231-42.

63. Rupp M, Pilo P, Müller B, Knüsel R, von Siebenthal B, Frey J. Systemic infection in European perch with thermoadapted virulent *Aeromonas salmonicida* (*Perca fluviatilis*). Journal of Fish Diseases. 2019;42(5):685-91.

64. Boily F, Malcolm G, Johnson S. Characterization of *Aeromonas salmonicida* and furunculosis to inform pathogen transfer risk assessments in British Columbia: Canadian Science Advisory Secretariat; 2019.

65. Rønneseth A, Haugland GT, Colquhoun DJ, Brudal E, Wergeland HI. Protection and antibody reactivity following vaccination of lumpfish (*Cyclopterus lumpus L*.) against atypical *Aeromonas salmonicida*. Fish & Shellfish Immunology. 2017;64:383-91.

66. Ellul RM, Walde C, Haugland GT, Wergeland H, Rønneseth A. Pathogenicity of *Pasteurella* sp. in lumpsuckers (*Cyclopterus lumpus* L.). Journal of Fish Diseases. 2019;42(1):35-46.

67. Dang M, Cao T, Vasquez I, Hossain A, Gnanagobal H, Kumar S, Jennifer H, Danny B, Santander J. Oral immunization of larvae and juvenile of lumpfish (*Cyclopterus lumpus*) against *Vibrio anguillarum* does not influence systemic immunity. Vaccines (Basel). 2021;9(8).

68. Erkinharju T, Strandskog G, Vågnes Ø, Hordvik I, Dalmo RA, Seternes T. Intramuscular vaccination of Atlantic lumpfish (*Cyclopterus lumpus* L.) induces inflammatory reactions and local immunoglobulin M production at the vaccine administration site. Journal of Fish Diseases. 2019;42(12):1731-43.

69. Erkinharju T, Lundberg MR, Isdal E, Hordvik I, Dalmo RA, Seternes T. Studies on the antibody response and side effects after intramuscular and intraperitoneal injection of Atlantic lumpfish (*Cyclopterus lumpus L*.) with different oil-based vaccines. Journal of Fish Diseases. 2017;40(12):1805-13.

70. Erkinharju T, Dalmo RA, Vågsnes Ø, Hordvik I, Seternes T. Vaccination of Atlantic lumpfish (*Cyclopterus lumpus* L.) at a low temperature leads to a low antibody response against *Aeromonas salmonicida*. Journal of Fish Diseases. 2018;41(4):613-23.

71. Lund V, Jørgensen T, Holm KO, Eggset G. Humoral immune response in Atlantic salmon, *Salmo salar* L., to cellular and extracellular antigens of *Aeromonas salmonicida*. Journal of Fish Diseases. 1991;14(4):443-52.

72. Olivier G, Evelyn TP, Lallier R. Immunogenicity of vaccines from a virulent and a virulent strain of *Aeromonas salmonicida*. Journal of Fish Diseases. 1985;8(1):43-55.

73. Pollard AJ, Bijker EM. A guide to vaccinology: from basic principles to new developments. Nature Reviews Immunology. 2021;21(2):83-100.

74. Gnanagobal H, Cao T, Hossain A, Vasquez I, Chakraborty S, Chukwu-Osazuwa J, Boyce D, Espinoza MJ, García-Angulo VA, Santander J. Role of riboflavin biosynthesis gene duplication and transporter in *Aeromonas salmonicida* virulence in marine teleost fish. Virulence. 2023 Dec 31;14(1):2187025..

75. Soto-Dávila M, Hossain A, Chakraborty S, Rise ML, Santander J. *Aeromonas salmonicida* subsp. *salmonicida* early infection and immune response of Atlantic cod (*Gadus morhua* L.) primary macrophages. Frontiers in Immunology. 2019;10(1237).

76. Soto-Dávila M, Valderrama K, Inkpen SM, Hall JR, Rise ML, Santander J. Effects of Vitamin D2 (Ergocalciferol) and D3 (Cholecalciferol) on Atlantic salmon (*Salmo salar*) primary macrophage immune response to *Aeromonas salmonicida* subsp. *salmonicida* infection. Frontiers in Immunology. 2020;10.

77. Santander J, Golden G, Wanda SY, Curtiss III R. Fur-regulated iron uptake system of *Edwardsiella ictaluri* and its influence on pathogenesis and immunogenicity in the catfish host. Infection and immunity. 2012;80(8):2689-703.

78. Sambrook J, Russell DW. The condensed protocols from molecular cloning: a laboratory manual. Cold Spring Harbor Laboratory Press; 2006.

79. Eslamloo K, Kumar S, Caballero-Solares A, Gnanagobal H, Santander J, Rise ML. Profiling the transcriptome response of Atlantic salmon head kidney to formalin-killed *Renibacterium salmoninarum*. Fish & Shellfish Immunology. 2020;98:937-49.

80. Santander J, Mitra A, Curtiss III R. Phenotype, virulence and immunogenicity of Edwardsiella ictaluri cyclic adenosine 3′, 5′-monophosphate receptor protein (Crp) mutants in catfish host. Fish & shellfish immunology. 2011;31(6):1142-53.

81. Valderrama K, Soto-Dávila M, Segovia C, Vásquez I, Dang M, Santander J. *Aeromonas salmonicida* infects Atlantic salmon (*Salmo salar*) erythrocytes. Journal of Fish Diseases. 2019;42(11):1601-8.

82. Gnanagobal H, Cao T, Hossain A, Dang M, Hall JR, Kumar S, Santander S. Lumpfish (*Cyclopterus lumpus*) is susceptible to *Renibacterium salmoninarum* infection and induces cell-mediated immunity in the chronic stage. Frontiers in Immunology. 2021;12.

83. St-Pierre J, Grégoire J-C, Vaillancourt C. A simple method to assess group difference in RT-qPCR reference gene selection using GeNorm: The case of the placental sex. Scientific Reports. 2017;7(1):16923.

84. Li Y, Dick WA, Tuovinen OH. Evaluation of fluorochromes for imaging bacteria in soil. Soil Biology and Biochemistry. 2003;35(6):737-44.

85. Russ N, Zielbauer BI, Koynov K, Vilgis TA. Influence of nongelling hydrocolloids on the gelation of agarose. Biomacromolecules. 2013;14(11):4116-24.

86. Villumsen KR, Raida MK. Long-lasting protection induced by bath vaccination against *Aeromonas salmonicida* subsp. *salmonicida* in rainbow trout. Fish & Shellfish Immunology. 2013;35(5):1649-53.

87. Lim J, Hong S. Characterization of *Aeromonas salmonicida* and *A. sobria* isolated from cultured salmonid fish in Korea and development of a vaccine against furunculosis. Journal of Fish Diseases. 2020;43(5):609-20.

88. Marana MH, Skov J, Chettri JK, Krossøy B, Dalsgaard I, Kania PW. Positive correlation between *Aeromonas salmonicida* vaccine antigen concentration and protection in vaccinated rainbow trout *Oncorhynchus mykiss* evaluated by a tail fin infection model. Journal of Fish Diseases. 2017;40(4):507-16.

89. Rømer Villumsen K, Dalsgaard I, Holten-Andersen L, Raida MK. Potential role of specific antibodies as important vaccine induced protective mechanism against *Aeromonas salmonicida* in rainbow trout. PLoS One. 2012;7(10):e46733.

90. Romstad AB, Reitan LJ, Midtlyng P, Gravningen K, Emilsen V, Evensen Ø. Comparision of a serological potency assay for furunculosis vaccines (*Aeromonas salmonicida* subsp. *salmonicida*) to intraperitoneal challenge in Atlantic salmon (*Salmo salar* L.). Biologicals. 2014;42(2):86-90.

91. Rømer Villumsen K, Koppang EO, Raida MK. Adverse and long-term protective effects following oil-adjuvanted vaccination against *Aeromonas salmonicida* in rainbow trout. Fish & Shellfish Immunology. 2015;42(1):193-203.

92. Braden LM, Whyte SK, Brown ABJ, Iderstine CV, Letendre C, Groman D. Vaccine-induced protection against furunculosis involves pre-emptive priming of humoral immunity in Arctic charr. Frontiers in Immunology. 2019;10:120.

93. Chart H, Shaw DH, Ishiguro E, Trust T. Structural and immunochemical homogeneity of *Aeromonas salmonicida* lipopolysaccharide. Journal of Bacteriology. 1984;158(1):16-22.

94. Dallaire-Dufresne S, Tanaka KH, Trudel MV, Lafaille A, Charette SJ. Virulence, genomic features, and plasticity of *Aeromonas salmonicida* subsp. *salmonicida*, the causative agent of fish furunculosis. Veterinary Microbiology. 2014;169(1):1-7.

95. Kay WW, Trust TJ. Form and functions of the regular surface array (S-layer) of *Aeromonas salmonicida*. Experientia. 1991;47(5):412-4.

96. Munn C, Ishiguro E, Kay W, Trust T. Role of surface components in serum resistance of virulent *Aeromonas salmonicida*. Infection and Immunity. 1982;36(3):1069-75.

97. Janda JM, Abbott SL. The genus *Aeromonas*: taxonomy, pathogenicity, and infection. Clinical Microbiology Reviews. 2010;23(1):35-73.

98. Mutoloki S, Brudeseth B, Reite OB, Evensen Ø. The contribution of *Aeromonas salmonicida* extracellular products to the induction of inflammation in Atlantic salmon (*Salmo salar* L.) following vaccination with oil-based vaccines. Fish & Shellfish Immunology. 2006;20(1):1-11.

99. Coleman G, Bennett AJ, Whitby PW, Bricknell IR. A 70 kDa *Aeromonas salmonicida* serine protease - β-galactosidase hybrid protein as an antigen and its protective effect on Atlantic salmon (*Salmo salar* L.) against a virulent *A. salmonicida* challenge. Biochemical Society Transactions. 1993;21(1):49S-S.

100. Ellis AE, Stapleton KJ, Hastings TS. The humoral immune response of rainbow trout (*Salmo gairdneri)* immunised by various regimes and preparations of *Aeromonas salmonicida* antigens. Veterinary Immunology and Immunopathology. 1988;19(2):153-64.

101. Maiti B, Dubey S, Munang'andu HM, Karunasagar I, Karunasagar I, Evensen Ø. Application of outer membrane protein-based vaccines against major bacterial fish pathogens in India. Frontiers in Immunology. 2020;11:1362.

102. Behera T, Swain P. Alginate–chitosan–PLGA composite microspheres induce both innate and adaptive immune response through parenteral immunization in fish. Fish & shellfish immunology. 2013;35(3):785-91.

103. Zhang Y-q, Zhang T-t, Li J-n, Liu X-l, Li L. Design and evaluation of a tandemly arranged outer membrane protein U (OmpU) multi-epitope as a potential vaccine antigen against *Vibrio mimicus* in grass carps (*Ctenopharyngodon idella*). Veterinary Immunology and Immunopathology. 2014;160(1-2):61-9.

104. Rauta PR, Nayak B. Parenteral immunization of PLA/PLGA nanoparticle encapsulating outer membrane protein (Omp) from *Aeromonas hydrophila*: evaluation of immunostimulatory action in *Labeo rohita* (rohu). Fish & Shellfish Immunology. 2015;44(1):287-94.

105. Behera T, Nanda P, Mohanty C, Mohapatra D, Swain P, Das B, et al. Parenteral immunization of fish, *Labeo rohita* with Poly D, L-lactide-co-glycolic acid (PLGA) encapsulated antigen microparticles promotes innate and adaptive immune responses. Fish & Shellfish Immunology. 2010;28(2):320-5.

106. Maji S, Mali P, Joardar S. Immunoreactive antigens of the outer membrane protein of *Aeromonas hydrophila*, isolated from goldfish, *Carassius auratus* (Linn.). Fish & Shellfish Immunology. 2006;20(4):462-73.

107. Kumar G, Rathore G, El-Matbouli M. Outer membrane protein assembly factor YaeT (omp85) and GroEL proteins of *Edwardsiella tarda* are immunogenic antigens for *Labeo rohita* (Hamilton). Journal of Fish Diseases. 2014;37:1055-9.

108. Viji VT, Deepa K, Velmurugan S, Donio MBS, Jenifer JA, Babu MM. Vaccination strategies to protect goldfish *Carassius auratus* against *Aeromonas hydrophila* infection. Diseases of Aquatic Organisms. 2013;104(1):45-57.

109. Braun V. Bacterial iron transport related to virulence. Contributions to Microbiology. 2005;12:210-33.

110. Ebanks RO, Goguen M, Knickle L, Dacanay A, Leslie A, Ross NW. Analysis of a ferric uptake regulator (Fur) knockout mutant in *Aeromonas salmonicida* subsp. *salmonicida*. Veterinary Microbiology. 2013;162(2):831-41.

111. Crosa JH, Walsh CT. Genetics and assembly line enzymology of siderophore biosynthesis in bacteria. Microbiology and Molecular Biology Reviews. 2002;66(2):223-49.

112. Braun V, Killmann H. Bacterial solutions to the iron-supply problem. Trends in Biochemical Sciences. 1999;24(3):104-9.

113. Bricknell IR, King JA, Bowden TJ, Ellis AE. Duration of protective antibodies, and the correlation with protection in Atlantic salmon (*Salmo salar*L.), following vaccination with an *Aeromonas salmonicida* vaccine containing iron-regulated outer membrane proteins and secretory polysaccharide. Fish & Shellfish Immunology. 1999;9(2):139-51.

114. Najimi M, Lemos ML, Osorio CR. Identification of iron regulated genes in the fish pathogen *Aeromonas salmonicida* subsp. *salmonicida*: Genetic diversity and evidence of conserved iron uptake systems. Veterinary Microbiology. 2009;133(4):377-82.

115. Kaur G, Nimker C, Bansal A. rIL-22 as an adjuvant enhances the immunogenicity of rGroEL in mice and its protective efficacy against *S. Typhi* and *S. Typhimurium*. Cellular & Molecular Immunology. 2015;12(1):96-106.

116. Romstad AB, Reitan LJ, Midtlyng P, Gravningen K, Evensen Ø. Development of an antibody ELISA for potency testing of furunculosis (*Aeromonas salmonicida* subsp *salmonicida*) vaccines in Atlantic salmon (*Salmo salar* L). Biologicals. 2012;40(1):67-71.

117. Thakur A, Mikkelsen H, Jungersen G. Intracellular pathogens: host immunity and microbial persistence strategies. Journal of Immunology Research. 2019;2019:1356540.

118. Van Den Eeckhout B, Tavernier J, Gerlo S. Interleukin-1 as Innate Mediator of T Cell Immunity. Frontiers in Immunology. 2020;11:621931.

119. Wang E, Wang J, Long B, Wang K, He Y, Yang Q. Molecular cloning, expression and the adjuvant effects of interleukin-8 of channel catfish (*Ictalurus Punctatus*) against *Streptococcus iniae*. Scientific Reports. 2016;6(1):29310.

120. Marsden MJ, Vaughan LM, Foster TJ, Secombes CJ. A live (delta aroA) *Aeromonas salmonicida* vaccine for furunculosis preferentially stimulates T-cell responses relative to B-cell responses in rainbow trout (*Oncorhynchus mykiss*). Infection and Immunity. 1996;64(9):3863-9.

4. Chapter four: Characterization of miRNAs in embryonic, larval, and adult lumpfish provides a reference miRNAome for *Cyclopterus lumpus.*

4.1 Abstract

MicroRNAs (miRNAs) are endogenous small RNA molecules involved in the post-transcriptional regulation of protein expression by binding to the mRNA of target genes. They are key regulators in teleost development, maintenance of tissue-specific functions, and immune responses. Lumpfish (*Cyclopterus lumpus*) is becoming an emergent aquaculture species as it has been utilized as a cleaner fish to biocontrol sea-lice (e.g., *Lepeophtheirus salmonis*) infestation in the Atlantic Salmon (*Salmo salar*) aquaculture. The lumpfish miRNAs repertoire was unknown. This study identified and characterized miRNA-encoding genes in lumpfish from three developmental stages (adult, embryo, and larvae). A total of 16 samples from six different adult lumpfish organs (spleen, liver, head kidney, brain, muscle, and gill), embryos, and larvae were individually small RNA sequenced. Altogether, 391 conserved miRNA precursor sequences (discovered in the majority of teleost fish species reported in miRbase), eight novel miRNA precursor sequences (so far only discovered in lumpfish), and 443 unique mature miRNAs were identified. Transcriptomics analysis suggested organ-specific and age-specific expression of miRNAs (e.g., miR-122-1-5p specific to the liver). Most of the miRNAs found in lumpfish are conserved in teleost and higher vertebrates, suggesting an essential and common role across teleosts and higher vertebrates. This study is the first miRNA characterization of lumpfish that provides the reference miRNAome for future functional studies.

4.2 Introduction

The discovery of microRNAs (miRNAs) in 1993 in *Caenorhabditis elegans* and further identification in humans and many other animals significantly altered the longstanding dogmas that defined gene regulation [1]. These studies revealed that miRNAs were a class of small non-coding RNAs that function as guide molecules in RNA silencing machinery, often termed the RNA-induced silencing complex (RISC). RISC regulates gene expression at the messenger RNA level either by degrading mRNAs targeted by the miRNAs or preventing their translation [1-3]. miRNAs constitute a large family of post-transcriptional regulators with ~22 nucleotides in length and are present in animals, plants, and some viruses [3, 4]. Functional studies indicate that miRNAs have diverse expression patterns and regulate almost every cellular process, including developmental, physiological, and pathophysiological processes [3, 5, 6].

miRNA biogenesis involves multiple steps; first, miRNAs are processed from precursor molecules (pri-miRNAs), which are transcribed by RNA-specific endoribonuclease (Drosha) and processed into an ~70-nucleotide pre-miRNA in the nucleus [2, 3, 6-9]. Pre-miRNAs are then transported to the cytoplasm for further processing by the enzyme Dicer to an ~22-bp miRNA/miRNA duplex [2, 3, 6-9]. The miRNA duplex is loaded into the RISC. Only one of the mature miRNAs (guide miRNA) is incorporated in RISC, and the other is degraded (passenger miRNA). The guide miRNA directs the RISC to target mRNAs, where the mature miRNA usually binds in the 3′ untranslated region (UTR) of the target mRNAs [2, 3, 6-9].

Teleosts are an essential component of aquatic ecosystems and a primary source of proteins for human and animal consumption worldwide. Teleosts are one of the most diverse vertebrates on the earth [10]. The exploration of the role of miRNA in teleost development, organogenesis, tissue differentiation, growth, regeneration, reproduction, endocrine system, and responses to

environmental stimuli, as well as their role in the maturation of the immune system and response to infectious diseases, is still under investigation [11-17]. miRNA characterization is the first step in any investigation of their regulatory roles. Such characterizations have been carried out in some economically important fish species such as Atlantic salmon (*Salmo salar*), Atlantic cod (*Gadus morhua*), rainbow trout (*Oncorhynchus mykiss*), Atlantic halibut (*Hippoglossus hippoglossus*), channel catfish (*Ictalurus punctatus*), turbot (*Scophthalmus maximus*), European seabass (*Lates calcarifer*), olive flounder (*Paralichthys olivaceus*) [18-26], and fish models like zebrafish (*Danio rerio*) and three-spined stickleback (*Gasterosteus aculeatus*) [27, 28].

Global production of farmed Atlantic salmon is estimated just over 2.6 million tonnes in 2019. This growth was mainly driven by Norway and Chile, the two leading producing countries. The Norwegian salmon industry alone earned some NOK 19-20 billion (USD 2.1-2.2 billion) in profits before tax in 2019 (FAO, 2021) (https://www.fao.org/in-action/globefish/market-reports/resource-detail/en/c/1268636/) (Last accessed: 21 January 2021. Atlantic salmon is the main species of the Atlantic Canadian aquaculture industry, which represents approximately 80% of Atlantic Canada's total aquaculture value [29].

Infectious diseases are a challenge for the aquaculture industry. Globally losses due to diseases in the aquaculture industry exceed US$6 billion annually [30, 31]. One of the most prominent disease challenges currently restraining Atlantic salmon aquaculture is the infestation by the parasite sea-lice, specifically *Lepeophtheirus salmonis* and *Caligus* spp. [32-36]. Sea-lice are a group of visible host-dependent ectoparasite copepods with vast reproductive potential [32-36]. The attached sea-lice feed on salmon mucus, blood, and skin, which leads to significant physical damage and immunosuppression [32, 36-39]. In addition, these effects on fish health lead to substantial economic impacts due to production losses and treatment costs [32, 37, 40]. The

salmon industry in the North Atlantic region has adopted cleaner fish, e.g., lumpfish (*Cyclopterus lumpus*), for biological control of sea-lice infestations [32, 41-44]. However, several aspects of lumpfish biology remain unknown, including their miRNA repertoire.

This study aimed to identify and characterize miRNA encoding genes in lumpfish by small RNAs high-throughput sequencing (HTS) followed by miRDeep2 analysis. The identification was carried out in two early developmental stages, embryos and larvae, and six organs of adult lumpfish, brain, muscle, gill, liver, spleen, and head kidney. A combination of HTS and computational analytical approaches (e.g., miRNA precursor prediction) has been successfully used for miRNA characterization, particularly in two early developmental stages and adult lumpfish organs. Therefore, here I provide the first reference miRNAome for lumpfish.

4.3 Materials and Methods

4.3.1 Fish holding

Five adult lumpfish (1,100 g ± 99.5 (mean ± SD), male = 4, female = 1) were obtained from the Dr. Joe Brown Aquatic Research Building (JBARB) at the Department of Ocean Sciences (DOS), Memorial University of Newfoundland (MUN), Canada. The animals were kept in a 23,000 L tank, with flow-through (14.0 L/min) of UV-treated seawater (6 °C), ambient photoperiod (winter-spring), and 95-110% air saturation. Biomass density was maintained at 20 kg/m^3. The fish were fed daily using a commercial diet (Skretting – Europa 18 (6.0-9.0 mm pellet)) with a ration of 0.25% of their body weight per day. Additionally, lumpfish embryos (300 degree days) and lumpfish larvae (one-week post-hatch) were obtained from the JBARB. Lumpfish egg masses were fertilized and maintained with flow-through in 5 L upwelling black nontranslucent incubators at 8-10 °C supplied with 95-110% air saturated and 5 µm UV-treated filtered flow-

through seawater (spring-summer) [45]. After completing the development of the embryos, the larvae hatched and were maintained at 10 ºC [46].

4.3.2 Ethics statement

The fish dissection and tissue sample collection were performed following the Canadian Council on Animal Care guidelines (https://ccac.ca/en/standards/guidelines/) and approved by Memorial University of Newfoundland's Institutional Animal Care Committee (https://www.mun.ca/research/about/acs/) under the protocols #18-1-JS and #18-03-JS.

4.3.3 Sample collection

Fish were euthanized with 400 mg of MS222 (Syndel Laboratories, Vancouver, British Colombia, Canada) per liter of seawater and dissected immediately after death confirmation. Tissue samples were collected from adult lumpfish brain, gill, skeletal muscle, liver, spleen, and head kidney. Tissue samples from five adult lumpfish, two pools (each pool contains 5 embryos) of lumpfish embryos, and two pools (each pool contains 5 larvae) of lumpfish larvae were immediately flash-frozen in liquid nitrogen (Air Liquide Canada Atlantic) and stored at -80 °C until further processing.

4.3.4 RNA extraction

Total RNA was extracted by using the mirVana RNA isolation kit (Invitrogen™, ThermoFisher, Waltham, Massachusetts, USA) following the manufacturer's protocol. RNA concentration and integrity were quantified using spectrophotometry (Genova-nano, Jenway, Stone, Staffordshire, England) and 1% agarose gel electrophoresis. The total RNA concentrations of 32 samples (four adult individuals with brain and muscle samples, five adult individuals with gill, liver, spleen, and head kidney samples, and four samples from two early life stages) were ranging from 100 – 3250 ng/μL (total volume 100 μL) (Table 4.1). Sixteen samples from two adult

lumpfish, two embryos pools, and two larvae pools were used for HTS by independent library preparation and sequencing of each sample (Table 4.1). In contrast, all 32 samples were used for RT-qPCR analysis.

Table 4.1. Concentration and quality of RNA samples.

Tissue samples for RT-qPCR	Concentration (ng/µl)	260/280[a]	260/230[b]
Brain 1	183	2.2	1.7
Brain 2	227	2.2	1.22
Brain 3	905	2.1	1.9
Brain 4	105	2.18	1.78
Muscle 1	159	2.25	1.5
Muscle 2	129	2.1	1.6
Muscle 3	182	2.23	1.83
Muscle 4	100	2.22	1.7
Gill 1	965	2.22	2.03
Gill 2	790	2.17	2.14
Gill 3	766	2.31	1.93
Gill 4	640	2.2	1.94
Gill 5	522	2.26	1.94
Liver 1	3250	2.21	2.16
Liver 2	262	2.2	1.5
Liver 3	904	2.16	1.95
Liver 4	653	2.29	2.01
Liver 5	887	2.23	2.1
Spleen 1	292	2.146	2.1
Spleen 2	241	2.147	2.1
Spleen 3	542	2.19	1.95
Spleen 4	904	2.1	1.9
Spleen 5	916	2.1	1.9
Head kidney 1	622	2.204	2.3
Head kidney 2	203	2.119	2.1
Head kidney 3	530	2.22	1.7
Head kidney 4	921	2.13	1.83
Head kidney 5	477	2.25	1.8
Embryo 1	393	2.189	2.1
Embryo 2	324	2.168	1.76
Larvae 1	320	2.207	2.03
Larvae 2	343	2.108	1.72

[a]260/280 Ratio: 260 nm and 280 nm are the absorbance wavelengths used to assess the purity of DNA and RNA. A ratio of ~2.0 is considered pure for RNA. A lower absorbance ratio may indicate the presence of protein, phenol, or other contaminants that have an absorbance close to 280 nm. Subtraction of non-nucleic acid absorbance at 320 nm, is also needed to calculate this ratio. Formula:

DNA Purity (A_{260}/A_{280}) = (A_{260} reading – A_{320} reading) ÷ (A_{280} reading – A_{320} reading)

[b]260/230 Ratio: The ratio of absorbance at 260 and 230 nm can be used as a secondary measure of DNA or RNA purity. In this case, a ratio between 2.0 - 2.2 is considered pure. If the ratio is lower than this expected range, it may indicate contaminants in the sample that absorb at 230nm.

4.3.5 High-throughput sequencing (HTS)

The library construction and small RNA sequencing were performed by the Genomics Core Facility Oslo (Oslo University Hospital, Norway). The NEBNext Small RNA Library Prep Set for Illumina (New England Biolabs, Inc. Ipswich, Massachusetts, USA) was used to prepare the libraries according to the manufacturer's protocol. One µg of total RNA from each of the samples was used as input for the preparation of the libraries, and a final size selection of 140–150 bp fragments using 6% polyacrylamide gel was used to enrich for small RNAs. The adapter sequences (5'- AGATCGGAAGAGCACACGTCTGAACTCCAGTCAC - 3') were used in the library preparation process. Following library preparation, next-generation RNA sequencing was carried out using the Illumina Genome Analyzer IIx sequencing platform described in Woldemariam et al. [19], generating single-end reads of length 75 bp.

4.3.6 Analysis of sequencing data

The quality of the sequencing raw and processed data was checked before miRNA discovery analysis. FastQC v0.11.9 [47] was used to check the quality of the raw sequencing data and the data obtained after adapter removal and size filtering. The adapter removal and size filtering were carried out using cutadapt v1.8.3 [48]. Reads shorter than 18 bp and longer than 25 bp after the adapter removal were discarded. The reads passing the filtering step were converted to fasta format with fastq_to_fasta from FASTX toolkit v0.0.14 (http://hannonlab

.cshl.edu/fastx_toolkit/). Each of the 16 samples were analyzed independently to detect miRNAs highly expressed in particular adult organs/tissues and early developmental stages. The lumpfish reference genome [49], and Bowtie v1.0.0 [50] were used for mapping the reads to the reference genome. The workflow applied to identify novel lumpfish miRNA sequences is illustrated in Figure 4.1.

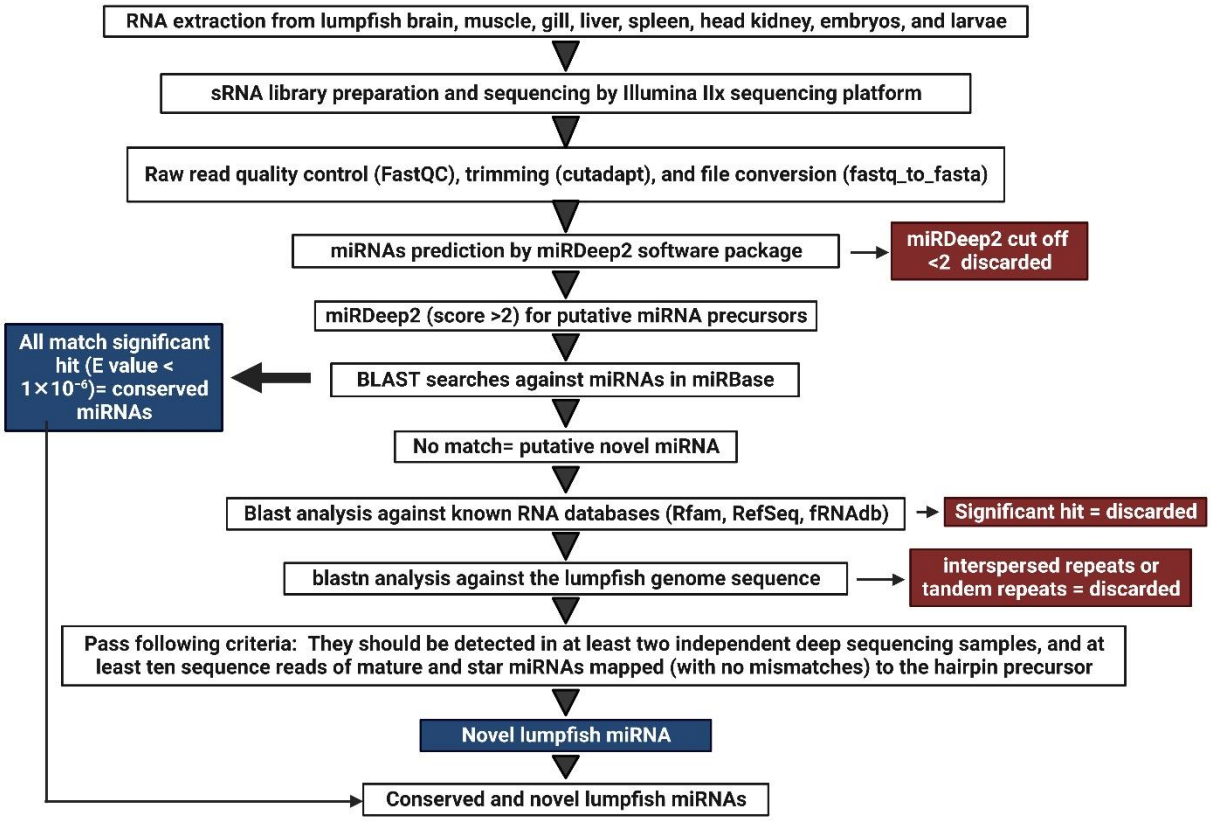

Figure 4.1. Experimental workflow used for characterization of lumpfish miRNAome.

High-quality trimmed reads were used to discover lumpfish miRNA using the miRDeep2 software package v0.0.7 (mapper and miRDeep2 analysis modules) applying default commands [51, 52]. The miRDeep2 tools assign a log-odds score (the miRDeep2 score) based on an algorithm that integrates the statistics of the read positions, the frequencies of reads within hairpins, and the posterior probability that the hairpin was derived from a true miRNA gene [51]. A miRDeep2 score of ≥ 2 was used as a cut-off to prevent false positive detection of miRNA precursors. In addition, they were inspected regarding the following criteria: i) reads between 5' and 3' end of a precursor should be aligned perfectly in a discrete manner; ii) miRNA precursors should be detected in at least 2 independent deep sequencing samples; and iii) at least 10 sequence reads of mature and miRNAs mapped to the hairpin precursor [53]. I further analyzed these putative precursor sequences by BLAST searches against known precursor sequences deposited in miRBase, (http://www.mirbase.org/index.shtml) (last accessed November 22, 2021). Any putative miRNA precursor sequence having a significant hit (E-value < $1E^{-6}$) in the BLAST analyses was regarded as a true evolutionarily conserved lumpfish ortholog of the miRNA gene in miRBase that retrieved the best hit and annotated as the evolutionarily conserved lumpfish ortholog of the miRNA gene according to the miRbase nomenclature guidelines (clu-prefix and same number as in other teleosts) [54, 55]. The putative miRNA precursor sequences that were identified by miRDeep2 and passed the additional criteria but did not show any significant match to the existing precursors in miRBase were considered as putative novel miRNAs. All those sequences were further analyzed by blastn searches against RNA databases in GenBank (http:// blast.ncbi.nlm.nih.gov/Blast), the small RNA databases Rfam (https://rfam.xfam.org/search), and the functional RNA database fRNAdb (https://dbarchive.biosciencedbc.jp/en/frnadb/desc.html). Sequences that had a significant hit against these databases were considered as other kinds of small

RNA and discarded from the analysis. The remaining precursors were used as queries in blastn analysis against the lumpfish genome sequence. Sequences with a significant BLAST hit (E value $< 1E^{-6}$) against multiple loci (> 10) in the lumpfish genome reference sequence were considered to be interspersed repeats or tandem repeats and discarded from the analysis. Sequences that passed all these filtering steps were regarded as true novel lumpfish miRNAs. A reference miRNAome of unique mature miRNA sequences (5p or 3p) for expression analysis of HTS data was generated by aligning all mature miRNAs by use of Sequencher software 5.3 (Gene Codes Corporation, Ann Arbor, Michigan, USA). Applying strict settings, the identical mature miRNAs from the same families were aligned, and the final reference, thus, consisted of only the unique different mature miRNAs.

4.3.7 Disclosing putative differentially expressed and/or organ and developmental stage enriched miRNAs

The HTS data from 16 tissue samples were used to estimate the expression of individual miRNAs across the different organs and developmental stages. The adapters were trimmed from the raw reads, and resulted reads were filtered based on size. The filtered reads from each of the 16 samples were mapped to the reference applying STAR aligner software (v.2.5.2b) [48]. The index for mapping was generated from the unique mature lumpfish miRNAs (see 2.6) with parameters genomeSAindexNbases 6. STAR aligner software (v.2.5.2b) with alignIntronMax1 and default parameters was then used for the mapping. Next, the output files of STAR mapping (BAM format) were processed further in R-Studio by using the feature Counts function from the Rsubread package (v.1.34.2) to produce count matrices [48]. The count tables were used as input in the DESeq2 R package (v.1.24.0) for differential expression analysis. Samples from an organ or developmental stage (n = 2) were compared to all other tissues sampled (n = 14). Putative

differentially expressed miRNAs were defined as those with Benjamini-Hochberg adjusted $p \leq 0.05$, $\log_2$ fold change threshold value of at least ≤ -3.0 or ≥ 3.0. The miRNA abundance of the different miRNAs within a particular organ or developmental stage was estimated as the percentage of a certain miRNA out of the total based on the average of normalized read counts from duplicated samples (reads less than 20 were filtered out). Enriched miRNAs were analyzed for each organ and developmental stage.

4.3.8 RT-qPCR

I selected 8 different miRNAs that were suggested as differentially expressed in literature and enriched in one of the organs by the DESeq2 analysis for further expression analysis with RT-qPCR. These miRNAs had previously shown similar organ-specific enrichment in other teleosts [19, 20]. The RNA-seq read numbers of these 8 miRNAs are provided in File S4.1. Those 8 miRNAs (clu-miR-135c-5p, clu-miR-9b-3p, clu-miR-133ab-3p, clu-miR-205-1-5b, clu-miR-203-3p, clu-miR-203a-5p, clu-miR-192a-5p, clu-miR-122-1-5p) were analysed by RT-qPCR to verify the DESeq2 results (Table 4.2). All forward primer sequences used for RT-qPCR were retrieved from the mature sequences of these miRNAs in the characterization step (methods 2.6). The primer sequences are listed in Table 4.2. The cDNA synthesis and RT-qPCR were carried out applying the miScript (miScript II RT Kit and miScript SYBR Green PCR Kit) assays following the manufacturer's instructions (Qiagen, Hilden, Germany). The RT-qPCR reaction mixture contained 12.5 µL 2x QuantiTect SYBR Green Master Mix, 2.5 µL 10x miScript Universal Primer, 2.5 µL of 10 µM forward miRNA-specific primer, 5 µL RNase free water, and 2.5 µL cDNA. The RT-qPCR analysis was carried out by Mx3000p (Stratagene, Agilent Technologies, LA Jolla, California, USA) using the following cycle, 95 °C for 15 min followed by 40 cycles of 94 °C for 15 sec, 55 °C for 30 sec and 70 °C for 30 sec as described in Andreassen et al. 2016 [20]. The

mature sequences of clu-mir-25-3p and clu-mir-17-5p were used as reference genes [20, 56]. The instrument-provided Ct values were applied to the LinRegPCR (v2021.1) software to calculate efficiency in all assays, and then the efficiency-adjusted Ct values were provided [57]. The efficiency-adjusted values were also used in the normalization (geomean from the two reference genes) to provide the dCt-values. The relative change in expression in each miRNA's target organ was calculated using the comparative Ct method ($2^{-\Delta\Delta Ct}$ method) [58]. All the comparisons were relative to the lowest expressed organ/tissue for the particular miRNA. All relative quantity (RQ) data are presented as mean ± SD. To compare gene expression across tissues, the RQ values for each target gene were subjected to a one-way ANOVA with Tukey's post-hoc test. All statistical tests were performed using GraphPad Prism 7.04 (La Jolla, San Diego, California, USA) with the p-value threshold set at ≤ 0.05. The number of organ samples was four or five for each group, while the early developmental stages had two biological replicates in each group (Table 4.1).

Table 4.2. Primers used in RT-qPCR analysis of mature miRNAs.

miRNAs	**Primer sequences (5´to 3´)**
clu-miR-25-3p	CATTGCACTTGTCTCGGTCTGA
clu-miR-17-1-5p	CAAAGTGCTTACAGTGCAGGTA
clu-miR-122-1-5p	TGGAGTGTGACAATGGTGTTTG
clu-miR-133ab-3p	TTTGGTCCCCTTCAACCAGCTGT
clu-miR-205-1-5p	TCCTTCATTCCACCGGAGTCTG
clu-miR-135c-5p	TATGGCTTTTTATTCCTATGTG
clu-miR-203-3p	GTGAAATGTTTAGGACCACTTG
clu-miR-203a-5p	AGTGGTTCTCAACAGTTCAACA
clu-miR-192a-5p	ATGACCTATGAATTGACAGCCA
clu-miR-9b-3p	TAAAGCTAGAGAACCGAATGTA

4.4 Results

4.4.1 Total RNA extraction, library preparation, and small RNA sequencing

Total RNA extracted from 32 samples (brain, muscle, gill, liver, spleen, and head kidney from five adult fish and two samples each from larvae and embryos) showed concentrations ranging from 100 to 3,250 ng/µL (Table 4.1) and intact 28S and 18S bands in 1% agarose gel indicated that they were of high quality. All these samples were qualified for further analysis by HTS and RT-qPCR. Small RNA libraries were successfully generated for 16 samples (12 tissue samples from two adult fish and two samples from each early developmental stages). The HTS resulted in a total of 147,972,041 raw reads, ranging from 6.6 to 13.3 million reads per sample. After adapter trimming there were a total of 86,054,423 reads ranging from 4.5 to 6.9 million reads per sample (Table S4.1). All raw HTS results were submitted to NCBI with BioProject accession number PRJNA679415. The individual SRA accession numbers are given in Table S4.1.

4.4.2 Characterization of lumpfish miRNA

The processed reads from each sample were analyzed with miRDeep2 software for miRNA gene discovery (Figure 4.1). Subsequent BLAST homology searches of all putative miRNA precursor sequences against miRbase revealed a total of 391 miRNA genes from 104 different families that were lumpfish orthologs to evolutionarily conserved miRNAs. They were subsequently annotated as the lumpfish orthologs of these miRNAs. miRDeep2 analysis also revealed 5p or 3p arm domination (most abundant mature miRNA from a given precursor) and the genome location of each miRNA gene. An overview of all precursor sequences along with their corresponding 5p and 3p mature sequences is given for all evolutionarily conserved miRNA genes in Table S4.2.

A total of 98 precursors identified by miRDeep2 did not show significant matches in the homology analyses against miRBase. These were considered as putative novel miRNA precursor sequences. They were further analyzed by blastn searches against RNA databases in GenBank, small RNA databases Rfam, functional RNA database fRNAdb, and lumpfish genome sequence (GenBank Accession: PRJNA625538). Sequences that had a significant hit against these databases were discarded from the analysis as described in the methods section. Following this filtering process, 8 precursor and corresponding mature sequences showed characteristics expected from true miRNAs. These eight miRNA precursor sequences are likely to represent novel lumpfish miRNAs, and all these novel miRNA genes along with their corresponding 5p and 3p mature sequences, the observed arm dominance of mature sequences, and the genome location of each miRNA gene are given in the last part of Table S4.2. Finally, the mature miRNAs were aligned by the use of Sequencher software to identify all unique mature miRNAs (many mature miRNAs from the same families were identical). There were 443 unique mature miRNAs. These unique miRNAs representing the lumpfish miRNAome are given in File S4.2.

4.4.3 Abundance of miRNAs within organs and developmental stages

I determined the diversity of miRNAs within the lumpfish tissues/organs and developmental stages based on the normalized read counts. The normalized read counts for all samples are shown in Table S4.3, while the average normalized read counts for each tissue/organ or developmental stage are shown in Table S4.4.

My results show the presence of 340 unique mature miRNAs in the lumpfish brain, 328 in muscle, 289 in gill, 288 in liver, 268 in spleen, 289 in head kidney, 328 in embryos, and 327 in larvae (Figure 4.2). Two hundred forty-one mature miRNAs were expressed in all six organs of adult lumpfish, 324 mature miRNAs were expressed commonly in embryos and larvae, and 223

mature miRNAs were expressed across all three developmental stages. All the miRNAs expressed in the early life stages, such as embryos and larvae, were also expressed in at least one organ of adult fish. The exceptions were clu-miR-19a-2-5p, which was only expressed in embryos, and clu-miR-137-1-5p, which was only expressed in larvae.

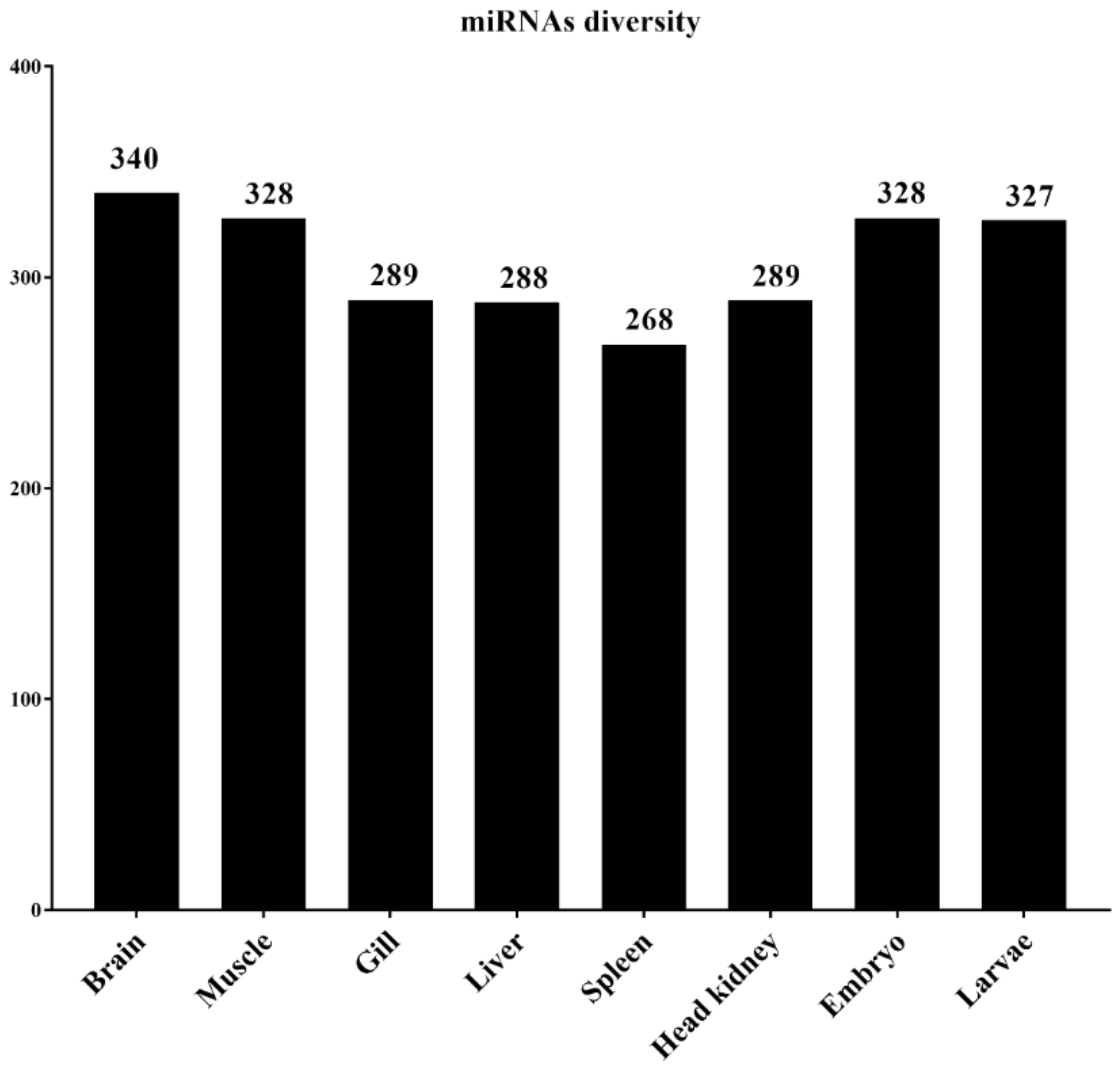

Figure 4.2. miRNA diversity in lumpfish tissue/organs and early developmental stages.

The abundance of the most common mature miRNAs within each organ and developmental stage is shown in Figures 4.3 and 4.4, respectively. These figures show the distribution of the top 20 enriched mature miRNAs within each of the six organs and in the two early developmental stages. The abundances for all miRNAs within each of the organs and early developmental stages are shown in Table S4.4. Five of the top 20 enriched mature miRNAs, clu-miR-21a-5p, clu-miR-22ab-3p, clu-miR-26-1-5p, clu-miR-100-2-5p, and clu-let-7g-5p were highly abundant within all organ and early developmental stages. While the five mature miRNAs clu-miR-146a-5p, clu-let-7a-3-5p, clu-miR-126-3p, clu-let-7e-5p and clu-miR-143-3p were highly abundant miRNAs within all six organs of adult lumpfish, but not among the highly expressed miRNAs within lumpfish embryos and larvae (Figures 4.3 and 4.4). Additionally, several miRNAs were highly abundant within one of the tissue/organs of adult fish compared to others. For example, Clu-miR-122-1-5p, clu-miR-192a-5p, clu-miR-152ab-3p, and one novel miRNA (clu-miR-nov-5-5p) were also among the top 20 most abundant miRNAs in liver, but with much lower abundance when comparing expression of miRNAs within other organs. Likewise, clu-miR-1-1-3p, clu-miR-206-3p, and clu-miR-133ab-3p were abundant only in muscle, clu-miR-451a-5p only in spleen, clu-miR-142-2-3p only in head kidney, and clu-miR-9-2-5p and clu-miR-7-3-5p only in brain (Figure 4.3, Table S4.4). Two miRNAs, clu-miR-217b-5p and clu-miR-181b-3-5p were common in the two early developmental stages while having relatively low expression within adult organs. In addition, there were some miRNAs common in one organ and early developmental stage. These were clu-miR-9-2-5p and clu-miR-7-3-5p (brain and early developmental stages), clu-miR-1-1-3p and clu-miR-206-3p (brain and early developmental stages) and clu-miR-192a-5p (liver and early developmental stages).

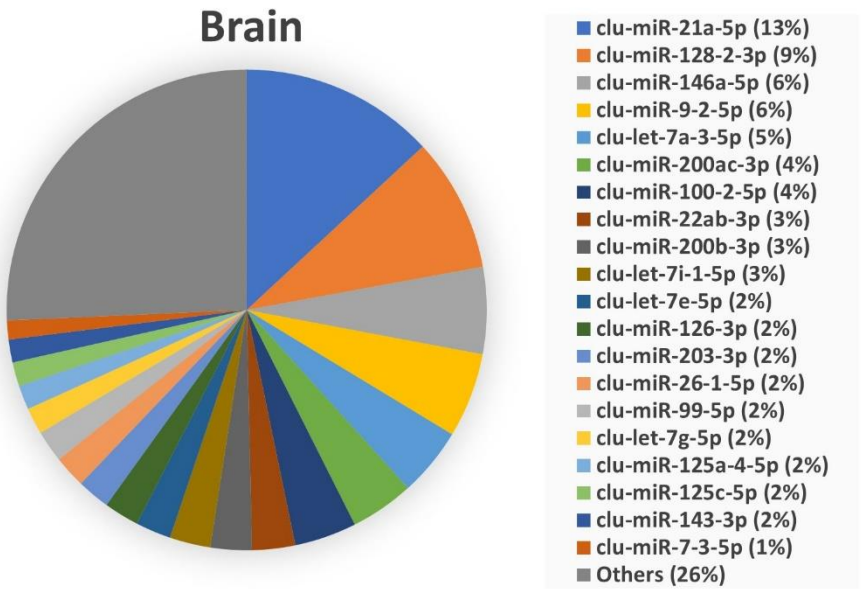
Brain
clu-miR-21a-5p (13%)
clu-miR-128-2-3p (9%)
clu-miR-146a-5p (6%)
clu-miR-9-2-5p (6%)
clu-let-7a-3-5p (5%)
clu-miR-200ac-3p (4%)
clu-miR-100-2-5p (4%)
clu-miR-22ab-3p (3%)
clu-miR-200b-3p (3%)
clu-let-7i-1-5p (3%)
clu-let-7e-5p (2%)
clu-miR-126-3p (2%)
clu-miR-203-3p (2%)
clu-miR-26-1-5p (2%)
clu-miR-99-5p (2%)
clu-let-7g-5p (2%)
clu-miR-125a-4-5p (2%)
clu-miR-125c-5p (2%)
clu-miR-143-3p (2%)
clu-miR-7-3-5p (1%)
Others (26%)

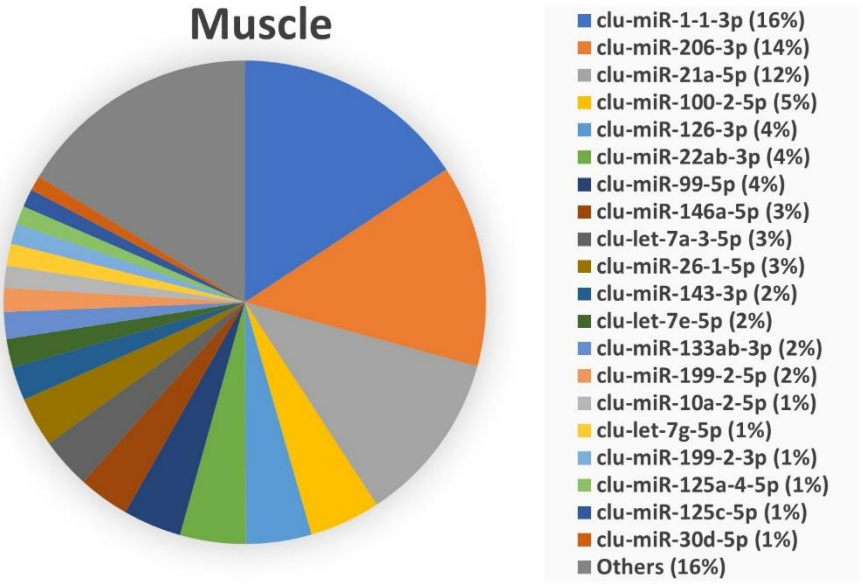
Muscle
clu-miR-1-1-3p (16%)
clu-miR-206-3p (14%)
clu-miR-21a-5p (12%)
clu-miR-100-2-5p (5%)
clu-miR-126-3p (4%)
clu-miR-22ab-3p (4%)
clu-miR-99-5p (4%)
clu-miR-146a-5p (3%)
clu-let-7a-3-5p (3%)
clu-miR-26-1-5p (3%)
clu-miR-143-3p (2%)
clu-let-7e-5p (2%)
clu-miR-133ab-3p (2%)
clu-miR-199-2-5p (2%)
clu-miR-10a-2-5p (1%)
clu-let-7g-5p (1%)
clu-miR-199-2-3p (1%)
clu-miR-125a-4-5p (1%)
clu-miR-125c-5p (1%)
clu-miR-30d-5p (1%)
Others (16%)

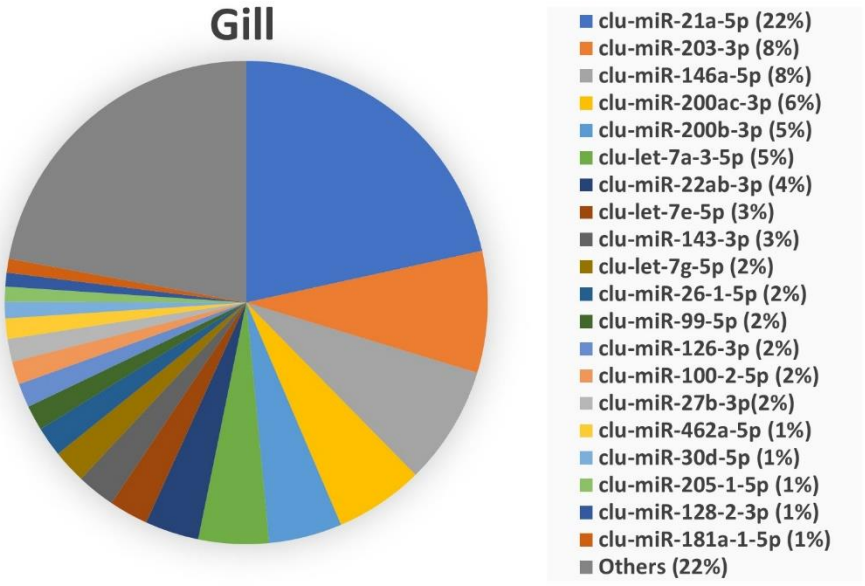
Gill
clu-miR-21a-5p (22%)
clu-miR-203-3p (8%)
clu-miR-146a-5p (8%)
clu-miR-200ac-3p (6%)
clu-miR-200b-3p (5%)
clu-let-7a-3-5p (5%)
clu-miR-22ab-3p (4%)
clu-let-7e-5p (3%)
clu-miR-143-3p (3%)
clu-let-7g-5p (2%)
clu-miR-26-1-5p (2%)
clu-miR-99-5p (2%)
clu-miR-126-3p (2%)
clu-miR-100-2-5p (2%)
clu-miR-27b-3p(2%)
clu-miR-462a-5p (1%)
clu-miR-30d-5p (1%)
clu-miR-205-1-5p (1%)
clu-miR-128-2-3p (1%)
clu-miR-181a-1-5p (1%)
Others (22%)

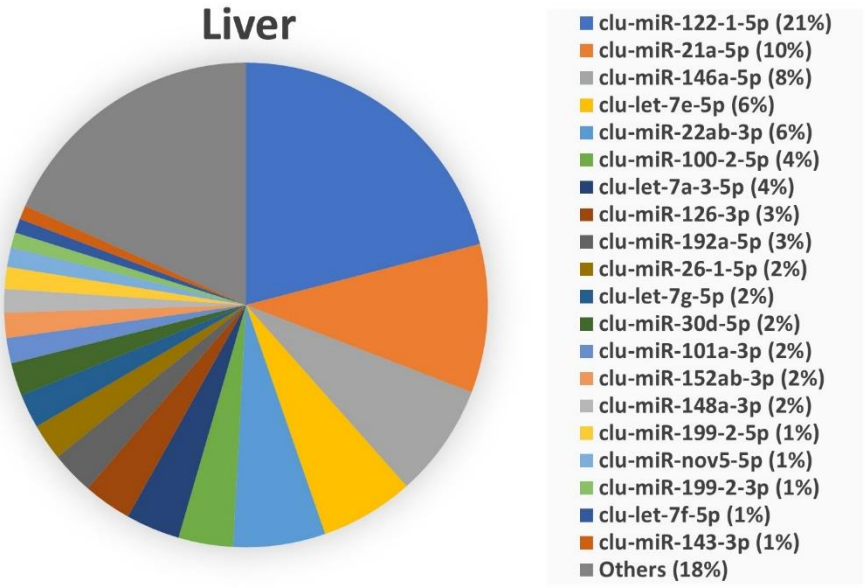
Liver
clu-miR-122-1-5p (21%)
clu-miR-21a-5p (10%)
clu-miR-146a-5p (8%)
clu-let-7e-5p (6%)
clu-miR-22ab-3p (6%)
clu-miR-100-2-5p (4%)
clu-let-7a-3-5p (4%)
clu-miR-126-3p (3%)
clu-miR-192a-5p (3%)
clu-miR-26-1-5p (2%)
clu-let-7g-5p (2%)
clu-miR-30d-5p (2%)
clu-miR-101a-3p (2%)
clu-miR-152ab-3p (2%)
clu-miR-148a-3p (2%)
clu-miR-199-2-5p (1%)
clu-miR-nov5-5p (1%)
clu-miR-199-2-3p (1%)
clu-let-7f-5p (1%)
clu-miR-143-3p (1%)
Others (18%)

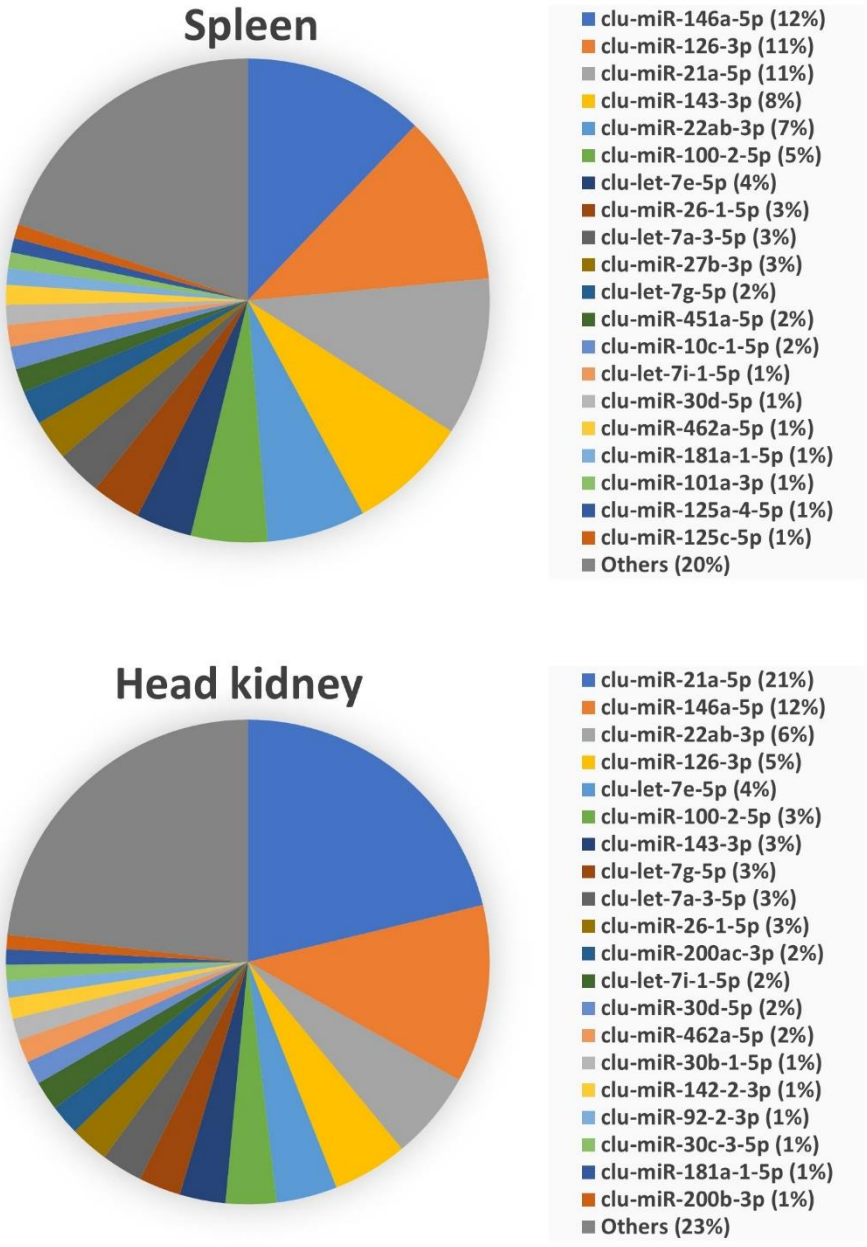

Figure 4.3. Twenty most abundant miRNAs in lumpfish brain, muscle, gill, liver, spleen, and head kidney.

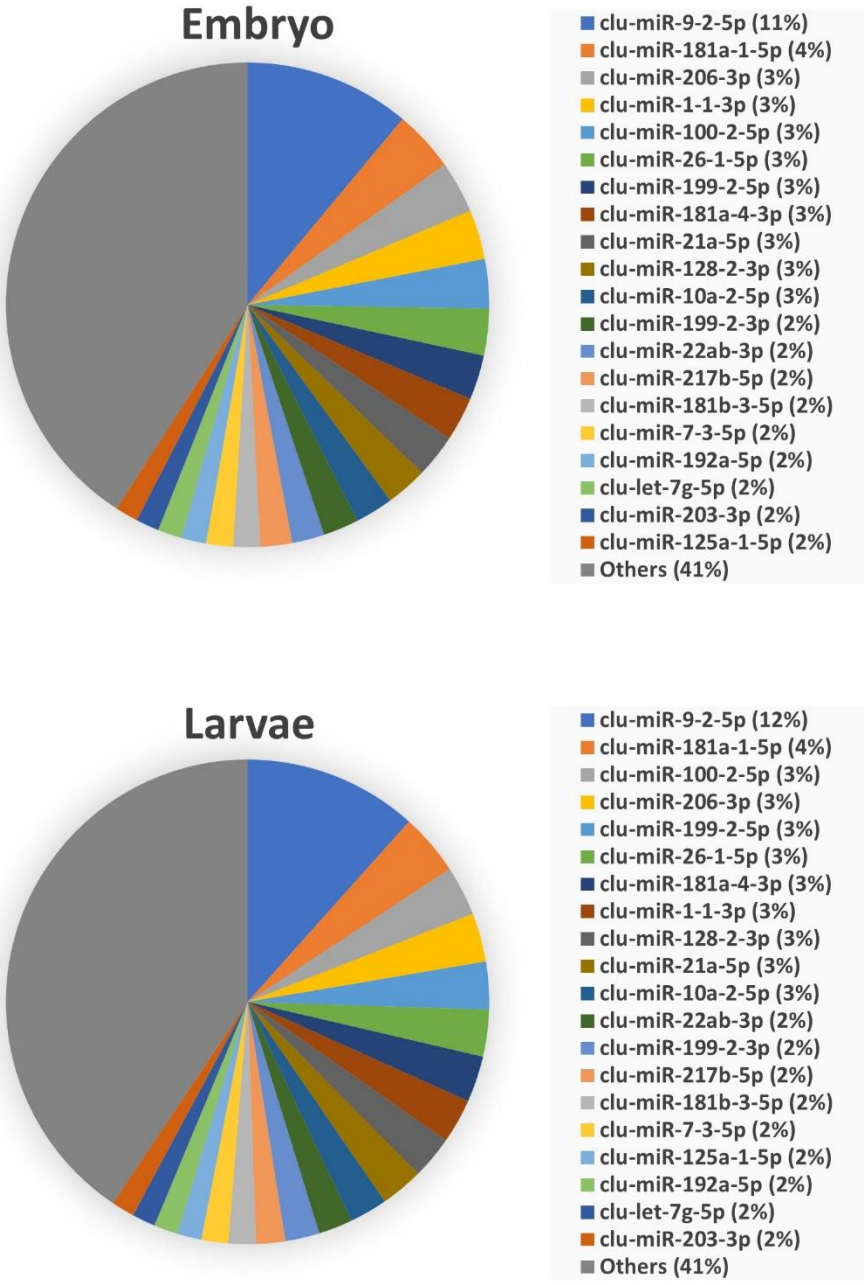

Figure 4.4. Twenty most abundant miRNAs in lumpfish embryos and larvae.

4.4.4 Comparison of mature miRNA expression between organs and early developmental stages

To further explore whether some miRNAs (any of the miRNAs, not only top common ones) were differentially expressed between adult organs or early developmental stages, I also carried out expression analysis of the HTS data and additional RT-qPCR of selected miRNAs. DESeq2 analysis of the HTS data was conducted by comparing one organ or early developmental stage (n = 2) to all other samples (n = 14). The results (File S4.3) suggested that several miRNAs have higher or lower expression in one organ or early developmental stages compared to all other samples. miRNAs suggested as with an increased expression (log_2 fold change > 3.0) in a certain organ or early developmental stage compared to expression in all others are given in Table 4.3 and Table 4.4, respectively. The numbers of such miRNAs were 9 in brain, 5 in muscle, 8 in gill, 15 in liver, 3 in spleen, 13 in embryos, and 22 in larvae. However, DESeq2 analysis did not suggest any enrichment of miRNAs in the lumpfish head kidney.

Table 4.3. Mature miRNAs suggested as highly expressed in one organ compared to others.

Organ[a]	**miRNAs[b]**	**Log_2FC[c]**
Brain	clu-miR-31-3p	6.14
Brain	clu-miR-153c-3p	5.96
Brain	clu-miR-153a-3p	5.33
Brain	clu-miR-1788-5p	4.91
Brain	clu-miR-212b-1-5p	4.10
Brain	clu-miR-212b-1-3p	3.14
Brain	clu-miR-128-2-3p	3.49
Brain	clu-miR-338-1-3p	3.40
Brain	clu-miR-132-1-5p	3.08
Muscle	clu-miR-133b-3p	6.08

Organ[a]	miRNAs[b]	Log2FC[c]
Muscle	clu-miR-133ab-3p	5.45
Muscle	clu-miR-1-1-3p	5.23
Muscle	clu-miR-1-3-5p	3.56
Gill	clu-miR-31-5p	6.91
Gill	clu-miR-1788-3p	6.21
Gill	clu-miR-203-3p	5.13
Gill	clu-miR-203a-5p	4.61
Gill	clu-miR-375-1-3p	4.82
Gill	clu-miR-205-1-3p	4.16
Gill	clu-miR-200b-3p	3.8
Gill	clu-miR-200b-5p	3.36
Liver	clu-miR-122-1-5p	8.23
Liver	clu-miR-122-1-3p	7.65
Liver	clu-miR-nov3-3p	6.78
Liver	clu-miR-nov3-5p	4.68
Liver	clu-miR-nov1-5p	5.58
Liver	clu-miR-101b-3p	4.83
Liver	clu-miR-101b-5p	4.41
Liver	clu-miR-722-3p	4.71
Liver	clu-miR-722-5p	4.38
Liver	clu-miR-92b-3p	4.04
Liver	clu-miR-92b-5p	3.91
Liver	clu-miR-192a-5p	3.75
Liver	clu-miR-94a-5p	3.43
Liver	clu-miR-152ab-3p	3.37
Liver	clu-miR-nov5-5p	3.36
Spleen	clu-miR-2187b-5p	5.10
Spleen	clu-miR-2187b-3p	3.47

Organ[a]	miRNAs[b]	Log_2FC[c]
Spleen	clu-miR-460-5p	3.27

[a] Organ samples were obtained from adult lumpfish

[b] The names are in a few cases with different lettered/numbered suffixes than in miRBase as several mature family members are identical. The miRNAs in the table are grouped in families, and the family member with the highest FC is used to list families in descending order.

[c] Log_2-transformed fold-change (FC) as determined by DESeq2 analysis

Table 4.4. Mature miRNAs suggested as highly expressed in embryos or larvae.

Embryos/Larvae[a]	miRNAs[b]	Log_2FC[c]
Embryos	clu-miR-430b-5-5p	5.61
Embryos	clu-miR-430b-4-3p	4.51
Embryos	clu-miR-430b-1-3p	4.37
Embryos	clu-miR-190b-5p	5.45
Embryos	clu-miR-726-5p	4.91
Embryos	clu-miR-184ab-2-3p	4.77
Embryos	clu-miR-184ab-3p	4.77
Embryos	clu-miR-301b-5p	4.73
Embryos	clu-miR-301b-1-5p	4.40
Embryos	clu-miR-124-1-5p	4.40
Embryos	clu-miR-217b-5p	4.23
Embryos	clu-miR-217a-5p	4.13
Embryos	clu-miR-216a-1-5p	4.20
Larvae	clu-miR-124-1-5p	4.41
Larvae	clu-miR-130-1-5p	3.15
Larvae	clu-miR-130-6-5p	3.62
Larvae	clu-miR-183-5p	4.09
Larvae	clu-miR-184ab-2-3p	4.71

Embryos/Larvae[a]	miRNAs[b]	Log_2FC[c]
Larvae	clu-miR-184ab-3p	4.71
Larvae	clu-miR-190b-5p	5.44
Larvae	clu-miR-194b-3p	3.46
Larvae	clu-miR-196a-1-5p	3.95
Larvae	clu-miR-216a-1-5p	4.00
Larvae	clu-miR-217a-5p	4.11
Larvae	clu-miR-217b-5p	4.11
Larvae	clu-miR-301b-1-5p	4.38
Larvae	clu-miR-301b-3p	3.44
Larvae	clu-miR-301b-5p	4.70
Larvae	clu-miR-430a-12-3p	3.97
Larvae	clu-miR-430a-3-3p	3.97
Larvae	clu-miR-430b-1-3p	4.28
Larvae	clu-miR-430b-4-3p	4.40
Larvae	clu-miR-430b-5-5p	5.41
Larvae	clu-miR-459-3p	4.01
Larvae	clu-miR-726-5p	4.64

[a] Lumpfish embryos were obtained at 300 degree days, and lumpfish larvae were obtained after one-week post-hatch.

[b] The names are in a few cases with different lettered/numbered suffixes than in miRBase as several mature family members are identical. The miRNAs in the table are grouped in families, and the family member with the highest FC is used to list families in descending order.

[c] Log_2-transformed fold-change (FC) as determined by DESeq2 analysis.

RT-qPCR was applied to verify the findings from the DESeq2 analysis in a few selected miRNAs. The two conserved mature miRNAs clu-mir-25-3p and clu-mir-17-5p, shown as suitable reference genes in other teleosts [20, 59], revealed stable expression across all samples in this study (mean Ct values were 22.8 ± 0.9 (SD), 22.4 ± 1.1 (SD), respectively) and were, consequently,

used as reference genes in the RT-qPCR analysis. Eight miRNAs known to be highly expressed in certain organs [19, 20] were selected for RT-qPCR (Table 4.2). These selected miRNAs showed significantly increased expression levels in the expected tissue/ organs (Figure 4.5) that align with the literature [19, 20]. For instance, clu-miR-135c-5p and clu-miR-9b-3p expression was significantly higher in brain, clu-miR-205b-5b, clu-miR-203a-3p, and clu-miR-203b expression was significantly higher in gill, clu-miR-133-3p expression was significantly higher in muscle, and clu-miR-122-5p and clu-miR-192a-5p expression was significantly higher in liver compared to other tissue/organs. These RT-qPCR results were in agreement with the DESeq2 results for 6 of the organ samples, while the increases observed for clu-miR-135c-5p and clu-miR-9b-3p in brain were similar in the DESeq2 analysis but not significant. However, I utilized four or five biological replicates for the RT-qPCR analysis, whereas two were used in the DESeq2 analysis. Additionally, the significance levels were adjusted according to a large number of tests in the DESeq2 analysis. This could explain why the increases did not reach the significant thresholds in the DESeq2 analysis for these two miRNAs.

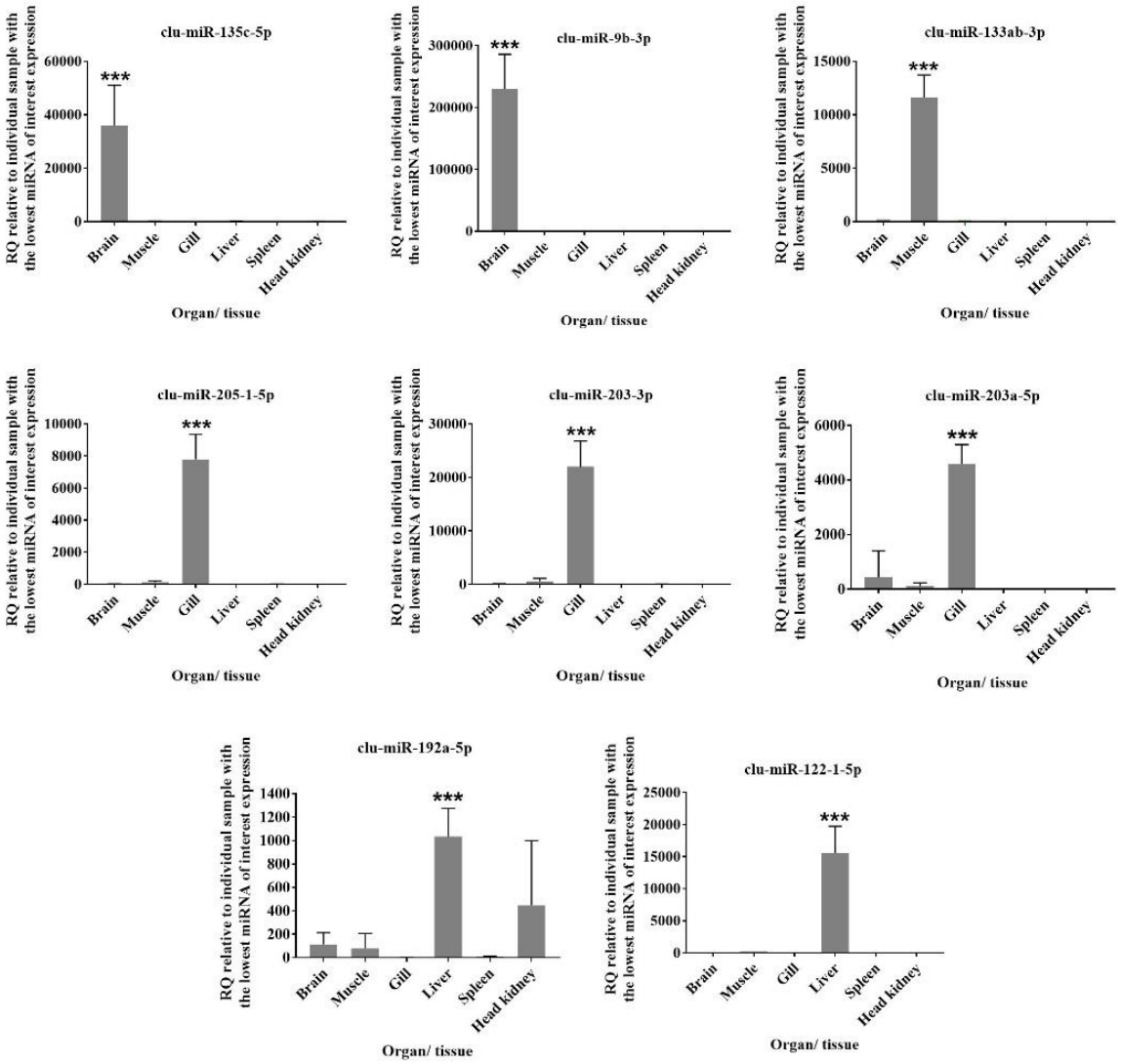
clu-miR-135c-5p
clu-miR-9b-3p
clu-miR-133ab-3p
clu-miR-205-1-5p
clu-miR-203-3p
clu-miR-203a-5p
clu-miR-192a-5p
clu-miR-122-1-5p
RQ relative to individual sample with the lowest miRNA of interest expression
Organ/ tissue
Brain
Muscle
Gill
Liver
Spleen
Head kidney
***

Figure 4.5. **Verification of tissue-specific expression of conserved miRNAs**. RT-qPCR results show the relative expression of eight miRNAs (clu-miR-135c-5p, clu-miR-9b-3p, clu-miR-133ab-3p, , clu-miR-205-1-5b, , clu-miR-203-3p, clu-miR-203a-5p, clu-miR-192a-5p, clu-miR-122-1-5p) across lumpfish organs (brain, muscle, gill, liver, spleen, and head kidney). The number of replicates for tissue samples was five (n = 5) except brain (n = 4) and muscle (n = 4). RQ: relative quantity normalized to clu-miR-25-3p and clu-miR-17-1-5p, and calibrated to the individual sample with the lowest miRNA of interest expression. *** on the top of a particular sample indicates that the expression of the particular miRNA is significantly higher when compared to others by one-way ANOVA ($p < 0.001$) with Tukey's post-hoc test.

4.5 Discussion

miRNAs play a significant role in embryonic development, determination of cell fate, and control of cell proliferation, differentiation, and death. Their dysregulation has a significant impact on critical cellular pathways and is linked to a variety of diseases [11, 13, 16, 48]. A species-specific and well-characterized miRNAome generated from small RNA sequencing of different developmental stages is required to study miRNA expression by analysis of HTS data. Characterization of miRNAs in multiple organs and developmental stages in a new aquaculture species like lumpfish will also facilitate further studies to determine their role in development, whether they regulate organ/developmental stage-specific functions, immune responses to infectious diseases, and disease progression. Therefore, this study was undertaken to define and characterize miRNAs expressed in the brain, muscle, gill, liver, spleen, and head kidney of adult lumpfish, as well as the two developmental stages, embryos and larvae. Together this resulted in a miRNAome consisting of 443 unique mature miRNAs that were used as lumpfish miRNA reference for analysis of HTS data and primer design (RT-qPCR analysis) of single miRNAs.

The expression of different miRNAs within an organ or developmental stage would reveal which ones were highly abundant and likely to have essential regulatory functions. Comparisons between adult organs and early developmental stages could further reveal the highly expressed ones in a few or single organs. Here, I applied DESeq2 analysis to demonstrate that the miRNAome worked well as a reference in such HTS analysis. However, as there were two biological replicates of each adult organ (or early developmental stages) compared to all other HTS samples (n = 14) in these analyses, I report them as suggestive expression differences. Ideally, there should be 3 or more biological replicates in each group compared in such analysis. However, I did choose a rather conservative $\log_2$FC (3 or more) to suggest them as differently expressed between organs (File

S4.3), and some of the miRNAs increased in particular organs were also supported in the additional RT-qPCR analysis (Figure 4.5).

My analysis identified that 10 mature miRNAs were highly abundant and among the top 20 enriched miRNAs within all six organs (five were also among the top 20 enriched in the early developmental stages). These 10 mature miRNAs (clu-let-7a-3-5p, clu-let-7e-5p, clu-let-7g-5p, clu-miR-21a-5p, clu-miR-22ab-3p, clu-miR-26-1-5p, clu-miR-100-2-5p, clu-miR-126-3p, clu-miR-143-3p, and clu-miR-146a-5p) are conserved miRNA families discovered in the majority of vertebrates in miRBase [19, 20, 60]. Their high expression within all adult organs could suggest that these miRNAs play a critical role in lumpfish cellular homeostasis. Still, as they are highly abundant in all adult organs, they are not likely to regulate organ-specific functions.

The brain receives information from sense organs that monitor conditions both within and around the fish. In the brain, the immune cells and the central nervous system interactions allow the immune system to fight against infection and enable the nervous system to regulate immune functioning [61, 62]. Any change in these interaction pathways can cause many pathological conditions attributed to organ dysfunction [61, 62]. However, miRNAs are critical brain development and function regulators, such as neuronal activity [63, 64]. miRDeep2 analysis identified 340 conserved mature miRNAs in the lumpfish brain. Among highly enriched in the brain are clu-miR-9-2-5p and clu-miR-7-3-5p. These two miRNAs do not have similar high relative expression levels within any other adult organs but are similarly enriched in the two early developmental stages indicating they could be important in developing neural tissue in lumpfish (Table S4.4). A similar enrichment pattern of miR-9-5p is seen in Atlantic salmon, cod, halibut, three-spined stickleback, and zebrafish brain [19, 20, 22, 28]. Enrichment of miR-7 in brain is also observed across vertebrates [65]. Several studies have shown that these two miRNAs are crucial

for brain development in zebrafish and other vertebrates [66-68], and it is likely that clu-miR-9-2-5p and clu-miR-7-3-5p may have similar functions in lumpfish. The DESeq2 analysis also suggested that clu-miR-128-2-3p, clu-miR-153c-3p, clu-miR-212b-1-5p, and clu-miR-338-1-3p were more than 10x higher expressed in brain than other organs (File S4.3). Similar findings were observed in Atlantic cod, three-spined stickleback, and zebrafish [19, 69]. In higher vertebrates, miR-128 controls neural motor behaviors by regulating the expression of various ion channels [70]. The three other miRNAs have also all been reported as having important brain functions in higher vertebrates [71-73].

Fish muscles are the major edible parts worldwide, which determines the nutritional and market value. The teleost muscle is also an immunologically active organ, which plays an important role against pathogens [74]. MicroRNAs are established modulators of muscle cell proliferation, differentiation, regeneration, and diseases [75]. miRDeep2 analysis identified 328 conserved mature miRNAs in lumpfish muscle. The muscle-specific top enriched miRNAs were clu-miR-1-1-3p, and clu-miR-133ab-3p (present in other organs but much less abundant). Like in this study, miR-133 and miR-1 were enriched in zebrafish, Atlantic salmon, and cod, suggesting the maintenance of muscle-specific miRNAs expression and function [18-20, 76]. As an example, miR-133 is one of the foremost studied and best-characterized miRNAs in vertebrates. It is required for proper skeletal and cardiac muscle development and function in mammals and fish [77, 78]. On the other hand, miR-1 is a conserved miRNA in the muscle tissue that plays a key role in maintaining muscle integrity [79].

Because of direct exposure to the water, teleost gills are the main mucosal surfaces for the entrance of pathogens, which trigger an immune response [80]. miRNAs are important regulators of immune response to those infections in the gills of fish [20, 81, 82]. However, DESEq2 analysis

was on apparently healthy organs and suggested the enrichment of clu-miR-200 and clu-miR-203 family members and clu-miR-205-1-3p, clu-miR-375-1-3p, clu-miR-31-5p, and clu-miR-1788-3p in lumpfish gill. RT-qPCR results confirmed the enrichment of clu-miR-203-3p, clu-miR-203a-5p, and clu-miR-205-1-5p. Some of these miRNAs, such as miR-200, miR-205, miR-375 were enriched in cod gill as well [20], while miR-200, miR-203, and miR-205 were enriched in gills of tilapia [83]. One of these miRNAs, miR-200, has been shown as important to gill function in cell studies of fish [84]. However, no study has been conducted to decipher the gill-associated role of the remaining five lumpfish miRNAs suggested as differentially expressed in teleost gill.

The liver is involved in various vital functions in controlling biochemical processes, including detoxification and metabolism [85]. miRNAs are essential for regulating liver development and functions, and alterations in intrahepatic miRNA networks have been associated with liver disease in humans [86]. They are also associated with hepatic lipid metabolism in Atlantic salmon [87]. miRDeep analysis identified 288 conserved mature miRNAs in the lumpfish liver (Table S4.4).

Four of the top 20 enriched miRNAs in liver; clu-miR-122-1-5p, clu-miR-152ab-3p, clu-miR-192a-5p, and clu-miR-nov5-5p did not show similar enrichment in any other adult organs (Figure 4.3). DESEq2 analysis also suggested these as having significantly increased expression in liver, and this was confirmed by RT-qPCR for clu-miR-122-1-5p and clu-miR-192a-5p (Figure 4.5). This finding is similar to other teleosts and mammals [20, 88, 89]. miR-122 is the most abundant miRNA in the liver of many species. In mammals, miR-122 is studied extensively and is known to be involved in lipid metabolism [88]. Furthermore, miR-192 is involved in cell growth, lipid synthesis, and apoptosis [90] and having such roles is also in agreement with this miRNA being among the top 20 miRNAs expressed in the early developmental stage samples

(Figure 4.4). Dysregulation of miR-152 is associated with liver disease in higher vertebrates indicating they are important hepatic miRNAs [87, 91]. Based on the high conservation of these miRNAs among vertebrates (miRBase 22.1) [60] and with a similar enrichment pattern as observed in lumpfish, we could assume they also play a similar liver-specific role in lumpfish.

As the body's major blood filter, the spleen plays a major role in detecting cell damage during infection [92]. The spleen is the home of different types of immune cells that trigger different immune responses [92-94]. Splenic miRNAs have been identified to modulate immune responses during diseases in humans, mice, chickens, dogs, and fishes [95-102]. miRDeep analysis identified 268 conserved mature miRNAs in the lumpfish spleen. One mature miRNA, clu-miR-451a-5p was only among the top 20 enriched miRNAs in spleen, and this particular miRNA has been shown to regulate erythroid maturation in zebrafish [103]. Furthermore, DESeq2 analysis suggested the enrichment of clu-miR-2187b-5p and clu-miR-460-5p in the lumpfish spleen. These two miRNAs are also enriched in Atlantic salmon and cod spleen [19, 20], but their particular function in spleen has not yet been investigated.

The anteriormost part of the kidney in the teleost is referred to as the head kidney. It is predominantly a lymphoid compartment. The head kidney is an essential hematopoietic organ and serves as a secondary lymphoid organ, a lymph node analog, vital in inducing and elaborating immune responses [93, 94]. Assessing changes in the expression of miRNAs in the head kidney could provide more comprehensive insight into the immune response to infection. miRDeep2 analysis identified 289 conserved mature miRNAs in lumpfish head kidney. DESeq2 analysis did not suggest any enrichment of miRNA in the head kidney.

The embryos and larvae samples did reveal several miRNAs suggested as early developmental stage enriched. Notably, the miR-430 family was suggested as enriched by the

DESeq2 analysis. These are known as highly expressed in early development, and among suggested functions is maternal RNA clearance during early embryogenesis in zebrafish [104, 105]. Another miRNA that was highly enriched and expressed only in the early developmental stages was clu-miR-217b-5p. This miRNA, as well as mature miRNAs from miR-124, miR-184, and miR-216 families that also were enriched in the lumpfish early developmental stages, have all been shown as important in zebrafish development [76].

4.6 Conclusion

In conclusion, this study represents the first characterization of a lumpfish miRNA transcriptome produced by independent analysis of small RNA sequences from several adult organs and early developmental stages. I identified 391 conserved and eight novel miRNA precursor sequences, which account for 443 unique mature miRNAs. My results demonstrate that most of the lumpfish miRNAs are highly conserved with highly similar precursor sequences to those observed in other teleosts. Many miRNAs also appear to have similar tissue-specific expression patterns as in other vertebrates. Thus, the miRNAs profile of lumpfish suggested a similar organ-specific expression pattern as other vertebrates. It is possible that these conserved miRNAs are regulating essential and conserved genes in vertebrates. Furthermore, the identification and characterization of lumpfish-specific novel miRNAs repertoire in this study will be crucial for further functional studies of the novel miRNAs in this species.

4.8 References

1. Bhaskaran M, Mohan M. MicroRNAs: history, biogenesis, and their evolving role in animal development and disease. Veterinary Pathology. 2014;51(4):759-74.

2. Michlewski G, Caceres JF. Post-transcriptional control of miRNA biogenesis. Cold Spring Harbor Laboratory Press for the RNA Society. 2019;25:1-16.

3. Krol J, Loedige I, Filipowicz W. The widespread regulation of microRNA biogenesis, function and decay. Nature Reviews Genetics. 2010;11(9):597-610.

4. Saliminejad K, Khorram Khorshid HR, Soleymani Fard S, Ghaffari SH. An overview of microRNAs: Biology, functions, therapeutics, and analysis methods. Journal of Cellular Physiology. 2019;234(5):5451-65.

5. Bronevetsky Y, Ansel KM. Regulation of miRNA biogenesis and turnover in the immune system. Immunological Reviews. 2013;253(1):304-16.

6. Matsuyama H, Suzuki HI. Systems and Synthetic microRNA Biology: From Biogenesis to Disease Pathogenesis. International Journal of Molecular Sciences. 2019;21(1).

7. Correia de Sousa M, Gjorgjieva M, Dolicka D, Sobolewski C, Foti M. Deciphering miRNAs' Action through miRNA Editing. International Journal of Molecular Sciences. 2019;20(24).

8. Ha M, Kim VN. Regulation of microRNA biogenesis. Nature Reviews Molecular Cell Biology. 2014;15(8):509-24.

9. Hammond SM. An overview of microRNAs. Advanced Drug Delivery Reviews. 2015;87:3-14.

10. Ravi V, Venkatesh B. Rapidly evolving fish genomes and teleost diversity. Current Opinion in Genetics & Development. 2008;18(6):544-50.

11. Bizuayehu TT, Babiak I. MicroRNA in teleost fish. Genome Biology and Evolution. 2014;6(8):1911-37.

12. Xue X, Woldemariam NT, Caballero-Solares A, Umasuthan N, Fast MD, Taylor RG, RiSe M. Dietary immunostimulant CpG modulates microRNA biomarkers associated with immune responses in Atlantic salmon (*Salmo salar*). Cells. 2019;8(12).

13. Smith NC, Christian SL, Woldemariam NT, Clow KA, Rise ML, Andreassen R. Characterization of miRNAs in cultured atlantic salmon head kidney monocyte-like and macrophage-like cells. International Journal of Molecular Sciences. 2020;21(11).

14. Woldemariam NT, Agafonov O, Sindre H, Hoyheim B, Houston RD, Robledo D, Andreassen R. miRNAs predicted to regulate host anti-viral gene pathways in IPNV-challenged Atlantic salmon fry are affected by viral load, and associated with the major IPN resistance QTL genotypes in late infection. Frontiers in Immunology. 2020;11:2113.

15. Andreassen R, Woldemariam NT, Egeland IO, Agafonov O, Sindre H, Hoyheim B. Identification of differentially expressed Atlantic salmon miRNAs responding to salmonid alphavirus (SAV) infection. BMC Genomics. 2017;18(1):349.

16. Andreassen R, Hoyheim B. miRNAs associated with immune response in teleost fish. Developmental & Comparative Immunology. 2017;75:77-85.

17. Eslamloo K, Inkpen SM, Rise ML, Andreassen R. Discovery of microRNAs associated with the antiviral immune response of Atlantic cod macrophages. Molecular Immunology. 2018;93:152-61.

18. Andreassen R, Worren MM, Høyheim B. Discovery and characterization of miRNA genes in atlantic salmon (*Salmo salar*) by use of a deep sequencing approach. BMC Genomics. 2013;14(482):1-11.

19. Woldemariam NT, Agafonov O, Hoyheim B, Houston RD, Taggart JB, Andreassen R. Expanding the miRNA repertoire in Atlantic salmon; discovery of IsomiRs and miRNAs highly expressed in different tissues and developmental stages. Cells. 2019;8(1).

20. Andreassen R, Rangnes F, Sivertsen M, Chiang M, Tran M, Worren MM. Discovery of miRNAs and their corresponding miRNA genes in Atlantic cod (*Gadus morhua*): Use of stable miRNAs as reference genes reveals subgroups of miRNAs that are highly expressed in particular organs. PLoS One. 2016;11(4):e0153324.

21. Ma H, Hostuttler M, Wei H, Rexroad CE, 3rd, Yao J. Characterization of the rainbow trout egg microRNA transcriptome. PLoS One. 2012;7(6):e39649.

22. Bizuayehu TT, Fernandes JM, Johansen SD, Babiak I. Characterization of novel precursor miRNAs using next generation sequencing and prediction of miRNA targets in Atlantic halibut. PLoS One. 2013;8(4):e61378.

23. Xu Z, Chen J, Li X, Ge J, Pan J, Xu X. Identification and characterization of microRNAs in channel catfish (*Ictalurus punctatus*) by using Solexa sequencing technology. PLoS One. 2013;8(1):e54174.

24. Fu Y, Shi Z, Wu M, Zhang J, Jia L, Chen X. Identification and differential expression of microRNAs during metamorphosis of the Japanese flounder (*Paralichthys olivaceus*). PLoS One. 2011;6(7):e22957.

25. Xia JH, He XP, Bai ZY, Yue GH. Identification and characterization of 63 microRNAs in the Asian seabass *Lates calcarifer*. PLoS One. 2011;6(3):e17537.

26. Robledo D, Martin AP, Álvarez-Dios JA, Bouza C, Pardo BG, Martínez P. First characterization and validation of turbot microRNAs. Aquaculture. 2017;472:76-83.

27. Chen PY, Manninga H, Slanchev K, Chien M, Russo JJ, Ju J. The developmental miRNA profiles of zebrafish as determined by small RNA cloning. Genes & Development. 2005;19(11):1288-93.

28. Desvignes T, Batzel P, Sydes J, Eames BF, Postlethwait JH. miRNA analysis with Prost! reveals evolutionary conservation of organ-enriched expression and post-transcriptional modifications in three-spined stickleback and zebrafish. Scientific Reports. 2019;9(1):3913.

29. DFO. Aquaculture in Atlantic Canada - Atlantic Salmon 2021.

30. DFO. Evaluation of Bacterial Kidney Disease (BKD) Impacts on the Canadian Salmon Aquaculture Industry FINAL REPORT. 2010.

31. Akazawa N, Alvial A, Baloi AP, Blanc P, Brummett RE, Burgos JM, Chamberlain GC, Chamberlain GW, Forster J, Hao NV, Ibarra R, Kibenge F, Lightner DV, Loc TH, Nikuli HL, Omar I, Ralaimarindaza, Reantaso M, St-Hilaire S, Towner R, Tung H, Villarreal M, Wyk M Van. Reducing disease risk in aquaculture (English). Agriculture and environmental services discussion paper. World Bank Group.

32. Brooker AJ, Papadopoulou A, Gutierrez C, Rey S, Davie A, Migaud H. Sustainable production and use of cleaner fish for the biological control of sea-lice: recent advances and current challenges. Veterinary Record. 2018 Sep;183(12):383.

33. Lam CT, Rosanowski SM, Walker M, St-Hilaire S. Sea-lice exposure to non-lethal levels of emamectin benzoate after treatments: a potential risk factor for drug resistance. Scientific Reports. 2020;10(1):932.

34. Karbowski CM, Finstad B, Karbowski N, Hedger RD. Sea-lice in Iceland: assessing the status and current implications for aquaculture and wild salmonids. Aquaculture Environment Interactions. 2019;11:149-60.

35. Aaen SM, Helgesen KO, Bakke MJ, Kaur K, Horsberg TE. Drug resistance in sea-lice: a threat to salmonid aquaculture. Trends in Parasitology. 2015;31(2):72-81.

36. Abolofia J, Asche F, Wilen JE. The Cost of Lice: Quantifying the impacts of parasitic sea-lice on farmed salmon. Marine Resource Economics. 2017;32(3):329-49.

37. Overton K, Dempster T, Oppedal F, Kristiansen TS, Gismervik K, Stien LH. Salmon lice treatments and salmon mortality in Norwegian aquaculture: a review. Reviews in Aquaculture. 2018;11(4):1398-417.

38. Barker SE, Bricknell IR, Covello J, Purcell S, Fast MD, Wolters W. Sea-lice, *Lepeophtheirus salmonis* (Kroyer 1837), infected Atlantic salmon (*Salmo salar* L.) are more susceptible to infectious salmon anemia virus. PLoS One. 2019;14(1):e0209178.

39. Torrissen O, Jones S, Asche F, Guttormsen A, Skilbrei OT, Nilsen F. Salmon lice-impact on wild salmonids and salmon aquaculture. Journal of Fish Diseases. 2013;36(3):171-94.

40. Costello MJ. The global economic cost of sea-lice to the salmonid farming industry. Journal of Fish Diseases. 2009;32(1):115-8.

41. Barrett LT, Overton K, Stien LH, Oppedal F, Dempster T. Effect of cleaner fish on sea-lice in Norwegian salmon aquaculture: a national scale data analysis. International Journal for Parasitology. 2020.

42. Imsland AK, Hanssen A, Nytrø AV, Reynolds P, Jonassen TM, Hangstad TA, Elvegård TA, Urskog TC, Mikalsen B. It works! Lumpfish can significantly lower sea-lice infestation in large-scale salmon farming. Biology Open. 2018;7(9).

43. Vasquez I, Cao T, Chakraborty S, Gnanagobal H, O'Brien N, Monk J, Boyce D, Westcott JD, Santander J. Comparative genomics analysis of *Vibrio anguillarum* isolated from lumpfish

(*Cyclopterus lumpus*) in Newfoundland reveal novel chromosomal organizations. Microorganisms. 2020;8(11).

44. Chakraborty S, Cao T, Hossain A, Gnanagobal H, Vasquez I, Boyce D, Santander J. Vibrogen-2 vaccine trial in lumpfish (*Cyclopterus lumpus*) against *Vibrio anguillarum*. Journal of Fish Diseases. 2019;42(7):1057-64.

45. Dang M, Cao T, Vasquez I, Hossain A, Gnanagobal H, Kumar S, Boyce D, Santander J. Oral immunization of larvae and juvenile of lumpfish (*Cyclopterus lumpus*) against *Vibrio anguillarum* does not influence systemic immunity. Vaccines. 2021;9(8):819.

46. Boyce D, Ang KP, Prickett R. Cunner and lumpfish as cleaner fish species in Canada. Treasurer JW, editor: Sheffield, UK: 5M Publishing.; 2018.

47. Andrews S. FastQC: a quality control tool for high throughput sequence data. Babraham Bioinformatics, Babraham Institute, Cambridge, United Kingdom; 2010.

48. Shwe A, Ostbye TK, Krasnov A, Ramberg S, Andreassen R. Characterization of differentially expressed miRNAs and their predicted target transcripts during smoltification and adaptation to seawater in head kidney of Atlantic salmon. Genes (Basel). 2020;11(9).

49. Knutsen TM, Kirubakaran GT, Mommens M, Moen T. Lumpfish (*Cyclopterus lumpus*) draft genome assembly. Figshare Dataset. 2018.

50. Langmead B, Trapnell C, Pop M, Salzberg SL. Ultrafast and memory-efficient alignment of short DNA sequences to the human genome. Genome Biology. 2009;10(3):R25.

51. Friedländer MR, Chen W, Adamidi C, Maaskola J, Einspanier R, Knespel S, Rajewsky N. Discovering microRNAs from deep sequencing data using miRDeep. Nature Biotechnology. 2008;26(4):407-15.

52. Friedlander MR, Mackowiak SD, Li N, Chen W, Rajewsky N. miRDeep2 accurately identifies known and hundreds of novel microRNA genes in seven animal clades. Nucleic Acids Research. 2012;40(1):37-52.

53. Kozomara A, Griffiths-Jones S. miRBase: annotating high confidence microRNAs using deep sequencing data. Nucleic Acids Research. 2014;42(Database issue):D68-73.

54. Griffiths-Jones S, Grocock RJ, van Dongen S, Bateman A, Enright AJ. miRBase: microRNA sequences, targets and gene nomenclature. Nucleic Acids Research. 2006;34:D140-4.

55. Ambros V, Bartel B, Bartel DP, Burge CB, Carrington JC, Chen X, Dreyfuss G, Eddy SR, Griffiths-Jones SA, Marshall M, Matzke M. A uniform system for microRNA annotation. RNA. 2003;9(3):277-9.

56. Johansen I, Andreassen R. Validation of miRNA genes suitable as reference genes in qPCR analyses of miRNA gene expression in Atlantic salmon (*Salmo salar*). BMC Research Notes. 2014;7(945):1-9.

57. Ruijter JM, Ramakers C, Hoogaars WM, Karlen Y, Bakker O, Van den Hoff MJ, Moorman A. Amplification efficiency: linking baseline and bias in the analysis of quantitative PCR data. Nucleic Acids Research. 2009;37(6):e45.

58. Schmittgen TD, Livak KJ. Analyzing real-time PCR data by the comparative C(T) method. Nature Protocols. 2008;3(6):1101-8.

59. Johansen I, Andreassen R. Validation of miRNA genes suitable as reference genes in qPCR analyses of miRNA gene expression in Atlantic salmon (*Salmo salar*). BMC Research Notes. 2014;8:945.

60. miRBase: the microRNA database. https://www.mirbase.org/.

61. Dantzer R, Wollman EE. Relationships between the brain and the immune system. Journal of Social and Biological Structures. 2003;197(2):81-8.

62. Dantzer R. Neuroimmune interactions: from the brain to the immune system and vice versa. Physiological Reviews. 2018;98(1):477-504.

63. Bizuayehu TT, Babiak I. MicroRNA in teleost fish. Genome Biology and Evolution. 2014;6(8):1911-37.

64. Brennan GP, Henshall DC. MicroRNAs as regulators of brain function and targets for treatment of epilepsy. Nature Reviews Neurology. 2020;16(9):506-19.

65. Tessmar-Raible K, Raible F, Christodoulou F, Guy K, Rembold M, Hausen H, Arendt D. Conserved sensory-neurosecretory cell types in annelid and fish forebrain: insights into hypothalamus evolution. Cell. 2007;129(7):1389-400.

66. Giraldez AJ, Cinalli RM, Glasner ME, Enright AJ, Thomson JM, Baskerville S, Hammond SM, Bartel DP, Schier AF. MicroRNAs regulate brain morphogenesis in zebrafish. Science. 2005;308(5723):833-8.

67. Radhakrishnan B, Alwin Prem Anand A. Role of miRNA-9 in Brain Development. Journal of Experimental Neuroscience. 2016;10:101-20.

68. Zhao J, Zhou Y, Guo M, Yue D, Chen C, Liang G, Xu L. MicroRNA-7: expression and function in brain physiological and pathological processes. Cell & Bioscience. 2020;10(1):77.

69. Vaz C, Wee CW, Lee GP, Ingham PW, Tanavde V, Mathavan S. Deep sequencing of small RNA facilitates tissue and sex associated microRNA discovery in zebrafish. BMC Genomics. 2015;16:950.

70. Tan CL, Plotkin JL, Venø MT, von Schimmelmann M, Feinberg P, Mann S, Handler A, Kjems J, Surmeier DJ, O'Carroll D, Greengard P. MicroRNA-128 governs neuronal excitability and motor behavior in mice. Science. 2013;342(6163):1254-8.

71. Tsuyama J, Bunt J, Richards LJ, Iwanari H, Mochizuki Y, Hamakubo T, Shimazaki T, Okano H. MicroRNA-153 regulates the acquisition of gliogenic competence by neural stem cells. Stem Cell Reports. 2015;5(3):365-77.

72. Wanet A, Tacheny A, Arnould T, Renard P. miR-212/132 expression and functions: within and beyond the neuronal compartment. Nucleic Acids Research. 2012;40(11):4742-53.

73. Howe JR, Li ES, Streeter SE, Rahme GJ, Chipumuro E, Russo GB, Litzky JF, Hills LB, Rodgers KR, Skelton PD, Luikart BW. MiR-338-3p regulates neuronal maturation and suppresses glioblastoma proliferation. PLoS One. 2017;12(5):e0177661.

74. Valenzuela CA, Zuloaga R, Poblete-Morales M, Vera-Tobar T, Mercado L, Avendaño-Herrera R, Valdés JA, Molina A. Fish skeletal muscle tissue is an important focus of immune reactions during pathogen infection. Developmental & Comparative Immunology. 2017;73:1-9.

75. Brzeszczyńska J, Brzeszczyński F, Hamilton DF, McGregor R, Simpson A. Role of microRNA in muscle regeneration and diseases related to muscle dysfunction in atrophy, cachexia, osteoporosis, and osteoarthritis. Bone & Joint research. 2020;9(11):798-807.

76. Bhattacharya M, Sharma AR, Sharma G, Patra BC, Nam JS, Chakraborty C, Lee SS. The crucial role and regulations of miRNAs in zebrafish development. Protoplasma. 2017;254(1):17-31.

77. Yu H, Lu Y, Li Z, Wang Q. microRNA-133: Expression, function and therapeutic potential in muscle diseases and cancer. Current Drug Targets. 2014;15(19):817-28.

78. Zhang R, Li R, Lin Y. Identification and characterization of microRNAs in the muscle of *Schizothorax prenanti*. Fish Physiology and Biochemistry. 2017;43(4):1055-64.

79. Horak M, Novak J, Bienertova-Vasku J. Muscle-specific microRNAs in skeletal muscle development. Developmental Biology. 2016;410(1):1-13.

80. Yu Y, Wang Q, Huang Z, Ding L, Xu Z. Immunoglobulins, mucosal immunity and vaccination in teleost fish. Frontiers in Immunology. 2020;11(2597).

81. Zhang QL, Dong ZX, Luo ZW, Jiao YJ, Guo J, Deng XY, Wang F, Chen JY, Lin LB. MicroRNA profile of immune response in gills of zebrafish (*Danio rerio*) upon *Staphylococcus aureus* infection. Fish & Shellfish Immunology. 2019;87:307-14.

82. Juanchich A, Bardou P, Rué O, Gabillard JC, Gaspin C, Bobe J, Guiguen Y. Characterization of an extensive rainbow trout miRNA transcriptome by next generation sequencing. BMC Genomics. 2016;17:164.

83. Su H, Fan J, Ma D, Zhu H. Identification and characterization of osmoregulation related microRNAs in gills of hybrid tilapia under three types of osmotic stress. Frontiers in Genetics. 2021;12(361).

84. Ng HM, Ho JCH, Nong W, Hui JHL, Lai KP, Wong CKC. Genome-wide analysis of MicroRNA-messenger RNA interactome in ex-vivo gill filaments, *Anguilla japonica*. BMC Genomics. 2020;21(1):208.

85. Sales CF, Silva RF, Amaral MG, Domingos FF, Ribeiro RI, Thomé RG, Santos HB. Comparative histology in the liver and spleen of three species of freshwater teleost. Neotropical Ichthyology. 2017;15(1).

86. Dai Z, Yang T, Song G. The roles of miRNAs in liver diseases. Non-coding RNA Investigation. 2019;3:25-.

87. Østbye TK, Woldemariam NT, Lundberg CE, Berge GM, Ruyter B, Andreassen R. Modulation of hepatic miRNA expression in Atlantic salmon (*Salmo salar*) by family background and dietary fatty acid composition. Journal of Fish Biology. 2021;98(4):1172-85.

88. Lagos-Quintana M, Rauhut R, Yalcin A, Meyer J, Lendeckel W, Tuschl T. Identification of tissue-specific microRNAs from mouse. Current Biology. 2002;12(9):735-9..

89. Trattner S, Vestergren AS. Tissue distribution of selected microRNA in Atlantic salmon. European Journal of Lipid Science and Technology. 2013;115(12):1348-56.

90. Liu XL, Cao HX, Wang BC, Xin FZ, Zhang RN, Zhou D, Yang RX, Zhao ZH, Pan Q, Fan JG. miR-192-5p regulates lipid synthesis in non-alcoholic fatty liver disease through SCD-1. World Journal of Gastroenterology. 2017;23(46):8140-51.

91. Su H, Yang JR, Xu T, Huang J, Xu L, Yuan Y, Zhuang SM. MicroRNA-101, down-regulated in hepatocellular carcinoma, promotes apoptosis and suppresses tumorigenicity. Cancer Research. 2009;69(3):1135-42.

92. Bronte V, Pittet MJ. The spleen in local and systemic regulation of immunity. Immunity. 2013;39(5):806-18.

93. Kaattari SL, Irwin MJ. Salmonid spleen and anterior kidney harbor populations of lymphocytes with different B cell repertoires. Developmental & Comparative Immunology. 1985;9(3):433-44.

94. Press C, Evensen Ø. The morphology of the immune system in teleost fishes. Fish & Shellfish Immunology. 1999;9:309-18.

95. Li G, Zhao Y, Wen L, Liu Z, Yan F, Gao C. Identification and characterization of microRNAs in the spleen of common carp immune organ. Journal of Cellular Biochemistry. 2014;115(10):1768-78.

96. Cao Y, Wang D, Li S, Zhao J, Xu L, Liu H, Lu T, Mou Z. A transcriptome analysis focusing on splenic immune-related mciroRNAs of rainbow trout upon *Aeromonas salmonicida* subsp. *salmonicida* infection. Fish & Shellfish Immunology. 2019;91:350-7.

97. Zhou Y, Wang YY, Fu HC, Huang HZ. MicroRNA expression and analysis of immune-related putative target genes in ISKNV-infected spleen of mandarin fish (*Siniperca chuatsi*). Aquaculture. 2022;547.

98. Grimes JA, Prasad N, Levy S, Cattley R, Lindley S, Boothe HW, Henderson RA, Smith BF. A comparison of microRNA expression profiles from splenic hemangiosarcoma, splenic nodular hyperplasia, and normal spleens of dogs. BMC Veterinary Research. 2016;12(1):272.

99. Li ZJ, Zhang YP, Li Y, Zheng HW, Zheng YS, Liu CJ. Distinct expression pattern of miRNAs in Marek's disease virus infected-chicken splenic tumors and non-tumorous spleen tissues. Research in Veterinary Science. 2014;97(1):156-61.

100. He JJ, Ma J, Wang JL, Xu MJ, Zhu XQ. Analysis of miRNA expression profiling in mouse spleen affected by acute *Toxoplasma gondii* infection. Infection, Genetics and Evolution. 2016;37:137-42.

101. Arribas AJ, Gomez-Abad C, Sánchez-Beato M, Martinez N, DiLisio L, Casado F, Cruz MA, Algara P, Piris MA, Mollejo M. Splenic marginal zone lymphoma: comprehensive analysis of gene expression and miRNA profiling. Modern Pathology. 2013;26(7):889-901.

102. Huang L, Ma J, Sun Y, Lv Y, Lin W, Liu M, Tu C, Zhou P, Gu W, Su S, Zhang G. Altered splenic miRNA expression profile in H1N1 swine influenza. Archives of Virology. 2015;160(4):979-85.

103. Pase L, Layton JE, Kloosterman WP, Carradice D, Waterhouse PM, Lieschke GJ. miR-451 regulates zebrafish erythroid maturation in vivo via its target gata2. Blood. 2009;113(8):1794-804.

104. Giraldez AJ, Mishima Y, Rihel J, Grocock RJ, Van Dongen S, Inoue K, Enright AJ, Schier AF. Zebrafish MiR-430 promotes deadenylation and clearance of maternal mRNAs. Science. 2006;312(5770):75-9.

105. Takacs CM, Giraldez AJ. miR-430 regulates oriented cell division during neural tube development in zebrafish. Developmental Biology. 2016;409(2):442-50.

5. Chapter five: Conclusions and prospects

5.1 Findings and future directions

Chapter 5 summarizes the research findings and highlights the main conclusions. It also presents directions for future research.

Chapter 1 provides the general introduction to this thesis work. Here, I highlighted the facts about aquaculture identified by FAO. The world needs more fish to meet the protein demand of the rising human population [1]. Annual fish consumption has increased by 3% from 1961 to 2019 [2, 3]. Aquaculture is likely the fastest-growing food-producing sector [3-5]. Aquaculture generated jobs for more than 20 million people worldwide in 2020 [4]. In Canada, aquaculture has become a large-scale commercial industry, while Atlantic salmon represent 63.43% and 74.3% of volume and value, respectively [6, 7]. Given the aquaculture sector's contribution to food security and the economy, its sustainable development is required. However, diseases are a challenge in any animal food production sector, including aquaculture. One of the most prominent disease challenges currently restraining the global Atlantic salmon aquaculture is infection by caligid sea-lice, specifically *L. salmonis* and *Caligus spp* [8-12]. I explained the characteristics of sea-lice, sea-lice impact on Atlantic salmon aquaculture, and current sea-lice control methods in chapter 1. An efficient biological pest control strategy is using cleaner fish, e.g., lumpfish (*Cyclopterus lumpus*) [8, 13-16]. Lumpfish feed on sea-lice at low temperatures (6-7 °C), indicating that lumpfish is a suitable cold-water option for the biological delousing of Atlantic salmon [13-15, 17, 18]. The number of cleaner fish used by the salmon farming industry has increased exponentially since 2008 [16, 19]. Lumpfish is a native fish in the North Atlantic Ocean. Commercial production of lumpfish is ongoing in Norway and Atlantic Canada. Due to its growing demand, I have focused on lumpfish during my Ph.D. research. Here, I have highlighted lumpfish's physical and genetic

characteristics, its distribution, reproduction, and commercial production in chapter 1. However, diseases caused by various pathogens preclude this industry's development. *A. salmonicida* subsp. *salmonicida* is one of the oldest known fish pathogens, endemic worldwide in both fresh and marine water in a broad host range, including Atlantic salmon and lumpfish, and is the etiologic agent of furunculosis [20-23]. A proper understanding of *A. salmonicida* and the host's resulting disease state is key to developing effective vaccines. The transcriptomic analysis techniques (e.g., RNA-Sequencing (RNA-Seq)) draw the scientific community's attention to elucidating host-pathogen interactions [24-27]. On the other hand, different post-transcriptional factors, including small RNAs (microRNA (miRNAs)), play a major role in determining an organism's disease state by regulating gene expression related to many cellular functions [28-36]. Recently, miRNA-mediated clinical trials have shown promising results for treating such diseases, including viral and bacterial infections [28, 29, 36]. Researchers use state-of-the-art tools, such as high throughput sequencing (HTS), to characterize the miRNAome repertoire, understand the host immune strategies activated against the pathogen, and how the pathogen overcomes host-mediated immune responses directed against it [26]. Such information could help develop vaccine therapeutics against the pathogen.

Nowadays, vaccination is the most critical measure to prevent bacterial infection in aquaculture [37]. The principle of vaccinology is described in chapter 1. The principle of vaccination is immune memory [38]. However, not all formulations confer immunological memory. Antigens prepared for vaccination, or the pathogen, could trigger adaptive immune suppression, hindering protective disease control measures [39-41]. Disease control or elimination requires the induction of protective immunity in a sufficient proportion of the population [42]. This is best achieved by immunization programs capable of inducing long-term protection, a hallmark

of adaptive immunity by maintaining antigen-specific immune effectors and/or by the induction of immune memory cells that may be sufficiently efficient and rapidly reactivated into immune effectors in case of pathogen exposure [43].

In chapter 1, I also described the major knowledge gaps in lumpfish biology and their immune functions. Overall, research is required to characterize the immune function of lumpfish, lumpfish-*A. salmonicida* interaction, and develop vaccines against *A. salmonicida*. It is also very important to characterize the miRNAome of lumpfish for future functional studies. Finally, I outlined the major thesis objectives in this chapter as i) determining *A. salmonicida* infection kinetics in lumpfish and multi-organ transcriptomic response of lumpfish during *A. salmonicida* infection; ii) investigating the immune protection and immune response of lumpfish to inactivated whole cell vaccine (WCV) or outer membrane proteins (OMPs) of *A. salmonicida*; iii) characterizing miRNAome of lumpfish.

The molecular interactions between lumpfish and *A. salmonicida* were unknown before this research. Therefore, in chapter 2, I characterized the kinetics of *A. salmonicida* infection in lumpfish. Lumpfish were intraperitoneally (ip) injected with different doses of *A. salmonicida.* This study showed that *A. salmonicida* J223 is highly virulent for lumpfish. After 3 days post-infection (dpi), lack of appetite, erratic swimming, and internal hemorrhagic septicemia were observed in the infected fish. Mortality began within 7-10 dpi, reaching 100% in the fish infected with the 10^3, 10^4, and 10^5 colony forming units (CFU)/dose, 68% in the fish infected with 10^2 CFU/dose and 7% in the fish infected with 10^1 CFU/dose. The calculated LD_{50} for *A. salmonicida* J223 in lumpfish was 10^2 CFU/dose. Subsequently, *A. salmonicida* infection kinetics in different organs were determined for the different doses used to infect lumpfish. All lethal doses (10^3-10^5 CFU) showed *A. salmonicida* in the head kidney at 3 dpi, suggesting that this organ is the primary

A. salmonicida target, and from then spread to the spleen and liver, and finally, after 7 dpi *A. salmonicida* infection in lumpfish became systemic. Lumpfish infected with a low dose of *A. salmonicida* (10^1 CFU) established a persistent infection as bacterial colonies were still detected after 30 dpi without mortalities. While *A. salmonicida* J223 strain's lethal doses caused acute infection, in low doses, it might cause chronic infections. Similarities and differences between bacterial physiology in acute and chronic infection are needed. Investigation of genetic requirements for *A. salmonicida* colonization and persistence during infection in the lumpfish model could encapsulate many key characteristics of infection. Future studies should reveal the strategies employed by *A. salmonicida* to evade host immune clearance to cause chronic infection. One possible approach could be dual RNA-sequencing analysis to simultaneously define changes in the transcriptomic profiles of the host and the pathogen, which would be helpful to explore the *A. salmonicida* pathogenicity in marine teleost.

In this study, I examined the transcriptome profile of central lymphoid organs, including the head kidney, spleen, and liver, during early (3 dpi) and late infection stages (10 dpi). I identified organ-specific and typical gene expression profiles using reference genome-guided and *de novo* transcriptome analysis. I investigated the molecular interactions and relationships between these organs. Principal component analysis (PCA) and heatmap results reveal clear tissue and time point clusterization. Among all the organs studied, the spleen has the clearest clusterization. Furthermore, I observed only 25.9% of the differentially expressed genes (DEGs) were shared between the *de novo* and reference-based analysis, 17.3% were unique in *de novo* analysis, and 56.8% were unique in reference-based analysis. This study suggested that each assembler was able to capture unique transcripts not detected by other. Therefore, I adopted an integrative approach for gene ontology (GO) enrichment analysis to bring more benefits for the better exploration of

pathogenicity. In addition, this study has provided a substantial transcriptomics database and a novel public platform for GO analysis.

I observed that the most significantly upregulated genes are associated with inflammation, complement activation, blood coagulation, and acute phase responses (APR). Furthermore, GO enrichment analysis revealed that inflammation and APR were activated pathways in all three organs. This study suggested that *A. salmonicida* infection could induce inflammation and APR by upregulating associated genes in lumpfish head kidney (e.g., *il1b, il6, il10, cxcl8a, serum amyloid A-3, hp*), spleen (e.g., *app, ccl19, il1b, il6, cxcl3, cxcl8a, hp*), and liver (e.g., *app, saa3, ccl19, il1b, il6, cxcl8a, hp*). In addition, blood coagulation and complement activation might co-occur in the head kidney and spleen because upregulation of genes related to blood coagulation was observed in lumpfish head kidney at 3 dpi (e.g., *fibrinogen, prothrombin, plasminogen, antithrombin-III*) and spleen at 10 dpi (e.g., *thrombomodulin, platelet glycoprotein 4, coagulation factor XIII, coagulation factor IIIa*, and *coagulation factor VIII, von Willebrand factor*). Interestingly, downregulation of genes encoding hemoglobin subunits alpha and beta was identified in spleen 3 dpi and hypoxia was suggested in the moribund lumpfish. In this study, the upregulation of genes *complement factor H, complement factor B, c3, c7, c8, c1r-A subcomponent-like complement component*, and *c6* was observed in head kidney and spleen.

Excessive activation of inflammation, complement, and coagulation systems damages the host tissues by breaking the blood/tissue barrier and organs, leading to multiple organ failures and death. Interestingly, excessive hemorrhages in the lumpfish body, eyes, gills, or at the base of the fins, muscles, organ tissues, and ascites were observed in moribund fish. These observations suggest that detrimental and uncontrolled inflammation, overactivation of blood coagulation, and complement components lead to a septic-like shock, which might play a significant role in the *A.*

salmonicida mediated lethal infection of lumpfish. However, the septic response is an extremely complex reaction of inflammatory, anti-inflammatory, humoral and cellular processes, and circulatory abnormalities, which are highly variable with the non-specific nature of the signs [44]. Therefore, further investigation is required to confirm sepsis in lumpfish.

Furthermore, I observed the downregulation of genes encoding MHCII and IgM in all analyzed organs. In addition, *cd79a*, *cd79b*, and *cd209* were downregulated in the head kidney, spleen, and liver. All these observations suggest that *A. salmonicida* mediated immune suppression in lumpfish. I also observed the downregulation of the low-affinity immunoglobulin gamma Fc region receptor II-b-like (*LOC117747925*) in the spleen at 3 dpi, suggesting that *A. salmonicida* J223 exerts an antiphagocytic effect in lumpfish.

In this study, host genes associated with cytoskeleton organization (e.g. *actin-binding LIM protein 1-like, cdc42 effector protein 1b, rho GTPase-activating protein 4-like, rho guanine nucleotide exchange factor 10-like protein, rho guanine nucleotide exchange factor 18, rho-related GTP-binding protein RhoH, tubulin beta chain, tubulin monoglycylase TTLL3-like, tubulin polyglutamylase TTLL7, rasgrf2a, tppp3*) were downregulated in the spleen at 10 dpi. In addition, downregulation of genes related to microtubule bundle formation was observed in the head kidney at 10 dpi (e.g., genes encoding dynein assembly factors, dynein heavy chains, *tppp3*). These findings suggest the disruption of the lumpfish cytoskeleton might be triggered by microfilament and microtubule depolymerization and mitotic arrest during *A. salmonicida* infection.

I observed the upregulation of several genes in head kidney and spleen at 10 dpi, which positively regulates the apoptosis process. However, no caspases were differentially expressed in this study. I detected the over-expression of several regulators of NFκB activity, including the *bcl-3*, *tnfrsf11b, aen, ddit4*, *nfkbia,* and *nfil3.* I did not observe the formation of furuncles in lumpfish

skin that is concurrent with no expression of caspases involved in apoptosis. Identification of the dysregulation of *A. salmonicida* virulence gene *AopP*, which is known to induce apoptosis during infection, could be valuable for future research.

A. salmonicida infection downregulates several genes (e.g. *bard1*, *dna2*, *ercc1*, *ercc4*, *herc2*, *msh2*, *parp1*, *rad52*, *ddit4*, *rad54l*) involved in DNA damage repair in liver 10 dpi. Therefore, several biological processes like DNA metabolic process, DNA replication, DNA repair, double-strand break repair, RNA metabolic process, gene expression, and cell cycle processes were enriched by GO enrichment analysis using the downregulated genes in liver 10 dpi. These findings suggest that *A. salmonicida* infection might provoke DNA damage and cause cell cycle arrest in the lumpfish liver.

This study suggested these genes as biomarkers for the molecular diagnosis of *A. salmonicida* early infection. Multiplex qPCR assays for these genes could then be developed to help to detect *A. salmonicida* infection in lumpfish, which could speed up the identification of potential biomarkers for various diagnostic and therapeutic developments in the future lumpfish aquaculture industry and explore the response to septic shock in marine teleosts.

Overall, in chapter 2, I proposed an infection model for lumpfish molecular responses at the early and lethal point of infection. The model suggested that *A. salmonicida* could induce lethal infection in lumpfish by uncontrolled and detrimental blood coagulation, complement activation, and inflammation. Such responses might lead to hypoxia, internal organ hemorrhages, suppression of the adaptive immune system, and impairment of the DNA repair system, which results in cell cycle arrest and, ultimately, death. Also, *A. salmonicida* might destabilize the cytoskeleton structure by depolymerizing microfilament and tubulin to colonize and survive inside the lumpfish. In addition to this, *A. salmonicida* may induce the apoptotic process. These findings fill the gap of

global understanding of the molecular network of *A. salmonicida*-lumpfish host interactions, which is essential for developing effective treatments. This information could be used for prophylactic and therapeutic vaccination in marine teleost. However, future studies will be needed to integrate the interaction of *A. salmonicida* virulence factors with the cells of the lumpfish immune system.

Driving from the need for vaccination against *A. salmonicida* in lumpfish, in chapter 3, I evaluated the immune protective effect of *A. salmonicida* bacterins and OMPs expressing iron-regulated outer membrane protein (IROMPs) in lumpfish. This study included wild-type *A. salmonicida* J223 strain that contains Vap A layer (A^+) and three other mutant strains, J225, J227, and J228, that do not have Vap A layer (A^-). Additionally, one set of bacterins contained extracellular products (ECPs, secreted by *A. salmonicida*) in the growth medium. Triplicated groups of passive integrated transporter (PIT)-tagged lumpfish (10.3 ± 2.4 g; n=48 per group) were ip injected with formalin-killed A^+ or A^- *A. salmonicida* bacterins ($ECPs^{+/-}$), A^+OMPs, A^+IROMPs, A^-OMPs or A^-IROMPs. However, all immunized and non-immunized control fish similarly died within 2 weeks post-challenge. Therefore, my results demonstrate that vaccines do not confer protection to lumpfish against *A. salmonicida* J223. ELISA and RT-qPCR analyses were conducted for bacterin-injected lumpfish to investigate further. Interestingly, ELISA results demonstrate that formalin-killed *A. salmonicida* J223 bacterins either in the presence or absence of Vap A layer do not increase IgM titers. Instead, *A. salmonicida* J223 bacterins significantly downregulate genes encoding MHCII, IgM, and CD4, which suggests immune suppression and the vaccine's inability to trigger humoral and cell-mediated immune responses. On the other hand, *A. salmonicida* A^- strains differentially modulate lumpfish's immune system. However, *A. salmonicida* A^- strains did not trigger humoral immune responses and confer protection in

lumpfish. Therefore, this study identified *A. salmonicida* subsp. *salmonicida* as a major lumpfish pathogen that can hijack fish defense mechanisms. However, the tactics employed by the J223 strain to inactivate host defense are still a mystery, which needs to be revealed to develop a new immune protective vaccine.

miRNAs are key regulators in teleost development, maintenance of tissue-specific functions, and immune responses [29, 33, 34]. Before this study, the miRNAs repertoire of lumpfish was unknown. In chapter 4, I identified and characterized miRNA encoding genes in lumpfish from three developmental stages (adult, embryo, and larvae). A total of 16 samples from six different adult lumpfish organs (spleen, liver, head kidney, brain, muscle, and gill), embryos, and larvae were individually small RNA sequenced. This study represents the first characterization of a lumpfish miRNA transcriptome produced by independent analysis of small RNA sequences from several adult organs and early developmental stages. I identified 391 conserved and 8 novel miRNA precursor sequences, which account for 443 unique mature miRNAs. My results demonstrate that most of the lumpfish miRNAs are highly conserved with highly similar precursor sequences to those observed in other teleosts. Many miRNAs also appear to have similar tissue-specific expression patterns as in other vertebrates. Thus, the miRNAs profile of lumpfish suggested a similar organ-specific expression pattern as other vertebrates. It is possible that these conserved miRNAs are regulating essential and conserved genes in vertebrates. Furthermore, the identification and characterization of lumpfish-specific novel miRNAs repertoire in this study will be crucial for further functional studies of the novel miRNAs in this species. Future studies must be carried out to identify the mRNA targets of lumpfish miRNA repertoire and miRNA-mRNA interactions. This could help functional enrichment analysis during *A. salmonicida* infection in lumpfish as well by mapping the genes uniquely regulated by candidate miRNAs to GO database

for analysis of enriched signaling pathway and disease ontology. There are studies in rainbow trout, turbot, and Atlantic salmon that characterized miRNA during *A. salmonicida* infection [45-48]. RT-qPCR experiment can be designed to identify the expression of these miRNAs in lumpfish by using primer sequences obtained in this study. Furthermore, miRNAs play a key role in the inflammatory response and have been validated to be potential sepsis biomarkers recently [49]. Future studies can apply a miRNA regulatory network-based method to identify novel miRNA biomarkers associated with the early diagnosis of sepsis. These could promote designing miRNA therapeutics for lumpfish during bacterial infections.

5.2 Conclusions

Firstly, this study characterized *A. salmonicida* subsp. *salmonicida* J223 infection kinetics in lumpfish and lumpfish molecular responses during lethal infection [24]. My research suggested that *A. salmonicida* J223 might cause septic-like shock and cell cycle arrest in lumpfish, which need to be verified by future experimental work [24]. Several biomarkers were also suggested in this study to identify *A. salmonicida* J223 infection [24]. Interestingly, I observed that both active and dead *A. salmonicida* J223 suppressed the immune system of lumpfish. Additionally, *A. salmonicida* J223 bacterin did not protect lumpfish, while many *A. salmonicida* WCV provided immune protection to several fish species [50-57]. These results indicated that not all WCV trigger immune protection. Therefore, my thesis identified that *A. salmonicida* J223 strain is hypervirulent and suggested that virulence factors in *A. salmonicida* J223 might hinder vaccine-induced protections in lumpfish even if in an inactivated form. This information will contribute to future lumpfish- *A. salmonicida* interactions studies. Furthermore, the lumpfish miRNA repertoire characterized in this thesis is crucial for future functional analysis and for identifying key miRNAs during bacterial infection (e.g., *A. salmonicida*) [58]. Overall, this thesis work contributed

significantly to understanding lumpfish- *A. salmonicida* interaction, revealed lumpfish miRNA repertoire, and provided guidelines for future vaccine and therapeutic vaccine design.

5.3 References

1. FAO. The future of food and agriculture: Trends and challenges. 2017. https://www.fao.org/3/i6583e/i6583e.pdf.

2. FAO. The State of World Fisheries and Aquaculture 2018. 2018. https://www.fao.org/3/i9540en/i9540en.pdf.

3. FAO. The State of World Fisheries and Aquaculture 2022. 2022. https://www.fao.org/publications/home/fao-flagship-publications/the-state-of-world-fisheries-and-aquaculture/en.

4. FAO. The State of World Fisheries and Aquaculture 2020. 2020. https://www.fao.org/documents/card/en/c/ca9229en.

5. DFO. Aquaculture collaboration. 2019. https://www.dfo-mpo.gc.ca/aquaculture/collaboration-eng.html.

6. DFO. Aquaculture Production and Value. 2021. https://www.dfo-mpo.gc.ca/stats/aqua/aqua21-eng.html.

7. Statistic Canada. Aquaculture Value Added Account. 2021. https://www150.statcan.gc.ca/t1/tbl1/en/tv.action?pid=3210010801.

8. Brooker AJ, Papadopoulou A, Gutierrez C, Rey S, Davie A, Migaud H. Sustainable production and use of cleaner fish for the biological control of sea-lice: recent advances and current challenges. Veterinary Record. 2018;183(12):383.

9. Lam CT, Rosanowski SM, Walker M, St-Hilaire S. Sea lice exposure to non-lethal levels of emamectin benzoate after treatments: a potential risk factor for drug resistance. Scientific Reports. 2020;10(1):932.

10. Karbowski CM, Finstad B, Karbowski N, Hedger RD. Sea lice in Iceland: assessing the status and current implications for aquaculture and wild salmonids. Aquaculture Environment Interactions. 2019;11:149-60.

11. Aaen SM, Helgesen KO, Bakke MJ, Kaur K, Horsberg TE. Drug resistance in sea lice: a threat to salmonid aquaculture. Trends in Parasitology. 2015;31(2):72-81.

12. Abolofia J, Asche F, Wilen JE. The cost of lice: quantifying the impacts of parasitic sea lice on farmed salmon. Marine Resource Economics. 2017;32(3):329-49.

13. Hemmingsen W, MacKenzie K, Sagerup K, Remen M, Bloch-Hansen K, Dagbjartarson Imsland AK. *Caligus elongatus* and other sea lice of the genus *Caligus* as parasites of farmed salmonids: A review. Aquaculture. 2020;522.

14. Imsland AK, Reynolds P, Eliassen G, Hangstad TA, Nytrø AV, Foss A. Assessment of growth and sea lice infection levels in Atlantic salmon stocked in small-scale cages with lumpfish. Aquaculture. 2014;433:137-42.

15. Imsland AK, Reynolds P, Eliassen G, Hangstad TA, Nytrø AV, Foss A, Vikingstad E, Elvegård TA. Assessment of growth and sea-lice infection levels in Atlantic salmon stocked in small-scale cages with lumpfish. Aquaculture. 2014;433:137-42.

16. Powell A, Treasurer JW, Pooley CL, Keay AJ, Lloyd R, Imsland AK, Garcia de Leaniz C. Use of lumpfish for sea-lice control in salmon farming: challenges and opportunities. Reviews in Aquaculture. 2018;10(3):683-702.

17. Eggestol HO, Lunde HS, Haugland GT. The proinflammatory cytokines TNF-alpha and IL-6 in lumpfish (*Cyclopterus lumpus* L.) -identification, molecular characterization, phylogeny and gene expression analyses. Developmental & Comparative Immunology. 2020;105:103608.

18. Imsland AK, Remen M, Bloch-Hansen K, Sagerup K, Mathisen R, Myklebust EA. Possible use of lumpfish to control *Caligus elongatus* infestation on farmed Atlantic salmon: a mini review. Journal of Ocean University of China. 2020;19(5):1133-9.

19. Barrett LT, Overton K, Stien LH, Oppedal F, Dempster T. Effect of cleaner fish on sea lice in Norwegian salmon aquaculture: a national scale data analysis. International Journal of Parasitology. 2020.

20. Fish FF. Furunculosis in Wild Trout. Copeia. 1937;1937(1):37-40.

21. Duijn JCV. Taxonomy of the fish furunculosis organism. Nature. 1962;4846:1127.

22. Janda JM, Abbott SL. The genus *Aeromonas*: taxonomy, pathogenicity, and infection. Clininal Microbiology Reviews. 2010;23(1):35-73.

23. R Beaz-Hidalgo MJF. *Aeromonas* spp. whole genomes and virulence factors implicated in fish disease. Journal of Fish Diseases. 2013;36(4):371-88.

24. Chakraborty S, Hossain A, Cao T, Gnanagobal H, Segovia C, Hill S, Monk J, Porter J, Boyce D, Hall JR, Bindea G, Kumar S, Santander J. Multi-organ transcriptome response of lumpfish (*Cyclopterus lumpus*) to *Aeromonas salmonicida* subspecies *salmonicida* systemic infection. Microorganisms. 2022;10(11):2113.

25. Wu R, Sheng X, Tang X, Xing J, Zhan W. Transcriptome analysis of flounder (*Paralichthys olivaceus*) gill in response to lymphocystis disease virus (LCDV) infection: novel insights into fish defense mechanisms. International Journal of Molecular Sciences. 2018;19(1):1-19.

26. Sudhagar A, Kumar G, El-Matbouli M. Transcriptome analysis based on RNA-Seq in understanding pathogenic mechanisms of diseases and the immune system of fish: a comprehensive review. International Journal of Molecular Sciences. 2018;19(1).

27. Eggestøl HØ, Lunde HS, Rønneseth A, Fredman D, Petersen K, Mishra CK, Furmanek T, Colquhoun DJ, Wergeland HI, Haugland GT. Transcriptome-wide mapping of signaling pathways and early immune responses in lumpfish leukocytes upon in vitro bacterial exposure. Scientific Reports. 2018;8(1):5261.

28. Bhaskaran M, Mohan M. MicroRNAs: history, biogenesis, and their evolving role in animal development and disease. Veterinary Pathology. 2014;51(4):759-74.

29. Bronevetsky Y, Ansel KM. Regulation of miRNA biogenesis and turnover in the immune system. Immunological Reviews. 2013;253(1):304-16.

30. Correia de Sousa M, Gjorgjieva M, Dolicka D, Sobolewski C, Foti M. Deciphering miRNAs' action through miRNA editing. International Journal of Molecular Sciences. 2019;20(24).

31. Ha M, Kim VN. Regulation of microRNA biogenesis. Nature Reviews Molecular Cell Biology. 2014;15(8):509-24.

32. Hammond SM. An overview of microRNAs. Advanced Drug Delivery Reviews. 2015;87:3-14.

33. Krol J, Loedige I, Filipowicz W. The widespread regulation of microRNA biogenesis, function and decay. Nature Reviews Genetics. 2010;11(9):597-610.

34. Matsuyama H, Suzuki HI. Systems and synthetic microRNA biology: from biogenesis to disease pathogenesis. International Journal of Molecular Sciences. 2019;21(1).

35. Michlewski G, Caceres JF. Post-transcriptional control of miRNA biogenesis. Cold Spring Harbor Laboratory Press for the RNA Society. 2019;25:1-16.

36. Saliminejad K, Khorram Khorshid HR, Soleymani Fard S, Ghaffari SH. An overview of microRNAs: Biology, functions, therapeutics, and analysis methods. Journal of Cellular Physiology. 2019;234(5):5451-65.

37. Assefa A, Abunna F. Maintenance of fish health in aquaculture: review of epidemiological approaches for prevention and control of infectious disease of fish. Veterinary Medicine International. 2018;2018.

38. Moser M, Leo O. Key concepts in immunology. Vaccine. 2010;28 Suppl 3:C2-13.

39. Takaya A, Yamamoto T, Tokoyoda K. Humoral immunity vs. *Salmonella*. Frontiers in Immunology. 2020;10:3155-.

40. Damrow TA, Williams JC, Waag DM. Suppression of in vitro lymphocyte proliferation in C57BL/10 ScN mice vaccinated with phase I *Coxiella burnetii*. Infection and Immunity. 1985;47(1):149-56.

41. Evenberg D, de Graaff P, Fleuren W, van Muiswinkel WB. Blood changes in carp (*Cyprinus carpio*) induced by ulcerative *Aeromonas salmonicida* infections. Veterinary Immunology and Immunopathology. 1986;12(1):321-30.

42. Pollard AJ, Bijker EM. A guide to vaccinology: from basic principles to new developments. Nature Reviews Immunology. 2021;21(2):83-100.

43. Clem AS. Fundamentals of vaccine immunology. Journal of Global Infectious Diseases. 2011;3(1):73.

44. Pierrakos C, Vincent J-L. Sepsis biomarkers: a review. Critical Care. 2010;14(1):R15.

45. Cao Y, Wang D, Li S, Zhao J, Xu L, Liu H. A transcriptome analysis focusing on splenic immune-related mciroRNAs of rainbow trout upon *Aeromonas salmonicida* subsp. *salmonicida* infection. Fish & Shellfish Immunology. 2019;91:350-7.

46. Xue T, Liu Y, Cao M, Tian M, Zhang L, Wang B. Revealing new landscape of turbot (*Scophthalmus maximus*) spleen infected with *Aeromonas salmonicida* through immune related circRNA-miRNA-mRNA Axis. Biology. 2021;10(7):626.

47. Xia YQ, Cheng JX, Liu YF, Li CH, Liu Y, Liu PF. Genome-wide integrated analysis reveals functions of lncRNA-miRNA-mRNA interactions in Atlantic salmon challenged by *Aeromonas salmonicida*. Genomics. 2022;114(1):328-39.

48. Hairul-Islam VI, Saravanan S, Sekar D, Karikalan K, Senthilkumar P, Chandrika R. Identification of microRNAs from Atlantic salmon macrophages upon *Aeromonas salmonicida* infection. Rna & Disease. 2014:1-8.

49. Huang J, Sun Z, Yan W, Zhu Y, Lin Y, Chen J. Identification of microRNA as sepsis biomarker based on miRNAs regulatory network analysis. BioMed research international. 2014;2014.

50. Bergh PV, Burr SE, Benedicenti O, von Siebenthal B, Frey J, Wahli T. Antigens of the type-three secretion system of *Aeromonas salmonicida* subsp. *salmonicida* prevent protective immunity in rainbow trout. Vaccine. 2013;31(45):5256-61.

51. Villumsen KR, Raida MK. Long-lasting protection induced by bath vaccination against *Aeromonas salmonicida* subsp. *salmonicida* in rainbow trout. Fish & Shellfish Immunology. 2013;35(5):1649-53.

52. Lim J, Hong S. Characterization of *Aeromonas salmonicida* and *A. sobria* isolated from cultured salmonid fish in Korea and development of a vaccine against furunculosis. Journal of Fish Diseases. 2020;43(5):609-20.

53. Marana MH, Skov J, Chettri JK, Krossøy B, Dalsgaard I, Kania PW. Positive correlation between *Aeromonas salmonicida* vaccine antigen concentration and protection in vaccinated

rainbow trout *Oncorhynchus mykiss* evaluated by a tail fin infection model. Journal of Fish Diseases. 2017;40(4):507-16.

54. Rømer Villumsen K, Dalsgaard I, Holten-Andersen L, Raida MK. Potential role of specific antibodies as important vaccine induced protective mechanism against *Aeromonas salmonicida* in rainbow trout. PLoS One. 2012;7(10):e46733.

55. Romstad AB, Reitan LJ, Midtlyng P, Gravningen K, Emilsen V, Evensen Ø. Comparision of a serological potency assay for furunculosis vaccines (*Aeromonas salmonicida* subsp. *salmonicida*) to intraperitoneal challenge in Atlantic salmon (*Salmo salar* L.). Biologicals. 2014;42(2):86-90.

56. Rømer Villumsen K, Koppang EO, Raida MK. Adverse and long-term protective effects following oil-adjuvanted vaccination against *Aeromonas salmonicida* in rainbow trout. Fish & Shellfish Immunology. 2015;42(1):193-203.

57. Braden LM, Whyte SK, Brown ABJ, Iderstine CV, Letendre C, Groman D. Vaccine-induced protection against furunculosis involves pre-emptive priming of humoral immunity in Arctic Charr. Frontiers in Immunology. 2019;10:120.

58. Chakraborty S, Woldemariam NT, Visnovska T, Rise ML, Boyce D, Santander J, Andreassen R. Characterization of miRNAs in embryonic, larval, and adult lumpfish provides a reference miRNAome for *Cyclopterus lumpus*. Biology. 2022;11(1):130.